Reinforced Dental Glass Ionomer Cements: From Conventional to Nanocomposites

Muhammad Amber Fareed

A Thesis Submitted To The School Of Metallurgy and Materials For The Degree of

Doctor of Philosophy

College of Engineering and Physical Sciences, University of Birmingham U.K.

August 2009

SUMMARY

The use of nanoclays as reinforcement to create “polymer-clay nanocomposites” with properties greater than the parent constituents has been well established over the past few decades. Nylon-6 has been the primary matrix material investigated reinforced with organically modified clays. Since then several other polymer-clay nanocomposites have been developed with various polymers employing diverse varieties of nanoclays. In this study a systematic investigation of the reinforcement possibility of poly(acrylic acid) (PAA) with polymer-grade nanoclays (PGV and PGN nanoclays) to develop glass-ionomer cements (GICs) is presented. Chemical characterisations in order to understand the dispersion mechanism of nanoclays and PAA-nanoclay interactions were performed using X-ray diffraction (XRD), X-ray photoelectron spectroscopy (XPS) and Fourier-transform infrared (FTIR) spectroscopy. Gel permeation chromatography (GPC) was conducted in order to measure the molecular weight of PAA used in cements. Several mechanical properties including, compressive strength (CS), diametral-tensile strength (DTS), flexural strength (FS), flexural modulus (E_f), and Vickers hardness (HV) of control groups (Fuji-IX and HiFi cement) and cements formed after the reinforcement of nanoclays were measured. The rheological studies were conducted with a Wilson’s oscillating rheometre to establish the working and setting times of cements after the reinforcement with nanoclays. Additionally, the wear resistance of cements was also measured by two different wear-test methodologies namely, reciprocating wear test (ball-on-flat) and Oregon Health & Sciences University (OH&SU) wear-simulator. Transmission electron microscopy (TEM), scanning electron microscopy (SEM), environmental SEM (ESEM) and cryo-SEM studies were also performed to study the microstructure.

XRD demonstrated that an interlayer space in nanoclays formed by a regular stacking of silicate layers along the [001] direction (d_{001}). The peaks in the diffraction pattern of PGN nanoclays at 2θ ~ 7.13° and PGV nanoclays at 2θ ~ 6.95° were attributed to the interlayer *d*-spacing. The interlayer space of PGN was expanded from 12.83 Å to 16.03 Å in PAA-PGN indicating that intercalation occurred whereas exfoliation occurred in PAA-PGV indicated by the lack of peak at d_{001}. XPS scans of PGV and PGN nanoclays depicted the main peak of O 1s photoelectron which was attributed to the various oxygen containing species such as Si-O-M (M: Mg, Al, Fe, etc) within the two layers of the silicate plate, while, Si-O-Al linkages were identified by Si 2p or Si 2s and Al 2p or Al 2s peaks. The disappearance of the Na peak in PAA-nanoclays in wide-angle XPS scans confirmed that PAA molecules exchanged sodium ions on the surface of silicate layers of nanoclays. It is suggested, that the removal of the cations from the interlayer galleries of nanoclays by the PAA chains reduced significantly the electrostatic Van-der-Waals forces between the silicate plates resulting in intercalation or exfoliation. FTIR spectra demonstrated the presence of a new peak at 1019 cm^{-1} in PAA-nanoclay suspensions and the absorbance intensity of the peak at 1019 cm^{-1} associated with Si-O- stretching vibrations increased with increasing nanoclays loading. The shift of the peak at 973 cm^{-1}, associated with Si-O- stretching vibrations in nanoclays, to 1019 cm^{-1} in PAA-nanoclay and to 1041 cm^{-1} in HiFi-nanoclay suspensions may be associated to the change of the chemical environment in the PAA-nanoclay suspensions. The setting reaction of GICs involves the neutralisation of PAA by the glass powder, which was linked with the formation of calcium and aluminium salt-complexes. The real-time study of the setting reaction of GICs over a period of one hour before and after nanoclays dispersion in Fuji-IX system and HiFi system presented slight differences in the FTIR spectra.

The working and setting times of GICs determined by the Wilson's rheometre exhibited a small decrease both in working and setting times of GICs prepared with the polymer liquids formed after the nanoclays dispersion, when compared to control groups (CPA-HP and CF-IX). Moreover, the mechanical properties (CS, DTS, FS, E_f and HV) of GICs were determined at various aging times 1 hour, 1 day, 1 week and 1 month of storage in distilled water. Generally, GICs formed with modified PAA liquid that contained less than 2 wt % nanoclays, exhibited slightly higher CS (range 124.0–142.0 MPa), similar DTS (range 12.0–20.0 MPa) and higher biaxial flexural strength (range 37.0–42.0 MPa) compared to the control cement groups (Fuji-IX and HiFi). E_f of GICs ranged between 8.0 to 14.5 GPa and the highest values of modulus were obtained for 1 wt % nanoclay reinforcement in the HiFi GIC system. HV of cements was calculated between 62-89 HV. However, the effect of nanoclays reinforcement on various mechanical properties was not statistically significant. The ball-on-flat wear test and the OH&SU wear simulation studies suggested that the determination of the wear volume is more reliable than the wear depth. A comparison between Fuji-IX and HiFi reflected that the HiFi system always showed better wear-resistance than the Fuji-IX. It is proposed, that the improved wear resistance of the HiFi system after the dispersion of nanoclays may be due to a better methodology employed for nanoclay dispersion. However, no significant difference was observed in wear volume for different wt % nanoclays loading. TEM micrographs indicated the microstructure of PAA matrix and glass particles as well as their interaction with dispersed nanoclays. The micro-structure of porous glass particles and the presence of siliceous hydrogel phases surrounding the remnant glass core were identified. In PAA matrix, the association of porous glass particles with the nanoclays was also observed.

ACKNOWLEDGMENTS

Einstein said, “If we knew what it was we were doing, it would not be called research, would it?” Coming from the background of clinical dentistry and then diving deep enough in the ocean of clay-nanocomposites may not accomplish and would have been an exigent task without the marvellous supervision of my supervisor, Dr. Artemis Stamboulis. Artemis, what can I say about her, a lady with good looks and beautiful smile, an extremely talented scientist and brilliant researcher, above all a very kind hearted person who cares for everybody around her. I would like to express my admiration for her time and the continuous support she had offered throughout this project. Thank you very much Dr Stamboulis!

I would like to thank the financial assistances and pecuniary awards from following organisations toward the completion of PhD degree. School of Metallurgy and Material at University of Birmingham for the PhD studentship award; Higher Education Commission Pakistan for the award to cover the final year university fees; British Society for Dental Research for the travel award to attend PEF-IADR London (September, 2008); Armourer and Brasiers Company for travel award to present a paper at IADR Miami USA (April, 2009); Charles Wallace Pakistan Trust for the doctoral bursary award to support the final stages of this research work.

I owe appreciation to many people who offered their substantial support to facilitate the experimental investigations and analysis. Especially, Dr Garry Fleming and Adam Dowling (Dr) at Dublin Dental School Trinity College Ireland contributed the expertise required for wear simulation study and respective data collection during my research visit to Ireland and proffered many constructive discussions. I am indebted to Adam who was enormously solicitous towards my comfort in Dublin. Many thanks are given to Dr M Dadras at University of Neuchatel Switzerland for cryo-SEM studies. Professor David Wood and Dr Neigel Bubb at Leeds Dental Institute granted access to rheological equipment. Prof Wood offered excellent ideas during our discussions on the research of dental materials. The efforts of Dr Ihtesham-ur-Rehman and Abdul S. Khan (Dr) at Queen Mary, University of London are recognized for Raman and FTIR experiments. Thanks are given to Dr Barry Woodfine at Advanced Health Care Limited Kent for his valuable time and munificent supply of the materials. I am grateful to Dr Owen Addison at Dental School Birmingham for his vital comments and assistance with statistical analysis. Finally, the generous supply of the materials form AHC, Nanocor, and BASF is highly appreciated.

Going through all the sweet memories and events at UoB has reminded me how many happy times I have had and the good friends I have made during my research career at Birmingham. I am indebted to the academic, technical and secretarial staff of Metallurgy and Materials for their invaluable assistance throughout this study. I am also thankful to my house-mates and friends who provided me the imperative moral support and made my stay in Birmingham a cherished experience. Last but not the least, overwhelming gratitude is given to my family members, little brother, brothers-in-law and sisters for their unconditional everlasting love. Most of all, to my parents, Mama Hazoor and Dady Ge, who raised me, taught me, loved me, encouraged me, remembered me in their prayers and enlightened me by saying, “A person who strives for knowledge is protected by angels of GOD”. It is to them, I dedicate this work.

In The Name Of Almighty ALLAH (GOD) The Most Beneficent, The Most Compassionate *to*

my parents

CHAPTER 1

CHAPTER 2

CHAPTER 3

CHAPTER 4

CHAPTER 5

CHAPTER 6

LIST OF FIGURES

CHAPTER 1

CHAPTER 2

CHAPTER 3

CHAPTER 4

LIST OF TABLES

LIST OF ABBREVIATIONS

ADA	American Dental Association
AGA	N-acryloylglutamic acid
ASTM	American Society for Testing and Materials
ATRP	Atom-transfer radical polymerization
Bis-GMA	Glycidyl-methacrylate and bisphenol-A
BO	Bridging oxygen
BS	British Standard
C1.0NPAH	Cement formed with D1.0NPA liquid and HiFi powder
C2.0NF75F	Cement formed with D2.0NF75 liquid and Fuji-IX powder
C2.0NFRTF	Cement formed with D2.0NFRT liquid and Fuji-IX powder
C2.0NPAH	Cement formed with D2.0NPA liquid and HiFi powder
C2.0VF75F	Cement formed with D2.0VF75 liquid and Fuji-IX powder
C2.0VFRTF	Cement formed with D2.0VFRT liquid and Fuji-IX powder
C4.0NPAH	Cement formed with D4.0NPA liquid and HiFi powder
CEC	Cation exchange capacity
CF-IX	Cement formed with Fuji-IX powder and Fuji-IX liquid
Compomer	Polyacid-modified composite resins
CPA-HP	Cement formed with 40% aqueous PA solution and HiFi powder
D0.5NP	Dispersion of 0.5%PGN in PA-110
D0.5VP	Dispersion of 0.5%PGV in PA-110
D1.0NP	Dispersion of 1.0%PGN in PA-110
D1.0NPA	Dispersion of 1.0% PGN in water and then addition of 40% PA (w/w) powder

D1.0VP	Dispersion of 1.0%PGV in PA-110
D2.0NF75	Dispersion of 2.0%PGN in Fuji-IX at 75 °C
D2.0NFRT	Dispersion of 2.0%PGN in Fuji-IX at room temperature
D2.0NP	Dispersion of 2.0%PGN in PA-110
D2.0NPA	Dispersion of 2.0% PGN in water and then addition of 40% PA (w/w) powder
D2.0VF75	Dispersion of 2.0%PGV in Fuji-IX at 75 °C
D2.0VFRT	Dispersion of 2.0%PGV in Fuji-IX at room temperature
D2.0VP	Dispersion of 2.0%PGV in PA-110
D_3MA	Decanediol di-methacrylate
D4.0NP	Dispersion of 4.0%PGN in PA-110
D4.0NPA	Dispersion of 4.0% PGN in water and then addition of 40% PA (w/w) powder
D4.0VP	Dispersion of 4.0%PGV in PA-110
D6.0NP	Dispersion of 6.0%PGN in PA-110
D6.0VP	Dispersion of 6.0%PGV in PA-110
D8.0NP	Dispersion of 8.0%PGN in PA-110
D8.0VP	Dispersion of 8.0%PGV in PA-110
EE	Edge-to-edge interaction
EF	Edge-to-face interaction
EGDMA	Ethylene glycol di-methacrylate
EgMA	Eugenol methacrylate
F	Fluorine
FDI	Fédération Dentaire Internationale

FF	Face-to-face interaction
FL	Fuji-IX liquid
FSD	Full-scale deflection
GPC	Gel Permeation Chromatography
ISO	International Organisation for Standardisation
MMA	Methyl methacrylate
MMT	Montmorillonite
M_w	Weight Average Molecular weight
M_w / M_n	Polydispersity
NBO	Non-bridging oxygen
nm	Nanometre
NVP	N-vinylpyrrolidone
P/L	Powder : Liquid ratio
PA	Poly(acrylic acid) powder
PA-110	Poly(acrylic acid) solution obtained from BASF
PAA	Poly(acrylic acid) solution
PAA-PGN	Poly(acrylic acid) – PGN montmorillonite
PAA-PGV	Poly(acrylic acid) – PGV montmorillonite
PA-sol	PAA liquid prepared with 40% PA (w/w) in 60% water
PEG	Poly-ethylene-glycol
PEO	Polyethylene oxide
PG	Polymer-grade
PGN	Polymer-grade montmorillonite type N nanoclays

PGV	Polymer-grade montmorillonite type V
PLS	Polymer-layered silicates nano-composite
Poly(AA-co-IA)	Copolymer of acrylic acid and itaconic acid
Poly(AA-co-MA)	Copolymer of acrylic acid and maleic acid
PVA	Poly(vinylphosphonic acid)
RBC	Resin-based composite
RMGIC	Resin-modified glass ionomer cement
Silorane	Siloxane and oxirane
TEGDMA	Tri-ethylene glycol di-methacrylate
USPHS	United States Public Health Service
w/w	Weight over weight
XPS	X-ray photoemission spectroscopy
XRD	X-ray diffraction
ZOE	Zinc-oxide eugenol

CHAPTER 1

1 LITERATURE REVIEW

1.1 Introduction

When a dentist considers the type of restorations to place in a patient's mouth, his decisions may be influenced by the variety of restorative materials available as well as by the choice of the patient. In this regard, the tooth-coloured filling materials have been increasingly used in restoring cavities in preference to amalgam or gold restorations due to the growing demand for aesthetics in dentistry [1]. Therefore, direct tooth-coloured restorative materials for example, glass ionomer cements (GICs), resin-modified glass ionomer cements (RMGICs), compomers, and resin-based composites (RBCs) are widely being used now-a-days. GICs exhibit higher fluoride release and bonding mechanism to dentine and enamel whereas, RBCs reveal good aesthetics appearance and improved mechanical performance [2]. However, RBCs are technique sensitive to place clinically, resulting in increased patient treatment time with an associated increased treatment cost to the patients [3]. Whereas, GIC restoratives can be easily manipulated, placed in single increment and offer the chemical adherence to the natural tooth structure. GICs are versatile dental materials which are advocated clinically as cavity bases and liners, luting cements, crown/core build-up applications and as restorative materials in deciduous and permanent dentitions [2, 4]. Since the emergence of original GICs [5, 6], these materials have undergone many developments and modifications resulting in the improvement of conventional system to offer successful results [7, 8].

Nanocomposites are a new class of composites, that are particle-filled polymer for which at least one dimension of the dispersed particle is in nanometre range [9]. Polymer nanocomposites, especially polymer-layered silicate nanocomposite represent a major alternative to conventionally (macroscopically) filled polymer [10]. Although the high aspect ratio layer-silicates such as montmorillonite nanoclays (MMT) is ideal for reinforcement but they are not easily dispersed in most the polymers due to the preferred face-to-face stacking [11]. In the present research work, chemical nature and the properties of the conventional GIC system after the reinforcement with nanoclays have been explored. Previously, Tran *et al.* have investigated the incorporation of nanoclays in the aqueous solutions of PAA [12, 13]. Tran *et al.* added 0.5 g of nanoclays to 50 g of a 5 wt % aqueous solution of PAA (molecular weight ~ 230,000) and stirred the mixture for 24 hours at four different temperatures of approximately 20, 30, 60 and 85°C. The resultant polymers nanocomposites were characterized to study the dispersion of nanoclay after the treatment with PAA. It was reported that the interlayer *d*-spacing of the nanoclay increased after mixing with PAA. Furthermore, the addition of small percentage of nanoclays in the conventional GI restorative has recently been reported by Dowling and Fleming, who examined the potential of clay reinforced GI restorative as posterior filling material [14, 15]. It was suggested that the addition of clay in GIC significantly improved the mean compressive strength of GI restorative without having an impact on wear behaviour [15]. According to the knowledge of the author of present study, the physio-chemical interaction of PAA-nanoclays and GIC system has not yet been reported in literature. Therefore, the findings of present work would be very beneficial to develop the further understanding of the dispersion of the nanoclays and the potential development of a glass ionomer system employing nanoclays.

1.2 History of dental cements

Dentistry is a science to maintain and improve the quality of dental care to patients. This goal can be achieved by preventing or treating a disease or relieving pain, and improving aesthetics or functions such as speech and mastication. Many of these objectives need the use of materials to alter or replace the lost or diseased tooth structure. There are more than 50,000 materials available at present and an operator (dentist) is required to select a material which is suitable for any particular clinical application [3]. To select an appropriate dental material, it is necessary that a clinician cautiously analyses the problem along with the careful consideration of clinical requirements, the choice of the available materials and different properties of the materials. Hence, a significant amount of research is required to develop complete understanding of the science of restorative materials.

In the earlier 19th century, metallic restorative materials such as amalgam and gold stimulated the search for dental cements for luting and lining purposes. Zinc oxide-phosphoric acid cements were developed by Pierce in 1879 [16]. These cements were more durable and less irritant to the pulp tissue than its predecessors the zinc oxychloride cement (1855) [16]. Silicate cements, which were based on alumino-fluoro-silicate glasses and phosphoric acid were the first tooth-coloured filling materials that were introduced in 1870s [17]. The dispersed phase of silicate cements was residual glass particles and matrix phase was an aluminium phosphate salt formed from the partial acid dissolution of glass particles. These materials were brittle, required mechanical retention, and had an average longevity of only a few years. Subsequently, the improved version of silicate cements containing fluoride was developed in the earlier 20th century and was mainly used as a filling material because of its improved aesthetics and translucence nature [3]. Afterwards, zinc phosphate cements were developed by Ames in 1892. During the same period zinc-oxide eugenol (ZOE) cements emerged as popular materials because of their therapeutic effect [1, 18]. ZEO had been continuously used as temporary filling materials, lining materials and luting cements for a long time. Till the mid of the last century, zinc phosphate, ZEO and silicate cements were employed extensively for bonding crowns, posts, bridges, inlays and orthodontic bands in addition to their use as cavity linings and filling materials In general, the clinical performance of dental cements had also been improved due to better understanding of physical, chemical, mechanical, biological and rheological properties of cements but their core chemistry remained unchanged [17].

In addition to cements, the use of acrylic filling materials and polymer composites also started in 1940s with the development of poly(methyl-methacrylate) based composites which consisted of a poly(methyl-methacrylate) powder, methyl methacrylate monomer, benzoyl peroxide, and n,n-dimethyl-paratoluidine [3]. These materials had some inherited problems associated with poor colour stability, high polymerization shrinkage, lack of bonding to tooth structure and large coefficient of thermal expansion. The acrylic-filling materials, however, stimulated the exploration of possible adhesive dental restorative materials and evolution of filled-resin materials. The first polymer matrix composite incorporated with silica fillers was introduced in 1950 which had improved mechanical properties and better aesthetics. However, polymer matrix composite could neither bond to the tooth structure nor had a good interfacial interaction between the silica particles and the polymer matrix [19].

In 1956 Buonocore *et al.* [20], proposed the concept of adhesion of materials to the tooth structure and investigated several dentine bonding agents after pre-treatment with 7% HCl and expanded this concept to enamel as well. Later, various dental manufacturers developed similar acidic primer containing methyl-acrylic, amide and phosphate monomers for application in restorative dentistry. Bowen in 1962, developed the resin-based composites (RBCs), containing glycidyl-methacrylate and bisphenol A (Bis-GMA or Bowen's resin) as a matrix of composite. Subsequent experiments incorporated tri-ethylene glycol di-methacrylate (TEGDMA) as a diluent in Bis-GMA to reduce viscosity of the system, resulted in the development of the most widely used matrix monomer combinations for dental composites to-date [21, 22]. Additionally, various RBCs formulations were prepared using a variety of diluent monomers such as methyl methacrylate (MMA) and ethylene glycol di-methacrylate (EGDMA), urethane di-methacrylate (UDMA) and decanediol di-methacrylate (D_3MA). A number of new compositions based on bis-(acrylamide) [DEAAP and DMAAH] and ring-opening monomers such as spiro-ortho-carbonates, vinyl-cyclo-propanes and a combination of siloxane and oxirane moieties (Silorane) that exhibit less shrinkage, have been reported [23-27].

Polyelectrolyte cements emerged in mid 1960s as a result of the development of first zinc poly-acrylate cement by Smith in 1967 using zinc-oxide powder and a PAA solution [28]. Later on, several metal oxides and fillers had been added and a variety of copolymers were explored to improve the properties of poly-electrolyte cements. In addition to the good physical properties and low toxicity, the significant new feature of poly-acrylate cements was their ability to bind with tooth structure which was studied by Mizrahi and Smith in 1969 [29]. It was reported by Mizrahi and Smith that the bonding mechanism of poly-acrylate cements to tooth structure resulted from the polar character of poly-carboxylic acids in poly-electrolyte cements. Despite the novel adhesive properties of these cements, poly-acrylate cements were not very popular at that time because of their opaque nature, non-aesthetic appearance and prolonged setting time. However, the idea of physico-chemical bonding with tooth enamel and dentine resulted in the discovery of PAA base cements. The first product of this series was poly-carboxylate cements followed by glass ionomer cements (GICs).

In response to the inadequate and insufficient properties of restorative materials, namely solubility in the oral environment, pulpal toxicity, and poor marginal adaptation, GICs became available in 1969 after the pioneering studies by Alan Wilson and Brian Kent in the laboratory of the Government Chemist in London [5, 6]. The acid-base reaction of GICs is initiated by depletion of metallic ions from the fluoro-alumino-silicate glass filler to the polymeric acid matrix. GICs were developed to overcome drawbacks of its predecessors, poly-carboxylates and dental silicates and to combine beneficial properties of both materials [6, 30]. The original glass ionomer cement was produced by the reaction of a powder (fluoro-alumino-silicate glass) and an aqueous solution of PAA at a concentration of about 45% [31]. The cements produced had extremely sub-standard handling and mechanical properties as compared to the GIC products available today. Since then new developments in GICs have come into realisation. GICs are hybrid materials exhibiting the combined properties of silicate cements (translucency and fluoride release) and poly-carboxylate cements (ability to chemically bond to tooth structure and elicit less unfavourable pulpal respone) [7, 8]. It is now well documented that GICs have various clinical advantages such as, physico-chemical bonding to tooth structure, prolonged release of fluoride and low coefficient of thermal expansion as compared to other restorative materials. To improve wear resistance of GICs, metal-reinforced GICs were developed by Simmons *et al.* in 1983 by incorporating silver alloy powder in glass powder which was named as Miracle Mix (a silver alloy admix) [32]. Similarly, a metal reinforced GIC cement "Cermet" was prepared by mixing equal volumes of powder of silver amalgam with glass powder of GICs followed by compressing and fusing at 800 ºC [33].

The acid-base reaction of GICs is known to have moisture sensitivity. Therefore, a new generation of command-set resin-modified glass-ionomer cements (RMGIC) was developed to overcome this problem. The idea of incorporating resin based polymer and glass ionomer salt formation within one system was employed in the RMGIC or hybrid ionomers. The RMGICs were developed as an improvement from the conventional GICs in terms of moisture sensitivity and the low early strength was associated with the slow acid-base setting reaction. In addition, RMGICs showed improved mechanical properties [34]. The polyacid-modified composite resins (Compomers) were introduced in the early 1990s and were presented as a new class of materials, which were designed to combine the favourable properties of resin based composites such as aesthetics and strength as well as the adhesion and fluoride release properties of glass ionomer cements. Although compomers do not contain any water, their ability to uptake water in the mouth is strongly related with the reduction in strength over a period of few weeks [35]. Nonetheless, acid primers are required to enhance the adhesion of both compomers and RMGICs in clinical applications.Both modified materials are associated with inherited shrinkage arising from polymerization.

1.3 Ideal properties of a dental/biomaterial

One of the main objectives of research and development in dental materials science is to explore and develop an “ideal restorative material”. The restorative materials are classified as indirect-filling materials and direct-filling materials. Indirect restorations such as crowns, bridges, inlays and onlays involve the laboratory stages in the provision of the restoration whereas, direct filling materials for example amalgam, RBCs, dental cements are placed directly to restore the tooth cavities. The *durability* of a material, for any application is generally used as a single factor to assess the success or failure of a restorative material in terms of life expectancy of restoration and the life expectancy of the surrounding tooth substance [1, 3]. Moreover, durability depends on the physical, mechanical, and biological properties of a restorative material. Therefore, an “ideal restorative material” would be identical to the natural tooth structure in durability, for instance in, strength, adherence and appearance. The properties of an ideal filling material can be categorised in a variety of ways for example, physical properties, biocompatibility, aesthetics and manipulation.

The physical properties of an ideal restorative material are expected to be similar to the tooth structure including resistance to different categories of forces in mouth such as compression, tension, shear, ductility, fracture toughness and creep. The characteristics of wear, bond strength, chemical resistance and heat insulation will be in a close resemblance to the tooth without shrinkage [3, 36]. **Biocompatibility** is one of the key requirements of an ideal restorative material. Since tooth fillings are in close contact with mucosa, tooth, and pulp therefore, by-products of the chemical reactions during different stages of material’s hardening may need to be considered. There are some issues with the current dental restorative materials including allergies, chemical leakage, toxicity, pulpal irritation and release of unwanted substances, which are required to be addressed to develop an ideal restorative material [37]. The **aesthetics** of an ideal restorative material would match the surrounding tooth structure in shade, translucency and texture. Finally, the **manipulation** and the application of dental filling materials are important factors to be considered in clinical practice. The operator's induced variables such as dispensing, mixing and appropriate powder to liquid ratios should be minimised to achieve optimum properties.

Recent improvements in the chemical, mechanical and physical properties of restorative materials have resulted in the development of several new products. However, we are still far away from finding an "ideal material" or a "permanent solution" for decaying tooth.

1.4 Development of GICs

During the development of dental materials, the main challenges are to find a biocompatible long lasting material that can bind to the tooth structure permanently and produce desirable therapeutic effects. Four main types of materials (metals, ceramics, polymers and composites) have been used in dentistry however, it is widely accepted that glass ionomer restorative cements represent a major shift in the restorative dentistry leading to encouraging results fighting against dental caries [38]. It is now well documented that GICs exhibit various clinical advantages such as physico-chemical bonding to tooth structure, prolonged release of fluoride and low coefficient of thermal expansion as compared to other restorative materials.

GICs were developed as a result of the pioneering work of Alan Wilson and Brian Kent at the Laboratory of the Government Chemist in London [5, 6]. In 1960s, Wilson and co-workers set about to improve the performance of dental silicate cements. Silicate cements were susceptible to staining and erosion and were also non-adhesive to the tooth structure and adversely reacted with dental tissues [7, 8]. Initially, Wilson and Batchelor discovered that aluminium and calcium phosphates formed part of the cement matrix which suggested that an improvement might occur if phosphoric acid was replaced by a less aggressive chelating acid, which could also interact with apatite [39-41]. As a result, in 1965, a series of acids (namely, pyruvic, tartaric, tannic, fluoroboric, glycerol phosphoric and tetraphosphoric) in 35-50% solutions were mixed with dental silicate cement glass powder (alumino-silicate glass) [42]. The cements formed had good handling and working features but they were hydrolytically unstable and susceptible to disintegration [43]. Interestingly, when a 25% solution of poly(acrylic acid) was mixed with the dental silicate glass, the resulting cement demonstrated hydrolytic stability however, the working time was too short for clinical use [30]. To ensure the satisfactory speed of the setting reaction of the cement, it was suggested that a third component was required in addition to the PAA and the alumino-silicate glass to achieve optimum setting and working characteristics [44]. Wilson *et al.* realised that the replacement of the phosphoric acid with other acid groups of different strengths and chelating abilities would require the preparation of a series of matching glasses with a range of reactivates [42].

In 1972, during the development of different glass compositions, Wilson and Kent found that the ratio of alumina to silica within the glass frit may control the reactivity of glass and as a result the setting characteristics of the final set cement [45].

Therefore, a series of glasses with alumina : silica ratios ranging from 1.75 : 1 to 2 : 1 (by mass) were prepared and mixed with solutions of 40 and 50 % PAA but the resultant cements were impractical because the working and setting times were too slow for clinical use [42, 45]. Further developments produced an extensive series of different glasses. Wilson and co-workers reported that cements which had adequate working-time, set too slowly, had poor compressive strength (CS) and were susceptible to aqueous attack. On the other hand, cements with sufficient setting time, reasonable CS and resistance to aqueous attack had working times which precluded their use clinically [42]. A breakthrough for Wilson and co-workers [45-48] came with the development of their 200th glass (a glass with higher fluoride and calcium content) and the cement formed was reported to have superior working time, improved CS and resistance to aqueous attack than any of its predecessors, although the translucency and the aesthetics of the cement were poor. Furthermore, Wilson *et al.* [49] investigated a series of additives (citric acid, salicylic acid, acetylacetone, sequestric acid, polyglycol and tartaric acid) and reported that tartaric acid was "effective beyond all expectations". Tartaric acid (+) has four favourable effects, it lengthens the working time, shortens the setting time, increases the CS and resistance to acid attack [42, 50, 51]. GICs develop their strength rapidly after mixing and the strength continues to grow slowly over a period of several months [52]. Wilson *et al.* investigated the development of strength, after the initial rapid increase that occurs on mixing, of four different cement types (polycarboxylate, zinc phosphate, silicate, and GICs) by empirically calculating the total water content of cements. They found that the initial acid-base reaction was followed by a slower process namely the hydration of the reaction products which was thought to be responsible for the slow development of strength in acid-base cements [53-55].

When the GICs was first introduced to the dental market as a replacement for dental silicate cements in anterior applications, it faced stiff competition from the resin-based composites developed by Bowen in 1958. However, clinical interest in GICs restorations continued to develop mainly due to favourable inherited properties of GICs which lead to the substantial improvement in the chemistry of the original product since their development in 1972. GlCs were marketed in Europe in 1976 and became available in the United States in 1977 with the trade name of **A**lumino-**S**ilicate **P**oly- **A**crylate (ASPA) by De Trey Company who made the first commercial glass-ionomer and it was distributed by the Amalgamated Dental Co in England and Caulk in the United States.

The modification and development of GICs had intermittently been introduced in the literature since their first appearance in dentistry nearly 40 years ago [56-62]. Several GIC systems are available in the market for dental professionals and due to the complexity of materials no two commercial systems are chemically or mechanically identical. Micro-mechanical adhesion to the dental tissue, bone and other materials, fluoride release capabilities and biocompatibility have all already been well documented. GICs have a number of advantages for use in dentistry namely high dimensional stability, no shrinkage during setting, no free monomer, no exothermic reaction and good adhesion to the tooth structure. They are highly suitable for applications such as restoration for anterior teeth, temporary filling material for poster region, tunnel restoration, cementing a metal or ceramic crown, a cavity liner, a base for resin based composites or amalgam and as repair material for abrasion and erosion lesion.

Additionally, GICs have been used for biomedical applications for instance in cochlear implant cementation, alveolar ridge augmentation, and as bone cements [63, 64]. However, due to their superiority and acceptability over existing products, attention is required to improve GIC properties. GICs based on bioactive glasses, alumino-silicate fibres and zirconia, have also been investigated with varying degrees of success to improve the biological and mechanical properties. Previously, GICs based on waste gasifier slags had also been proposed for the building industry because of the fast setting repair cements. Moulded products such as roof tiles had also been developed [65]. However, the dental industry is still one of the largest areas of GICs application and by eliminating the drawbacks associated with their weak mechanical properties it would be possible to expand the range of their application.

Despite the numerous benefits of GICs, the major disadvantages associated with this system are their early moisture sensitivity and vulnerability to desiccation. In comparison to RBCs, GICs show poor wear resistance and lower mechanical properties (tensile, compressive, flexural strength) and they are unsuitable materials for load bearing applications in posterior restoration [3, 17, 44, 66]. Over the past decade there has been a great improvement in the research of GIC formulations, micro-structural understanding and characterisation. Various new concepts of glass development [67], polymer and monomer compositions [68-70], ultrasound application [71] and nanoclays incorporation [14] were employed to improve the cross-linking in the matrix phase to improve the properties.

1.5 Systematic study of the GIC literature

The dental market in UK is worth over £ 2.5 billion per year of which dental restoration represents over a third of the whole revenue [72] . This market is likely to grow over the coming years because the materials clinically may become more affordable and readily available. However, the cost effective and predictable dental treatment is central to the achievement of patient satisfaction regardless of whether the treatment is purchased privately by the patient or provided by a third party such as the NHS General Dental Services (GDS). The patients are now more aware of the advances in aesthetic ceramic materials, restorative materials and dental implants.

According to the British Medical Journal “A systematic review is an overview of primary studies which contains an explicit statement of objectives, materials and methods that have been conducted according to explicit and reproducible methodology” [73]. A brief review of the available literature on GICs was carried out to find about the most emerging interests in this material. A quick strategy using key words “glass ionomer, glass polyalkenoate and glass ionomer cement” were used in the comprehensive data bases search engines, SCOPUS and ISI Web of Knowledge. A schematic presentation of the number of studies on GICs over the last 30 years by several authors is summarised in Figure 1.1. It is clear, that the understanding of the chemistry of GICs, the mechanical testing, the ion release, the setting reaction, the glass structure and clinical investigations have been the main areas of GICs research. A quick search of Cochrane Library was also performed by using similar key-words and only four Cochrane reviews and nine other reviews were found on the use of GICs in addition to 557 articles on clinical trials.

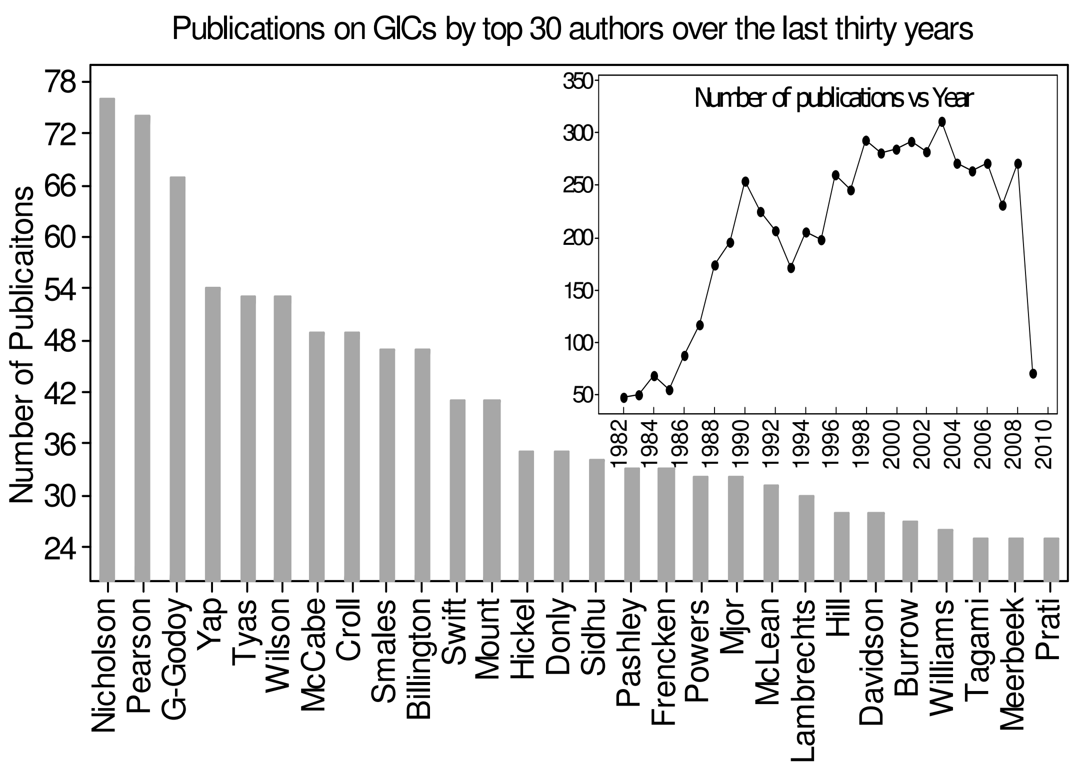

Figure 1. 1: An illustration of the number of GIC publications over the last 30-years.

In 2005, an extensive study was undertaken by Lucarotti *et al.* [74-76] which included over eighty thousand adult patients for a total of 719,009 payment claims submitted by GDS dentists to the Dental Practice Board (DPB) to assess the outcome of the type of the direct restorations placed in patients. The researchers of the study found that dental amalgam was the material of choice with single surface amalgam restorations producing a survival probability of 58% after ten years [74]. Interestingly, patient's demand for aesthetic restorative treatment of cavities in posterior teeth combined with the potential fear of mercury toxicity [77] has led the dental profession to consider alternative materials to dental amalgam. However, the GDS regulations in England and Wales restrict the use of either RBCs or GICs in load-bearing surfaces of posterior teeth. Therefore, the resin-based composites had been placed in Class III, IV and V cavities and GICs in Class III and V cavities with associated survival probabilities at ten years of 43 % and 38 %, respectively [75]. Lucarotti *et al.* also reported that it was not possible to directly compare the performance of amalgam and tooth-coloured materials in posterior teeth because of the GDS limitations for the application of tooth coloured materials in such situations [74]. Moreover, in the above mentioned study, the tooth coloured restoratives were not randomly assigned to different cavities and as a result, the relative performance of the tooth coloured materials compared with the dental amalgam could not be determined as they had not been applied to similar clinical cases.

GICs are probably the most versatile materials among dental restoratives due to the inherent adhesion to the tooth substance and release of fluoride [8]. The role of GICs in the progress of caries was evaluated by Randal and Wilson in a systematic review published 1999 [78]. Randal and Wilson found no conclusive evidence for or against a treatment effect on the inhibition of secondary caries by GICs and therefore the ultimate effect of GIC properties on carries inhibition was not very clear. In 2004, GICs were used in the placement of over 1.9 million restorations in the NHS in England and Wales alone, mainly in Class V non-load-bearing cavities. Burke and Lucarotti recently reported a study of the data available over the past 11 years to determine the re-intervention of GIC restorations [79]. They concluded that there were remarkable variations according to tooth position and time interval to re-intervention in the selection of next restoration material but GIC restorations in anterior and molar teeth are not likely to be followed by another GI restoration.

1.6 The chemistry of GICs

The conventional GICs set via an acid–base reaction between an ion-leachable inorganic glass (powder) and an aqueous solution of acrylic acid or co-polymers (liquid). The acid-base reaction is initiated by the release of ions from the fluoro-aluminosilicate glass filler to the polymeric matrix. The setting chemistry of GICs has been studied by several analytical techniques including Fourier-transform infrared spectroscopy (FTIR) [80, 81], Raman spectroscopy [26, 82], solid state MAS-NMR spectroscopy [83-85], electron probe analysis and pH change [86]. The extent of the ionic cross-linking of the polysalt matrix and the properties of cement are determined by the number and the type of cations and anions released from the glass [87]. After mixing the PAA liquid with the glass powder, PAA rapidly attacks (H^+ ions are formed from -COOH groups) the glass particles preferentially at the more reactive calcium-rich sites resulting in the release of calcium and aluminium into the matrix phase which form calcium acrylate and aluminium acrylate salt units [88] as shown in Figure 1.2.

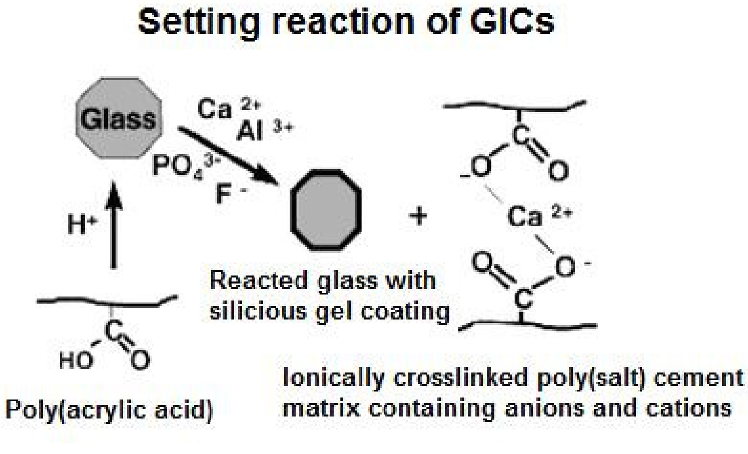

Figure 1. 2: Dissolution of the glass powder and cross-linking of poly-acrylic acid chains by the released cations following the poly-acid attack during the setting reaction of GICs [88].

The above mentioned reaction involves the neutralisation of the polyacid by the basic glass powder which continues for a long period of time. After mixing the powder and the liquid components, the glass is attacked by the acid. The main mechanism involves hydrolysis of Si–O–Al bonds and is thought to be the first step in the setting reaction of GICs [89]. Moreover, Ca^{2+} and Al^{3+} cations along with the fluoride and phosphate anions are released from the glass and migrate into the gel-phase of the cement forming metal cation salt-bridges with the carboxylate anions on the polymer backbone resulting in the cement hardening [90]. It has been reported, that in the case of phosphorus containing glasses the above mechanism does not apply because Al, in the latter case, is charged balanced by phosphorus and not by calcium making the hydrolysis of the Si-O-Al bonds not feasible [91]. On the other hand, Griffin *et al.* reported the depletion of phosphorus and suggested that the mechanism of cations release is different and does not occur by hydrolysis of Si-O-Al bonds [91, 92]. Moreover, the small amount of (+)-tartaric acid that can be added facilitates the transfer of Ca^{2+} or Al^{3+} cations from the inorganic phase to the organic matrix for salt-bridge formation and provides the control of working and setting time [93]. Hatton and Brook showed, that the matrix complex not only consists of simple metal poly-acrylate salts but also some remnants of glass network such as sodium (Na), phosphorus (P) and silicon (Si) known to be distributed throughout matrix [94]. Wasson and Nicholson reported that an inorganic network formed by Na, Si and P within the matrix plays probably a role in improving the strength properties of cements by contributing to the insolubility of cements [95]. On the other hand, Hill *et al.* [96-98] reported that the main phase that plays a role in improving the mechanical properties is indeed the polymer matrix and the molecular weight of the polymer together with the number of entanglements formed are very important factors to determine the strength and the fracture toughness of glass ionomer cements. The role of fluorine present in the glass component seems to be also very important for the cement setting. Although, fluorine does not take part in the cross-linking of matrix and forms fluoride-complexes which may retard the binding of cations to the anionic sites on the polyelectrolyte chains, it increases the reactivity and delays the gelation by prolonging the working time [99]. According to studies by Wilson *et al.* [31, 42, 100, 101] not all the carboxyl groups of PAA are converted to carboxylate groups during the acid-base reaction due to the intramolecular Al^{3+} tricarboxylate salt bridge formation. Additionally, the acid-base reaction of GICs influenced by a variety of factors such as the molar-mass of polymer, the concentration of PAA solution, the powder : liquid (P/L) ratio, the mixing time, the mixing temperature, the presence of chelating agents and the ratio of bounded : unbounded water. Some of these factors are described here briefly:

Glass Composition: Up to a certain value, if the ratio of alumina/silica and fluoride content are higher, the setting reaction will be faster and the working time will be shorter [99]. Glass **particle size: A** finer powder of glass has larger surface area which accelerates the setting. This results in faster maturation of the cement [33]. **Temperature:** An increase in temperature, decreases the working time and accelerates the setting reaction [102]. **Powder/liquid (P/L) ratio:** If the relative proportion of powder is greater than the liquid, then the working time will be shorter and the setting of cement will be faster, also the viscosity of the system increases. The changes in P/L ratios have an effect on the mechanical properties of the GIC system [103, 104]. **Choice of a polymer or copolymer:** The molecular weight of polymer, the water concentration and the presence of (+)-tartaric acid, influence strongly the setting reaction [105, 106].

1.7 Composition of GICs

1.7.1 Glass powder

The glass component of GICs is not just merely an expensive filler or a reservoir for the cross-linking ions but it is an important inorganic structure and the main reactant in the cements formation process [107]. Moreover, the size of the powder particles should be less than 45 µm for filling grade and 15 µm or less for luting cement which can be obtained by grinding in a ball mill or a gyro mill. Further treatment of the glass powder may be done to reduce the reactivity of the glass either by annealing or by washing with a dilute solution of acid (5% acetic acid) [17]. It is important to note, that the reactivity of the glass is influenced by a relatively lower frit temperature 1100°C due to the incomplete fused glass particles [33]. A typical composition of two commercial glasses is presented in Table 1.1.

Table 1. 1: Two of the commonly used GIC glass powder compositions [33].

Compound	Composition A (wt %)	Composition B (wt %)
SiO_2	41.9	35.2
Al_2O_3	28.6	20.1
AlF_3	1.6	2.4
CaF_2	15.7	20.1
NaF	9.3	3.6
$AlPO_4$	3.8	12.0

Most of the glass compositions are of high fluorine content, which is an important attribute of GIC because of its cariostatic properties. Fluorine in the glass favours amorphous phase separation to produce a very reactive glass droplet phase and a less reactive matrix phase which provides cations for the formation of salt-bridges between the PAA chains [108].

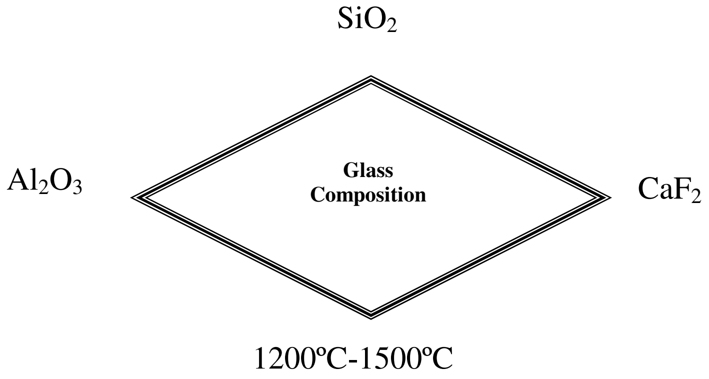

Figure 1. 3: An ionomer glass composition

In order to achieve optimum mechanical properties, efforts have been concentrated to develop new glasses that contribute to the formation of improved final set glass-ionomer cements. The original composition of ion leachable glasses [SiO_2-AlO_3-CaF_2-$AlPO_4$-Na_3AlF_6] used in GIC systems was described in a patent by Wilson 1973 and it was reported that in CaO-Al_2O_3-SiO_2 glasses the Al_2O_3:SiO_2 ratios is required to be 0.5 or more as it plays a critical role in determining the reactivity of the glass and subsequently cement properties. Till today hundreds of glass compositions have been studied for their potential application particularly in dentistry, for the formation of glass ionomer cements (Figure 1.3). Three main categories of glasses can be identified and are described bellow:

(a) Aluminosilicate glasses; are the oldest known glasses used for their chemical durability, tolerance in higher temperatures and superior strength properties as glass ceramics but are also one of the least understood materials for their structure and chemical bonding [109]. They are based on the general composition of SiO_2-Al_2O_3-CaO or SiO_2-Al_2O_3-CaF_2 which were initially employed to make GICs and have been studied extensively by Wilson and co-workers for the development of conventional GI system [109-111]. The individual compositional ingredients of these glasses have been modified by various researchers resulting in several new compositions of aluminosilicate glass series containing SiO_2, Al_2O_3, CaO, CaF_2, NaF, K_2O and P_2O_5 [112, 113].

(b) Aluminoborate glasses; are of interest due to their susceptibility to hydrolysis after appropriate heat treatment leading to controlled reactivity of the glass ionomer cements and also due to the high electrical resistivity [114]. Aluminoborate glasses are based on the general composition Al_2O_3-B_2O_3 with addition of Na_2O, Li_2O, BaO, ZnO and ZnF_2. The use of aluminoborate glasses in dental applications have been restrained due to the low compressive strength of the corresponding cements compared to the aluminosilicate glass formed ionomer cements [115].

(c) Zinc silicate glasses are based on the compositions CaO-ZnO-SiO_2 or Al_2O_3-ZnO-SiO_2 but there is a high percentage of ZnO and SiO in both glass compositions with only a little amount of the third oxide [116]. Although zinc silicate glasses have a great potential as cement formers and as a hard tissue replacement material, zinc glass based cements have inferior mechanical properties compared to the corresponding aluminosilicate glasses for use in clinical dentistry [117].

Furthermore, Wilson *et al.* [118] substituted calcium oxide for fluorite and noted an increase in the compressive strength with fluorine content. Various series of glasses such as SiO_2-Al_2O_3-CaO-P_2O_5, SiO_2-Al_2O_3-Nb_2O_5-CaO, SiO_2-Al_2O_3-CaO-CaF_2 and SiO_2-Al_2O_3-CaO-ZrO-CaF_2 were developed later in which an acid-base reaction degraded the glass network resulting in the release of metal cations (F, P, Ca^{2+} and Al^{3+}) into the matrix to cross-link the polymer chain. In some of the glass series, the fluorine content was up to 23%. However, in more complex glasses containing fluorine (F) and phosphorus (P) the Al : Si ratio has the least influence on the properties of cements.

In addition, most of silicon and aluminium tetrahedra are polymerized to form bridging oxygen (BO) sites Si-O-Si, Si-O-Al and Al-O-Al with a small amount of non-bridging oxygens (NBO) in charge balanced aluminosilicate glasses [119]. The acid degradability of alumino-silicate glasses is related to the destabilisation of the coordination state of aluminium due to the exchange of charge balancing cations connected with the charge deficient AlO_4 tetrahedra. The ratio of aluminium to phosphorus can also have an effect on the number, type and rate of ion release from the glass [120]. Also, alkali metal ions like sodium and fluorine are added to ionomer glasses with the intention to decrease the melting temperature during glass production and to help the release of fluoride ion with offering a soluble counter ion [110]. The role of fluoride and fluorine content has attracted a significant attention both in glass compositions and GICs restorations. Fluoride contributes to the formation of fluorapatite structures which involves a variety of mechanisms including; the reduction in demineralization, the enhancement of remineralization, the interference of pellicle and plaque formation and the inhibition of microbial growth [23, 110]. Generally, the release of fluoride from GICs is considered to strengthen the neighbouring enamel and dentine due to the formation of fluoride complexes with hydroxyapatite [99, 121, 122]. The fluorine serves two major roles in a glass composition, firstly, it decreases the refractive index of the glass and facilitates melting of the glass at lower temperatures and secondly, it disrupts the glass network facilitating the acid attack during cement formation [123]. Hill *et al.* [84, 99] reported that when the calcium fluoride (CaF_2) content was increased, the glass became too reactive for cement formation because the addition of fluorite increased the reactivity of the glass resulting in a shorter working and setting times of the cements as well as increased the Young's modulus and compressive strength of the set cements. Additionally, solid state MAS-NMR studies by Stamboulis and Hill on the structure of fluorine containing aluminosilicate glasses described the role of fluorine as a network disruptor and reported that the addition of calcium fluoride may lead to the formation of non-bridging fluorines as well as non-bridging oxygens [83, 84, 97]. The role of phosphorus is also important in the setting reaction since Al–O–P bonds present in the glass alter the rate of glass dissolution and ion release. The low phosphate contents in the glass can improve the compressive strength and extend the working and setting time of cements whereas, the higher phosphate content disrupts the cross-linking process in the matrix by competing with -COOH groups resulting in mechanically inferior cements [124].

2.1.1 Poly(acrylic acid) liquid (PAA)

A polyelectrolyte, by definition is any polymer with an ionisable group present in its repeating unit [125]. The poly(acrylic acid) (PAA) is a polyelectrolyte made out of acrylic acid monomer units. The acrylic acid monomer is obtained from ethylene cyanohydrin. Cyanohydrins are organic compounds which contain both cyano and hydroxyl groups usually linked to the same carbon atom. Cyanohydrins are obtained from the reactions of aldehydes (or ketones) with hydrogen cyanide in base [126]. To synthesize the acrylic acid, a mixture of ethylene cyanohydrin and sulphuric acid is blown with steam resulting in distilling out 50% acrylic acid solution. PAA is produced when the sodium salt of acrylic acid is polymerised and subsequently acidified to generate poly(acrylic acid) [127]. Furthermore, PAA is insoluble in its monomer but highly soluble in water and exhibits the typical behaviour of a polyelectrolyte. Therefore, when dissolved in water it attains the following structure –[CH_2-CH]- COO^- [128]. The hydrogen atom is removed from the carboxylic acid group to show the reactive carboxyl ion (COO^-) groups which in most cases take part in polymerisation reactions. A freeze-dried PAA powder is also used in dental cements and is mixed with glass powder in commercial products. PAA is a water-soluble polymer and is widely used in various applications in the industry. PAA is also considered super absorbent because of its ability to absorb water many times more than its weight in water. Therefore, this class of materials is used in many applications including diapers and personal hygiene products, ion exchange resins, membranes for hemodialysis and ultrafiltration and controlled-release devices [129]. PAA and its copolymers have received a lot of interest because they are very useful as thickening agents for adhesives, in formulation of pharmaceuticals, cosmetics, coatings, and agricultural chemicals. In dental materials science, PAA was first explored by Wilson in 1972 for the development of glass ionomer cements after mixing with aluminosilicate glass powders [45].

The liquid used for the traditional GICs was the aqueous solution of poly(acrylic acid) in a concentration of 40-50% but in that concentration this liquid tends to gel with time. This problem was resolved by the introduction of di-carboxylic or tri-carboxylic acid into the polymer chains, which not only prevent gelation of the liquid but also provide greater reactivity due to the increased number of reactive carboxyl groups in a chain unit [55, 130]. However, the main additive found in the PAA liquid for GICs is (+)-tartaric acid (5-10%) which can form metal carboxylates more quickly than PAA resulting in improved handling properties such as extending the working time and sharpening the setting time measured by NMR and FTIR analyses. But the precise involvement of (+)-tartaric acid in the setting mechanism and in improving the strength properties of GICs requires further explanation. The aqueous solution of PAA is also known to form chain extension from random coil to rod-like structure, which has a greater excluded volume and chain stiffness than random conformation. This kind of coil expansion has been noted in high concentration solutions used for cement formation and can be reduced by adding a low-molar mass sodium chloride [131]. Moreover, current formulations contain a copolymer of itaconic acid, maleic acid and tricarboxylic acid that are used to reduce the viscosity and tendency for gelation which can increase the reactivity of the liquid [132]. To increase the shelf life and acceptability of a GIC, a freeze-dried polyacid powder is mixed with glass powder and is kept in the same container. In this case, the powder is mixed with water which dissolves the acid powder to form the liquid acid and initiate the acid-base reaction. A variety of other unsaturated carboxylic acids have been proposed over the last few decades including the copolymer of acrylic acid and itaconic acid [poly(AA-*co*-IA)], acrylic and maleic acid [poly(AA-*co*-MA)] and the copolymer of acrylic with methacrylic acid [70, 133, 134].

2.1.2 Developments in the polymer-liquid of GIC

Conventional GICs or RMGICs commercial systems may contain copolymers of PAA with either itaconic acid or maleic acid forming a more rigid polymer matrix [135]. There have been attempts to improve the glass-ionomer cement properties by exploring the new routes for PAA copolymer formation in which acid groups are made more available for salt-bridge formation. Various homopolymers or copolymers [poly(AA-*co*-IA), poly(AA-*co*-MA)] of unsaturated mono-, di- and tri-carboxylic acid have been employed in order to improve the polymer matrix as previously mentioned. However, very few studies on new ionic polymer systems were conducted until the early 1990s to explore new polymer systems.

Subsequently, the use of poly(vinylphosphonic acid) (PVA) in GICs was proposed by Eills and Wilson in 1991 [136]. They found that the cements based on PVA were far more reactive and hydrolytically stable than those based on polycarboxylic acid but the polymer was too acidic for its application in dentistry. Later, novel polyacid formulations were also developed by Kao *et al.* through the incorporation of amino acid-derived monomers with carboxylic acid [N-acryloylglutamic acid (AGA) and N-acryloyl-6-aminocaproic acid (AACA)-modified] [70]. Acrylic acid, itaconic acid, and amino acid monomers were combined in different proportions to make water soluble copolymers that produce a chemical-cured glass ionomer system with improved physical properties [69, 70]. The same research group proposed an amino acid modified acrylic acid copolymer *N*-vinylpyrrolidone (NVP) readily polymerized by a free radical polymerization that is also soluble in water [137, 138]. It was thought, that incorporation of a low amount of NVP in the backbone chain of PAA would result in improved properties of both conventional and light cure GICs. However, due to the increased viscosity of polymer solution, the working properties were compromised due to the strong chain entanglements formed in these high molecular weight (M_w) linear polyacids.[68]. More recently, Xie *et al.* developed a low viscosity, light-curable 4-arm star-shape poly(acrylic acid) system via an atom-transfer radical polymerization (ATRP) technique to formulate light curable GICs [139]. The use of this polymer in GICs resulted in significantly higher compressive and diametral tensile strength. The concept of combining the advantages of eugenol such as analgesic and anti-inflammatory properties, antimicrobial and anti-aggregating functions, antipyretic activity and anti-anaphylactic properties with GICs has been exploited in a recent study by Rojo *et al.* [140]. The acrylic derivative of eugenyl methacrylate (EgMA) was blended with PAA to form a water soluble copolymer [p(AA-co-EgMA)]. The cements formed with p(AA-co-EgMA) copolymer showed some therapeutic benefits but the improvement in physical properties of the eugenol-GIC systems was not demonstrated. A number of variations in the chemistry of GICs have been produced either to enhance the physical properties or extend the usage in clinical applications. For example, endodontic GICs were developed with the potential to have increased working, setting times and radio-opacity as well as advantages of high tissue tolerance and anti bacterial effects [141].

1.8 Classification of GICs

A number of classifications for cements have been suggested on the basis of their chemistry, application, setting reaction and additives. Wilson and Nicholson classified cements into three broad categories namely hydraulic, condensation and acid-base [132]. Hydraulic cements, for example, Portland cement and Plaster of Paris, are formed from two constituents one of which is water. On the other hand, in condensation cement, for instance silicate cements, the essential cement forming features are the loss of water and the condensation of two hydroxyl groups to form bridging oxygens [132] which can be represented by the following reaction:

$$\text{R-OH} \quad + \quad \text{HO-R} \quad \longrightarrow \quad \text{R-O-R} + H_2O$$

Finally, acid-base cements, such as GICs, involve the cement formation by both acid-base and hydration reaction [54]. In GICs, the reaction between the proton accepting glass powder and proton donating acidic liquid is generally considered to be the mechanism involved in the cements formation. The product of the reaction is a salt-like hydrogel which binds the unreacted powder particles into a cement mass [54] and the general reaction may be simplified as:

$$\underset{\text{basic oxide}}{MO} \quad + \quad \underset{\text{acidic liquid}}{H_2A} \quad \longrightarrow \quad \underset{\text{salt hydrogel}}{MA} \quad + \quad \underset{\text{water}}{H_2O}$$

Besides, GICs can be classified on the basis of their chemistry in the following five types namely: Conventional GICs, RMGICs, Hybrid Ionomer Cements (Dual-cured), Tri-cure Glass Ionomer Cements and Metal-reinforced Glass Ionomer Cements. Moreover, depending upon the desired clinical dental application, the glass-ionomer cements are classified in the following three types [4, 58]:

Type I: Luting and bonding materials are used according to the following specifications [4, 58]:

- For cementation of crowns, bridges, inlays, onlays and orthodontic appliances.
- Powder : liquid ratio is 1.5:1 up to 3.8:1 depending on the type of liquid used.
- Ultimate film thickness is about 20 microns maximum.
- Quick setting with early resistance to water uptake.

Type II.1: Restorative aesthetic materials are used in aesthetic applications with minimal occlusal load [4, 58]:

- Powder : liquid ratio (P/L) is 3:1 up to 6.8:1.
- Excellent shade range and translucency.
- Auto-cure cements, due to prolonged setting time, require immediate protection from moisture to avoid water uptake or loss.
- Resin-modified cements set immediately and do not need water protection.

Type II.2: Restorative materials are used where aesthetics are not a consideration but quick set and high physical properties are the requirements [4, 58]:

- Powder : liquid ratio ranges from 3:1 to 4:1.
- Fast set and early resistance to water uptake, susceptible to dehydration for two weeks after placement.

Type III: Lining and base cements can be used as lining or base in the cavities depending on the P/L ratio [4, 58]:

- For lining purposes, P/L used is 1.5:1
- For base cements purpose, P/L ratio is 3:1 up to 6.8:1 depending on the type of base.
- Physical properties improve as powder content increases.
- Can be auto-cure or resin modified.

1.9 Biological properties of GICs

One of the properties of GICs is that they release fluoride in the oral environment and recharge as well which renders them to an attractive choice as a dental restorative material. Therefore, the understanding of the biological effects of GICs on living hard and soft tissues are very important for their long term application in the human body. Some of the important biological properties of GICs are discussed bellow:

Biocompatibility: Biomaterials are intended to interact with biological systems and designed to be implanted in the body for the replacement of diseased or damaged tissues [33, 142, 143]. Biomaterials must be biocompatible. Biocompatibility is one of the most important requirements for a material which is potentially used in the human body at any site and in any form. In dental materials science, biocompatibility has evolved into a comprehensive, complex and interdisciplinary area of research. Several factors such as chemical composition, structure, degradability, site of application and inflammatory response may influence the biocompatibility of a material. Although, GICs are considered biocompatible but they may produce a greater pulp response than zinc oxide eugenol cements [33]. Freshly prepared GICs are mildly cytotoxic and their cytotoxicity further reduced with the passage of time. Pulpal biocompatibility may be affected by the weak nature of PAA, which is unable to penetrate the dentinal tubules due to very high molecular weight, so mild pulp reaction may be expected [144]. Heys *et al.* reported that the possibility of the pulpal reaction may increase if the permeability of dentine is increased due to the acid-etching procedure of the dentine [145] but GICs do not require such procedure. Moreover, due to the formation of the ion exchange adhesion layer at the interface of GICs and the enamel or dentine, there is a good biocompatibility and the pulp irritation is not common. Additionally, GICs also prevent from micro-leakages, bacterial invasion and introduction of bacterial toxin [146]. Although, dentine itself is a very good buffer against variation in pH levels, the dentine remineralisation process initiated by the formation of minerals from the release of ions from GICs increases the chances to retain the vitality of the tooth and ultimately helps the pulp to heal [2, 3, 38].

Internal Mineralization: This is a unique property of GICs as the inner structure of the tooth is benefited by the exchange of minerals [147]. Although this fact cannot be observed easily, it had been revealed in different studies when old GICs restoration were removed from the tooth due to any reason and high level of remineralisation was observed underneath [38, 148]. GICs play an important role by providing a nearly perfect seal and inhibit the ingress of bacteria or their products. Due to ion exchange adhesion with the tooth structure, GICs can be used without the fear of developing irreversible pulp inflammation and the affected demineralised dentine may be left under the GICs restoration [149].

Antibacterial efficacy: Different studies proved the antibacterial activity of GICs as these materials decrease bacterial penetration and increase physical exclusion of bacteria because of its fluoride releasing activity and low pH at initial stage [150, 151] or through the release of metal cations [152]. Several studies have shown that GICs have an antimicrobial and cariostatic effects. It was found that the plaque surrounding GIC restorations have significant low bacteria as compared to either composite or amalgam restoration [3, 153, 154]. However, the mechanism for this activity is not very clear and Meiers and Miller reported that inhibition of cariogenic bacteria may potentially encourage demineralization at tooth-restoration interferences [155].

Nonetheless, GICs are used in a variety of dental restoratives and preventive applications due to some of their versatile properties such as chemical adhesion to enamel and dentine, fluoride-release over a prolonged period of time and very insignificant change in volume during setting. These factors contribute to prevent the bacterial micro-leakage hence satisfactory adaptation to the tooth margins. Despite such biological advantages, GICs, have certain inappropriate mechanical properties such as low wear resistance and fracture toughness, and lesser control over moisture sensitivity that make their use in high load bearing areas questionable. Therefore, several attempts have been made to improve the mechanical properties and to make GICs more acceptable for posterior restorations with variable success [156-158]. However, successful clinical use of GICs, both as bone cements and as preformed implants for hard tissue replacement, have been reported in the fields of otologic surgery (Cochlear implant fixation, repair of the tympanic chain, eustation tube obliteration and as ear ossicles), and oral and reconstructive surgery [159].

1.10 Introduction of Characterisation Methods

There are three main steps in the study of the development of any material namely (a) preparation of materials (b) characterisation of the properties and (c) determination of the performance of the material for specific applications [160]. Many traditional techniques are used to achieve this goal. The preparation of materials involves processing methods to prepare the raw ingredients and actual specimen. For example, in case of GIC system the development of glass powder and polymer liquid are the key steps. The characterisation of nanoclays dispersion involve the structural analysis using a variety of X-ray techniques, spectroscopy and microscopy techniques while the property characterisation involved the mechanical testing of glass ionomer cements. Therefore, in the present study the potential of the dispersion of nanoclays to reinforce the polymer matrix was analysed in order to determine the eventual influence on the GICs properties. This section will deal with the introduction and the background of the chosen characterisation methodology.

X-ray diffraction (XRD) is a most commonly used method to characterise the degree of nano-dispersions and to measure the structure of layered silicates such as MMT nanoclays in a specific polymer. XRD is a non-destructive technique and does not require complex sample preparation. By using XRD it is possible to measure the spacing between the ordered crystalline layers of clay by using **Bragg's law: $\lambda=2d\sin\theta$** where d is the spacing between the atomic planes of a crystalline phase and λ is the wavelength of X-rays [161]. The intensity of the diffracted X-rays is measured as a function of the diffraction angle 2θ and the specimen's orientation. The Bragg's equation based on XRD patterns is generally used to detect the layer expansion of

MMT nanoclays and the information regarding the change in the "d" spacing (increase or decrease) can be used to determine the type of polymer nanocomposites formation (intercalated, delaminated or exfoliated etc.). The peaks in the XRD spectra are described by the Miller indices which is a notion system in crystallography for planes and direction in a crystal lattice as shown in Figure 1.4. The coordinates in square brackets such as [100], [001] and [101] denote a direction vector (in real space).

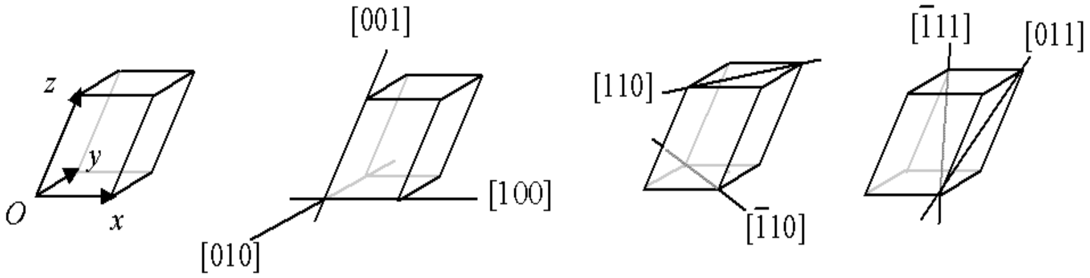

FIgure 1. 4: Miller indices of planes and direction vectors [162].

X-ray photoelectron spectroscopy (XPS) is a spectroscopic technique employed to perform the elemental analysis of a material in terms of its composition (top 1-10 nm usually) and chemical state [161]. XPS is a surface chemical-analysis technique based on the principle of photoemission and is used to analyze the surface chemistry of nanoclays treated with a PAA solution. A typical XPS spectrum is plotted by the number of electrons detected on the Y-axis versus the binding energy (eV) of the electrons detected on the X-axis. The binding energy of electrons (eV) can be determined by using the following equation:

$$E_{binding} = E_{kinetic} - E_{photon} \quad (EB= EK - hv)$$

where $E_{binding}$ is the energy of the electron emitted from one electron configuration within the atom, E_{photon} is the energy of the X-ray photons being used and $E_{kinetic}$ is the kinetic energy of the emitted electron as measured by the instrument [163].

XPS spectra were obtained by irradiating the specimen with a beam of X-rays while measuring the kinetic energy and number of electrons that escape from the top 1 to 10 nm of the specimen. XPS requires ultra-high vacuum conditions because electron counting detectors in XPS instruments are typically one meter away from the material being irradiated with X-rays.

Fourier transform infrared (FTIR) spectroscopy is used to identify chemical compounds present in nanoclays, PAA and PAA-nanoclay solutions formed by the dispersion of MMTs. The setting reaction of GICs after the dispersion of nanoclays can also be studied by this technique. FTIR is most useful for identifying both organic and inorganic elements and is based on the principle that molecules have specific wavenumbers or frequencies at which they rotate or vibrate corresponding to distinct energy levels (dipole moments) [164]. Generally, an FTIR spectrum shows the infrared intensity versus the wavelength (wavenumber) of light. An FTIR spectrometer obtains infrared spectra by first collecting an interferogram of a sample signal with an interferometer, which measures all of infrared frequencies simultaneously. The detected interferogram can not be directly interpreted. It has to be "decoded" with a well-known mathematical technique in terms of "Fourier Transformation". An OMNIC computer software can perform the Fourier transformation calculation and present a plot of absorbance versus wavenumber [165]. When infrared light interacts with the specimen, the chemical bonds will stretch, contract and bend resulting in adsorbance of infrared radiation in a specific wavenumber range regardless of the structure of the rest of the molecule. For example, in the case of PAA, the C=O stretching vibration of the carbonyl group appears at around 1705 cm-1.

The mechanical behaviour of a material is mainly related to the response to a force or load and this behaviour ultimately decides the usefulness of a material in a specific application. The mechanical tests and measurements to determine the properties of a material are usually carried out according to existing standards. International specification standards for materials in general and dental materials in specific, are dictated by the American Dental Association (ADA), the British Standards (BS), the Federation Dentaire Internationale (FDI), the American Society for Testing and Materials (ASTM) or the International Organisation for Standardisation (ISO). One of the main purposes of these standards is to provide the technical information with an impartial and reliable selection process for the materials used in the clinical dental practice. Certain claims for the materials quality arise from manufacturers as a result of a set of standard property tests either physical, chemical, biological or mechanical that lends them to duplication [33]. Therefore, the conventional test methods, employed by the manufacturers to assess standard mechanical properties such as compression strength (CS), tensile strength, flexural strength (FS), working characteristics, resistance to aqueous attack, wear, creep, modulus, biocompatibility, etc. must be performed under the specific test conditions designed to identify the safest and most effective materials for clinical performance [3].

Moreover, a comparison between dental materials testing can only be achieved if the protocol of specimen preparation and testing methodology occurs under these standard test conditions to produce a good reproducibility of results. Unfortunately, there are only few standards available which describe the mechanical testing parameters for dental filling materials, specifically, GICs and resin-based composites. Table 1.2 presents the main guidance for dental materials laboratory tests recommended by ISO.

The specification standard for acid-base cements (ISO 9917-1: 2007) describes the CS, working time and setting time specifications, the standard for light activated system (ISO 9917-2: 2000) describes FS, depth of cure, shade and colour stability, the ISO 10477-2004 provides standard specification for bond strength, FS and water sorption and the ISO 4049: 2000 describes the specification for FS, film thickness, depth of cure, working and setting time.

Table 1. 2: ISO specifications to perform mechanical testing for dental materials.

10271:2001	Dentistry–Water-based cements Part1:Powder/liquid acid-base cements
14569-1:2007	Dental materials – Guidance on testing of wear part 1: wear by tooth brushing
14569-2:2001	Dental materials – Guidance on tooth wear Part 2: Wear by two and/or three body contact
1559:1995	Dental materials – Alloys for dental amalgam
11245:2000	Dental restorations – Phosphate-bonded refractory die materials
11405:2003	Dental metallic materials- Corrosion test methods
9917-1:2007	Dental materials – Testing of adhesion to tooth structure
9917-2:2000	Dentistry-Dental water-based cements Part 2:Light-activated cements
7491:2000	Dental materials – Determination of colour stability
10477-2004	Dentistry – Polymer-based crown and bridge materials
4049:2000	Dentistry- Polymer-based filling, restorative and luting materials

Tribology; is the science of friction, wear and lubrication which deals with the interaction of contacting surfaces in relative motion [166]. Wear can be described as damage to a solid surface due to the relative motion between that surface and contacting substances. The wear behaviour of a material is dependent not only on the properties of the material but also on the contact conditions. Thus, the parameters used to characterise the wear of a material are considered as “system properties” of the materials, rather than the “intrinsic properties” such as elastic modulus or strength [163]. According to the American Society of Materials (ASM), there are a variety of parameters which may influence the wear mechanisms [166] as described in Table 1.3. Such parameters include, the material itself, the shape and contour of the antagonist, the surface roughness, the motion and frequency of motion, the loading rate, the lubrication, the local environment and lubrication. Furthermore, the traditional methods of classifications of wear are either based on the relative type of motion (reciprocating, rolling, impact oscillation and flow) or the mechanism of wear, such as adhesion, abrasion, attrition, surface fatigue and tribochemical [167].

The fundamental wear mechanisms which operative in the oral environment include abrasion, three-body abrasion, attrition, adhesion, fatigue and erosion wear [168]. However, these mechanisms rarely act in isolation and therefore the determination of the wear resistance of direct-restorative materials is a challenging task. The assessment of the *in-vivo* wear of dental restoratives has previously been conducted either by direct observation of the restoration at regular patient visits or by the indirect analysis of tooth replicas of the restoration [169, 170]. On the other hand, the i*n-vitro* wear resistance of restorative materials have been determined by pin-on-disc or ball-on-flat methods [171] and by employing several human oral simulator devices [172].

Table 1. 3: Effect of various parameters on the wear resistance (modified from the ASM handbook [166])

Material parameters	Composition, microstructure, mechanical properties (modulus, yield strength, ductility), fracture toughness, hardness, Poisson's ratio
Design parameters	Shape and type of antagonist, loading, force/impact level, type of motion, roughness, cycle time
Environmental parameters	Temperature, humidity, atmosphere, wet or dry condition, pH, contamination and so on
Lubrication parameters	Type of medium, presence of slurry, stability of slurry

In 1971, the United States Public Health Service (USPHS) was introduced a method to clinically assess the wear of filling materials. The USPHS technique was reported by Cvar and Ryge [173], in which two or more independent clinical observers directly evaluated the wear of the dental restorations at regular patient visits and rated the wear in accordance with a written criterion. Due to the limitation of the USPHS methods, Leinfelder *et al.* proposed an indirect analysis of tooth replicas technique which involved the comparison of the stone cast replicas of the teeth in 1986 [170]. However, the impression and cast stone materials are known to be susceptible to dimensional changes on setting which result in dimensional inaccuracy that is not desirable for wear measurements [3]. Later, the problems associated in order to assess the *in-vivo* wear of dental restoratives with the direct USPHS and indirect Leinfelder techniques, led to the development of a variety of devices to simulate the wear of restorative materials *in-vitro*. *In-vitro* wear test methods attempt to mimic the masticatory processes encountered in the oral environment. One of the main purposes of *in-vitro* wear simulators was to assess wear resistance of restorative materials prior to the placement in the oral environment in order to provide an initial indication about potential restorative materials. In the dental literature, the *in-vitro* wear assessment of restorative materials has been conducted using a number of machines which simulate a variety of different wear mechanisms. These wear testing machines include the IVOCLAR [174], the Zurich [175], the MTS [176], the Academic Centre for Dentistry Amsterdam (ACTA) [177], the Oregon Health & Science University (OH&SU) [178], the Dento-munch-robo-simulator [179] and the University of Alabama [180] wear simulators. Conversely, there is no internationally recognised standard for the *in-vitro* wear assessment of dental restoratives and it is assumed that lack of internationally recognised standards is due to the difficulties involved in simulating the complexity of the wear behaviour mechanisms operative in the oral environment. As a result, there is no single *in-vitro* wear machine currently available that can simulate all clinical wear mechanisms operative in the oral environment [168]. Therefore, considerable difficulties are associated in correlating both *in-vivo* and *in-vitro* wear studies on dental restoratives. Similarly, there are challenges associated with the interpretation of wear data of different *in-vitro* wear machines and even similar *in-vitro* wear machines in different test centres [172].

1.11 Nanocomposites

Composite is a wide term, which usually specifies a material with two or more constituents providing the synergistic properties leading to the better mechanical, thermal, optical, or even biological properties of the system [163]. Therefore, GICs are also considered composite materials that set by a neutralization (acid-base) reaction between fluoroalumino silicate glass and PAA aqueous medium. It is surprising that the vast majority of general dental practitioners consider the term “composite” as a resin-based dental composite material only and they do not include glass ionomer cements. However, in metallurgy and engineering terms a composite material is the material which is consisted of two or more constituent materials namely the matrix and the reinforcement.

Generally, polymeric nanocomposites are hybrid materials, products of an organic polymer and an inorganic layered silicate which reinforcing additives (clay silicates) have one or more of their dimension in nanoscale [181]. Hybrid organic-inorganic materials have shown superior mechanical properties when compared to conventional materials. The layered-silicates which are used in the fabrication of nanocomposites belong chemically to the family of 2:1 phyllosilicates which include mica, talc, montmorillonite and hectorite [182]. There are various applications of nanocomposites in the automotive industry because they are lightweight, gloss and fire resistant. Other applications are in food packaging, as biomedical materials and dental materials etc. are also emerging.The field of nanocomposites is one of the most popular in nanotechnology.

Several types of nanocomposites can be formed by adding either isodimentional fillers such as nano-powders, where all three dimensions are on a nanometer scale, or two-dimensional materials such as nano-rods, nano-wires or nanotubes. Polymer nanocomposites can be defined as two-phase systems where at least one dimension of the reinforcing filler is on nanometer scale and in case of layered silicate (nanoclay) polymers only the thickness is of the nanometer scale [183]. Polymeric materials have been reinforced with several macroscopic materials such as organic synthetic and/or natural compounds in order to improve several mechanical, thermal and barrier properties. However, the structural perfection in the above mentioned properties is more likely to be achieved if the reinforcing elements become smaller and smaller [184].

Dental nanocomposites (e.g., GICs reinforced with nanoclays), is a new class of filling materials which is derived from a highly refined form of nanoclays that may be dispersed in a polymer which is then mixed with an aluminosilicate powder to make a cement. The reinforcement of GICs with nanoclays has been developed more recently with some improvements in the mechanical properties as compared to conventional GI cements [14, 15]. Polymer grade (PG) nanoclays (PGV and PGN nanoclays) are high purity aluminosilicate minerals and are frequently used as additives to hydrophilic polymers such as polyvinylalcohols, polysassharides and PAA. In this study, the focus is on the design and synthesis of PAA-nanoclays (PAA-PGV and PAA-PGN) materials with layered silicate as the inorganic phase. This approach exploits the ability of PGV and PGN nanoclays for their potential intercalation and/or exfoliation in PAA and eventually to develop novel glass ionomer cements.

1.12 Structure and Properties of Montmorillonite (MMT)

The MMTs are members of the smectite clay family, which is generally known as 2:1 layered silicates or phyllosilicates. MMTs are generally referred as “nanoclays”, have a larger adsorption capacity due to the unique crystal structure and are widely used in the plastic industry for the reinforcement of polymers [185]. Nanoclays have a layered structure formed by tetrahedral silicate sheets which are linked to octahedral aluminium sheets through sharing of apical oxygens. The tetrahedral sheets contain mainly Si(IV) as the central atom, while the octahedral sites are occupied mostly by Al(III), Fe(III) or Mg(II) as shown in Figure 1.5. MMT clays have a sheet-type or plate-like structure with a thickness of only 1 nm, although the other dimensions (width and length) may vary from 30-1000 nm or even larger depending on the particular layered silicate.

Concerning the structure of nanoclays, if one tetrahedral sheet and one octahedral sheet are bonded together then the structure is called 1:1 layer silicate structure. Whereas, if the nanoclays are created from two tetrahedral sheets sandwiching an octahedral sheet is called 2:1 layer silicate [161] (Figure 1.5). Generally, two types of octahedral sheets occur in clay minerals: (a) dioctahedral type, where two-thirds of the octahedral sites are occupied mainly by trivalent central atoms such as Al(III) or Fe(III) and, (b) trioctahedral type, where most of the octahedral sites are occupied by the divalent central atoms for example Mg(II) or Fe(II) [186, 187]. Silica is the dominant constituent of MMTs with alumina being an other essential element of nanoclays. The crystal structure consists of layers made up of two tetrahedrally coordinated silicon atoms, which are fused to an edge-shared octahedral sheet of aluminium or magnesium hydroxide.

The tetrahedral silicate layer consists of SiO_4 groups which are linked together to form a hexagonal network of composition of Si_4O_{10}, whereas the alumina layer consists of two sheets of closely packed oxygens or hydroxyls. The two tetrahedral layers sandwich the octahedral layer by sharing their apex oxygen resulting to form "one clay sheet" that has a thickness of 0.96 nm (Figure 1.5). In the natural state Na^+ cations reside on the surface of MMTs and the chemical formula of the MMT clays can be presented as $Na_{1/3}(Al_{5}/_{3}Mg_{1//3})Si_4O_{10}(OH)_{2.}$ This structure of the layers leads to a Van-der-Waals space between the layers and the gap is called the interlayer space or clay gallery which can trap the polymer molecules during the nanocomposites formation [188].

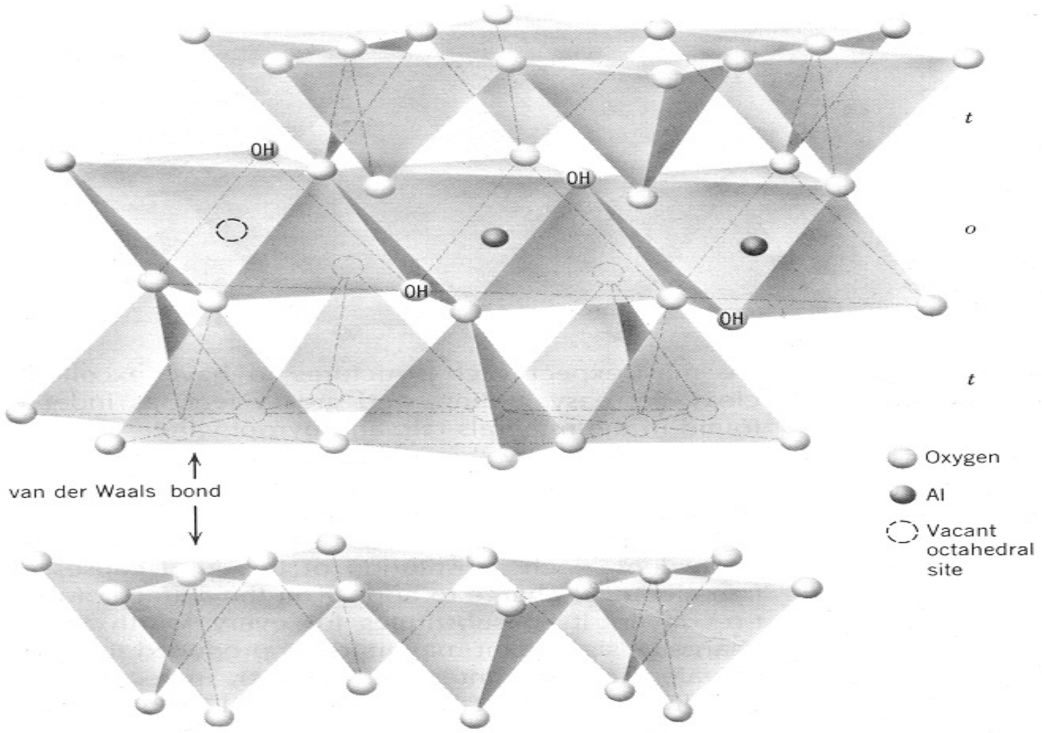

Figure 1. 5: The structure of montmorillonites (MMT). The crystalline layered nanoclays has a central alumina octahedral sheet which is sandwiched between two silica tetrahedral sheets [189].

The crystals of nanoclays carry a charge which arises from isomorphous substitutions of certain atoms in their structure for other atoms of a different valence. In the tetrahedral sheet, Si^{4+} may be replaced by trivalent cations (Al^{3+} or Fe^{3+}), or divalent cations (Mg^{2+} or Fe^{2+}) may replace Al^{3+} in the octahedral sheet (Figure 1.5). The exchanges of the ions result in charge deficiency and a negative potential at the surface of nanoclays is created, which is compensated by the adsorption of cations on the surface [190]. Cations and anions are also held at the crystal edges because the interruption of the crystal results in broken valence bonds. Moreover, in an aqueous solution, both sets of ions may exchange with ions in the bulk solution which are known as exchangeable cations.

The total amount of cations adsorbed on the surface of nanoclays is expressed in miliequivalents per hundred grams of dry clay and is called the cation exchange capacity (CEC). The description of the CEC of nanoclays used in present research is given in section 2.1.1. To achieve the optimum properties of nanocomposites, the degree of dispersion of nanoclays in a particular polymer matrix depends on the interlayer cations. Although, the isomorphic substitution within the clay layer and the surface treatment of the clay have led to the development of various types of commercial clays for different applications but, in polymeric nanocomposites, the ability of the silicate particles to disperse into individual layers through ion exchange reactions with organic and inorganic cations is considered to be important [191].

1.13 Types of nanocomposites

Polymer nanocomposites have been known for more than 50 years [192] but in the recent years polymer layered silicate nanocomposites have attracted great interest because they often exhibit remarkable improvement in materials properties when compared with conventional micro- and macro-composites. A wide range of inorganic materials, such as glass powder, glass fibres, talc, calcium carbonate, and clay minerals have been used as additives or reinforcement of polymers. Nanoclays have been used for a long time as catalysts, absorbent and rheological modifiers in the chemical and coating industries.

However, polymer-clay nanocomposites attracted most of the attention after the first report by researchers at Toyota in 1988 for their application in timing belt cover in which they proposed an improved method for producing nylon 6–clay nanocomposites by using in situ polymerization [188, 193]. The same group also developed some other nanocomposites and they reported that these polymer–clay nanocomposites exhibited superior strength, modulus, heat distortion temperature, water and gas barrier properties [194]. The success in the improvement of nanocomposite properties stimulated the intense research efforts world wide and the use of clays in nanocomposites has recently been increased because they are inexpensive and easily available. The reinforcement effect of nanoclay dispersion on polymers has largely been observed in epoxy resin [195], nylon [196], poly-styrene [197], poly-(methyl methacrylate) [198], poly-caprolactone [188], poly-ethylene [199], poly-urethanes [200], poly-imides [201, 202], and chitosan [203, 204], based composite systems over the past couple of decades.

Extensive amount of research is being carried out to understand the structure-chemical analysis of nanocomposites where small molecules of polymers may enter into clay galleries to increase the interlayer spaces. One of the methods to study the exfoliation of nanoclays is the mixing or treatment of nanoclays with polymers that usually results in the formation of exfoliated silicate nanoplates (Si-O-M) or silica (Si-O-Si), which are then incorporated into a polymer system or dispersed in a liquid phase to develop a nanocomposite. Moreover, the ionic or non-ionic character of a polymer determines the interactions with the clay particles because an ionic polymer produces electrostatic interactions whereas non-ionic polymers are adsorbed onto the surface of nanoclays simply by Van der Waals interactions [203].

The dispersion of layered silicates within polymers has been proven to be the successful approach to synthesize polymer layered-silicate (PLS) nanocomposites. However, the polymer-nanoclay interactions in nanocomposites can be influenced by the polymer concentration, molecular weight and hydrolyzing groups of the polymer; concentration of clay in nanocomposites, size and shape of nanoclay particles, their surface charge, aspect ratio, pH, and temperature of mixing system [205-208]. In the nanocomposites, the multilayer structure is well preserved allowing the calculation of the interlayer space between the silicate layers in order to determine the degree of nanoclay dispersion. The interaction of nanoclays with the polymer chains usually results in an increase of the interlayer spacing in comparison to the spacing of the nanoclay used which lead to a shift of the diffraction peaks towards lower angle values [209]. On the basis of the degree of exfoliation of nanoclays, the polymer-clay nanocomposites can be categorized in the following four groups:

(a) Conventional (unmixed) nanocomposites; If the polymer is unable to interact with nanoclays sheets then a phase separated composite is obtained which has the properties in the same range as the traditional micro-composites. In this type of composites, the nanoclay particles are present in their usual aggregated form [205].

(b) Intercalated nanocomposites; are formed when few polymer chain molecules penetrate inside the clay galleries resulting in the expansion of the ordered multilayers or sometime individual interlayered platelets of nanoclays. The lamellar structures of the clay remain intact in intercalated nanocomposites. In intercalated nanocomposites the d_{001} values are shifted towards lower 2θ values [207].

(c) Exfoliated nanocomposites; are obtained when individual 1nm thick nanoclay layers are separated and well dispersed throughout the polymer matrix. In exfoliated structures no more diffraction peaks are visible in the XRD spectra either because of the too much large spacing between the layers (exceeding 8 nm) or because nanocomposites are not present. To achieve a fully exfoliated structure in nanocomposites is very advantageous and is one of the main aims of nanocomposites formation because this leads to maximizing the polymer–clay interactions [210]. Usually, the clay content of an exfoliated nanocomposite is much lower than that of an intercalated nanocomposite.

(d) Highly-delaminated nanocomposites; this group lies between (b) and (c) and makes a distinction between the fully exfoliated and intercalated dispersion however, small stacks of about 2-20 layers of clays are well dispersed in the matrix [211].

However, it is sometimes challenging to distinguish between completely exfoliated and highly delaminated nanocomposites.

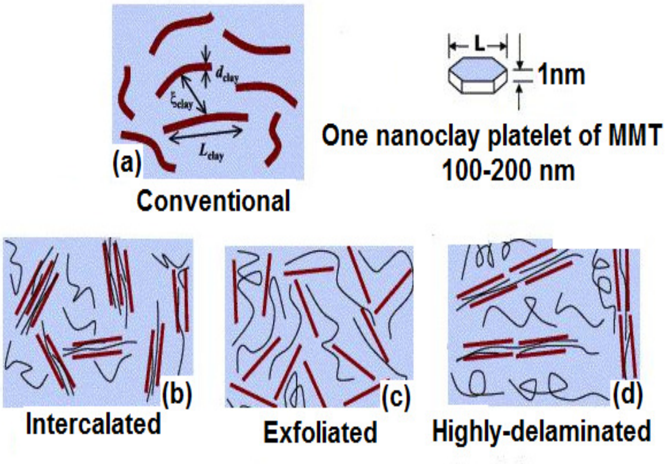

Figure 1. 6: Classification of dispersion of MMT's in polymer nanocomposites (Adapted from Sinha *et al.*) [206].

1.14 Preparation methods for nanocomposites formation

Several preparation methods have been considered for the preparation of polymer-layered silicate (PLS) nanocomposites. There are four main experimental methods that have been used to fabricate the polymer-clay nanocomposites, i.e. solvent mixing (solution blending), in situ polymerization, template synthesis and melt blending.

(i) Exfoliation-adsorption (Solvent Mixing or solution blending):

In this method nanoclays are exfoliated into single layers using a solvent in which a polymer is soluble (or a pre-polymer in case of an insoluble polymer). This method has been widely used with water soluble polymers such as PAA, poly(vinyl alcohol) and poly(ethylene oxide) to produce intercalated nanocomposites and it normally involves the use of a solvent (water, chloroform, toluenexylene or benzonitrile) to disperse nanoclays which is then mixed with the polymer solution [212, 213]. The silicate layers are easily separated in adequate solvent, and then the polymer is adsorbed on the delaminated sheets after the solvent is evaporated. In this method the intercalation only occurs for certain polymer-solvent pairs. Exfoliation-adsorption is a good method for the intercalation of polymers with little or no polarity into layered structures. The removal of the solvent results in a uniformed mixture of the polymer and nanoclays however, the dispersion and properties of nanocomposites depend largely on the intermolecular interactions, surface energies, solvent evaporation rate and shear mixing [11].

(ii) In situ polymerization:

In this method, the nanoclays are swollen within the liquid monomer or a monomer solution so that the polymer formation can occur between the intercalated sheets of the clay. The monomer is polymerized after the absorption into the interlayer space of the nanoclay by heat, a suitable initiator, or an organic initiator or catalyst [214].

(iii) Template synthesis:

This is a far less developed technique in which the polymer aids the nucleation and growth of the inorganic crystals and gets trapped within the layers as they grow [9].

(iv) Melt blending:

In this technique nanoclays are mixed with the polymer matrix in the molten state and no additional liquid is required. This is a more widely used technique to develop commercial nanocomposites because it is more versatile and least environmentally controversial than the above mentioned procedures. This manufacturing process involves annealing (statically or under shear) of the mixture of nanoclays with the polymer in the molten state above the softening point of the polymer and shear flow is obtained by using conventional compounding equipment to facilitate the mixing process and to control the alignment of the layers of the polymer and nanoclays [215]. If the chosen polymer is sufficiently compatible with the nanoclays, the polymer chains will move into the interlayer space and form either intercalated or exfoliated nanocomposites.

Finally, the preparation method to disperse the PGV and PGN nanoclays in PAA solution will be discussed in detail in section 2.1.2, briefly, PGV and PGN nanoclays were dispersed by using the first exfoliation-adsorption method.

1.15 Aims and Objectives

As a part of the broader effort to develop a mechanically superior GIC for use as restorative for the posterior dentition, the findings of the present study on the modification of poly(acrylic acid) with purified polymer grade (PG) montmorillonite; PGV and PGN are reported. Exfoliation of PGV and PGN clays within PAA is the first step towards the development of glass ionomer based dental nanocomposites which generally involves the interaction of silicate nano-plates of clays with the polymer matrix. The reinforcing effects of PGV and PGN nanoclays were characterized by, XRD, XPS, FTIR, ESEM, SEM and TEM to establish the interaction of PAA with PGV and PGN nanoclays. The micro-structure of nanoclays and their effect on the properties of PAA and glass ionomer dental restorative cements were also studied. The aim of the current study was to investigate the influence of the addition of nanoclays to the liquid constituents of experimental and conventional GI restorative systems at concentrations of 0.5 - 4.0 wt% in terms of their chemical and mechanical properties. The objective was to determine if the addition of nanoclays in the liquid portion (PAA) of conventional GI restoratives resulted in a reinforcing effect with better mechanical and wear behaviour of the novel glass ionomer clay nanocomposites. The findings of the current work may be useful to consider when the effect of the reinforcement of nanoclays will eventually be used to develop commercial products in the near future.

CHAPTER 2

2 MATERIALS AND METHODS

In the present work, clays or nanoclays, is a general name for layered silicate minerals including polymer-grade montmorillonites (PGV and PGN nanoclays). PAA-PGV and PAA-PGN suspensions were prepared by mechanically mixing of nanoclays and PAA solutions. PAA-nanoclays suspensions were heated continuously during the process of mechanical mixing. Nanoclays were also dispersed in the liquid portion of Fuji-IX system by the similar procedure. However, in HiFi system, nanoclays were initially dispersed in water followed by the addition of HiFi-PAA in nanoclay water mixture and stirred mechanically. The ultimate goal was to determine the performance of GICs after nanoclays dispersion for their potential applications in load bearing area.

2.1 Materials

Purified Nanomer or polymer-grade (PG) montmorillonites (PGV and PGN nanoclays) were generously supplied by Nanocor Inc. (Chicago IL, USA) through NRC Nordmann, Rassmann GmbH (Hamburg, Germany). Poly(acrylic acid) solution (PAA) [Sokalan PA-110, M_w ~ 110,000, water content 65 wt % and pH ~2] was provided by BASF plc, Cheshire, UK. PAA powder (PA) (M_w ~ 60,000 according to the manufacturer), LG26 experimental glass powder and HiFi glass powder (alumino-silicate) were obtained from Advanced Health Care Limited Kent, UK. Fuji-IX (GC co-operation Tokyo, Japan) batch number 0704281 used as a commercial reference dental restorative materials and P/L ratio was kept at 3.6 : 1 according to manufacturer's instructions.

2.1.1 Polymer Grade Montmorillonites (PGV and PGN nanoclay)

PGV nanoclays and PGN nanoclays have sheet or plate-like structure having thickness one nanometer (nm), although other dimensions (length and width) can be in hundreds of nanometers (Figure 1.5). The chemical composition analysis and physical properties of PGV and PGN used in the present work are given in Table 2.1. Both PGV and PGN were purified to a level greater than 98% montmorillonite by the manufacture.

Table 2. 1: Chemical Analysis Grade of PGV and PGN

Element	PGV	PGN
O	48.43	48.7
Na	4.01	3.21
Mg	2.97	1.65
Al	11.06	12.35
Si	29.82	29.65
P	0.03	0.03
S	0.12	0.06
K	0.15	0.04
Ca	0.19	0.20
Ti	0.20	0.10
Mn	0.02	0.02
Fe	3.00	3.99
TOTAL	100.00	100.00

Table 2.2 shows some of the physical and the chemical properties of nanoclays such as the degree of cations exchange capacity (CEC) in milli-equivalents and aspect ratio determined by the Nanocor. Various loading levels of PG nanoclays ranging from 0.5-25 wt % depending upon the degree of hydrogen bonding with the host polymer and

the requirement of the application have been reported [216]. In the current work, however, 0.5 - 8 wt % of nanoclays was mixed with PAA solutions to study the dispersion behaviour of nanoclays in PAA. The viscosity of PAA-PGV and PAA-PGN potentially increased when nanoclays content was more than 4.0 wt %. Therefore, 0.5 - 4.0 wt % of PGV and PGN nanoclays were used to disperse in aqueous polymer solutions to prepare GICs.

Table 2. 2: Physical Properties of the Purified Nanomers, PGV and PGN nanoclays.

PROPERTY	PGV	PGN
Colour	White	Off-white
CEC (meq/100g) ± 10%	145	120
Aspect Ratio	150-200	300-500
Specific Gravity	2.6	2.6
Maximum Moisture (%)	18%	12%
pH (5% dispersion)	9-10	9-10
Average Dry Particle Size (μ)	16-22	16-22

2.1.2 Preparation of PAA-nanoclay solution

Poly(acrylic acid) – PG nanoclays (PAA-PGV and PAA-PGN) solutions were formed by mixing and heating procedure similar to the exfoliation–adsorption method however, no solvent other than water was used for dispersion of nanoclay in PAA. Tran *et al.* [12, 13] previously reported the similar technique for the formation of PAA nanocomposites. This method involves the statically or under shear mixing of the polymer solution and nanoclays without employing any solvent. Initially, 0.25, 0.50, 1.0, 2.0, 3.0 and 4.0 grams of PGV and PGN nanoclays were weighed on a balance accurate to 0.01 g (TS4000, Ohaus, Pine Brook, NJ, USA) and added to 50 g of 65 % aqueous solution of PAA (PA-110). The initial hand-mixing was performed for three minutes using a glass-rod. The polymer solutions became light-yellow after nanoclays were preliminary mixed. Table 2.3 shows the description of polymer-nanoclay suspensions prepared at different nanoclays loading (0.5 - 8 wt %) in this study. PAA-PGV (D0.5VP-D8.0VP) suspension and PAA-PGN (D0.5NP-D8.0NP) suspension were then mechanically mixed by a mechanical-stirrer (IKA lab, Sweden) in a 100 ml round-bottomed, two necked flask along with a condenser fitted with cooling tubes was used as a reactor. PAA-PGV and PAA-PGN suspensions were heated on an isomantle at ~75-80 °C in a fume cupboard for 24 hours. After 24 hours, solutions were allowed to cool at room temperature. The solid residue was collected from the PAA-nanoclays suspensions via a centrifuge (J2-21M/E centrifuge Beckman, UK) at 18,000 rpm and 15 °C. The solid mass of nanoclays (PAA treated nanoclays) was obtained after centrifuge and then washed with water and dried in air prior to further characterization. Moreover, to study the effect of nanoclays dispersion at different temperatures on the properties of cements, the dispersion of nanoclays in Fuji-IX liquid (FL) was performed both at room temperature and at 75°C. The polymer solutions to prepare GICs cements were also made according to procedure mentioned above. The temperature variable was studied by mixing the Fuji-IX (L) with nanoclays both at room temperature (RT) and 75°C. To prepare the Fuji-IX liquid containing 2 wt % PGN and 2 wt % PGV nanoclays, 0.16 g of each PGV nanoclays and PGN nanoclays weighed on a balance accurate to 0.01 g and mixed with 8.0 g of Fuji-IX liquid for 24 hours to form the PAA-PGV and PAA-PGN solutions. 2 wt % PGV and 2 wt % PGN nanoclays were mixed in liquid portion of Fuji-IX in a plastic container, sealed with parafilm (Parafilm Pechinney Lastic Packaging Menasha WI, USA) to avoid the loss of water during the stirring process, on a hot plate (Stable Temp Cole-Parmer IL, USA) at 100 rmp using a magnetic-stirrer. The polymer solutions of Fuji-IX after the mixing of nanoclay were assigned the following specimen names; D2.0VF75, D2.0NF75, D2.0VFRT and D2.0NFRT (Table 2.3).

Final series of polymer solutions was formed using PGN nanoclays by dispersing via a different processing route. Distilled water at room temperature was used to form a suspension of PGN nanoclays with three different concentrations of PGN nanoclays (1.0 wt %, 2.0 wt % and 4.0 wt %). HiFi-PGN solutions were prepared by mixing PGN nanoclays in distilled water for 2 hours. After 2 hours, HiFi PAA powder was added slowly to aqueous solution of nanoclays. PAA-PGN solutions were obtained after mixing HiFi PAA powder and PGN solution. 1.0 wt %, 2.0 wt %, 4.0 wt % PGN nanoclays (0.10, 0.20 and 0.40 g) was mixed in 10 g of water for 2 hours using a magnetic stirrer in sealed plastic container on a hot plate (Stable Temp Cole-Parmer IL, USA) at 100 rmp at room temperature. The plastic container was sealed with plastic parafilm to avoid the loss of water during the stirring process.

Table 2. 3: Dispersion of polymer grade nanoclays in various PAA solutions.

Specimen ID	Clay wt %	Clay Type	Liquid	PAA Powder *** (P)	Mixing Temp [^{0}C]	Mixing Time [Hours]
D0.5PGV/PA-110 [D0.5VP]	0.5	PGV	PA-110 *	---	75-80	24
D1.0PGV/PA-110 [D1.0VP]	1.0	PGV	PA-110	--	75-80	24
D2.0PGV/PA-110 [D2.0VP]	2.0	PGV	PA-110	---	75-80	24
D4.0PGV/PA-110 [D4.0VP]	4.0	PGV	PA-110	---	75-80	24
D6.0PGV/PA-110 [D6.0VP]	6.0	PGV	PA-110	---	75-80	24
D8.0PGV/PA-110 [D8.0VP]	8.0	PGV	PA-110	---	75-80	24
D0.5PGN/PA-110 [D0.5NP]	0.5	PGN	PA-110	---	75-80	24
D1.0PGN/PA-110 [D1.0NP]	1.0	PGN	PA-110	---	75-80	24
D2.0PGN/PA-110 [D2.0NP]	2.0	PGN	PA-110	---	75-80	24
D4.0PGN/PA-110 [D4.0NP]	4.0	PGN	PA-110	---	75-80	24
D6.0PGN/PA-110 [D6.0NP]	6.0	PGN	PA-110	---	75-80	24
D8.0PGN/PA-110 [D8.0NP]	8.0	PGN	PA-110		75-80	24
Fuji-IX (L) [FL]	---	---	FL **	---	---	---
D2.0PGV/FL-75 [D2.0VF75]	2.0	PGV	FL	---	75	24
D2.0PGV/FL-RT [D2.0VFRT]	2.0	PGV	FL	---	RT	24
D2.0PGN/FL-75 [D2.0NF75]	2.0	PGN	FL	---	75	24
D2.0PGN/FL-RT [D2.0NFRT]	2.0	PGN	FL	---	RT	24
40%PAA-SOL [PA]	0	---	60% water	40% PAA	75	2+22
D1.0PGN/PAA [D1.0NPA]	1.0	PGN	59% water	40% PAA	75	2+22
D2.0PGN/PAA [D2.0NPA]	2.0	PGN	58% water	40% PAA	75	2+22
D4.0PGN/PAA *[D4.0NPA]*	4.0	PGN	56% water	40% PAA	75	2+22

[*] PA-110 solution was supplied by BASF. M_w was 110,000 with 40 % PAA contents

[**] Fuji-IX liquid (FL) was obtained GP Fuji-IX P/L system made by GC Cop, Japan.

[***] PAA (powder) supplied by AHC Ltd. to preapre 40 wt % PAA solution.

Further mixing of this solution after the addition of HiFi PAA powder (Advanced Health Care, UK) for 22 hours using a magnetic stirrer was preformed at a temperature of 75 °C. After 24hr of the mechanical mixing the solution was left overnight in the same sealed container to cool down and to prevent any loss of water. The schematic presentation of the PAA solutions prepared for this study is shown in detail in Table 2.3

2.1.3 Preparation of glass ionomer cements (GICs)

The details of the cement preparation for chemical evaluation are given in this section. Two groups of cements were form namely, Fuji-IX and HiFi by mixing the appropriated polymer liquid mentioned in section 2.1.2 and glass powder of either Fuji-IX or HiFi system. The details of both cement systems formation are give in Table 2.4. Glass ionomer cements of Fuji-IX system were prepared by hand mixing of the corresponding liquid phase with the Fuji-IX powder according the manufacturer recommended powder to liquid ratio, 3.6:1. The commercial Fuji IX GP cement was used as a control formulation. The powder component of the commercial GIC, Fuji-IX, was used as the basic glass in cement formulations by using the Fuji-IX liquid polymer solution obtained after nanoclay dispersion (Table 2.3). A plastic weighing boat was placed on a balance accurate to 0.01g (TS4000, Ohaus, Pine Brook, NJ, USA) to weigh 0.72 g of the Fuji IX powder, 0.20 g of an appropriate liquid according to the weight percentage was also measured on a mixing glass-slab, separately.

Table 2. 4: A detailed description of the glass ionomer cement formation of two GICs systems after the dispersion of PGV and PGN nanoclays in PAA liquid.

Cement Specimen ID		Liquid	Glass Powder	P/L ratio
Fuji-IX	CF-IX	FL	Fuji-IX (FP) ##	3.6:1
	C2.0VF75F	D2.0VF75	Fuji-IX (FP)	3.6:1
	C2.0VFRTF	D2.0VFRT	Fuji-IX (FP)	3.6:1
	C2.0NF75F	D2.0NF75	Fuji-IX (FP)	3.6:1
	C2.0NFRTF	D2.0NFRT	Fuji-IX (FP)	3.6:1
HiFi	CPA-HP	PA	HiFi (HP) ###	4.2:1
	C1.0NPAH	D1.0NPA	HiFi (HP)	4.2:1
	C2.0NPAH	D2.0NPA	HiFi (HP)	4.2:1
	C4.0NPAH	D4.0NPA	HiFi (HP)	4.2:1

Fuji-IX glass powder (FP) was obtained GP Fuji-IX P/L system made by GC Cooperation, Japan.

HiFi (HP) glass powder from HiFi system was supplied by Advanced Health Care

The powder was dispensed onto the other end of glass slab and was separated in two equal portions. During the mixing process, the first portion of glass-powder was mixed with the polymer liquid for 20s using the stainless steel spatula. After 20s the second powder portion was added to the cement mixture and it was spatulated for a further 20s so that the total mixing time was 40s. After the mixing, cements were subjected to the further characterization which will be discussed in section 2.2. Cement specimens for Fuji-IX systems were named as **CXXVF00F**, where **C** represents the cement followed by XX percentage of clays in liquid polymer, **FL** represents the Fuji-IX liquid, **00** represents whether the nanocomposites solution was prepared at room temperature or 75°C and **F** is the symbol of Fuji-IX powder (FP).

Similarly, glass ionomer cements of HiFi series were prepared using HiFi glass powder (Advanced Health Care. UK) and the corresponding liquid as mentioned in Table 2.4. HiFi cements were prepared by using a powder to liquid ratio of 4.2:1. A glass-slab and the stainless-steel spatula were used to mixing the cements at room temperature. A 0.82 g of HiFi glass-powder and 0.20 g of appropriate polymer liquid were measured by weight percentage on a weight balance accurate to 0.01 g. The HiFi glass powder was mixed with an appropriate polymer liquid in two equal increments, initially for 20s and the remaining powder was added to the mix and spatulated for a further 20s so that the total mixing time was 40s. The plastic mass of the cement was subjected to further characterization mentioned in section 2.2. HiFi cement specimens were named as **CXXNPAH,** where **C** represent the cement followed by XX percentage of clays in liquid polymer, **PA** represent the poly(acrylic acid) liquid and **H** is the symbol of HiFi powder (FP). The above mentioned cements were subjected to further characterisations which will be discussed in the next section.

2.2 Methods

2.2.1 X-ray Diffraction (XRD)

X-ray diffraction (XRD) was used to study the dispersion of nanoclay treated with poly(acrylic acid). XRD of the PGV nanoclays, PGN nanoclays and nanoclays specimens obtained after the centrifuge were carried out to determine the interlayer basal space from the position of the d_{001} peak in the XRD pattern. Bragg's law was employed to determine the interlayer spacing. Bragg's Law can be derived by considering the conditions necessary to make the phases of the beams coincided when the incident angle equals and reflecting angle. The rays of the incident beam are always in phase and are parallel up to the point at which the top beam strikes the top layer at atom z (Figure. 2.1). The second beam continues to the next layer where it is scattered by atom B. The second beam must travel the extra distance AB + BC if the two beams are to continue travelling adjacent and parallel. This extra distance must be an integral (n) multiple of the wavelength (λ) for the phases of the two beams to be the same therefore, nλ = AB +BC [163]. Recognizing “d” as the hypotenuse of the right triangle ABZ, trigonometry can be used to relate d and θ to the distance (AB + BC). The distance AB is opposite θ so AB = d sinθ. Because AB = BC in above equation so it becomes as nλ = 2AB. Substituting the AB derives the Bragg’s law:

$$n\lambda = 2d.\sin\ \theta$$

where, ***n*** is an integer determined by the order given, **λ** is the wavelength of X-ray, ***d*** is the spacing between the planes in the atomic lattice, and ***θ*** is the angle between the incident ray and the scattering planes.

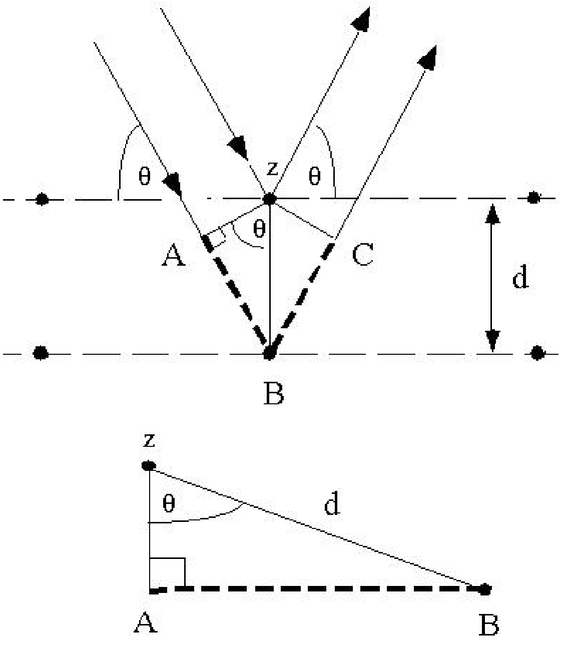

Figure 2. 1: A diagram showing the principle of the XRD technique [163].

In the present work, XRD characterization was carried out on the solid residues collected via a centrifuge at 15 °C and 18,000 rpm (J2-21M/E centrifuge Beckman, UK). The solids were washed with water and dried in air prior to the experiments. XRD analysis was conducted using a Philips analytical X-Pert XRD, at 40 kV and 40 mA using Cu Kα radiation with a wavelength of λ = 1.5418 Å. The diffraction data were recorded between 2θ angles of 2° and 30° at a step size of 0.014° and a count time of 1 sec/step.

2.2.2 X-ray photoelectron spectroscopy (XPS)

X-ray photoelectron spectroscopy (XPS) provides a quantitative analysis of the surface composition. XPS is a more sensitive elemental analysis technique which can determine the presence of element at the top < 10 nm surface of the specimen. Photoelectron spectroscopy utilise photo-ionization and energy dispersive analysis of the emitted photoelectrons to study the composition and electron state. It is a widely employed method to characterise the surface chemistry of polymer nanocomposites because the intensity of the peaks is related to the concentration of the elements within the sample region. XPS spectra of the solid reside of specimens collected after centrifuge were carried out using an Auger VG ESCALLAB 200i XL with a photoelectron spectrometer and a monochromated AlKα source (*hv*= 1486.6 eV). The spectra were acquired in the normal conditions with the photoelectron take-off axis perpendicular to the sample surface. For each and every element there is a characteristic binding energy associated with a specific atomic orbital and the presence of particular energy indicates the presence of specific element on the sample.

2.2.3 Fourier Transform Infrared (FTIR) Spectroscopy

The working principle of the FTIR is to find the absorption of energy in a wavelength or wavenumber to investigate the chemical structure of the material being tested. This technique is useful to study the chemical structure of the lower few microns of the sample in contact with the diamond attachment. FTIR spectra were collected using a mid-infra red source using a DTGS detector. XT-KBr beam-spliter was employed, the resolution was set at 4 cm^{-1} and the number of scans were fixed at 100. An infrared source in Transmission E.P.S mode having a velocity of 0.6329 m/sec^2 was used to collect the spectra. At room temperature, one drop of each control group polymer solution and the liquid suspension formed after the dispersion of nanoclay was placed on a brass ring of 10 mm of diameter positioned centrally on the Golden Gate Single Reflection Diamond ATR attachment of a Nicolet FTIR spectrometer (FT-Roman Module, MGNA-IR 860). FTIR spectra of the nanoclays and the glass powders were also collected by using the same machine. FTIR spectra of at least three samples of each group were collected to measure the data reproducibility. Furthermore, the setting reaction of the control cement groups (Fuji-IX, CPA-HP) and cements formed after the dispersion of 2 % of nanoclay (C2.0VF75F, C2.0NPAH) was studied using FTIR. The cements were prepared by spatulating the powder and the liquid portion according to the mixing ratio mentioned in section 2.1.3. Plastic mass of cement was placed on the Diamond ATR attachment of FTIR spectrometer at 1 minute after the start of mixing. After three minutes of the start of the mixing, the cement mass was surrounded by a wit tissue paper to prevent dislocation by dehydration and to reproduce the humid oral environment. Series spectra were collected for one hour since one minute after the start of mixing. At least two cement samples of each GIC groups were analysed to access the data reproducibility of the setting reaction

2.2.4 Molecular Weight Measurement

The conventional Gel Permeation Chromatography (GPC) method was employed at Rapra Technology Limited (Shrewsbury, UK) to determined Molecular weight of the polymer used in the present study. The number-average molecular weight (M_n), the weight-average molecular weight (M_w) and polydispersity (M_w/M_n) of polymers can be generally measured by employing GPC (size exclusion chromatography). GPC is a very valuable analytical technique for polymers ranging from low to high molecular weight. GPC is conducted almost exclusively in chromatography columns to determine the relative molecular weight of a polymer sample as well as the distribution of molecular weights. The samples for GPC are dissolved in appropriate organic solvents and after filtering the solution it is injected onto a column. The multiple detectors may be used to gain additional information about the polymer sample. Gels are used as stationary phase for GPC and the pore size of a gel must be carefully controlled in order to be able to apply the gel to a given separation [217]. Moreover, the significance of weight and number-average molecular weight is very important. The quantity of Mw is always higher than M_n except for a mono-disperse system. The polydispersity is the ratio of the weight to the number-average molecular weight (M_w/M_n) and is a measure of the breadth of the molecular weight distribution. Polydispersity is also a measure of the distribution of molecular mass of a polymer sample. M_w is particularly sensitive to the presence of high-molecular-weight species, whereas M_n is influenced by the species at the lower end of the molecular weight distribution. The distribution of chain lengths and degree of polymerisation of polymers can be illustrated by plotting the weight of polymer of a given molecular weight against the molecular weight as shown in Figure 2.2 [217].

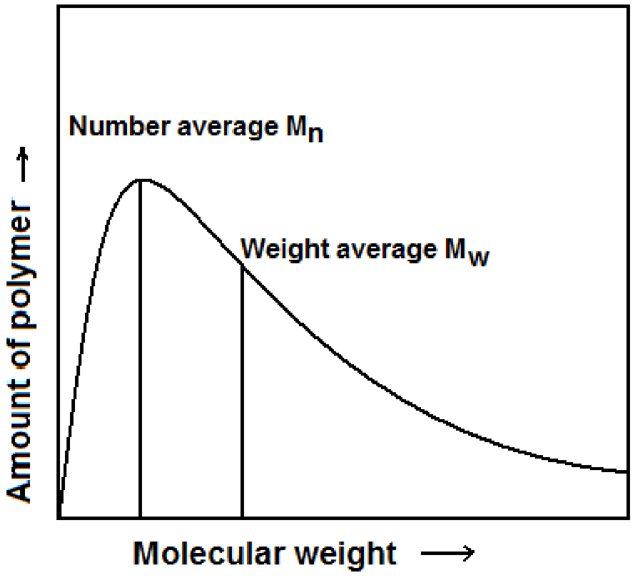

Figure 2. 2: Distribution of molecular weight in a typical polymer [217].

M_w analysis of a commercial polymer solution (Fuji-IX) and polymer powder (HiFi PA) were studied using Vicotek TDA 301 (Column Oven and Detector System with associated Pump and Auto-sampler) at 30 °C and at a flow rate of 1.0 ml/min. GPC utilized the static light scattering method according to the refractive index of PAA to determine M_w. Solutions for GPC analysis were prepared by dissolving 50 mg samples in 10 ml of eluent (0.2M $NaNO_3$, 0.01M NaH_2PO_4 pH~7). All solutions were left overnight to dissolve and were then filtered through 0.45μm PVDF membrane prior to chromatography. The data was collected and analysed using Polymer Laboratories "Cirrus" software. Billmeyer reported that in the presence of added salt, correct molecular weight of polyelectrolytes can be measured by membrane osmometry. GPC provides a more convenient method of determining the molecular weights of polymers and most samples can be thoroughly analyzed in an hour or less. However, one of the disadvantages of GPC is the pre-filtration of the sample, having the possibility of removing higher molecular weight sample before it can be loaded on the column [218].

2.2.5 Rheology of cements (Setting time and Working time)

The working and setting times of the cements described in the section 2.1.3 were determined by Wilson's Oscillating Rheometre. The oscillating rheometre is a simple but crude instrument and the actual measurement of this kit is a complex mixture of the dynamic viscosity and the storage modulus of the materials as well as the spring constant of the rheometre [31, 219]. The oscillating rheometre of Wilson gives more information and better measure of working time than indentation test therefore, the working and setting times of the cements were determined using a "modified Wilson's oscillating" rheometre shown in Figure 2.3. The oscillating rheometre consists of two aluminium platens having 0.50 mm deep groves to hold the plastic cement mass. The lower platen oscillates continuously by means of the spring coil attached to it. The platens maintained at room temperature to measure the working and setting time of the cements.

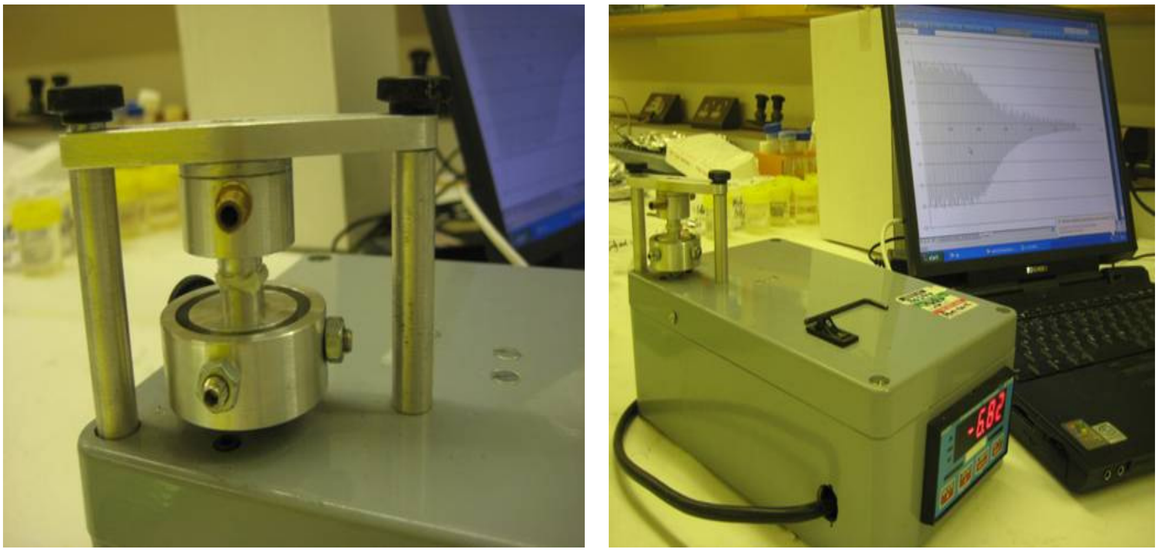

Figure 2. 3: The custom made Wilson's Oscillating Rheometre used in the present study.

The powder and liquid were weight to an accuracy of ± 0.01 g prior to mixing and the cement specimens were prepared according the ratios mentioned in Table 2.1. Setting and working times were determined for the specimens in both cement groups (Fuji-IX and HiFi) described in Table 2.4. After the end of cement mixing, the plastic mass of the cement was placed onto lower platen and the upper platen was positioned on top and was secured screw so that the distance between the two platens was 1mm. the working and setting times were calculated by mean of a software programme (RDP Electronics Limited Wolverhampton, UK using MS excel manual for the 650 and E725 modules) soon the mixing was initiated. As the setting reaction proceeded, the viscosity increases which impend the oscillatory motion of the lower platen. The changes in the oscillatory motion of the lower platen were recorded on an excel chart. The working time was taken at which the amplitude of oscillation reached at 95% of initial (maximum) value. Whereas, the setting time was taken at 5 % of initial value [31]. At least two traces were recorded for each cement specimen. The trace of the amplitude of the oscillation was recorded and the working and setting times of the materials were determined. Figure 2.4 illustrates a typical rheometre trace obtained in the current study of glass-ionomer cement showing the working time, 95% of the full-scale deflection (FSD) of the amplitude and the setting time of cements, 5 % of FSD.

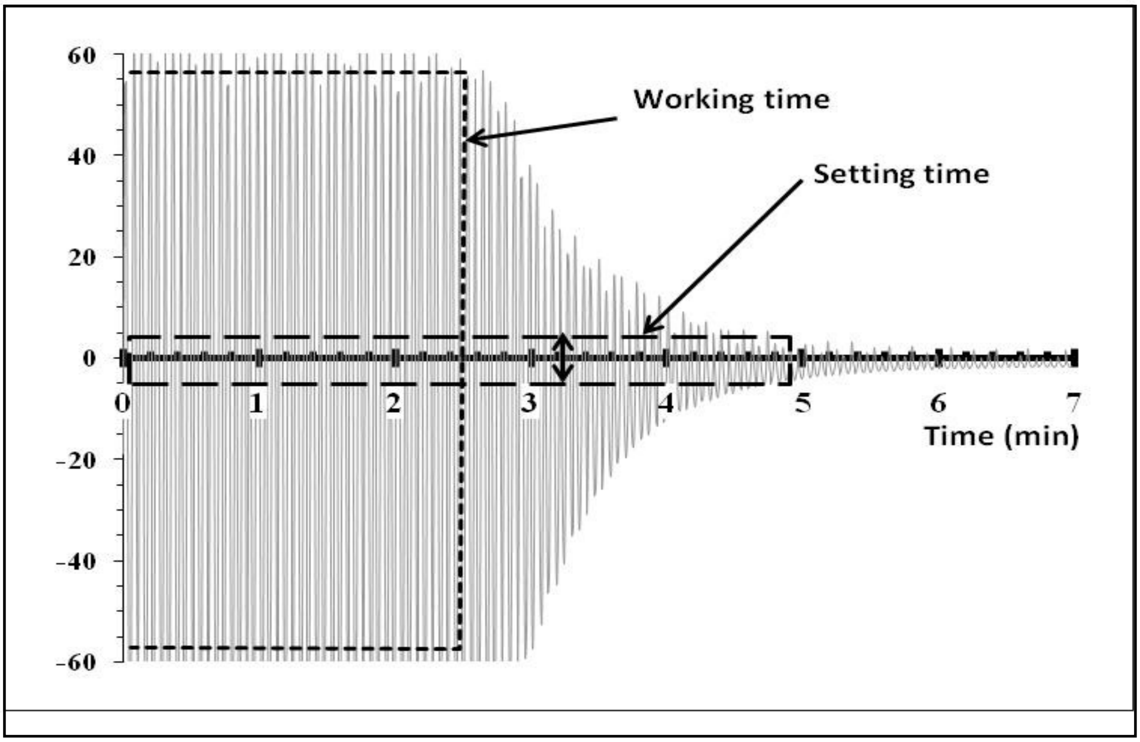

Figure 2. 4: Schematic presentation working time and setting time of a typical GIC trace obtained form Wilson's Oscillating Rheometre.

2.2.6 Mechanical Properties

Cement specimens of the Fuji-IX system were prepared with a P/L ratio of 3.6:1 according to the manufacturer's instructions to determine the various mechanical properties. Likewise, HiFi cement specimens were also prepared with a P/L of 4.2:1. The mechanical properties evaluated for the cements during the current work are descried below.

2.2.6.1 Compressive Strength (CS)

The CS of the cements was determined according to the protocol mentioned in British Standard ISO 9917-1:2007 for Dentistry - water-based cements - Part 1: Powder/liquid acid-base cements [220]. A split brass mould which can take up to 12 specimens was machined. The mould has internal dimensions of 6.0 ± 0.1 mm in height and 4.0 ± 0.1 mm diameter. A PTFE dry-film spray (PR Mould release RS-7 Rocol Leed, UK) was applied to the brass mould to prevent the adhesion of cements. The cements were prepared according to the P/L ratio mentioned in section 2.1.3 and Table 2.4. The cements were packed inside the split mould to a slight excess and were pressed with a stainless-steel spatula to avoid any air trapping. Meticulous attention was observed to pack the cements within the 60 seconds of the end of mixing. The split mould was squeezed together and any bulk extruded cement was removed. The top and the bottom surfaces of the split mould were also covered with an acetate sheet after inserting the cement. A glass slab was placed over the top surface of the mould which was then tightened using a C-shaped screw clamp. The whole assembly was transferred to a desiccator which was maintained at 37.5 ± 1 °C and 95% humidity no later than 120 seconds after the end of mixing. One hour after the end of mixing the mould assembly was taken out from the desiccator and the end of the specimens were polished flat at right angle to its long axis. A wet 800 grade silicon carbide paper followed by 1200 silicon carbide paper was used for this purpose. The specimens were removed from the mould immediately after surfacing. After removing from the mould, the specimens were checked visually for any air-voids or chipped edges and the defective specimens were discarded. Immediately after the preparation, the samples were immersed and stored in a sealed glass container containing distilled water for 1 hr, 1 day, 1 week and 1 month and was kept in the water-bath maintained at 37.5 ± 1.0 °C. The 20 samples of each cement specimen were tested at 1hr, 1 day, 1 week and 1 month. The compression testing of specimens was performed on a screw-driven Instron machine (Model 5566, Instron Corporation, High Wycombe, UK) with a cross-head speed of 1 mm.min^{-1} and 5 KN load cell. A sheet of damp filter paper (Whatman No 1) was placed to both top and bottom surfaces of the attachments of machine in the area contacted the sample. The CS was calculated in MPa from the following equation:

$$CS = 4P / \pi d^2$$

where, *P* is the maximum force applied at fracture and *d* is the diameter of the sample cylinder in mm.

2.2.6.2 Diametral-Tensile Strength (DTS)

The diametral-tensile strength (DTS) of cements was evaluated according the test method reported in literature [3, 33]. The DTS test is also called diametral compression test for tension or indirect tension. A split brass mould was machined having internal dimensions, 2.0 ± 0.1 mm height and 4.0 ± 0.1 mm diameter. The disk shaped samples of cements were prepared according to the P/L ratios mentioned in section 2.1.3. A PTFE mould-releasing agent was applied to the brass mould. The protocol to mix the cement, to prepare and to condition the disk-shaped DTS samples was kept the same as described for CS in section 2.2.6.1. A screw-driven Instron-extra (Model 4467 Instron Corporation, High Wycombe, UK) with a 1 KN load cell at a cross-head speed of 1 mm min^{-1} to compress samples diametrically, to introduce tensile stress in the material in the plane of force application (Figure 2.5). The 20 samples of each cement group were tested for DTS at 1 hours, 1 day, 1 week and 1 month. DTS was calculated in MPa from the equation:

$$DTS = 2P / \pi DT$$

where, *P* is the maximum load applied, *D* is the diameter of the disk and *T* is the thickness of the disk.

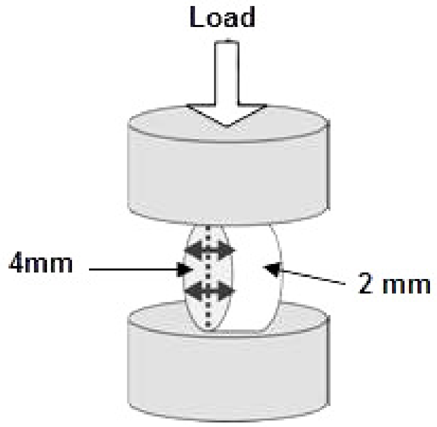

Figure 2. 5: An illustration of the DTS test method.

2.2.6.3 Flexural Strength (FS):

Flexural Strength (FS) is the ability of a material to bend before it breaks and it is obtained when the ultimate flexibility of one material is achieved before its proportional limit [3, 36]. The FS of the cements was calculated according to the procedure mentioned in British Standard ISO 4049:2000 [221]. A split brass mould was fabricated for the preparation of test specimens (25 ± 2) mm in length ×(2.0 ± 0.1) mm in height ×(2.0 ± 0.1) mm width (Figure 2.6). 15 bar-shaped samples of cements (M-U) were prepared according to P/L ratio mentioned in CS test samples fabrication method were tested for FS after 1hours, 1 day, 1 week and 1 month. A screw-driven Instron-extra (Model 4467 Instron Corporation, High Wycombe, UK) at a cross-head speed of 1 mm min^{-1} and 1 KN load cell was used to fracture the bar-shaped samples. Samples were placed on two supports and a load was applied at the centre; this test method is also known as three-point bending test. FS was calculated by the following formula:

$$\sigma = 3Fl / 2bh^2$$

where, F is the ultimate load at fracture, l is the distance between the two supports, b is the width and h is the height of the bar shaped sample.

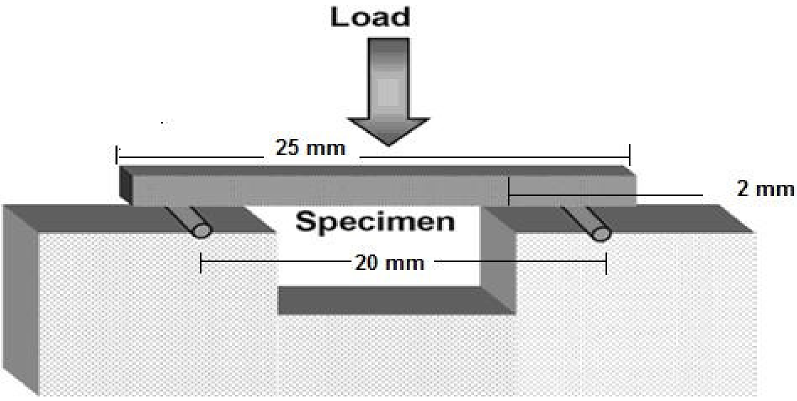

Figure 2. 6: Schematic representation of a three-point FS test method.

2.2.6.4 Flexural Modulus (E_f)

The flexural Modulus is the ratio, within the elastic limit, of stress to corresponding strain [33]. E_f is an intrinsic property of a material which was calculated from three-point bend test FS data according to the ASTM standard D 790-07 [222]. The three-point bending test provides the values for the modulus of elasticity in bending, flexural stress, flexural strain and the flexural stress-strain response of a material. The flexural Modulus was calculated by drawing a tangent to the steepest initial straight-line portion of the load-deflection curve and calculated by using the following formula:

$$E_f = \frac{l^3 m}{4bd^3}$$

where, E_f is the modulus of elasticity in bending in MPa, l is the distance between the two supports, m is the slope of the tangent to the initial straight-line portion of the load-deflection curve N/mm of deflection, *b* is the width of beam in mm and *d* is the depth (height) in mm of the bar shaped sample.

A typical stress-strain graph obtained from the three-point bending test is shown in Figure 2.7 which describes the modulus (E) as the initial straight portion of the curve after the toe region. In this typical stress-strain curve there is a toe region that does not represent a property of the material and this defect may have been caused by the padding used to keep the specimen wet while the test was in progress. In order to obtain the correct values of modulus, this artefact was ignored and the next immediate available point was chosen to draw the slope of stress-deflection curve.

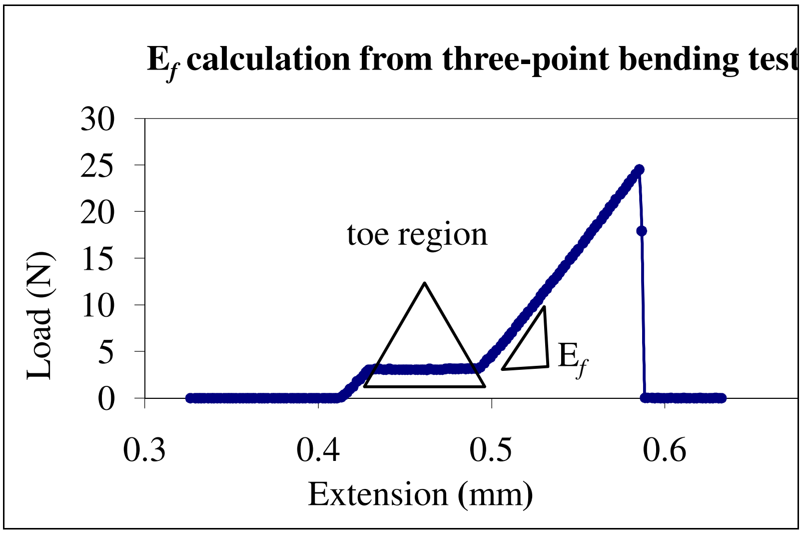

Figure 2. 7: Stress-Strain curve of a GIC cement specimen obtained from the three-point bending test showing E_f and the Hookean region.

2.2.6.5 Vickers Hardness (HV)

Vickers hardness (HV) test method consists of indenting the GICs with a diamond indenter, in the form of right pyramid with a square base and an angle of 136 degree between opposite faces. Hardness test was carried out using a Micro-indentor (MVK-

H1 Mitutoyo, UK) hardness tester with a Vickers diamond indenter. The polished cement specimens were tested in accordance with ASTM standard C1327-08 [223]. The surface of the specimens was wet-ground with 800 and 1200-grit silicon carbide paper at room temperature before the test. A load of 300 N was applied for 10 seconds. A diamond Vickers indenter creates a square impression from which two surface-projected diagonal lengths were measured using an optical microscope (Mitutoyo, UK) and average was calculated. At least three samples were tested for each GIC and each sample was indented three times and a mean hardness value was obtained.

2.2.7 Wear

Wear studies of GICs were performed by employing two different wear test methods namely, reciprocating wear test and OH&SU wear simulator. The details of each test method are given below in the following sections.

2.2.7.1 Reciprocating Wear test

A reciprocating tribometer was used to determine the sliding wear resistance of the cements in accordance with ASTM standard G133-05 [224]. Figure 2.8 shows the schematic arrangement for a reciprocating ball-on-flat wear test machine. The alumina ball (Spheric Trafalger Limited Sussex, UK) of 12.5 mm diameter having an average surface roughness (Ra) of about 0.01 μm was used as an antagonist. Alumina ball was tightly mounted in a steel holder to prevent slippage during the test. Prior to the each wear tests the alumina ball was cleaned in acetone and rinsed in distilled water. Before wear testing, the rectangular shaped cement specimen was prepared using a split brass mould (10 × 5 × 2) mm and stored in distilled water maintained at 37 °C according to the protocol mentioned in section 2.1.3. After 23 hours of the start of mixing, GICs samples were removed from water and were attached to a 10 × 3 mm custom made aluminium disk. The flat cement specimens were attached to the aluminium disks were secured with super-glue to the base of machine to prevent slippage or buckling during the test. The top surfaces of the cement samples were wet-ground with the 800 and 1200-grit silicon carbide paper at room temperature using water as lubricant.

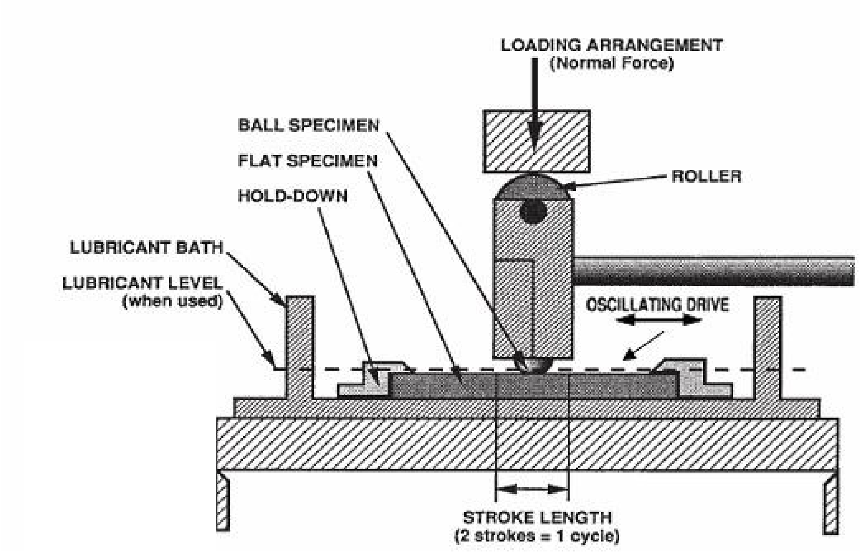

Figure 2. 8: Schematic representation of a reciprocating wear test machine (adapted from ASTM standard G133-05)

The reciprocating wear tests were repeated three times for three different rectangular shape specimens of each cement group. A 20 N load (equivalent to the light biting force of human applied) was applied [225] and a provision was made for applying the uniform force to the contact between the alumina ball and the flat cement specimen. The sliding stroke length was 6 mm and frequency was set at 1 Hz. A total number of 10,000 cycles were repeated while the test was conducted in the distilled water at room temperature. The spherical tip of alumina ball slides back and forth across the surface of a polished flat cement specimen to produce a wear facet. The area across the wear scar profile was measured by a surface roughness measuring stylus profilometer (Surf-corder, Mitutoyo, UK). The wear area was calculated using Microcal Origin version 6.0 analytical software (Northampton, MA USA) by integrating the area across the wear scar profile measured by a stylus profilometer, and then multiplying by the circumference length of the track. Post wear examination of wear track was conducted using SEM and an optical microscope.

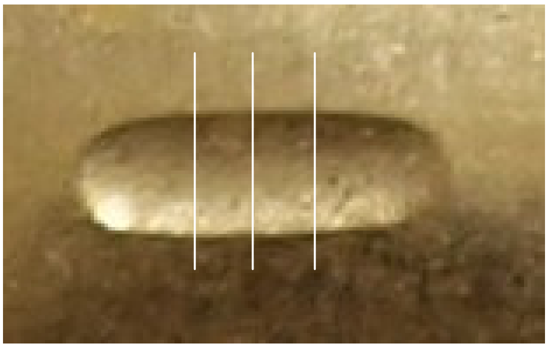

Figure 2. 9: Wear facet produced by the reciprocating wear test method. The white lines represent three estimated position of the scans measured by stylus profilometer.

Three/Four measurements were performed for each wear track and the average value was used to calculate wear area (Figure 2.9). The employed volume measurement procedure is the most common and direct method for wear calculation and does not require complicated mathematical expressions or simplifying assumptions [166]. The wear volume was determined by multiplying the wear area and length of the wear track which is expressed as volume loss per unit sliding distance per unit contacting load. Post wear examination of wear track was conducted using SEM and an optical microscope. Following equation was used according to the above mentioned ASTM standard to compute the sliding distance or number of cycles [224]:

$$X = 0.002 \times t \times f \times L \qquad \text{or} \qquad N = t \times f$$

where, X is sliding distance of ball in meters, N is number of cycles of test, t time in seconds, f is oscillating frequency Hz (cycles/sec) and L is length of stroke in mm.

2.2.7.2 OH&SU wear simulator test

The *in-vitro* wear resistance measurement was carried out by Oregon Health & Science University (OH&SU) four chamber oral wear simulator. OH&SU wear simulator produces an abrasion and attrition wear simultaneously in the presence of food-like slurry [178]. The steatite antagonists (Union Process Inc., Akron, OH, USA) is a ceramic material consisting of magnesium silicate which has wear characteristics similar to that of enamel when opposing dental restorative materials [226].

The wear regime of the OH&SU oral wear simulator forces the steatite antagonist into contact with the specimen through the food-like slurry and applies a 20 N sliding abrasion force to the surface along a 7 mm linear path. At the end of the 7 mm linear sliding path a direct static 90 N force is applied to each specimen to simulate attrition wear [227]. The steatite antagonist was raised at the end of each wear cycle and returns to the start of the 7 mm path and the wear regime is repeated for the required number of wear cycles. The 5.0 ± 0.1 mm diameter steatite antagonists were fixed to nylon screws (Radionics Ltd., Dublin, Ireland) using a light cured resin-based composite (Grandio; Voco GmbH, Cuxhaven, Germany). The height of the antagonist was adjusted using a custom made jig so that the head of the antagonist was positioned 1 mm above the disc-shaped specimens prior to wear testing (Figure 2.10).

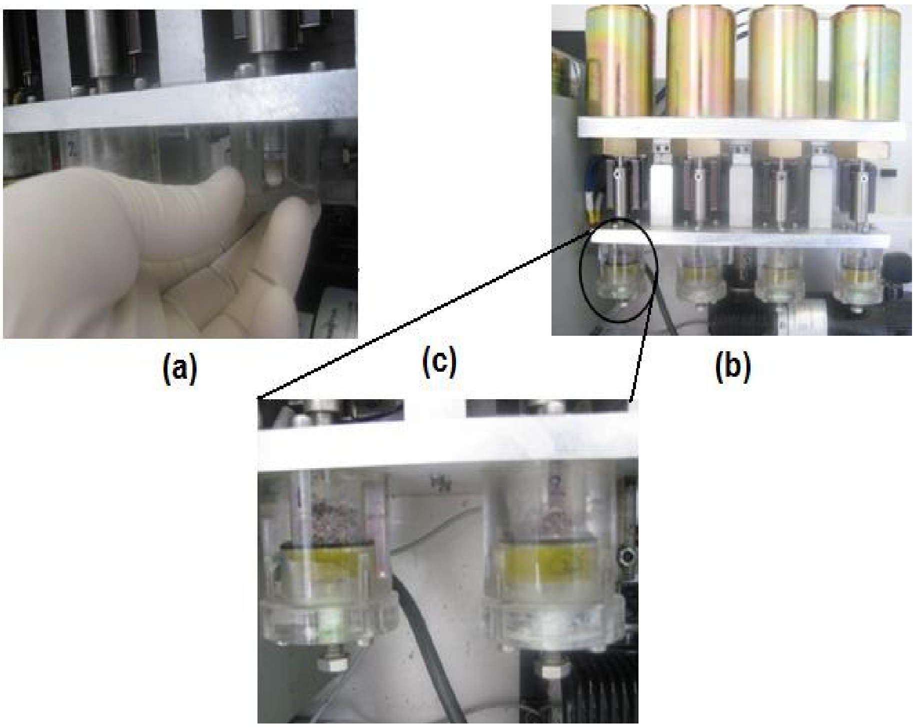

Figure 2. 10: OH&SU oral wear simulator; (a) adjustment of the height of antagonist with custom-made jig and (b, c) chambers containing embedded GICs specimen, slurry and antagonist.

Disc-shaped specimens (12.5 ± 0.1 mm diameter and 2.0 ± 0.1 mm thickness) were prepared from the teflon vestals mould according to the cement mixing protocol mentioned above in section 2.1.3 and stored in the ionized water for 1hr. The specimens were removed from the mould 1hr after the start of mixing and stored in distilled water at 37 ± 1 °C in an incubator for a further 22hr followed by the resin mounting using a two part cold-setting acrylic resin (Varidur; Beuhler, Lake Bluff, IL, USA) with a P/L ratio 2:1 to produce cylinders (25.0 ± 0.1mm diameter and 10.0 ± 0.1mm height) compatible with the chambers of the wear testing apparatus. Beta grinder-polisher machine (Beuhler, Lake Bluff, IL, USA) with P600 SiC and P1200

SiC abrasive paper was used to provide a reproducible surface finish for wear testing as recommended by original investigator [178].

The embedded disc-shaped specimens were secured into individual wear chambers and attached to the OH&SU oral wear simulator (Figure 2.10). To simulate three-body wear food-like slurry which consisted of 1 g of poppy seeds (Holland and Barrett, Burton-upon-Trent, England), 0.5 g of PMMA beads with a mean particle size of 50-100 µm (Special Tray; Dentsply DeTrey, Kanstanz, Germany) and 5ml of distilled water was placed into each wear chamber prior to the commencement of testing (Figure 2.11). The slurry has been reported in literature over 20 years ago to produce wear rates for a variety of dental restorative materials [228]. Each specimen was subjected to 50,000 wear cycles at a frequency of 1Hz which was equivalent to six months wear in the oral environment [178].

The OH&SU oral wear simulator produced a tear drop wear facet on the surface of each disc-shaped specimen which contained two regions, abrasion wear and attrition wear [178]. The tear-drop shaped wear facets were scanned using a non-contact optical profilometer (Talysurf CLI 2000; Taylor-Hobson Precision, Leicester, England) shown in Figure 2.10. The optical profilometer utilised a 3 mm range chromatic length aberration gauge with a resolution of 0.1µm (z-axis) when scanning at a speed of 2 mm/sec. A series of horizontal traces (perpendicular to the sliding direction of the OH&SU wear simulator) were conducted across the wear facet at 4µm intervals (y-axis) with longitudinal measurements (parallel to the sliding direction of the OH&SU wear simulator) taken at 4µm intervals (x-axis) and a detailed three-dimensional representation of the tear drop wear facet was generated using the TalyMap analysis software package (Taylor-Hobson Precision, Leicester, England).

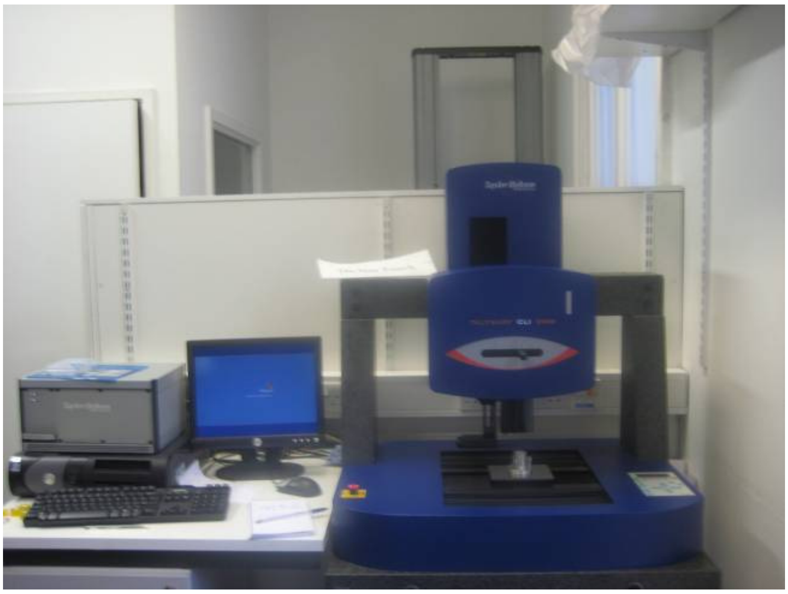

Figure 2. 11: The non-contact optical profilometer used in this work (Talysurf, Leicester England)

2.2.8 Statistical Analysis

Statistical analysis of raw data was performed by using the Minitab 15.0 statistical software programme (Minitab Limited Coventry, UK) and SPSS 14.0 statistical software programme (SPSS Ltd Surrey, UK). A multiple comparison of mechanical properties (CS, DTS, FS) of both cement systems (Fuji-IX and HiFi), with different storage conditions (1hr, 1day, 1week and 1month) and different nanoclay contents, was conducted. A general linear model (GLM) analysis of variance (ANOVA) was conducted on the combined CS, DTS and FS data following different nanoclay content , at the storage conditions on the GICs with post hoc Tukey's test comparisons ($P < 0.05$) in SPSS 14.0v. One-way analysis of variance (ANOVA) and post-hoc Tukey's multiple range tests at $P < 0.05$ of E_f, VH and wear resistance values were employed by using Minitab 15.0v at the associated 95% confidence interval was established to highlight the difference. Box, whisker plots and interaction plots were produced to highlight the general trend in the data to identify mean, median and inter-quartile ranges.

2.2.9 Scanning Electron Microscopy (SEM)

The beam shaped specimens from three-point bend test were used to study the fracture surface of GICs. A JEOL 7000 (Philips Co Japan) scanning electron microscope was used to study the surface of the cements. The scanning electron microscope was operated under low vacuum conditions, in back-scattered electron mode at a voltage of 15 kV, to characterise the morphology of the PGV reinforced cements and the control group cement specimens. A focussed beam of electrons was fired from an electron gun under vacuum towards an anode and pass through a series of condenser lenses to produce the focussed beam of electrons is generated in SEM which scans back and forth across a specimen resulting in an image of the surface. Cement specimens were coated with a thin film of gold to make them conductive before placing it the vacuum chamber of election microscope. Environmental scanning electron microscope (ESEM) Philips XL30 ESEM-FEG (Philips Co Japan) was also used to study the surface of cement where humidity level was kept at 95%. In a cryo scanning electron microscope (Cryo-SEM) images can be made of the surface of frozen material. The cryo-method has the great advantages such as, rapidly frozen GICs are less susceptible to crack formation allowing the detailed examination of cement surface. Cryo-SEM is also useful for the vulnarable biological structures because they are rapidly frozen to preserve the structure. The GIC samples were cryo-fixed, generally by plunging it into sub-cooled nitrogen (nitrogen slush) close to the freezing point of nitrogen at -210 ^{o}C and then the samples were transferred to the cold-stage of the SEM cryo-preparation chamber. After sputter coating with metal (usually gold or platinum), the sample is transferred into the SEM chamber, where it remains frozen during imaging on another cold-stage, cooled by nitrogen.

2.2.10 Transmission Electron Microscopy (TEM)

A JEOL-1200EX transmission electron microscope (80 kV) was used to examine clay morphology, dispersion and orientation within the polymer matrix. GICs cement samples were then embedded in a cold moulding resin by using bullet shaped polypropylene moulds. GICs samples were ultra-microtomed to a thickness of 80-110 nm at room temperature using a Leica Ultracut E ultramircotome equipped with a diamond knife. The TEM samples were placed on a Formvar-cated 200 mesh copper grid. The contrast of the samples was sufficient to permit electron micrograph imaging without staining.

CHAPTER 3

3 RESULTS

3.1 Dispersion of PGV and PGN in an aqueous solution of PAA

3.1.1 X-ray Diffraction (XRD)

XRD is a common method to measure the interaction of layer silicate nano-particles with the polymer matrix. The structure of nanocomposites can be identified by observing the position, shape, and intensity of the basal reflections from the distributed nano-silicate layers within the polymer. The intercalation and exfoliation of nanoclays usually result in increased interlayer space which then leads to the shift of the diffraction peaks towards lower angle values. XRD was employed to identify these intercalated structures and to measure the interlayer distance of polymer grade montmorillonites (PGV and PGN) after mixing with the PAA aqueous solution (PA-110).

Figure 3.1 and 3.2 show the XRD graphs of nanoclays dispersed in PA-110 at different content (w/w %) of PGV and PGN, respectively. It is well documented that polymer molecules may be trapped in the interlayer spaces within the nanoclays. This usually leads to an increase in the interlayer spacing resulting in a multilayered structure [229]. The PAA-nanoclay interaction is identified by a shift of the XRD diffraction peaks towards lower angle values in comparison with the original interlayer spacing of PGV and PGN. The main peaks in the diffraction pattern of PGN nanoclay ($2\theta \sim 7.13°$) and PGV nanoclay ($2\theta \sim 6.95°$) were attributed to the formation of the interlayer space by a regular stacking of the silicate layers along the [001] direction (Figure 3.1 and 3.2).

The interlayer distance at 2θ = 6.95° for PGV was calculated by using *Bragg's Law* to be 12.83 Å in Figure 3.1 and it demonstrates the absence of the main peak (2θ ~ 6.95°) in all of PAA-PGV samples (D0.5VP to D8.0VP). The increase in the interlayer distance is due to the segregation and adsorption of PAA molecules into the interlayer spaces of PGV nanoclay. The lack of the XRD peak in the measured range implies that the PGV nanoclays were exfoliated within the PAA-PGV suspensions. An additional peak at 2θ ~ 19.74° identified in PGV nanoclay can be attributed to the in-plane structures formed by stacking along the (*a,b*) direction [230, 231]. The peak at 2θ ~ 19.74° associated with the [101] plane becomes very broad and insignificant in PAA-PGV sample after the dispersion of nanoclays.

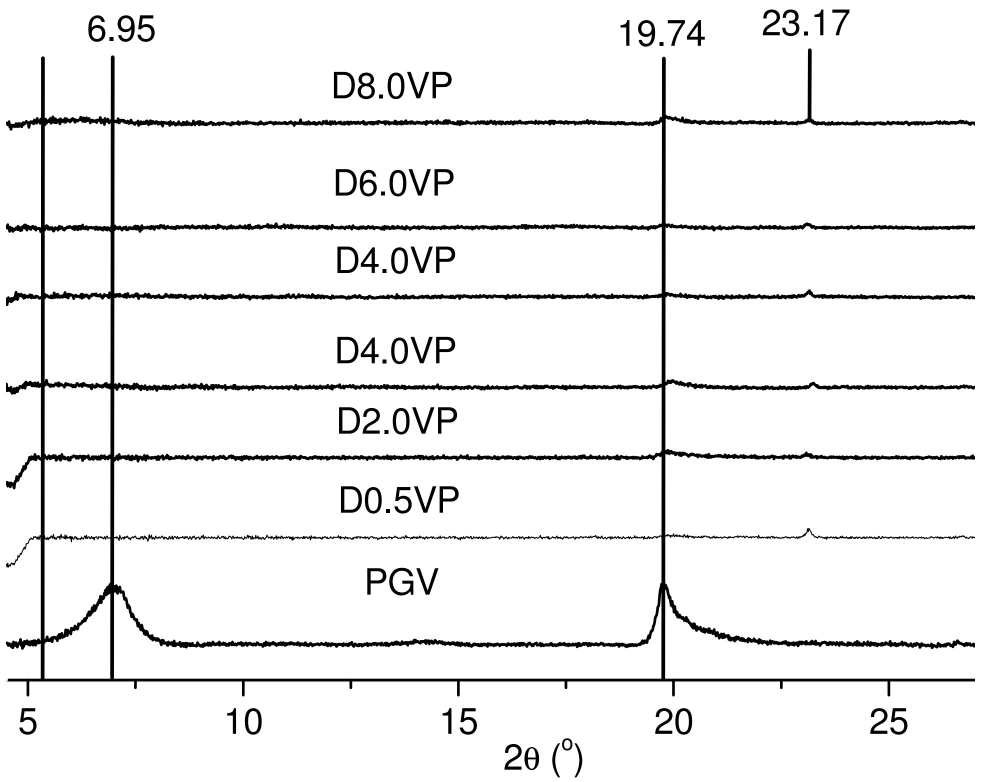

Figure 3.1: X-ray diffraction graphs of PGV nanoclays and different content of centrifuged PGV (D0.5VP to D8.0VP) nanoclays dispersed in aqueous PAA solution.

Figure 3.2 shows the XRD graph of PGN nanoclay and PAA-PGN samples (D0.5NP to D8.0NP). The interlayer distance shown for PGN at 2θ ~ 7.13° was calculated by using *Bragg's Law* to be 12.42 Å and the d_{001} space between the silicate layers of PAA-PGN (D0.5NP to D8.0NP) samples increased to 18.83 Å. This increase in the interlayer space depicted the partial intercalation of PGN montmorillonites in PAA. There are two more peaks observed at 2θ ~ 19.74° and ~ 26.51° in the X-ray pattern of PGN which can be attributed to the in-plane structures formed by stacking along the (*a,b*) direction [230, 231]. The peak at 2θ ~ 19.74° associated with the [101] plane becomes very broad and insignificant in PAA-PGN (D0.5NP to D8.0NP) groups after the dispersion of nanoclays.

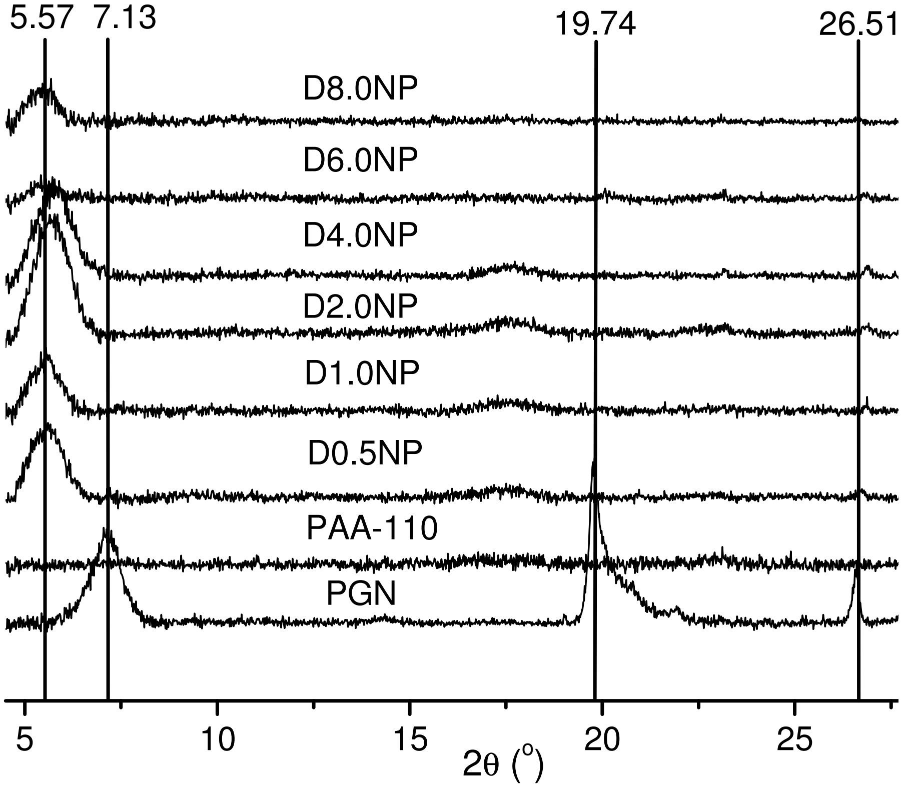

Figure 3.2: X-ray diffraction graphs of PGN nanoclays and different content of centrifuged PGN (D0.5NP to D8.0NP) nanoclays dispersed in aqueous PAA solution.

3.1.2 X-ray Photoelectron Spectroscopy (XPS)

Element-specific techniques such as XPS provide detailed information about the structure of materials and specifically the bonding and the chemical interactions. Figure 3.3 shows the wide scan XPS spectra of PAA, PGV nanoclay and PAA-PGV suspensions (D4.0VP and D6.0VP) formed by two different nanoclay contents (4% and 6%). Figure 3.4 presents the XPS spectra of PAA, PGN nanoclay and PAA-PGN suspensions formed by two different nanoclay contents (4% and 6%).

In the wide scan of both PGV and PGN nanoclays, the main peak of O 1s photoelectron was attributed to the various oxygen containing species such as Si-O-M (M: Mg, Al, Fe, etc) within the two layers of the silicate plate, whereas Si-O-Al linkages can be identified by the Si 2p or Si 2s and Al 2p or Al 2s peaks. Similarly, the minor peaks of Mg KLL and Fe 2p were attributed to the presence of a small amount of Si-O-Mg and Si-O-Fe species (substitution between Fe^{+2}, Al^{+3} and Mg^{+3} ions generates negatively charged silicate layers which are balanced by the adsorption of Na^{+} ions) [12]. The Na 1s (or Auger Na KLL) photoelectron peak in nanoclays was due to the Na ions on the surface of the silicate plates. The main peaks of O 1s and C1s from the wide scan of PAA were attributed to the presence of oxygen and carbon from the –COOH and C-C groups. In the XPS wide scan of solid residue collected from PAA-PGV (D4.0VP and D6.0VP) and PAA-PGN (D4.0NP and D6.0NP) prepared at 75 °C, the C 1s peak was assigned to the presence of PAA whereas all the other peaks e.g. Si 2p, Al 2p and Fe 2p were due to the presence of the polymer-grade montmorillonites. However, the Na 1s and Na KLL peaks were not detected in the wide scan of both PAA-PGV and PAA-PGN suspensions.

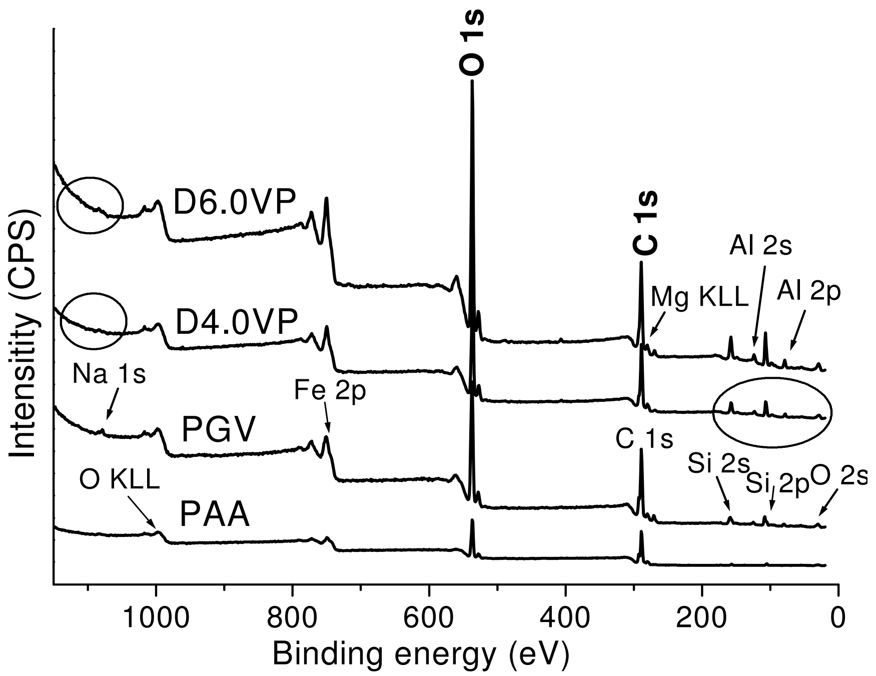

Figure 3.3: Wide-angle XPS spectra of PAA, PGV nanoclays and centrifuged PGV after dispersion in aqueous PAA solutions of different PGV content (D4.0VP, D6.0VP)

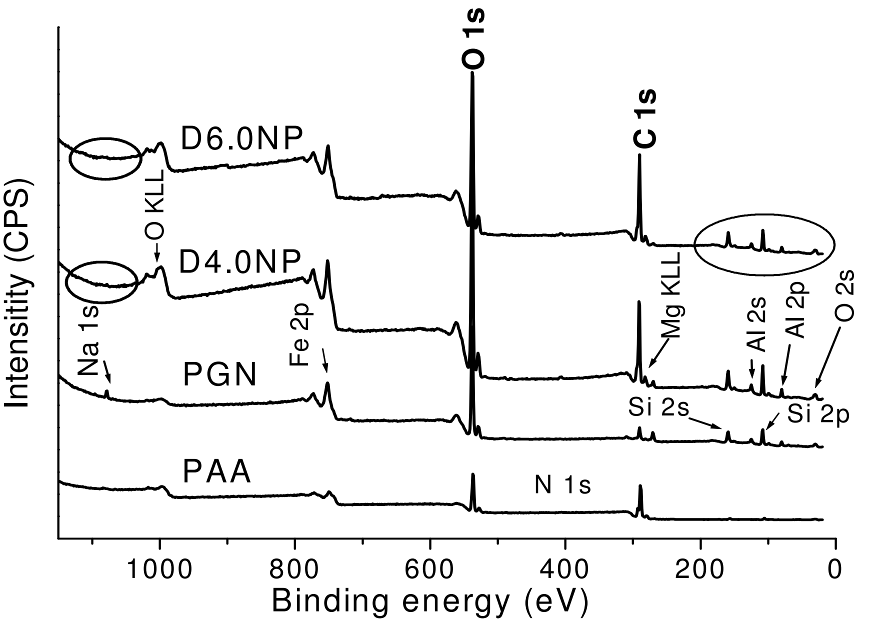

Figure 3. 4: Wide-angle XPS spectra of PAA, PGN nanoclays and centrifuged PGN after dispersion in aqueous PAA solutions of different PGV content (D4.0NP, D6.0NP).

Figure 3.3 and 3.4 indicate, that Na ions have been removed from the surface of silicate plates during the interaction of PAA with the nanoclays at 75 °C and are probably replaced by the protons from the PAA solution [12]. It is clear from the wide angle XPS scan that the XPS spectra show small differences between the untreated nanoclays and the treated nanoclays. Therefore, in order to emphasise the differences a more detailed analysis of XPS results was carried by high resolution scans of C 1s and O 1s which are shown in Figure 3.5 and 3.6, respectively.

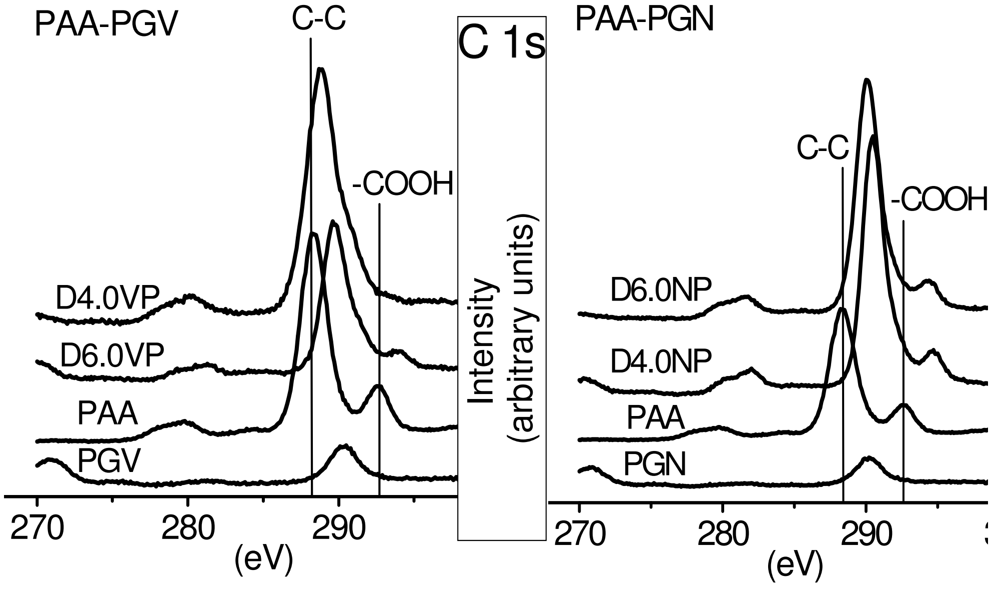

Figure 3. 5: Narrow-angle C 1s XPS spectra of PAA, PGV and PGN nanoclays, PAA-PGV (D4.0VP, D6.0VP) and PAA-PGN (D4.0NP, D6.0NP) suspensions.

In the C 1s region scan of PAA, the peak at 287 eV was attributed to C-C whereas the peak at 293 eV was attributed to C-COOH of PAA backbone [232]. In addition to the broadening and shifting of the C-C peak in the C 1s spectrum of PAA-PGV there was also shifting and gradual decrease of –COOH peak in the C 1s spectra for both D4.0VP and D6.0NP. Specifically for the latter, the peak is so small that it could be considered as non present. On the other hand, the narrow-angle scans of C 1s of PAA-PGN shows both C-C and –COOH peaks which moved towards higher binding energies with the addition of nanoclays. It is clear, that the peak associated with –COOH groups also shifts to higher binding energies with the addition of nanoclays and its intensity seems to decrease (Figure 3.5). Generally, 4 wt % nanoclays containing PAA solutions show more wide and strong peaks when compared to the PAA reference standard indicating the higher degree of interaction of nanoclays with the poly(acrylic acid) chains. The presence of C 1s peak in the spectrum of nanoclays at a binding energy of 290eV was unexpected and although it was a small peak compared to the relevant peak in PAA's spectrum, it could not be ignored. The nanoclays were not organically treated and any trace of carbon could be originated from the environment either as contamination or from the air and therefore the above peak was attributed to the presence of the surface adventitious carbon ions [233].

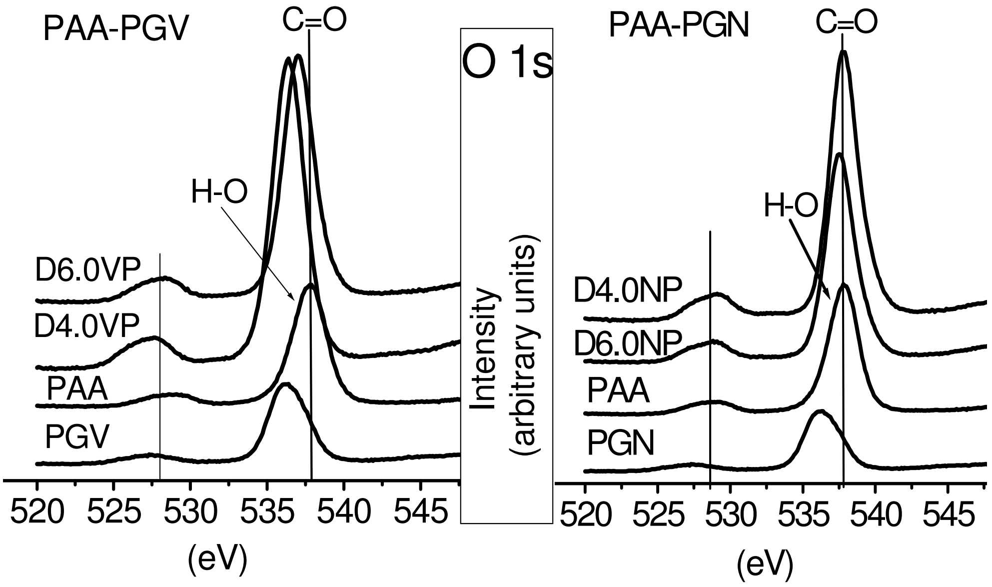

Figure 3. 6: Narrow-angle C 1s XPS spectra of PAA, PGV and PGN nanoclays, PAA-PGV (D4.0VP, D6.0VP) and PAA-PGN (D4.0NP, D6.0NP) suspensions.

In the O 1s scan of PAA (Figure 3. 6) the peak at 537 eV was attributed to the presence of the carbonyl and hydroxyl components of the carboxylic group [13]. The O 1s peak in the scans of PGV and PGN nanoclays was due to the presence of metallic oxides O-M (M: Si, Al, Fe, Mg) and appeared at 538 eV. The O 1s scan of D4.0VP exhibits a very strong peak at 536 eV, which was moved slightly towards a lower binding energy compared to the peak present in PAA's spectrum. Generally, a shifting towards lower binding energies and broadening of the O1s peak in the case of the treated PAA-PGV nanoclays were observed indicating changes in the environment around the chemical species containing oxygen and consequently most likely stronger interactions with PAA. However, the O 1s peak in the PAA-PGN suspension was similar to the reference peak of PAA but increased in intensity.

3.1.3 Fourier Transform Infrared (FTIR) Spectroscopy

3.1.3.1 FTIR spectra of the PAA solutions after nanoclay dispersion

The spectra with major peak position assignments for the PGV and PGN nanoclay, PAA-PGV suspensions after dispersion in PAA solutions (D0.5VP to D8.0VP) of various concentrations of nanoclays are provided in Figure 3.7. In addition, the description of the main peaks is presented Table 3.7 The FTIR spectra of both nanoclays PGV and PGN show characteristic bands at 3620 cm^{-1} due to O–H stretching vibrations, 3370 cm^{-1} due to inter- and intra-layer H-bonded O–H stretching vibrations, 1654cm^{-1} due to H–O–H bending vibrations, 973cm^{-1} due to Si–O stretching vibrations in the tetra-hydrate layer in PGV and PGN nanoclay , 913cm^{-1} due to the presence of Al–OH and 833 and 792cm^{-1} due to (Al, Mg)–OH vibration modes [234-237]. The spectrum of PAA (PA-110) also shown in Figure 3.7 demonstrates clearly the presence of a strong C=O peak around 1705 cm^{-1} due to stretching vibrations in the free (i.e. non-hydrogen bonded) carboxyl groups and a peak at 1629 cm^{-1} due to the presence of hydrogen bonded carboxyl groups.

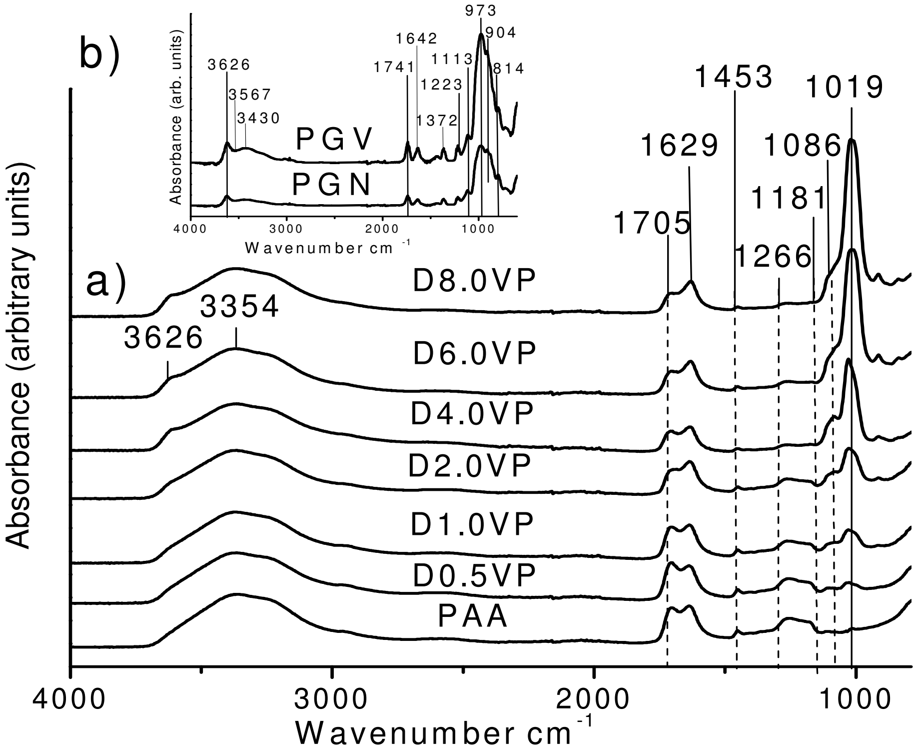

Figure 3. 7: FTIR spectra of (a) PAA, PAA-PGV after dispersion in aqueous PAA solutions of different PGV content (D0.5VP to D8.0NP), (b) spectra of PGV and PGN nanoclays powder (b)

Figure 3.8 shows the FITR spectra of Fuji-IX liquid (FL) and the solutions prepared from the liquid portion of Fuji-IX after the dispersion of 2% of PGV and 2% PGN montmorillonites at room temperature (D2.0VFRT and D2.0NF75) and at 75 °C (D2.0VFRT and D2.0NF75). The peak at 1706 cm^{-1} is attributed to the C=O stretching vibrations in the carboxylic group, whereas the peak at 1628 cm^{-1} is associated with –OH bending vibrations of carboxyl group. It is however, a fact that most of the peak positions are consistent in all groups of suspensions after the dispersion of nanoclays. The peak at 1633 cm^{-1} can be attributed to the H-O-H bending vibrations in FL. In the spectrum of FL and its solutions prepared after the dispersion of nanoclay, there are two additional peaks at 1088 cm^{-1} and 1134 cm^{-1} which suggests the presence of 5-10 % tartaric acid in the solution of Fuji-IX (Figure 3.7), however tartaric acid was not observed in the FTIR spectrum of PAA-PGV (D0.5VP-D8.0VP) (Figure 3.7).

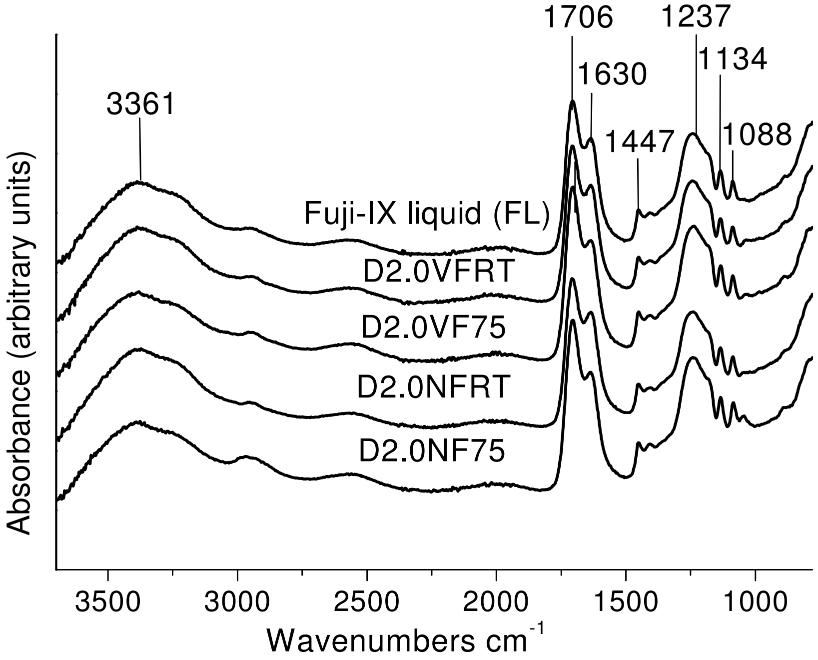

Figure 3. 8: FTIR spectra of Fuji-IX liquid (FL) and its solution after dispersion of 2% PGV (D2.0VRT, D2.0V75) and 2%PGN (D2.0VRT, D2.0V75) at room temperature and 75 °C, respectively.

Similarly, Figure 3.9 presents the FTIR spectra of the polymer solution of the HiFi control group (PA) with respective PA solutions formed after the dispersion of 1wt %, 2 wt % and 4 wt % PGN nanoclay in PA (D1.0NHPAH, D2.0NHPAH and D4.0NHPAH) at 75 °C according to the protocol described in 2.1.2. The peak at 1710 cm^{-1} is attributed to the C=O stretching vibrations in the carboxylic group, whereas the peak at 1628 cm^{-1} is associated with –OH bending vibrations in water molecules fact that is consistent in all groups of suspensions after the dispersion of nanoclays. The presence of a new peak at 1041 cm^{-1} in the case of 4 wt % PGN in D4.0NHPAH is attributed to the Si-O stretching mode in PGN nanoclay. A week peak at 1041 cm^{-1} in D1.0NHPAH and D2.0NHPAH is also attributed to Si-O stretching vibration. In addition, there is a very broad OH stretching band at 3360 cm^{-1} present in both of the polymer systems (Fuji-IX and HiFi) associated with –OH groups in water molecules.

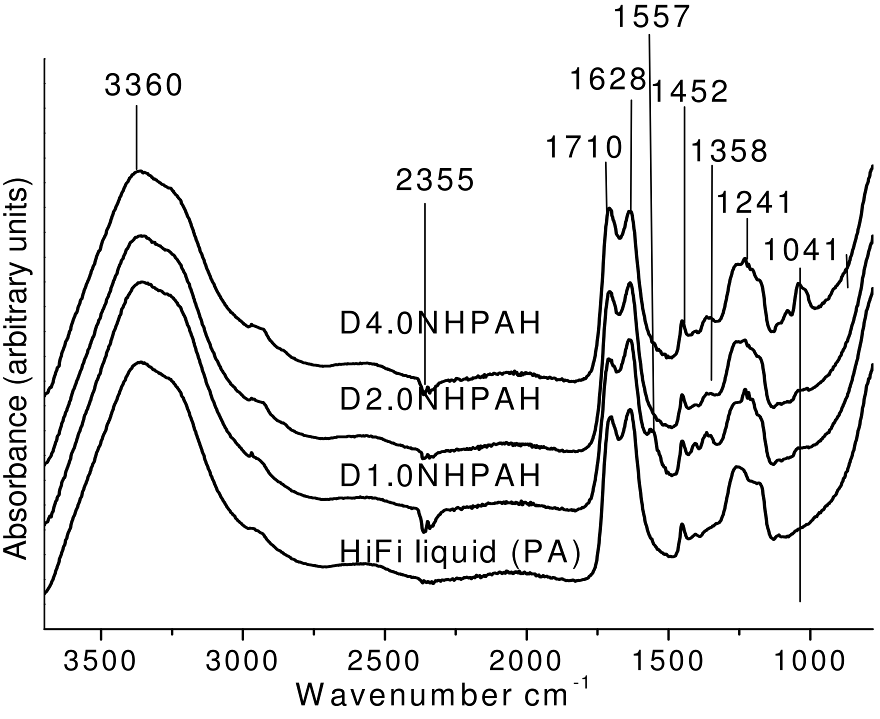

Figure 3. 9: FTIR spectra of HiFi liquid (PA) and its solutions prepared after dispersion of 1% (D1.0NHPAH), 2% (D2.0NHPAH) and 4% (D4.0NHPAH) of PGN nanoclay.

Table 3. 1: Description of FTIR peaks present in spectra shown in Figures 3.7, 3.8, and 3.9.

	Wavenumber cm^{-1}	Assignment	Reference
Nanoclay	3626	Si-OH stretching vibrations	[234, 236]
	1741	H-O-H bending vibration	[235, 236]
	1642	H-O-H bending vibration	[235, 236]
	973	Si–O stretching vibration	[234-237]
	904	Al–OH stretching vibration	[234-237]
	814	(Al, Mg)–OH vibration mode	[234-237]
	797	Si-O-Al vibration	[236]
	527	Al(Mg)-O-Si	[236]
	480	Si-O stretching vibration	[236]
PAA-nanoclay	3354	H bonded O-H stretching vibration	[234-237]
	1705	C=O stretching vibration	[237]
	1642	C-O vibration	[237]
	1642	H-O-H bending vibration	[236, 237]
	1453	C-H bending vibration	[236, 237]
	1266	C-O stretching vibration	[236, 237]
	1019	Si-O stretching vibration	[236, 237]

3.1.3.2 Setting reaction of GI cement followed by FTIR spectroscopy

Glass ionomer cements are formed when an acidic polyelectrolyte (PAA) reacts with an alumina-silicate glass powder. It has been previously shown, that the acid attack of the glass surface by the protons in PAA results in the release of various metallic cations from the glass, which react with the poly-anions to form a poly-salt matrix [111, 238]. A series of ATR-FTIR spectroscopy studies over the duration of one hour has been employed allowing the investigation of the setting reaction in the cements studied in this thesis. Moreover, the FTIR spectra of the glass compositions used in the preparation of cements are presented in Figure 3.10. The most intensive absorption bands is present in the region of 900-1400 cm^{-1}, which usually represents a super-position of some bands situated close to each other and are assigned to the stretching vibration of SiO$_4$ tetrahedra with a different number of bridging oxygen atoms and P-O bonds [239, 240].

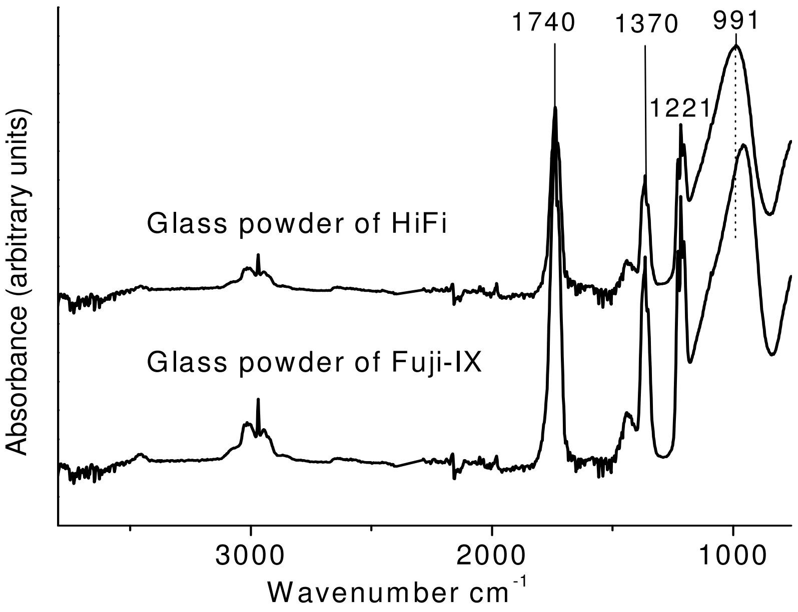

Figure 3. 10: FTIR spectra of Fuji-IX and HiFi glass powder.

The main peak in the spectra of Fuji-IX glass powder present at 991 cm^{-1} and was attributed to the Si-O-Si stretching vibrations of the glass. The Si-O-Si peak in the HiFi glass powder is present at a slightly lower wavenumber 960 cm^{-1} when compared to the Fuji-IX glass powder. The strong peak at 1740 cm^{-1} is assigned to Si-OH, which appears at the same wavenumber in both glass components.

In this section, the setting reaction of each cement system (Fuji-IX or HiFi) containing two groups (one control and one prepared after the dispersion of 2% nanoclays) is described. Figure 3.11 shows the setting reaction of Fuji-IX cement (CF-IX). It is found, that the strong band around 1405 to 1451 cm^{-1} is due to the formation of calcium and aluminium tartrate salts which increased in intensity and became prominent one hour after the start of mixing [241, 242]. The weak peak at 1160 cm^{-1} can be assigned to the C-OH in tartaric acid. The band decreased in intensity and moved to lower wavenumber at 1055 cm^{-1}. The bending vibrations at 1594 and 1644 cm^{-1} were attributed to the formation of calcium and aluminium polyacrylate salts and the symmetric and asymmetric stretching vibrations of COO^{-} were present at approximately 1420 and 1540 cm^{-1}, respectively [243]. A new peak formation was noted at 1594 cm^{-1} 1 hr after the start of mixing of cements and it may be assigned to C-O asymmetric stretch vibrations of Ca-tartrate. A strong absorbance band at 948 cm^{-1} due to the stretching vibrations of Si-OH is present continuously over the time periods studied and overlapped with the asymmetric stretching vibrations in Si-O that usually appears between 940 and 1000 cm^{-1}. Furthermore, Figure 3.12 shows the setting reaction of cements formed after the dispersion of 2% PGV nanoclay (C2.0VF75F) in Fuji IX liquid. The bending vibrations at 1594 and 1625 cm^{-1} are attributed to the formation of calcium and aluminium polyacrylate salts.

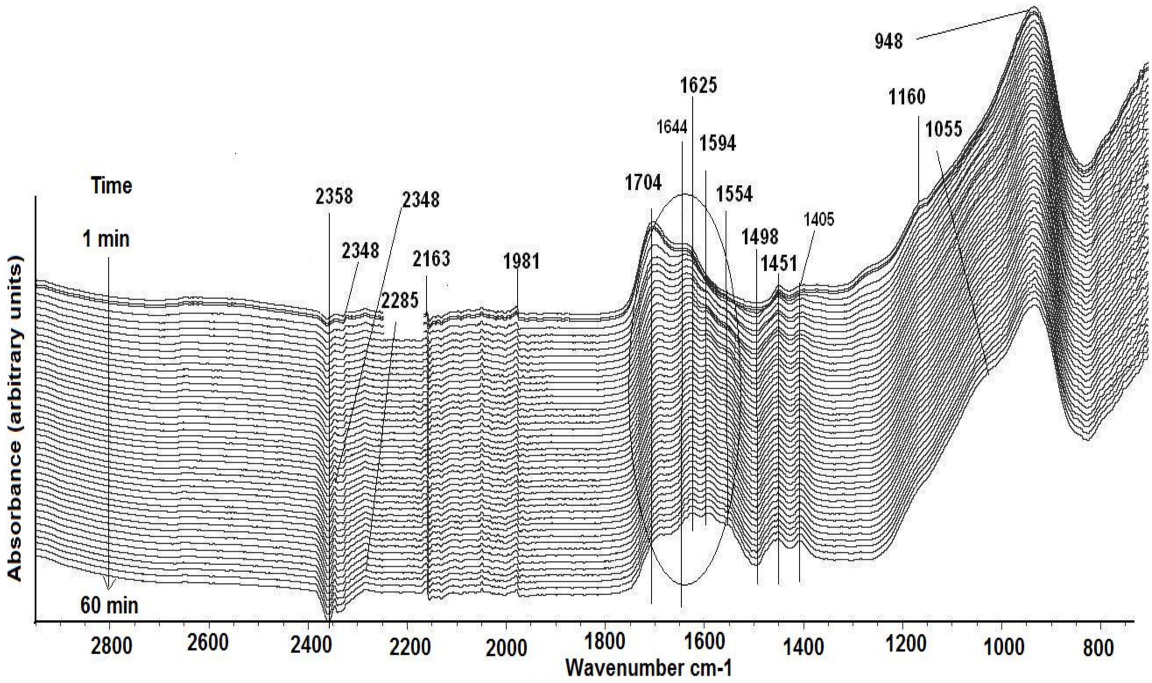

Figure 3. 11: Real time ATR-FTIR analysis of the setting reaction of Fuji-IX cement at different time intervals for 1 hour,

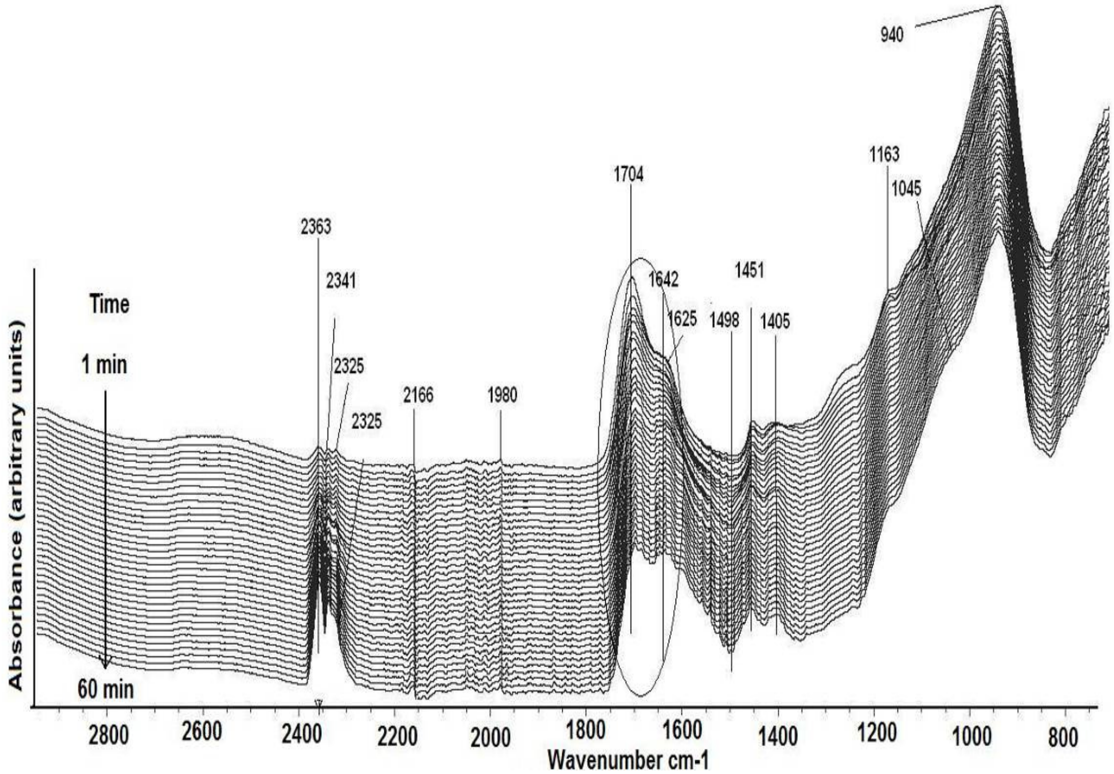

Figure 3. 12: Real time ATR-FTIR spectra of the setting reaction of C2.0VF75F at different time intervals for 1 hour.

A gradual increase in the peak intensity at 1642 cm^{-1} was observed with cements aging as expected (Figure 3.12). The peak at 1625 cm^{-1} in C2.0VF75F moved also to higher wavenumbers whereas unlike CF-IX, the peak at 1594 cm^{-1} was not present. The strong peak at 940 cm^{-1} is associated with the asymmetric stretching vibrations in Si-OH. The relatively weak peaks at 2325 and 2328 cm^{-1} in the spectra of cements are associated most likely with the presence of atmospheric CO_2.

The setting reaction of the HiFi glass ionomer cement system (CPA-PA) is presented in Figure 3.13. A medium peak at 1594 cm^{-1} is attributed to the C-O asymmetric stretching vibration of Al-PAA polysalts. The appearance of a new peak at 1522 cm^{-1} was observed that may be associated with –(C=O)O- asymmetrical stretching vibrations of mono or divalent poly salts. The strong peak at 1451 cm^{-1} is assigned to C-O symmetric stretching vibrations of Ca-PAA [244]. A strong absorbance band at 950 cm^{-1} due to the stretching vibrations of Si-OH is present constantly over the period of setting of HiFi cement.

Figure 3.14 shows the setting reaction of the cement formed after the dispersion of 2% PGN (C2.0NPAH) in the HiFi system. The setting reaction of C2.0NPAH follows similar trend to CPA-PA, however the peaks at 2358 and 2310 cm^{-1} increased in intensity as compared to CPA-HP. Generally, the spectrum of C2.0NPAH appears similar to the spectrum of CPA-HP over the duration of 1 hour. The main peaks found in Fuji-IX (CF-IX and C2.0VF75) and HiFi (CPA-HP and C2.0NPAH) glass ionomer cements are described in Table 3.2.

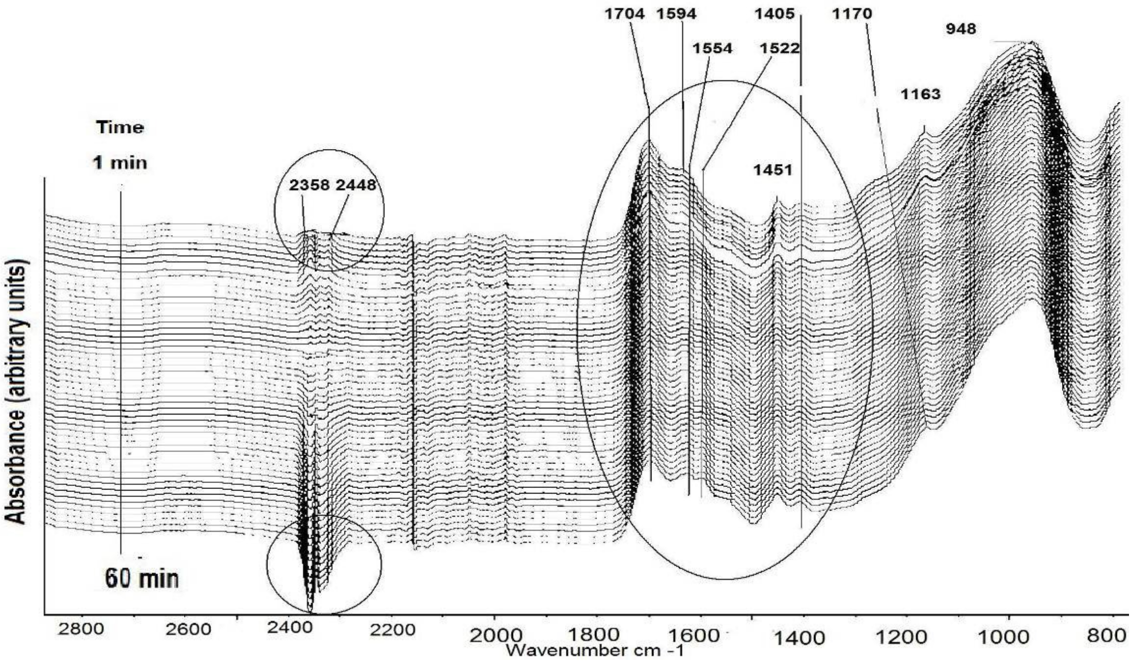

Figure 3. 13: Real time ATR-FTIR spectra of the setting reaction of CPA-HP at different time intervals for 1 hour with the assignment of major peaks

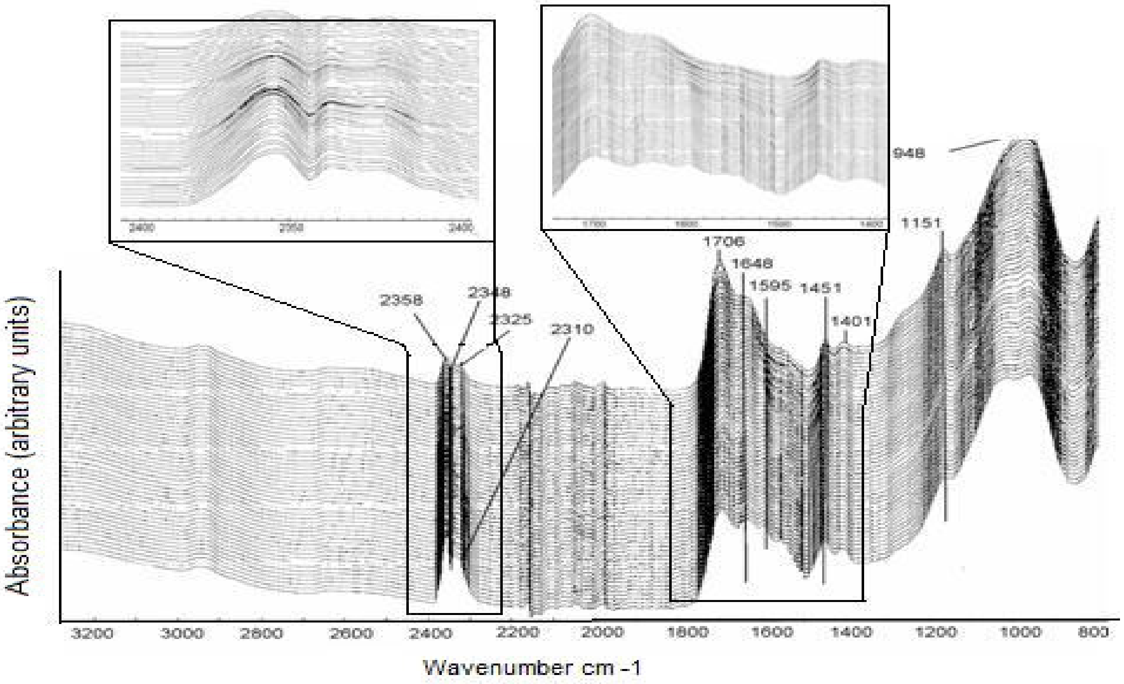

Figure 3. 14: Real time ATR-FTIR spectra of the setting reaction of C2.0NPAH at different time intervals for 1 hour formed after the dispersion of 2% PGN nanoclays.

Table 3. 2: FTIR peak assignment in glass ionomer cements

Wavenumber cm^{-1}	Assignment	Compound	Reference
3200-2600	-OH stretching vibration	Water, PAA, TA	[243]
1705	C=O stretching vibration	PAA TA	[243]
1635	O-H stretching vibration	Water	[243]
1554	C-O asymmetric stretching vibration	Ca-PAA	[243]
1410	C-O symmetric stretching vibration		[243]
1560	COO- asymmetrical stretching vibration	Al-PAA	[243]
1460	COO-symmetrical stretching vibration		[243] [245]
1540 (1522)	COO-asymmetrical stretching vibration	Mono/divalent polyacrylate salts	[241, 242]
1420-	COO-symmetrical stretching vibration		
1595	C-O asymmetric stretching vibration	Ca-tartrate	[241, 242]
1385	C-O symmetric stretching vibration		[241, 242]
1670	C-O asymmetric stretching vibration	Al-tartrate	[241, 242]
1410	C-O symmetric stretching vibration		[241, 242]
1240 (1249)	C-O stretching vibration	AA	[241, 242]
1136,1088	C-OH stretching vibration	TA	[244]
948	Si-OH stretching vibration	glass	[244]
940-1000	Si-O stretching vibration	glass	[244]

3.2 Molecular weight determination

Gel permeation chromatography (GPC) was employed to measure the molecular weight of poly(acrylic acid) in two different polymer solutions namely, Fuji-IX liquid (FL) and HiFi liquid (PA). The GPC measurements were performed by RAPRA. The GPC system was calibrated with different concentrations of sodium polyacrylates. Figure 3.17 shows the molecular weight distribution of a FL, PA and PA powder and, Table 3.3 shows the summarised results M_w, polydispersity (M_w /M_n) and refractive index peak area. Figure 3.16 shows an overlay of the computed M_w distribution for a duplicate run of the three samples. The polymer solution of FL has a peak in the lower range as compared to the polymer solution of PA and PA powder. The plots of X-axis are all to the same area, the Y-axis being a function of the weight fraction.

Table 3. 3: GPC result of the two PAA solutions.

Sample	M_w	M_n	M_w /M_n	Peak Area	Polymer (%)
Fuji-IX Liquid [FL]	15,600	3,970	39	33,800	33
40% PAA-SOL [PA]	52,100	11,000	4.8	39,000	39
PA Powder	56,500	10,100	5.7	4,020	100

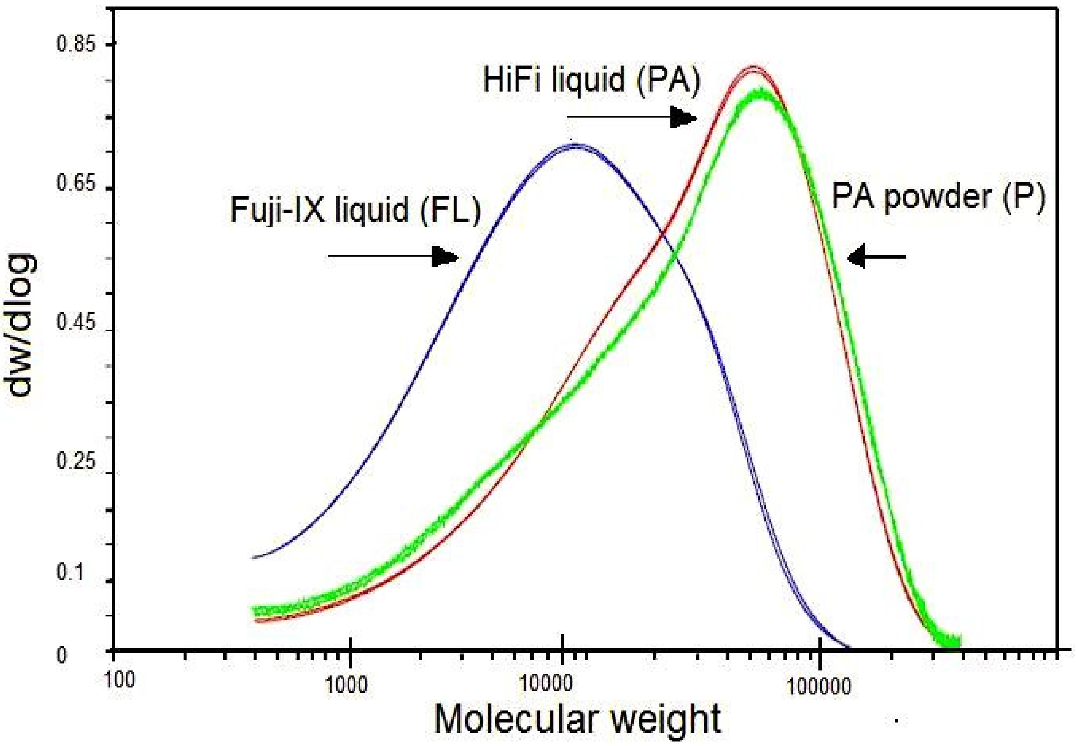

Figure 3. 15: GPC plot showing the molecular weight distribution of FL, PA, and PA powder (P).

The polymer content could be calculated from the refractive index detector response and is shown in Table 3.3 along with the peak area and M_w of the individual polymer samples. In practice when the refractive index chromatogram peak area for the FL and PA solution are similar, indicating the similar amount of polymer concentration present in the solution, it is possible to calculate the concentration of polymer in the solution. The polymer content in the aqueous solution was calculated form refractive index peak area is also shown in Table 3.3. The average M_w of FL was calculated 15,700 which is much lower than the expected range for a cement liquid required for posterior restoration cements (40,000-60,000).

3.3 Rheological studies of cements

Working and setting times are determined for cements by the Wilson's oscillating rheometer at ambient temperature (21-25 ºC) and two values were recorded for each cement mixture. The results of the setting and working time measurements are shown in Table 3.4 which demonstrates that there is a slight increase in both the working and the setting times of cements made from polymer liquids after the nanoclays dispersion as compared to control groups (CF-IX). A slight decrease in working and setting times was observed for HiFi cements formed after the dispersion of nanoclay when compared to control group (CPA-HP).

Table 3. 4: Rheological properties of control cements and cements formed with the polymer solutions after the nanoclay dispersion.

Cement specimen		Working Time (min)	Setting Time (min)
Fuji-IX	CF-IX	4.16 ± 0.15	6.35 ± 0.10
	C2.0VF75F	4.15 ± 0.25	6.55 ± 0.15
	C2.0VFRTF	4.30 ± 0.18	6.40 ± 0.15
	C2.0NF75F	4.50 ± 0.20	6.50 ± 0.25
	C2.0NFRTF	4.40 ± 0.30	6.55 ± 0.15
HiFi	CPA-HP	3.28 ± 0.10	6.30 ± 0.10
	C1.0NPAH	3.35 ± 0.25	6.50 ± 0.15
	C2.0NPAH	3.05 ± 0.10	5.60 ± 0.10
	C4.0NPAH	3.00 ± 0.15	5.50 ± 0.20

It was observed that cements (C2.0NPAH and C4.0NPAH) formed with HiFi glass powder and polymer liquids after the dispersion of PGN (D2.0NPA and D4.0 NPA) exhibit lower working and setting times than control group (CPA-HP) of HiFi cement and rheological properties of C1.0NPAH was not very much different of CPA-HP. However, a slight increase of 10-20 seconds was observed in the setting time of Fuji-IX cements formed with FP and, D2.0VF75, D2.0VFRT, D2.0NF75 and D2.0NFRT. The slight deflection in the results to the higher values of working and setting time may be due to the room temperature used during the experiments.

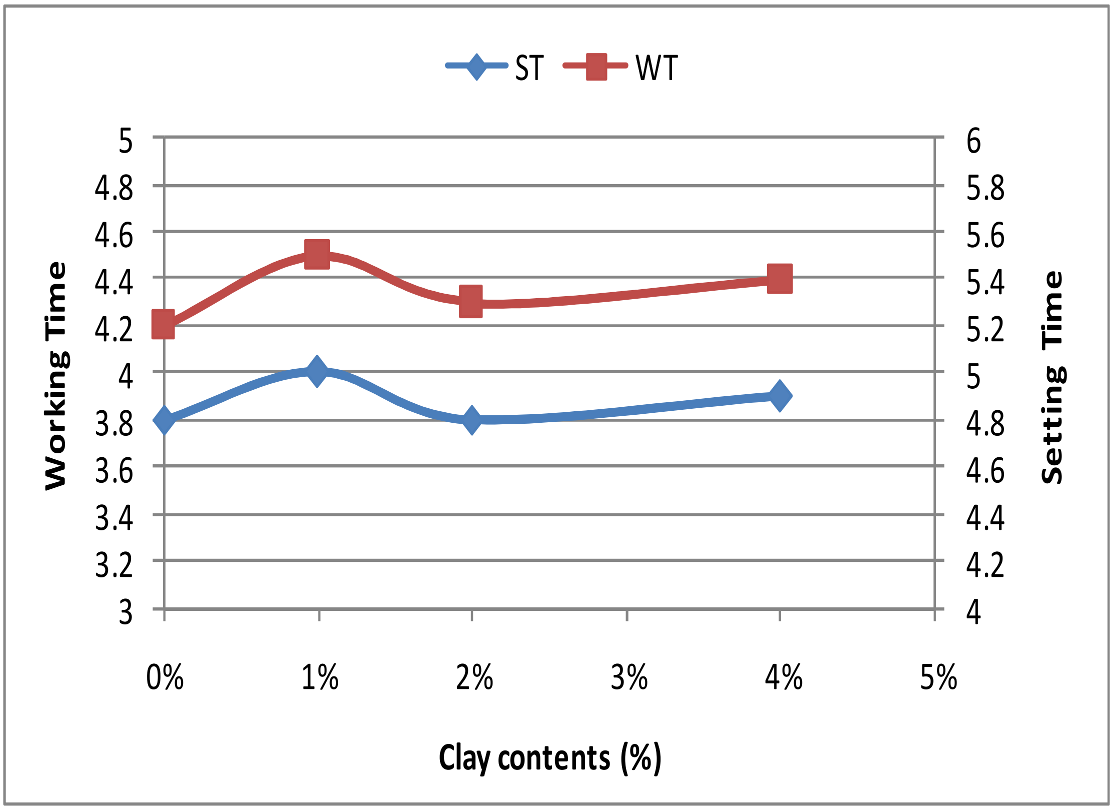

Figure 3. 16: A comparison of working and setting times at different clay contents (wt %)

3.4 Mechanical properties of cements

In the oral environment teeth and/or materials are subjected to stresses due to mastication forces and therefore it is important to determine the various mechanical properties before their application in the human teeth. In the current work several mechanical properties such as CS, DTS, FS, HV, E*f*, and wear rate have been determined to study the effect of nanoclays on the behaviour of cement after the dispersion of different percentages of PGV and PGN nanoclays. CS, DTS and FS were also determined after different aging time such as, 1 hr, 1 day, 1 week and 1 month.

3.4.1 Compressive Strength (CS)

After the successful dispersion of nanoclay in PA-110, initially experimental cement based on an experimental ionomer glass (LG 26; $4.5SiO_2$-$3Al_2O_3$-$1.5P_2O_5$-3CaO-$2CaF_2$) was formulated in order to identify the effect of nanoclays incorporation in a GIC system. D2.0VP and D2.0NP was employed as modified polymer liquid and PA-110 was used as control. The CS results of the cements made by mixing LG26 glass powder and polymer liquid D2.0VP, D2.0NP and PA-110 are shown in Figure 3.17. The cements formed with LG26 glass powder showed much lower compressive strength values however, there were some improvements observed in the CS of cements formed after nanoclays dispersion (C2.0VPL and C2.0NPL). CPL (control group without nanoclays) shows the lowest values where as, C2.0VPL (2 wt% PGV dispersion) exhibited the highest values of CS both after 1hr and 1day. There was clearly an indication that CS could be improved after the dispersion of nanoclay in a glass ionomer system.

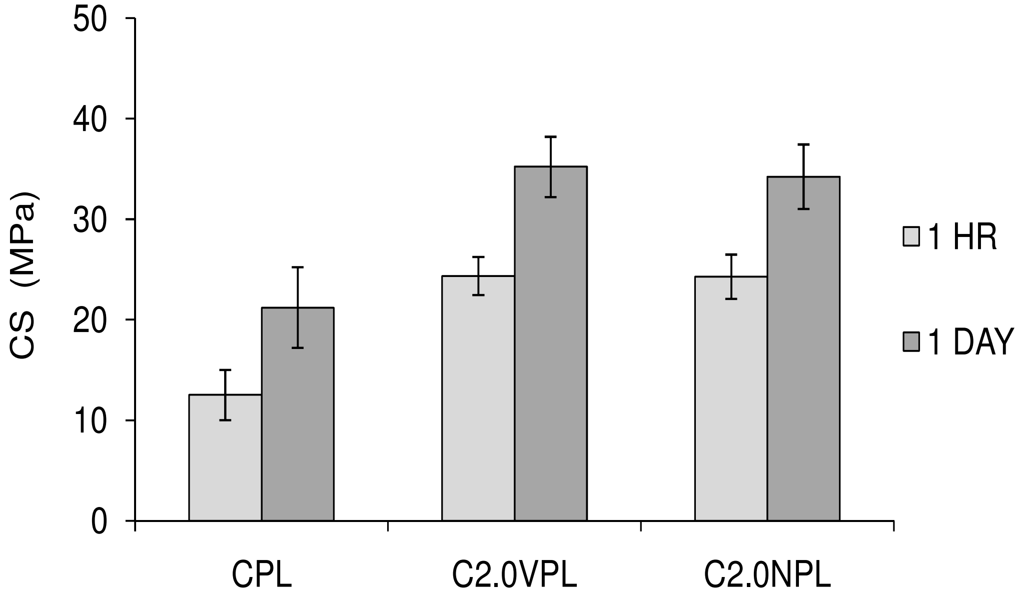

Figure 3. 17: CS results of initial experimental cements made from LG26 glass powder and PA-110 after nanoclays dispersion.

The CS of the control specimens (Fuji-IX and HiFi) were consistent with the CS recommendations set by ISO 9917-1 2007 of 100 MPa. However, in the present study, the CS of the control groups tested after 1 hour was lower than the manufacturer's values which may be related to the difficulties associated with mixing these materials. The author proposed that the ability to mix reliably to achieve the CS in accordance with ISO 9917-1 2007 provides validity for the further comparison with nanoclays reinforced cements. Table 3.5 shows the mean CS values with the standard deviation of the cements formed from the Fuji-IX glass powder after the dispersion of nanoclays at different aging time. Generally, an increase in the CS values of Fuji-IX system was observed with aging of cements. The dispersion of 2 wt % PGV nanoclays and 2 wt % PGN nanoclays in the liquid polymer of Fuji-IX both at room temperature and 75 °C do not show a significant difference ($P > 0.05$) in the compressive strength of cement.

The CS results of cements prepared with HiFi glass powder and polymer solutions after the dispersion of nanoclays are shown in Table 3.5. Cements formed with polymer solution after 1 wt % PGN nanoclays dispersion (C1.0NHPAH) resulted in most improved CS values in comparison to other groups. However, 4 wt % PGN nanoclays dispersion (C4.0NHPAH) resulted in weakest cements in the group. It is obvious from the compressive strength results that nanoclays (PGV and PGN nanoclays) containing polymer liquid with the reactive glass powder generally shows a trend of higher CS values than the control group but the addition of 4 wt % nanoclays reinforcement may result in poor cement possibly because of the agglomeration of clays in the system.

Table 3. 5: Compressive strength of two cement systems (Fuji-IX and HiFi) after the dispersion of nanoclays at different storage times.

Cement Specimen		Compressive Strength (MPa)		
		1 Hour	**1 Day**	**1 Month**
Fuji-IX	CF-IX	99.8 (10.9)	120.3 (19.4)	124.0 (19.8)
	C2.0VF75F	94.8 (8.9)	137.2 (16.0)	122.4 (17.5)
	C2.0VFRTF	93.6 (7.9)	107.2 (14.4)	134.1 (24.9)
	C2.0NF75F	100.9 (14.4)	107.2 (15.7)	130.6 (26.8)
	C2.0NFRTF	100.4 (13.1)	136.8 (25.4)	142.1 (28.9)
		1 Day	**1 Week**	**1 Month**
HiFi	CPA-HP	99.8 (10.6)	120.3 (19.4)	124.0 (19.8)
	C1.0NPAH	94.8 (8.9)	137.2 (16.0)	132.4 (19.8)
	C2.0NPAH	93.6 (7.1)	107.2 (14.4)	134.0 (24.9)
	C4.0NPAH	100.9 (14.4)	107.2 (15.7)	130.6 (26.8)

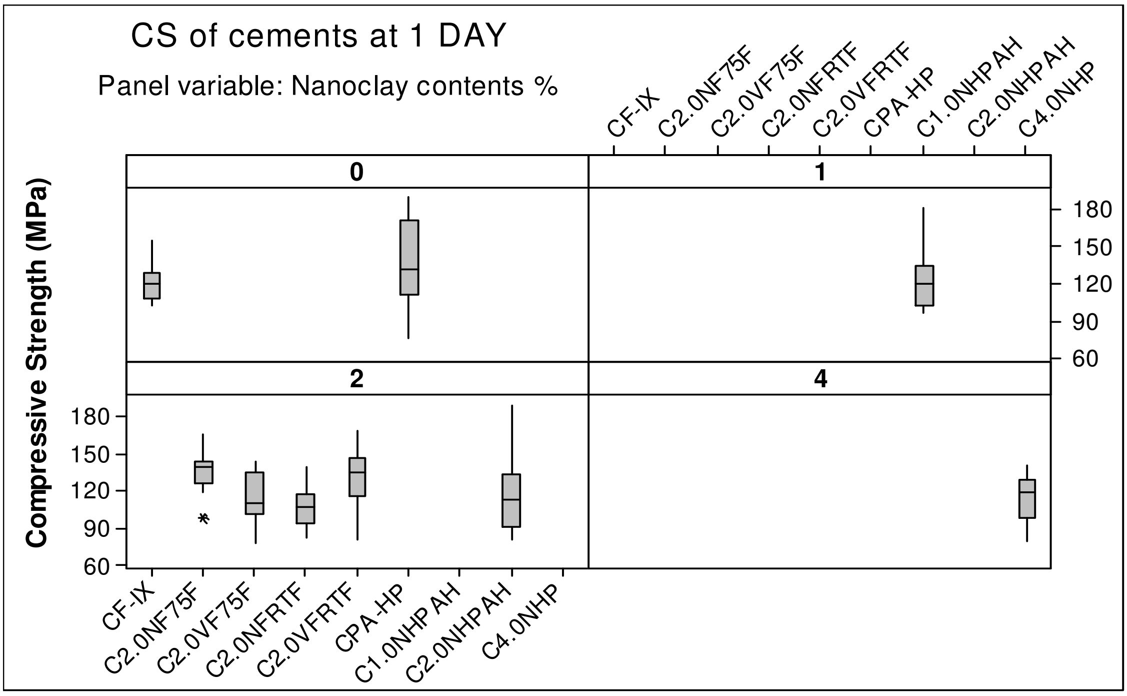

Figure 3. 18: A comparison of the CS of the cements with different nanoclay contents at 1 day.

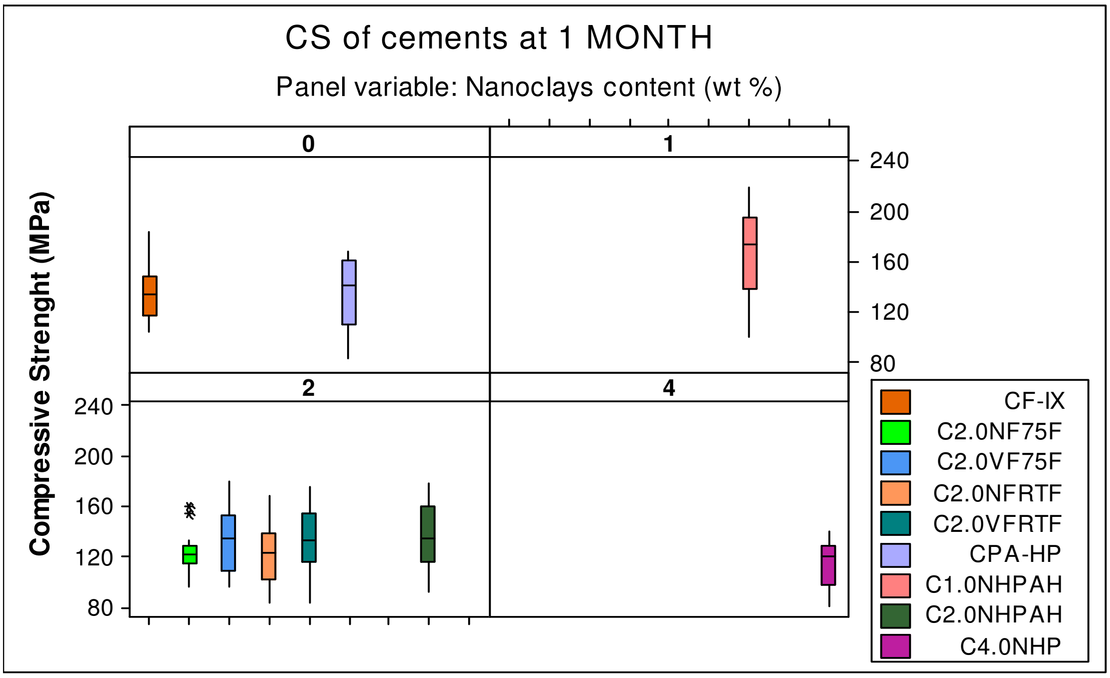

Figure 3. 19: Comparison of CS of cements at 1 month with different nanoclays contents.

The effect of the nanoclays content (0 wt %, 1 wt %, 2 wt % and 4 wt %) on the CS cement after 1 day (Figure 3.18) and 1 week (Figure 3.19) is shown by whisker plots. In all CS measurements, HiFi system showed higher values than Fuji-IX system however, univariate general linear model (GLM) analysis of variance (ANOVA) and post-hoc Tukey's test do not show significant difference ($P > 0.05$) in CS when both systems were compared. CS values of 1 month group of both cement systems were significantly higher ($P < 0.05$) CS than 1 day cement ($P > 0.05$). Univariate GLM analysis of HiFi cement formed with the dispersion of 1 wt % PGN nanoclays resulted in a significant increase ($P < 0.01$) in the mean CS to 137.5 (MPa) as compared to control group of HiFi (CPA-HP) 120.0 (MPa). Conversely, there was no significant change ($P > 0.05$) in the CS was observed at 95% confidence intervals by the dispersion of 2 wt % or 4 wt % nanoclays content.

3.4.2 Diametral Tensile Strength (DTS)

The bar charts in Figures 3.20 and 3.21 show the mean results of DTS with standard deviations of two GIC systems at different storage time after nanoclays dispersion. Fuji-IX system do not show any significant difference ($P > 0.05$) in DTS of cements formed after 2 wt % PGV and 2 wt % PGN dispersion when data was analysed with univariate GLM statistical analysis. There was a gradual increase in DTS values when cement specimens were tested after 1 hour and 1 month of aging. However, the control group cements (CF-IX) has higher DTS at 1 hour (12.1 MPa) and 1 day (15.2 MPa) but C2.0VF75F (18.9 MPa) and C2.0NF75F (18.6 MPa) have better DTS after one month.

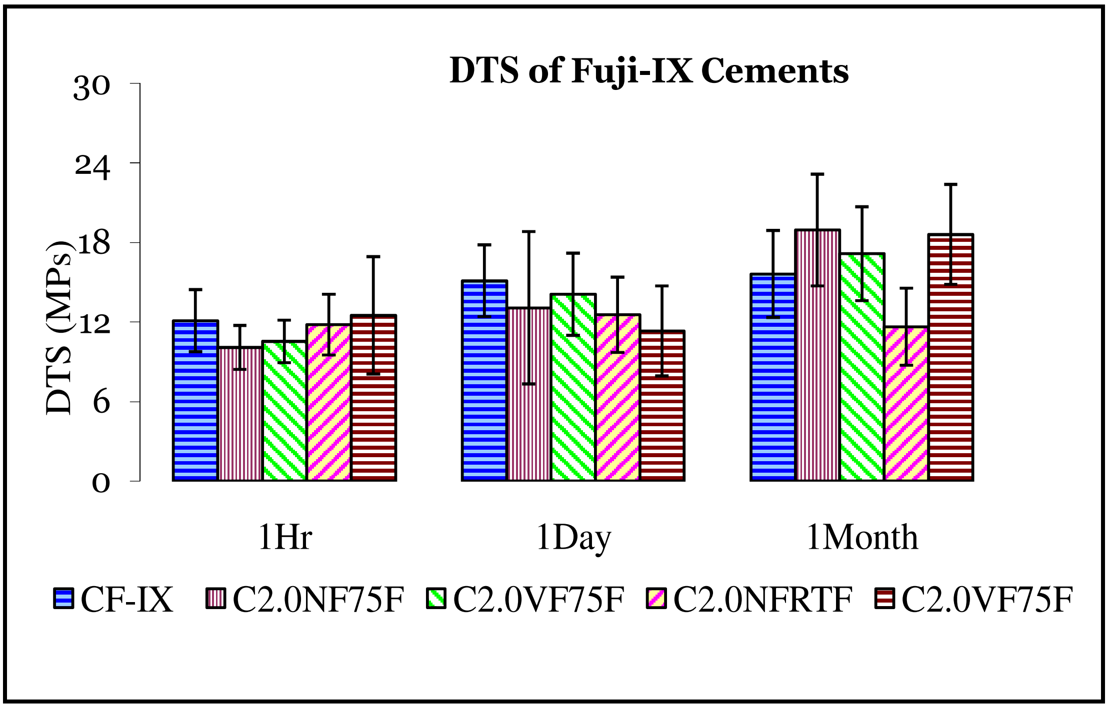

Figure 3. 20: Diametral tensile strength of Fuji-IX cements after nanoclay dispersion in Fuji-IX liquid at different storage times.

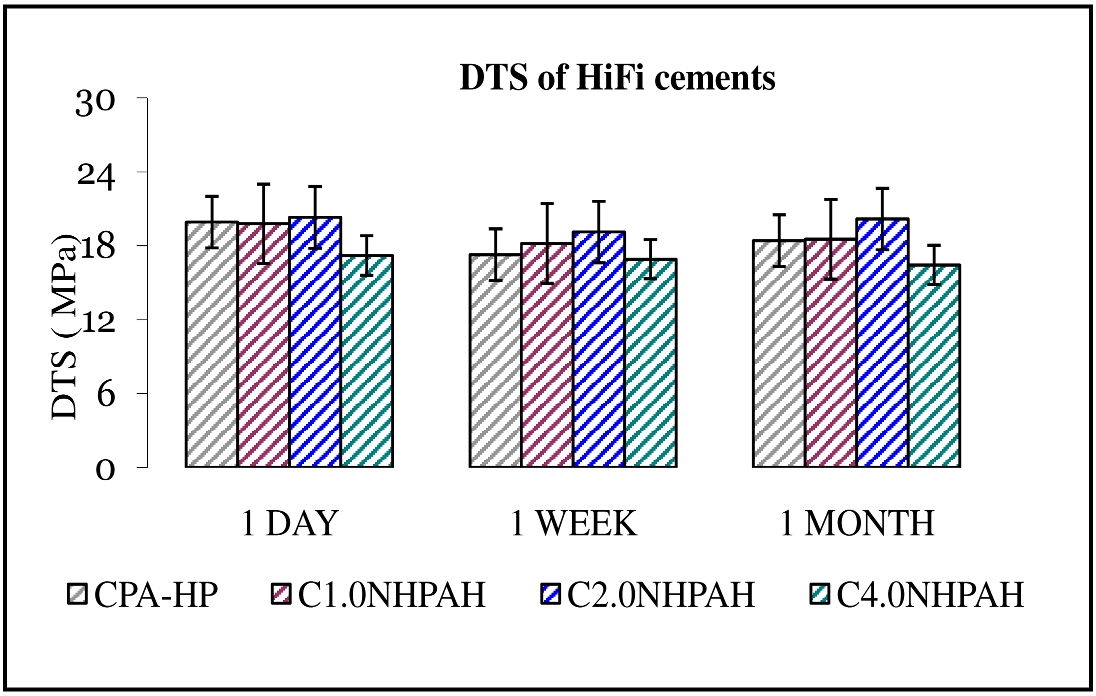

Figure 3. 21: Diametral tensile strength of HiFi cements after nanoclay dispersion in PAA liquid at different storage times.

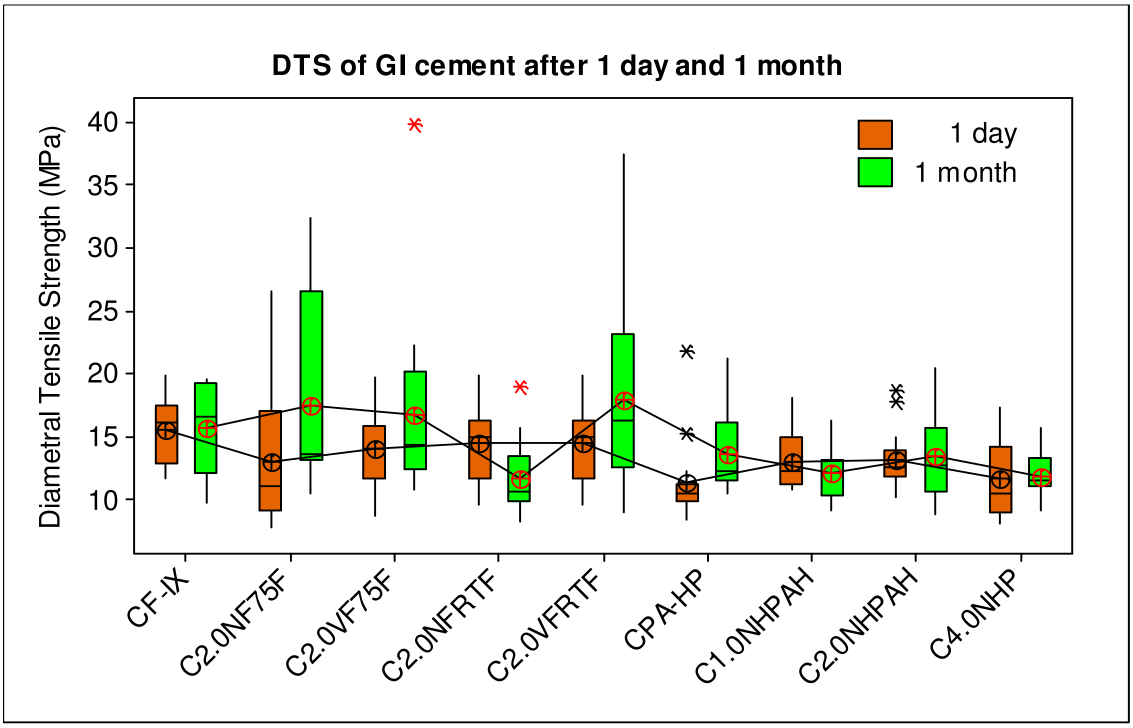

Figure 3. 22: Diametral tensile strength of cement specimens after the storage time of 1day and 1 month.

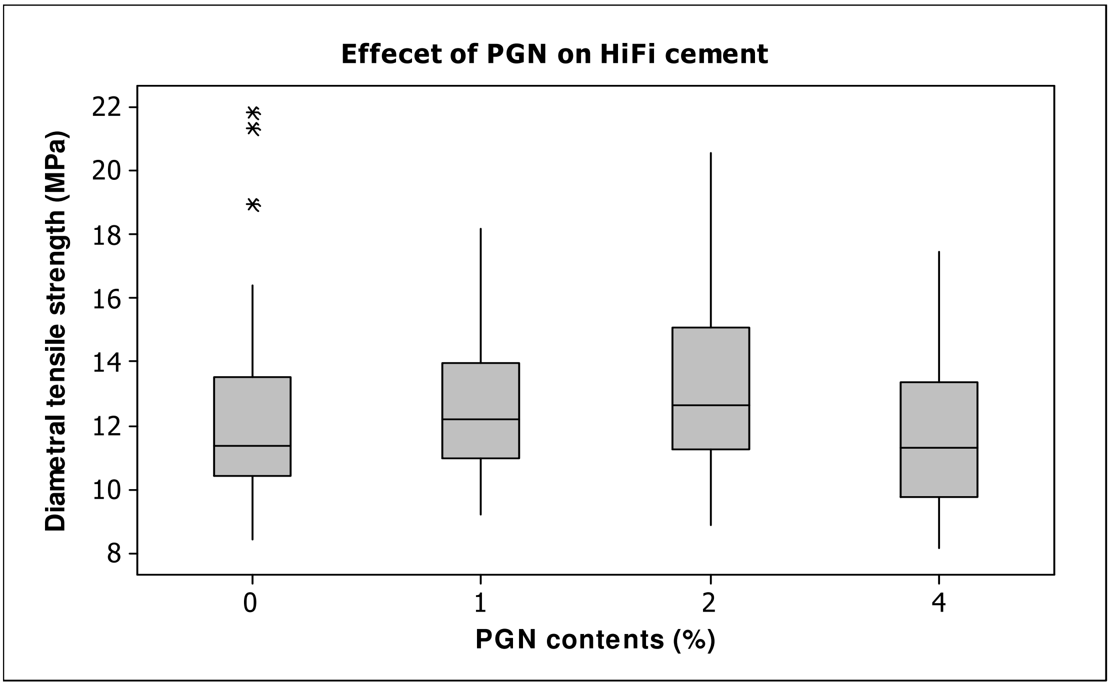

Figure 3. 23: Effect of PGN nanoclays content on the diametral tensile strength of HiFi cements.

The cements formed with the HiFi system after the dispersion of 2 wt % PGN nanoclays (C2.0NHPAH) resulted in significantly better DTS values (*P* < 0.05) in comparison to other cements for 1 day, 1 week and 1 month storage time whereas, 4 wt % PGN dispersion (C4.0NHPAH) generally demonstrated the lowest DTS. A comparison of DTS of two systems at 1 day and 1 month storage is given in Figure 3.22. Univariate GLM ANOVA and post-hoc Tukey's test highlighted no significant differences among the DTS of Fuji-IX cements tested after 1 day and month (*P* > 0.05) although cement tested at 1month showed higher mean values of DTS, likewise post-hoc Tukey's test of HiFi cement identified no significant difference (*P* > 0.05) in the mean DTS after the dispersion of different w/w percentage of PGN nanoclays. The affect of nanoclays content on the DTS of HiFi system is presented in Figure 3.23 and box plots represent a mild improvement in DTS after the addition of 2 wt % PGN which generally showed higher DTS value, however there was no significant difference (*P* > 0.05) in DTS was observed after the nanoclays dispersion when data was analysed with GLM analysis.

3.4.3 Flexural strength (FS)

The average values and standard deviation of two cement systems are given in Figure 3.25 (Fuji-IX) and Figure 3.26 (HiFi). In Fuji-IX system C2.0NF75F showed highest values (31.1 MPa) at 1 hour, CF-IX control group was better after one day (30.0 MPa) and a highest FS value was shown by C2.0NFRTF (35.1 MPa) for the cements tested after one month. Furthermore, a group comparison of the FS results of Fuji-IX system and HiFi systems at two time storage (1 day and 1month) is presented by means of box plot in Figure 3.24. In HiFi system, the dispersion of 2 wt % PGN nanoclays in polymer liquid (C2.0NHPAH) resulted in the highest values of FS for 1 day, 1 week and 1 month in comparison to other cement samples however, FS of C2.0NHPAH at 1 month (42.8 MPa) was not very much different from 1 day (42.7 MPa). Flexural strength data of both Fuji-IX system and HiFi system analysed with univariate GLM ANOVA and post-hoc Tukey's test with the confidence interval of 95% did not show any significant difference ($P > 0.05$) of the impact of nanoclays addition of both systems. The cements tested after 1 month yielded significantly higher values than 1 day group as expected. The FS values at 1 day storage time of C2.0NHPAH (2 wt% PGN nanoclays) was significantly higher ($P < 0.001$) in HiFi system but there was not difference ($P > 0.01$) found when the HiFi materials aged for 1 month before three point test.

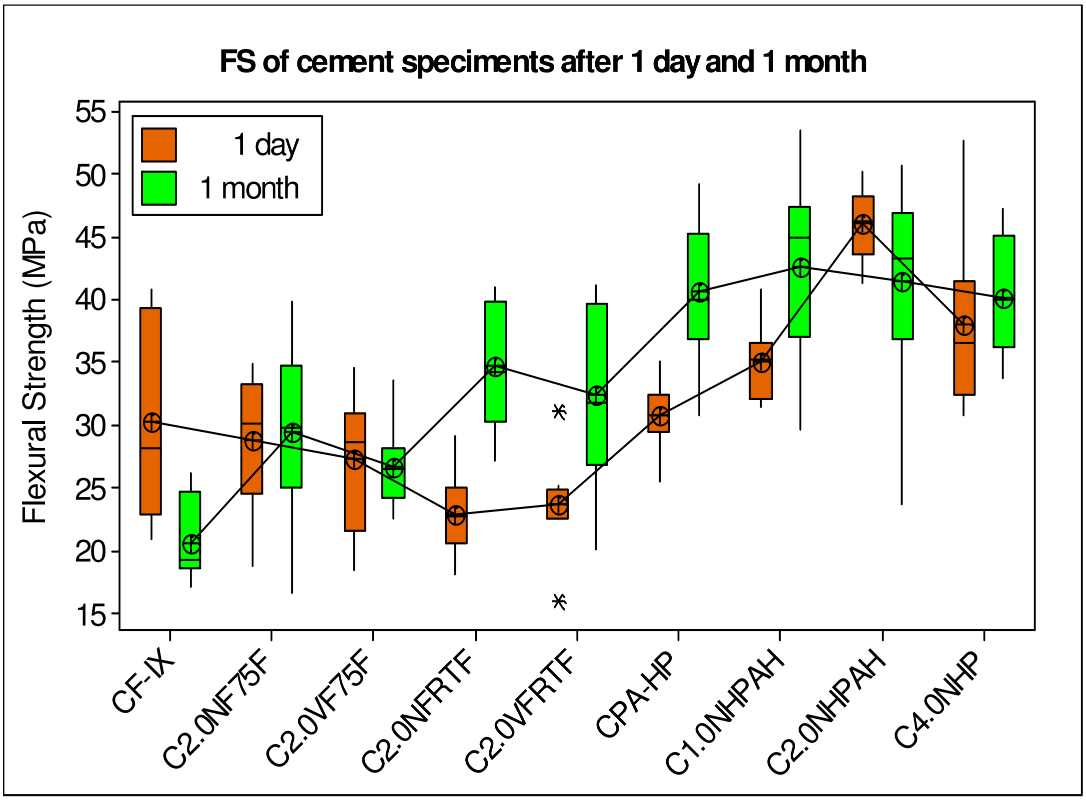

Figure 3. 24: A comparison of the flexural strength of cements tested after 1 day and 1 month.

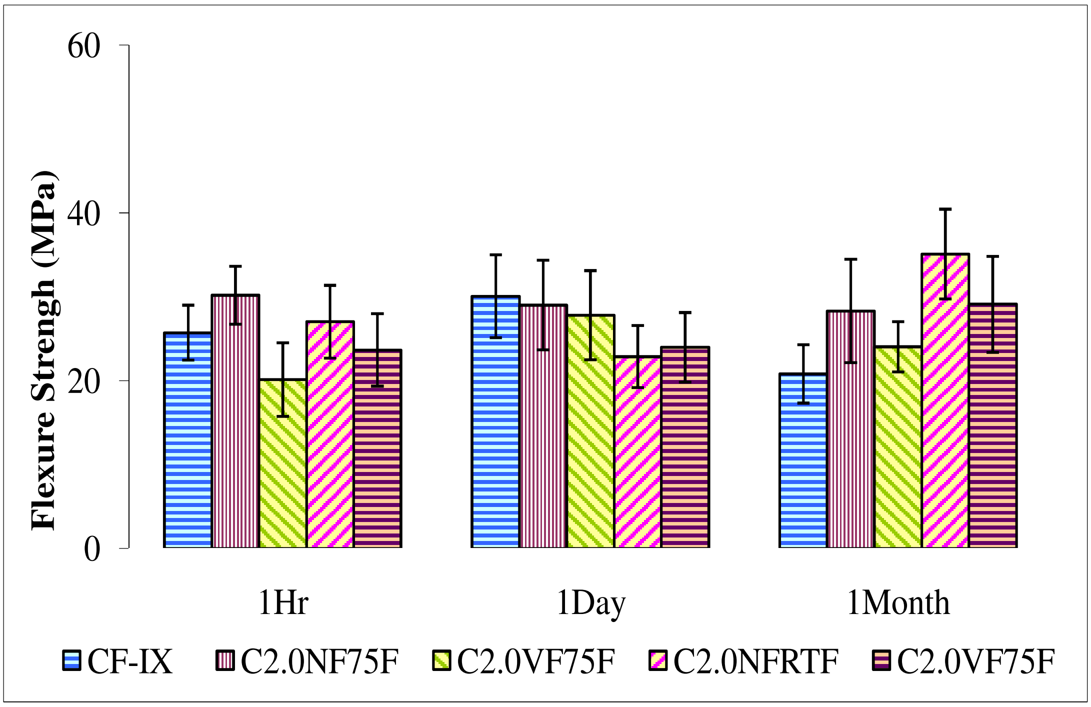

Figure 3. 25: Flexural strength of Fuji-IX system at different storage times after nanoclay dispersion.

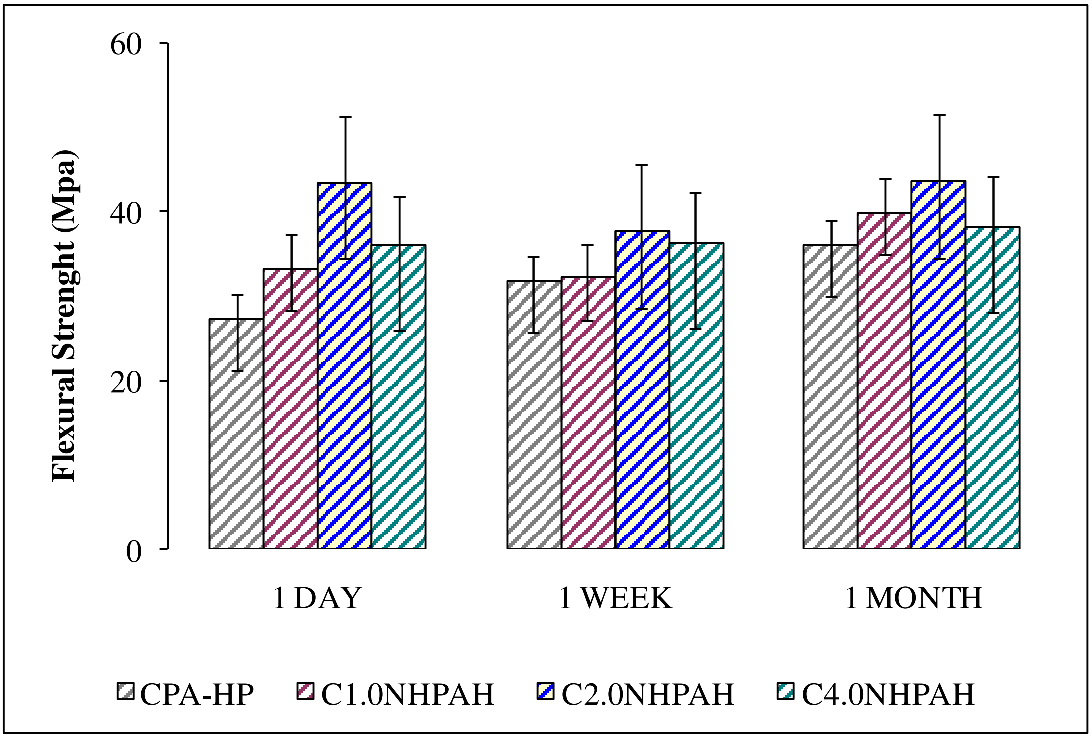

Figure 3. 26: FS of HiFi system at different storage time after nanoclays dispersion.

3.4.4 Flexural Modulus (E_f)

Flexural modulus of the Fuji-IX and HiFi systems after the dispersion of nanoclays was calculated from three-point bend test data of cements tested after 1 month storage time. Figure 3.27 presents the box and whisker plot comparison of E_f of the Fuji-IX and the HiFi systems after the nanoclays dispersion. One-way ANOVA and Tukey's test comparison of cement groups showed that the E_f of HiFi cement formed after the dispersion of 1 wt % nanoclays (C1.0N PAH) was 14.8 G Pa which was significantly higher ($P < 0.001$) at 95% significance level when data was analysed with one-way ANOVA and Tukey't test. However, there was no significant difference ($P > 0.05$) between both cement systems after the 2 wt % nanoclays dispersion in the liquid portion.

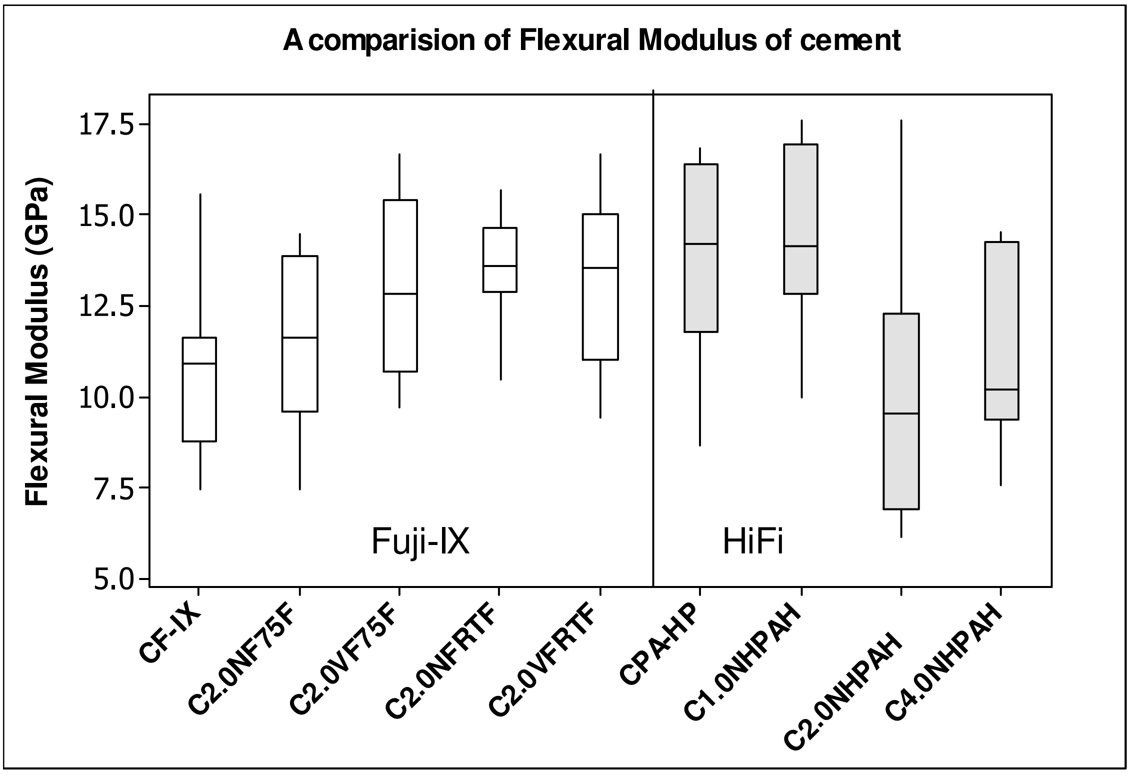

Figure 3. 27: Flexural modulus of GI cements calculated from three-point bend test.

Figure 3.28 presents the interval plot with 95% confidence interval of the mean values of the flexural modulus of four different concentrations of nanoclays and the highest value of modulus 14.50 GPa was obtained with 1 wt % nanoclays content in cement system, however, the effect of nanoclays content on the modulus of cements was not identified statistically significant (*P* > 0.058) when data was analysed with one-way ANOVA.

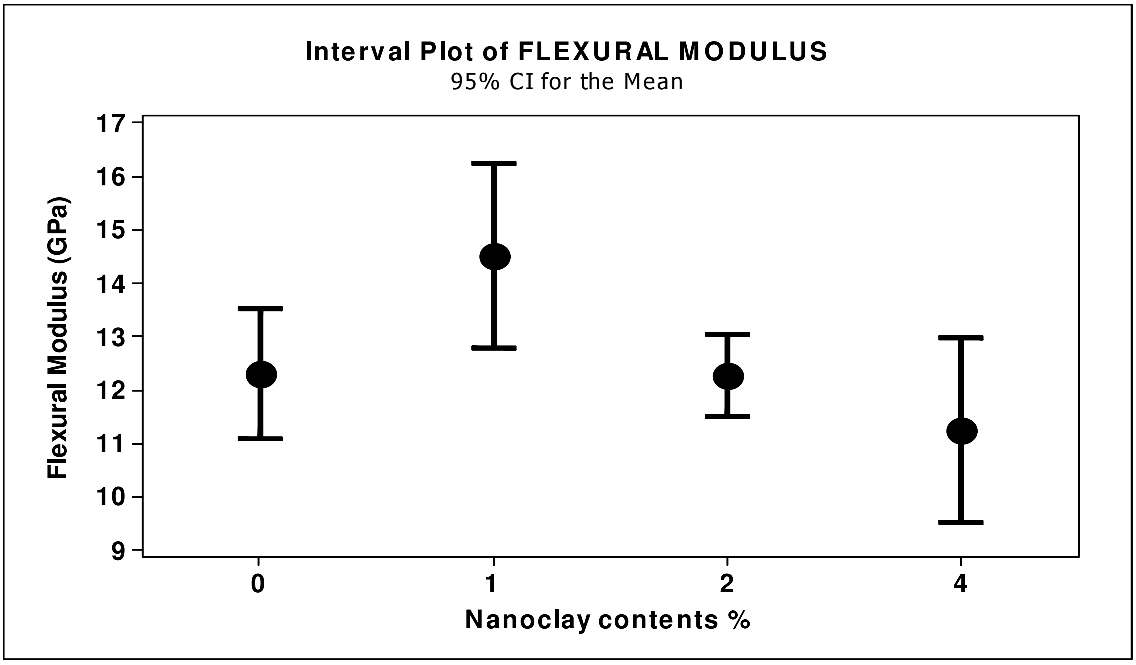

Figure 3. 28: Effects of nanoclay contents on flexural modulus of cements.

3.4.5 Vickers Hardness (HV)

The results obtained from Vickers Hardness (HV) test are summarised in Table 3.6. Since the value obtained gives the depth of indentation formed, the higher the value obtained from Vicker's indent test mean that the harder the specimen under test. At least 9 measurements were taken from a minimum of three cement specimen in each group. The data was analysed with one-way ANOVA and Tukey's test with 95 %

confidence interval. The results of HV shown in Table 3.6 depicted no significant difference ($P > 0.01$) in HV value of all of the cements despite the fact that C4.0NPAH (85.4 ± 9) showed the highest hardness among all other groups but there were also higher standard deviations. However, there is no clear indication that incorporation of nanoclays in small amount has got the tendency to improve the HV of cements when the results were analysed with one way ANOVA and Tukey's test.

Table 3. 6: Vickers micro-hardness and standard deviation of tested cements.

Cement Specimen	HV (300g)
CFuji-IX [CF-IX]	74.9 (5.6)
C2.0PGV/FL-75/FP [C2.0VF75F]	72.5 (7.2)
C2.0PGV/FL-RT/FP [C2.0VFRTF]	68.7 (6.6)
C2.0PGN/FL-75/FP [C2.0NF75F]	69.2 (4.1)
C2.0PGN/FL-RT/FP [C2.0NFRTF]	77.4 (8.9)
C40%PAA-SOL/HP [CPA-HP]	72.5 (3.2)
C1.0PGN/PAA/HP [C1.0NPAH]	62.7 (6.6)
C2.0PGN/PAA/HP [C2.0NPAH]	69.2 (4.1)
C4.0PGN/PAA/HP [C4.0NPAH]	85.4 (9.9)

3.5 Wear behaviour of cements

The nature of wear is very complex because there are several mechanisms for wear and each of which is sensitive to a wide number of parameters however, the fact is that these parameters are not necessarily the same or act in the same way. Another important point which need to be familiar with is that unlike modulus or strength of a material, wear testing, does not measure the intrinsic property of a material. Also there is no single universal parameter which can be used to characterize the wear behaviour of dental cements [246].

Table 3. 7: Description of the wear results of two GICs systems obtained by employing two different wear testing methods.

Cement specimens		**Reciprocating wear test**		**OH&SU wear test**	
		Volume (mm)^3	Depth (µm)	Volume (mm)^3	Depth (µm)
Fuji-IX	CF-IX	8.30 (2.58)	419.2 (24.0)	1.13 (0.16)	300 (15)
	C2.0NF75F	15.64 (5.35)	419.6 (24.0)	1.48 (0.14)	334 (27.0)
	C2.0VF75F	8.73 (2.19)	424.3 (30.0)	1.03 (0.19)	259 (32.0)
	C2.0NFRTF	9.33 (3.26)	423.1 (40.0)	**	**
	C2.0VFRTF	7.23 (0.61)	321.9 (18.0)	**	**
HiFi	CPA-HP	6.08 (2.1)	481.0 (43.0)	0.69 (0.13)	221 (17.0)
	C1.0NHPAH	4.90 (0.6)	418.6 (43.0)	0.94 (0.21)	291 (35.0)
	C2.0NHPAH	5.66 (1.0)	512.2 (117.0)	0.97 (0.28)	291 (33.0)
	C4.0NHPAH	6.22 (1.3)	419.0 (63.0)	1.49 (0.24)	342 (44.0)`

The type of the opposing material (antagonist), loading force and movement patterns are the critical factors when wear test are designed for reproduce the oral dental wear and it is not unnecessary to mention that there is no single universal test for wear assessment for dental materials due to challenging nature of the mastication process [15].

Table 3. 8: A comparison of the various parameters used in two wear testing methods.

Parameters		**Reciprocating Wear test**	**OHSU wear test**
Mechanism		Ball-on-flat	Simulation
Type		Two-body wear	Three-body wear
Force (N)		20	20 and 90
Sliding distance (mm)		6	7
Contact duration		All time (to-and fro)	Plough
Antagonist	Material	Alumina Al_2O_3	Steatite magnesium silicate
	Diameter (mm)	12.5	5.0
	Hardness (HV)	1700	650
	Tendency to wear	Yes	No
No. of cycles	Total cycles	10,000	50,000
	Total time (hr)	4	12
	Frequency (Hz)	1	1
Medium	Distilled water	Yes	Yes
	Slurry	No	yes
	Temperature	Room temp.	Room temp.
Profilometer	Type	Contact stylus	Non-contact optical
	Number of scans	3	1750
	Step size	1 mm	0.004 mm

Hence, a comparison of two wear test method employed in current study is given in Table 3.7 for the descriptive purpose as it is not possible to assess the result on the basis of these variables. Furthermore, the loss or displacement of a material may be reported in term of loss of mass, wear area, wear depth or wear volume. Dental cements may potentially behave differently in different wear test methods to produce different wear values resulting in different ranking of the same group of materials. Although, "volume" is the fundamental measure for wear when it is associated with the loss of a material but in dental literature two parameters namely, "total wear depth" and "total wear volume" have been reported to assess this complex behaviour [20-23].

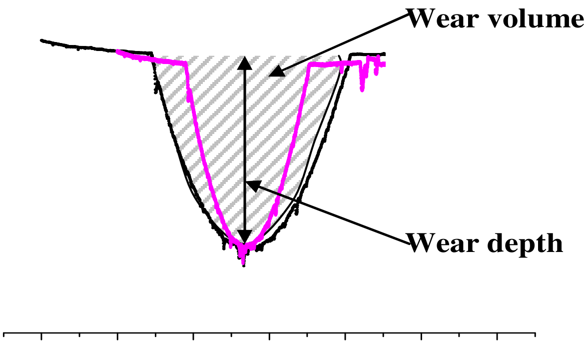

Figure 3. 29: Two wear profiles from reciprocation wear test showing same wear depth but different volume.

Wear Depth, which has been used in the past has limited clinical value because of its dependence on occlusal factors and wear area is also has inadequate value for the similar reason. Whereas, wear volume is associated with the oral environment it is thought to be independent of occlusal factors and has clinical value because it is a measure of the work done [247, 248]. However, in the *in-vitro* environment, if a material and environmental factors remain constant, volume loss is linear with time but, the relationship of wear volume and wear depth is not necessarily to be linear as presented in Figure 3.29. The wear results of current study have been analysed both in terms of depth and volume (Table 3.7) but mainly the results of wear volume will be described in detail because it is considered that the preferred parameter for measuring wear is volume [248].

3.5.1 Reciprocating wear test

The wear volume and wear depth determined by reciprocating wear test is shown in Table 3.7. Although the wear rate under the same conditions tended to differ across wear facets from area of first contact to facet centre to the area of last contact but wear volume values presented here are based on the central deepest part of the wear track to depict overall wear rates, values in parentheses represent the standard deviation for three samples. Mean wear volume for CF-IX (control group) was measured 9.60 (2.58) mm^3. C2.0NF75F showed slight higher values of wear volume 15.64 (3.35) mm^3 as compared to the wear volume of the other three cement specimens C2.0VF75F, C2.0VFRTF and C2.NFRTF in Fuji-IX cement system. There was no significant difference in the wear volume of the cements prepared with the polymer liquid after the mixing of nanoclay at two different temperatures.

HiFi cement group generally showed the better wear resistance when compared to the Fuji-IX system (Table 3.7). The dispersion of 1 and 2 wt % of nanoclays, C1.0NPAH 7.60 (2.33) mm^3 and C2.0NPAH 8.15 (1.55) mm^3 showed a slightly superior wear resistance than the control group CAP-HP 8.50 (1.56) mm^3. C4.0NPAH, which contain 4 wt % PGN nanoclays showed the highest wear volume 12.09 (1.08) mm^3 indicating the worst wear resistance among all the cements in HiFi group. However, no significant difference ($P > 0.05$) was found in wear volume of HiFi cement system with the different nanoclays content when data was analysed by one-way ANOVA and post-hoc Tukey test. Figure 3.30 shows the comparison of the wear volume and HV values of the HiFi system at different nanoclays content (wt %). A linear relationship between the wear volume and hardness of the materials is generally obtained when the materials are compared by using this parameter [171].

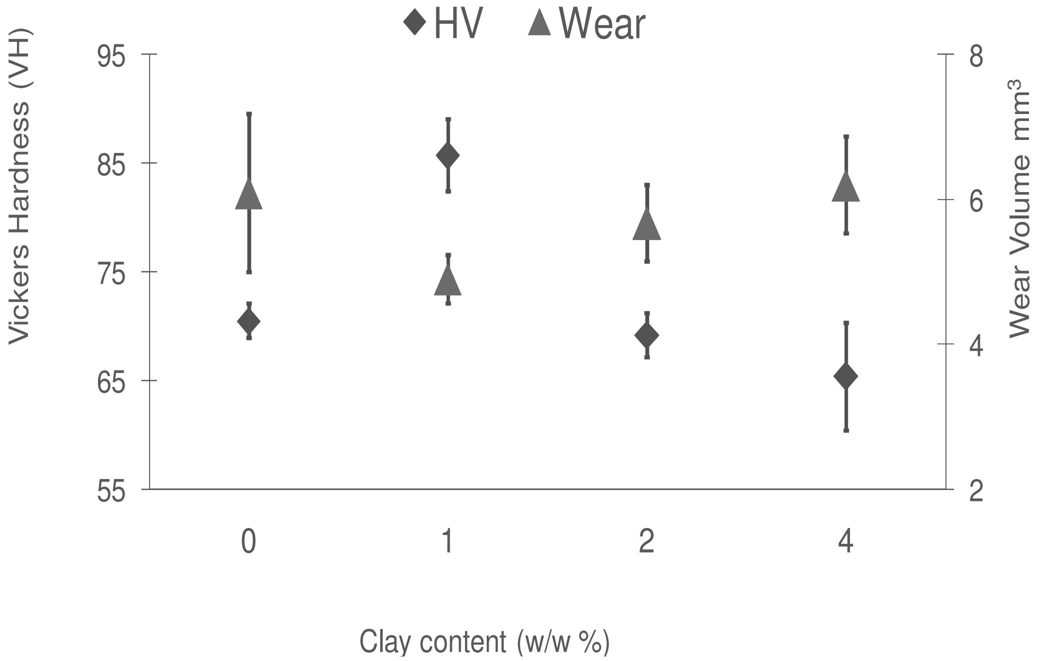

Figure 3. 30: A comparison of the reciprocating wear volume and HV of HiFi cements with different nanoclays content (wt %).

3.5.2 OH&SU wear test

The effect of nanoclays on total wear volume and total wear depth is presented in Figure 3.31. A significant difference ($P < 0.013$) of total wear volume was identified for 4 wt % PGN nanoclays content (C4.0NHPAH) and similar trend was observed for total wear depth of cements ($P < 0.019$) when result of different clay content was analysed using one-way ANOVA and Tukey’s test with the confidence interval of 95%. Figure 3.32 and 3.33 present the comparison of total wear volume and total wear depth of the four specimens in each cement group in relation to the mean abrasion and mean attrition values extracted from the raw data. The analysis of variance (on the raw data) was performed using a one-way ANOVA and Tukey's test for the analysis of the mean total volumetric wear and the mean total wear depth. There was no significant difference (*P* > 0.001) found in total wear depth and total abrasion depth in all cement groups. The total attrition depth of CPA-HP (control group of HiFi) was calculated as 189.23 microns and was significantly different (*P* < 0.001) when compared to total attrition wear depth of other cement groups. On the other hand, one-way ANOVA and Tukey's analysis of total wear volume found no significant difference (*P* > 0.001) in cement groups. The total attrition volume and total abrasion volume of C2.0NF75F was significantly different (*P* < 0.001) and the total abrasion volume of C4.0NHPAH was also statistically different (*P* < 0.001) when compared to the other cement in the similar group. The relationship of an average facet length (mm) of four samples of each group of cement is shown in Figure 3.34 and there was no significant interaction (*P* > 0.057) observed among different cement groups evaluated using Tukey test. Figure 3.35 shows the 3D images of the tear drop shaped wear facet produced by OH&SU wear simulator.

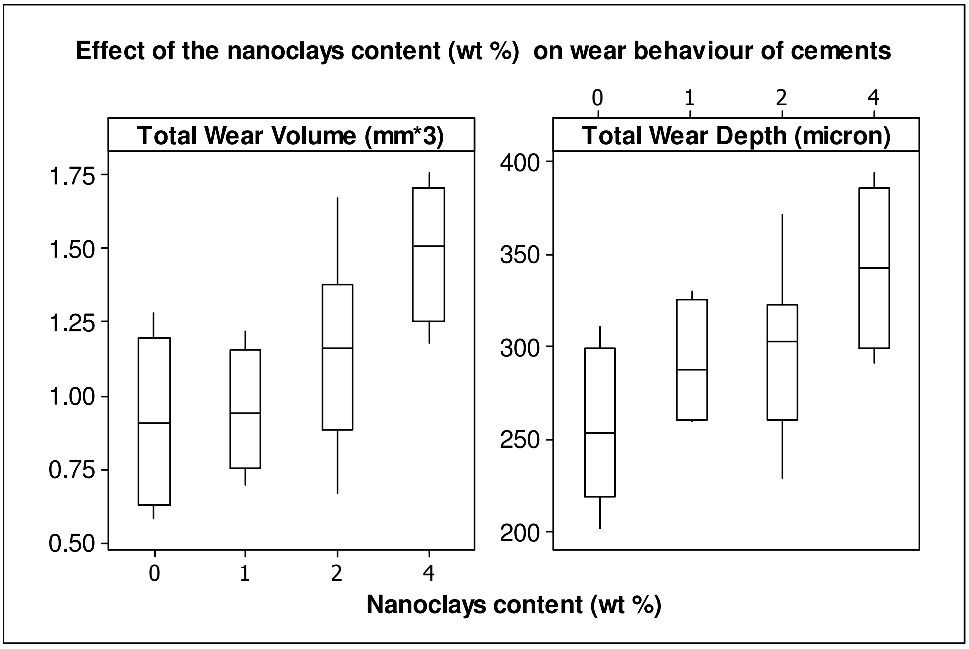

Figure 3. 31: Effect of nanoclays content on the wear resistance of cements.

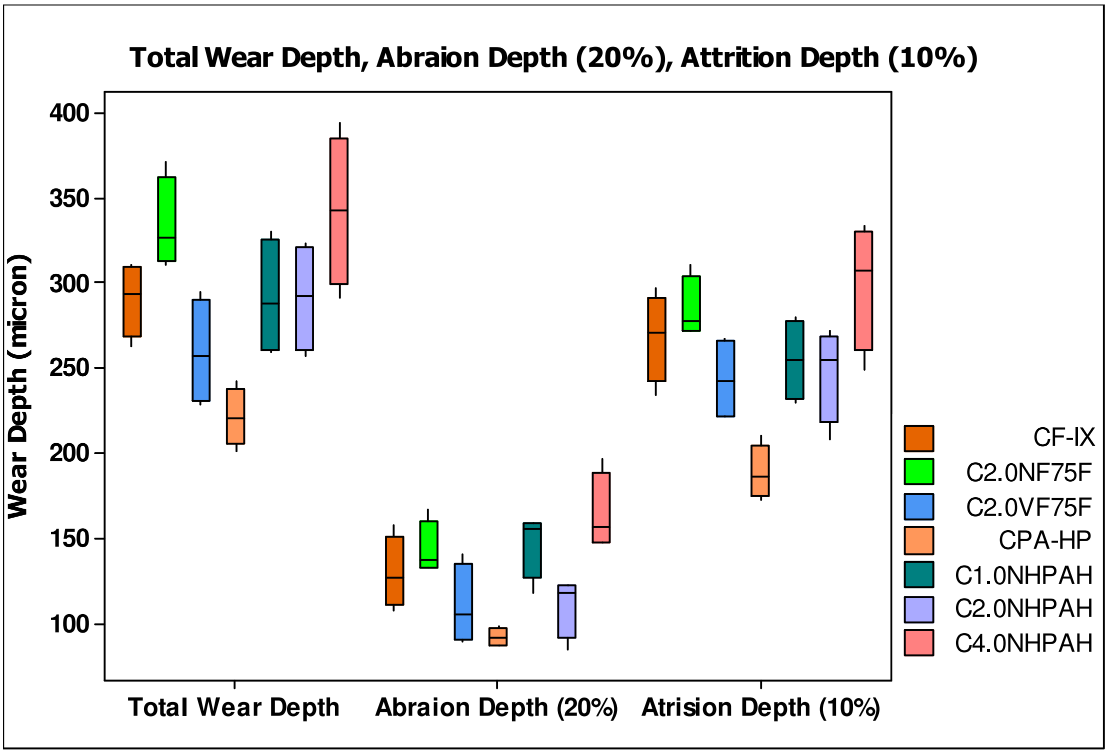

Figure 3. 32: A comparison of total wear depth, abrasion and attrition wear depth area across the wear facet.

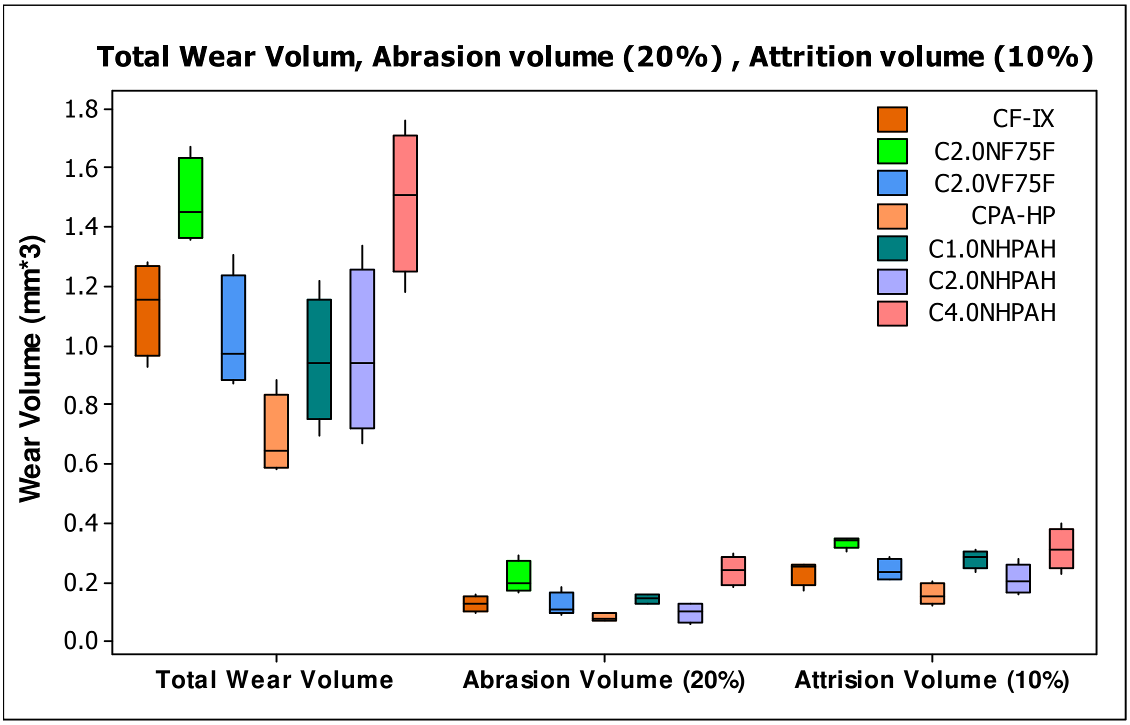

Figure 3. 33: A comparison of total wear volume, abrasion and attrition wear volume of the wear facet.

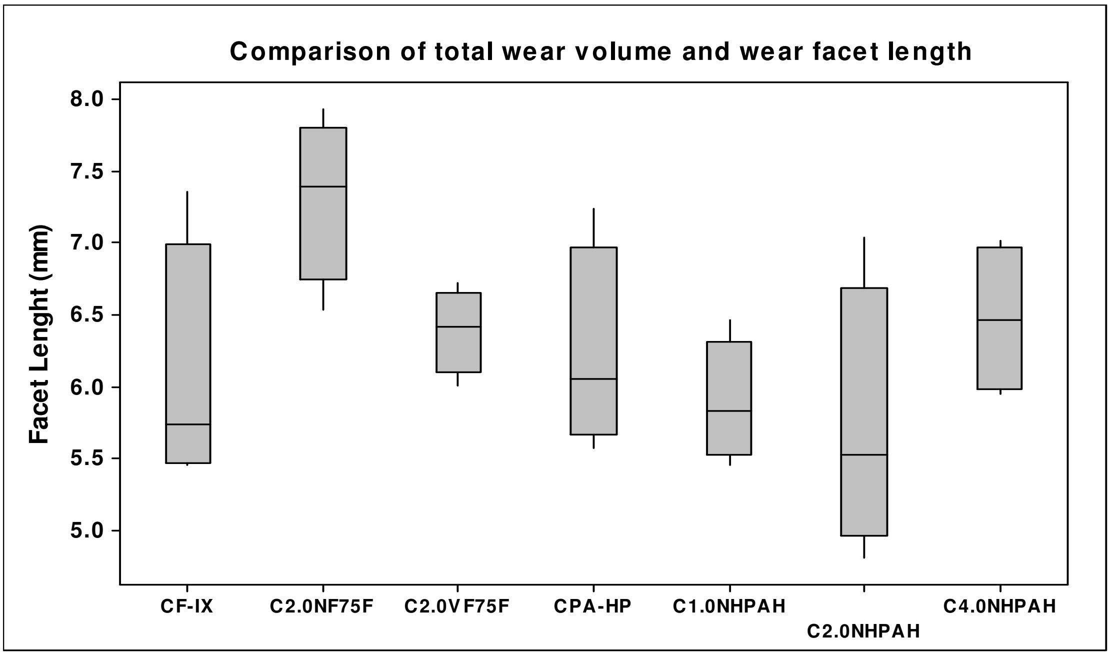

Figure 3. 34: Schematic representation of the effect of the wear facet length on wear volume.

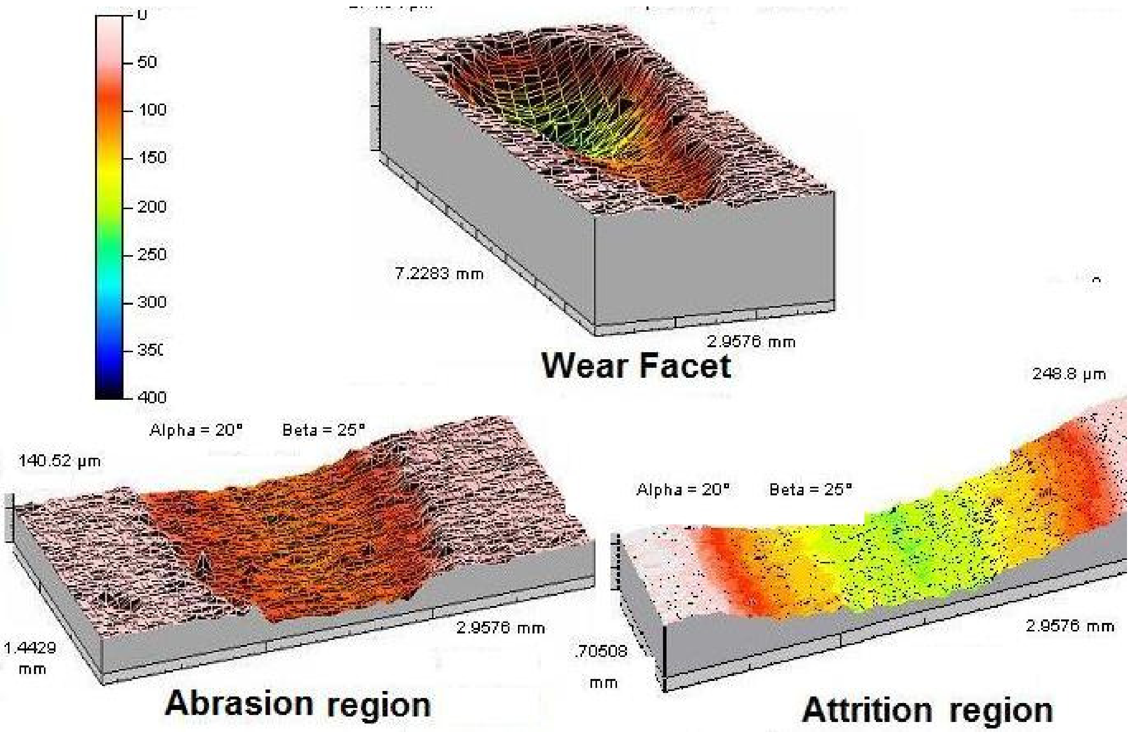

Figure 3. 35: A tear-drop shaped wear facet produced by OH&SU wear simulator showing abrasion and attrition region.

3.6 Electron Microscopy of Cements

Electron microscopy was carried out on the fractured surface of beam shaped specimens after three-point bend test. Figure 3.35 illustrate the cryo-SEM micrographs of the representative regions of the fractured surface for Fuji-IX (CF-IX) cement after three-point bending at lower magnification as well as high magnifications. Generally, the artifactual cracks were ubiquitously observed when within the glass ionomer cement matrix when GIC's specimens were examined by conventional SEM due to the dehydration of cement. However, the representative cryo-SEM micrographs of the fractured surface of bar-shaped specimens demonstrated that only a few or no micro-cracks on the surface of glass ionomer cements matrix were observed. The presence of some pores and air voids on the surface of GICs can also be observed. The size of the glass particles was measured under 5 µm in the micro-graph of Fuji-IX cement. Due to the small amount of nanoclay wt % used, it was difficult to study the dispersion of nanoclays in GIC by scanning electron microscopy. Therefore, transmission electron microscopy was employed to study the structure and interaction of nanoclays and GICs. The TEM micro-morphological appearance of glass fillers, GIC matrix and nanoclays is presented in Figure 3.36. The different phases of glass ionomer cement were readily observed from the TEM micrographs of C2.0VF75 (Fuji-IX with 2 wt % PGV nanoclays). The porous structure of glass filler particles indicated the acid attack of PAA resulting in the formation of siliceous hydrogel layers all around the glass core. The porous nature of glass filler particles is retained within the silica gel layers after depletion of ions from the surface of glass particles [249]. The presence of nanoclays with in GIC matrix was also observed which supported the finding of the interaction of PAA with nanoclays described in section 3.1. TEM observation confirmed that the layers of nanoclays were mostly exfoliated and dispersed in the matrix of GICs after the mixing the PAA liquid constituent containing nanoclay with the aluminosilicate glass powder

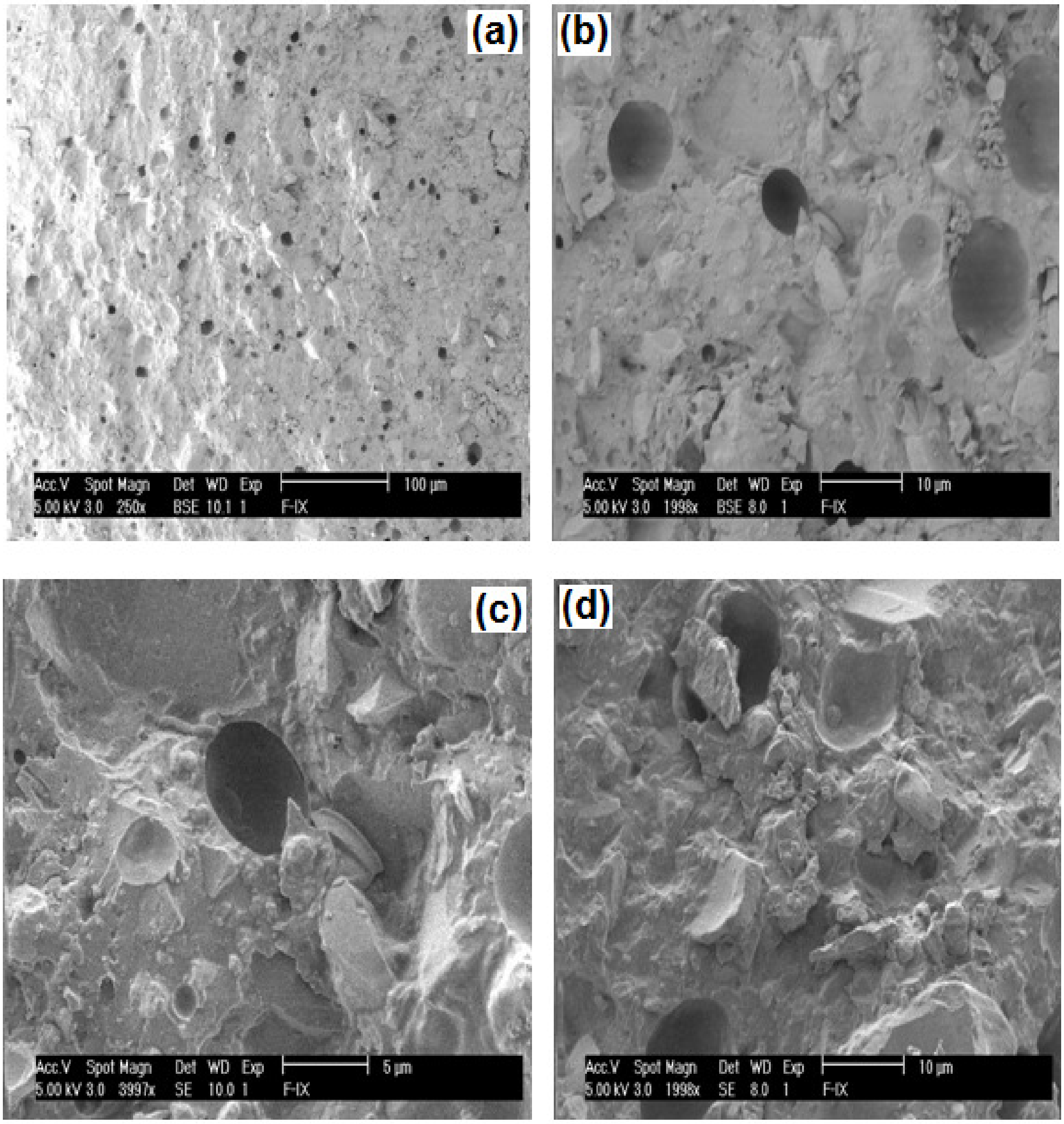

Figure 3. 36: Cryo-SEM micrographs of the fractured surface of Fuji-IX (CF-IX) at various magnifications demonstrating, (a) micrograph at lowest magnification (× 250) showing the absence of the cracks, (b, c, d) micrographs at high magnifications (× 1998 and × 3997) indicating the presence of pores, glass particles and the matrix phase of GIC.

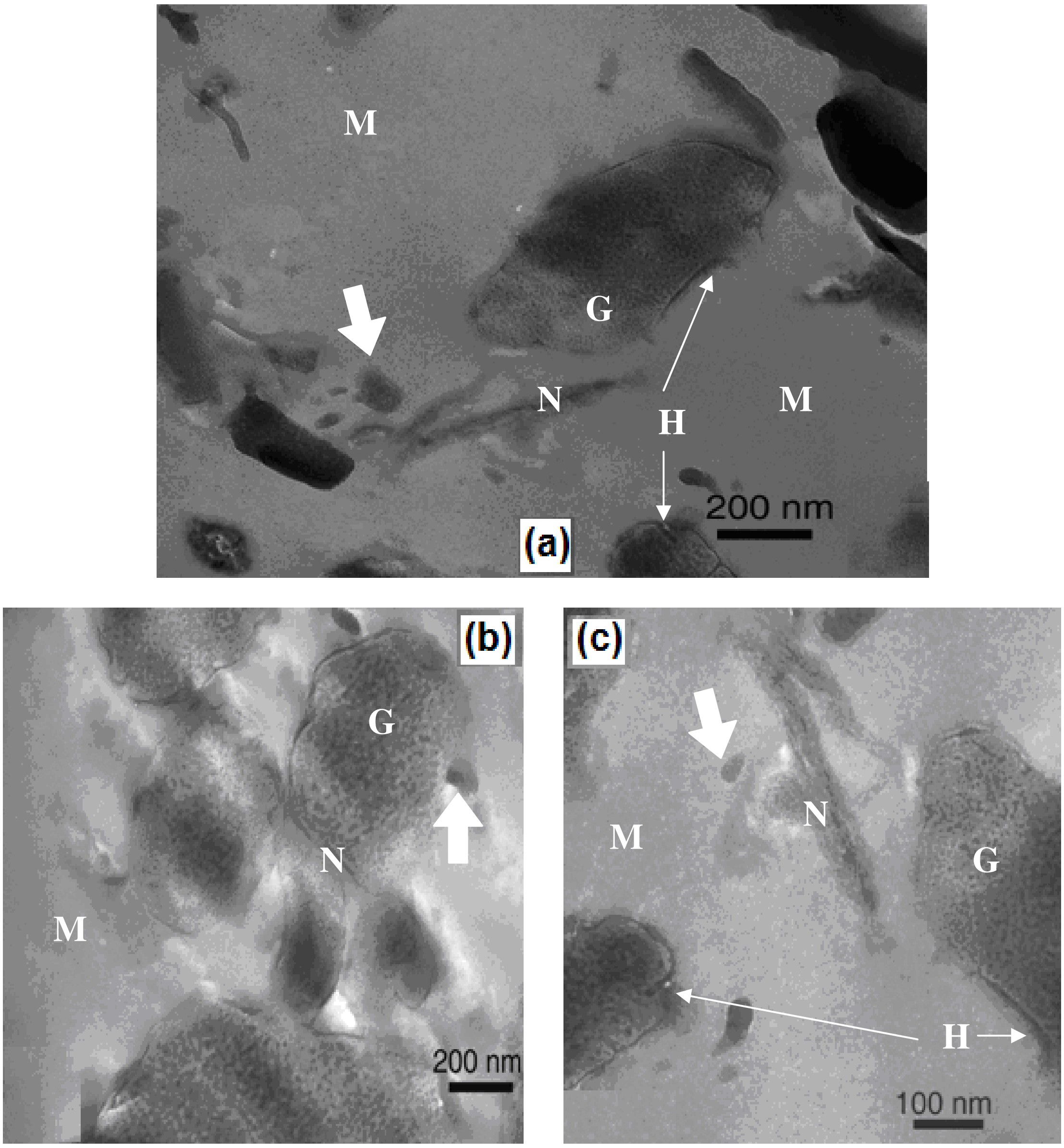

Figure 3. 37: TEM micrographs of Fuji-IX cement after the dispersion of 2 % nanoclay in liquid portion (C2.0NF75) showing the interaction of nanoclays within GIC system, (a and b), at lower magnification and, (c) at higher magnification indicating remnant glass core (G), nanoclay (N), siliceous hydrogel layers around the periphery of glass filler core (H), cement matrix (M), fully reacted hydrogel within the matrix (white bold arrow).

CHAPTER 4

4 DISCUSSION

A cursory glance at the available literature showed that polymer–clay nanocomposites are the focus of strong research interest worldwide due to the remarkable improvements in various properties of polymer composites at low filler loadings. According to SCOPUS data-base, the papers on “polymer-clay nanocomposites” in major international journals exceeded 700 in 2008 alone. In some review papers on “polymer-clay nanocomposites”, Alexandre [9], Vaia and Giannelis [10, 250], Ray [207, 251], Pinnavaia [11, 183], Fischer [252] and Okada [253, 254] confirmed, that significant research is still required to develop further the understanding of structure-property relationships in several polymer-clay systems. However, the current commercial applications of polymer–clay nanocomposites are limited due to the difficulty in achieving exfoliated structures across the polymer matrix and optimization of the processing methods. Such difficulties are due to incomplete understanding of the complex experimental factors and the interactions that may control the development of different nanocomposites and particularly GICs, which are discussed here. The present study focuses on the reinforcement of GIC systems with nanoclays. Therefore, the acquisition of quantitative and qualitative information of PAA-nanoclay and GIC-nanoclay interactions are the basis for developing a potential commercial product. In the next sections, such interactions are discussed which are particularly important for advancing the fundamental understanding of dispersion of nanoclays in the GIC systems.

4.1 Dispersion of polymer-grade (PG) montmorillonite

The incorporation of low concentration of nanometer-sized fillers has become a popular strategy to improve polymer materials in recent years. A uniform dispersion and controlled association of nano-particles with the matrix is also thought to significantly improve the properties of a material. The exfoliation of montmorillonite type nanoclays in a polymer matrix provides at least 10 Å thick silicate layers with the high in-plan bond strength and aspect ratios comparable to those found for fibre-reinforced polymer composites, for example, nanoclays exfoliation in nylon-6 matrix by Toyota researchers was shown to greatly improve the mechanical properties of the matrix. Since the invention of polymer (nylon-6) clay nanocomposites by Toyota Central R&D Labs Inc. [255] and the pioneering studies on nanoclay-epoxy systems by Pinnavaia [256-258], extensive research on the dispersion, intercalation and exfoliation of clays has been carried out and has been reported in the literature [191, 207, 254, 259-264].

To achieve maximum polymer-nanoclay interaction, the choice of an appropriate grade of nanoclays suitable for use with poly(acrylic acid) (PAA) is the first step towards the development of nanoclay-based glass ionomer dental cements. In the present work, two different polymer-grade nanoclays (PGV and PGN) were selected. The nanoclays were purified by the manufacturer (Nanocor Inc) and were regarded as GRAS (Generally Regarded As Safe) substances by the U.S.A Food and Drug Administration (FDA) [265]. The differences between these nanoclays are mainly the amount of sodium, aluminium, magnesium, potassium and iron content (Table 2.1) and the cation exchange capability index (CEC) which is larger for the PGV than for the PGN (Table 2.2).

The nanoclays are considered to be of a medical grade according to the suppliers and therefore it was thought that it would be valuable and interesting to investigate their potential application as reinforcing agents in dental and biomedical materials. After the selection of the appropriate nanoclays there are two main challenges; the interaction of nanoclays with the polymer matrix and the choice of an appropriate processing method to achieve uniform distribution of the nanoclays within the polymer matrix [9, 216]. The interactions occurring at the polymer-nanoclay interface are very complex. Shi *et al.* studied the interfacial interaction of organoclays with epoxy resin and proposed a model presented in Figure 4.1.

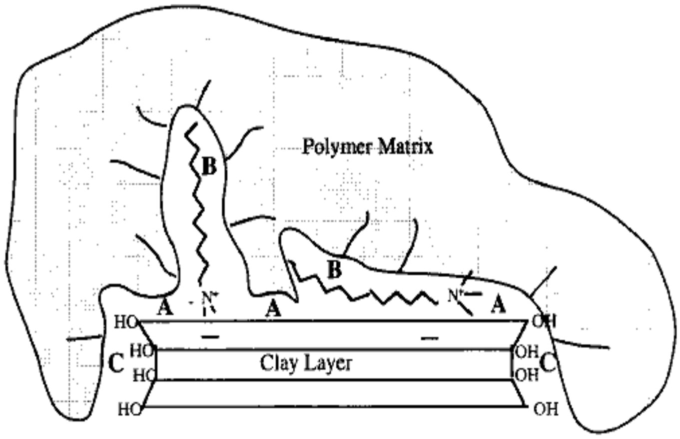

Figure 4. 1: Schematic illustration of different types of interfacial interaction, (A) adsorption (direct bonding) of polymer on nanoclay surface, (B) dissolution of onium chain into polymer matrix, (C) polymer binding to hydroxylated edge site [266].

The ion exchange of the Na^+ gallery cations in nanoclays by organic cations, particularly alkylammonium ions allows the modification of the nanoclays gallery surfaces for the dispersion of the polymer precursors. Shi *et al.* [266] described the three types of poly-nanoclays interactions in epoxy-clay nanocomposites as shown in Figure 4.1. In type A, the polymer is adsorbed directly to the chemically inert network of siloxane oxygen atoms on the basal-surfaces of the silicate plates, in type B, the alkylammonium chains dissolve into the polymer matrix and, in type C, the hydroxylated edges of the silicate layers bind with the polymer matrix [266].

Traditionally, nanoclays are combined with the host polymer either by a neat or volatile solvent followed by extensive mechanical mixing of the clay-solvent in the polymer by employing a mixing kit [160]. Three types of mixing equipment are recommended to disperse the nanoclays in resin namely, high-shear mixer or 3 roll mill for liquid resin, Brabender mixer for viscous resin or twin extruder for solid resin [160]. However, in the current study a relatively simple procedure has been adapted for the dispersion of nanoclays either by mixing them in a PAA solution at 75°C or by exfoliating initially the clays in water and then adding an appropriate amount of dehydrated PAA powder continuously stirring the mixture at 75°C for 24 hours. Tran *et al.* [267] previously reported a similar technique and suggested that mixing of nanoclays with the polymer resulted in the formation of silicate (Si-O-M) or silica (Si-O-Si) nano-plates, which were incorporated in the liquid phase of the polymer. Generally, nanoclays are hydrophilic materials and chemical modifications with surfactants such as alkyl or quaternary ammonium salts, alkyl imidazoles and coupling agents are required to improve hydro-phobicity in order to make them compatible with the hydrophobic nature of certain polymers [160, 268]. The ammonium group of these surfactants reacts with the silicate surface of nanoclay via sodium cations and the hydrophobic alkyl chains interact with the organic polymer [269].

According to Nanocor Inc. the supplied nanoclays did not require any pre-treatment with surfactants and could be directly added to PAA systems [265]. Previous studies, on epoxy nanocomposites [270-274], and PAA-nanoclay interactions [12, 13, 267] showed that increasing the temperature, resulted usually in better exfoliation of nanoclays within the polymer matrix. The mechanism involved in the formation of such nanocomposites is that the polymer chains extend the silicate layers until a thermodynamic equilibrium is reached between the polymer and the higher surface energy of the silicate plate. However, the charge density of silicate layers, the nature of the interlayer exchanged ions, the curing conditions as well as the nature of the polymer determine if an intercalated or an exfoliated structure can be achieved [274]. The reinforcing capability of nanoclays is due to its high modulus, high strength and high aspect ratio [275]. The better the exfoliation of nanoclays in the polymer matrix, the greater is the reinforcing effect resulting in superior polymer nanocomposites. The use of high-speed mixing may cause the breaking up of nanoclay sheets resulting in reducing their aspect ratio and achieving better polymer-nanoclay interactions. More recently, the effects of temperature, speed, and duration of mixing on the dispersion of nanoclays (e.g., cloisites) in epoxy resin were studied by Ngo *et al.* [276] using XRD and TEM analyses. They reported that although the mixing temperature, speed and time do not significantly affect the intercalation of organo-clays at the pre-mixing step in epoxy resins but these factors contributed in splintering of nanoclays into smaller aggregates. Ngo *et al.* also recognized that the effect of mixing speed was more evident than the mixing temperature in terms of nanoclays dispersion. The mixing temperature at 120 °C and the mixing speed at 24,000 rpm was recommended to achieve the appropriate dispersion of organically treated nanoclays in epoxy nanocomposites [276].

4.1.1 XRD analysis

The XRD graphs shown in Figures 3.1 and 3.2 demonstrated that PGV and PGN nanoclays were respectively exfoliated and intercalated and the increase in the interlayer distance was due to the adsorption and segregation of PAA chains into the interlayer space. The main diffraction peak in the XRD pattern of PGV was present at $2\theta = 6.95°$ and the interlayer space was 12.39 Å whereas in PGN the main diffraction peak appeared at $2\theta = 7.13°$ and the interlayer space was 12.71 Å, a little bit larger than in the case of PGV. Although the lack of d_{001} peak in the XRD pattern of PAA-PGV indicated the full exfoliation of the nanoclays in PAA, it is important to note that due to the limitation of the XRD equipment used in the present work it was not possible to collect the spectra in lower angle than $2\theta = 3.5°$. Therefore in the case of PAA-PGV, there is possibility that the [001] diffraction peak may have further moved to a lower angle which was not in the detectable range. However, in PAA-PGN samples the shifting of 2θ values to a lower angle indicated most likely only intercalation due to the small increase in the interlayer space. In PAA-PGN samples it is clear that increasing the PGN nanoclays content from 0.5 to 8.0% did not influence the interlayer space between the silicate plates of PGN and the d_{001} peak was present at similar 2θ values for all samples. Based on the information obtained by the available literature [10, 12, 207, 277] we can assume that intercalated nanoclays should be these structures which the interlayer space increased due to the adsorbed PAA chains on the surface of nanoclays and the XRD graph still showed a broad peak shifted to lower angles associated with the out-of plane direction of the silicate plates. Similarly, the XRD pattern of fully exfoliated nanoclays should not exhibit the d_{001} peak at low angle values.

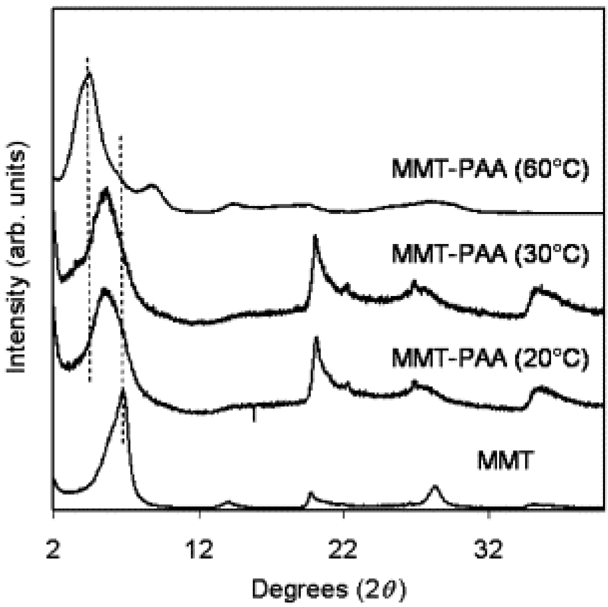

Figure 4. 2: XRD spectra of MMT-PAA prepared at different temperature [12].

Tran *et al.* [12] investigated the nanoclays dispersion in PAA at various temperatures (Figure 4.2) and proposed a model suggesting that the increase in the interlayer distance is dependent upon the reaction temperature as shown in Figure 4.3. According to this model under low pH conditions, a possible exchange of Na^+ ions by H^+ ions can form surface hydroxyl groups leading to hydrogen bonding with the carboxyl groups in PAA (Figure 4.3). Tran *et al.* also observed that when the mixing temperature was increased (from 30 to 60°C), the interlayer spacing increased from 16 to 20 Å. Several mechanisms could explain the above observation. First, according to the model in Figure 4.3, there could be other additional layers of PAA adsorbed within the interlayer space. Another explanation could be, that the entropy of the polymer was higher at 60°C than at 30°C and there was not enough time for the polymer to reorganise itself on the surface of nanoclays resulting in random binding of the carboxyl groups to the nanoclays surface instead of binding to adjacent carboxyl groups. This would also result in a disordered surface and a reduced surface coverage per molecule whereas, a more thick layer of PAA can most likely form, sterically stabilising the nanoclays surface with increasing the temperature [12].

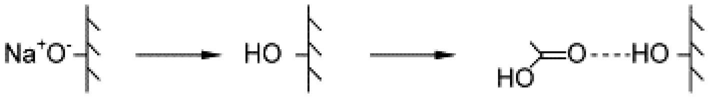

Figure 4. 3: A possible PAA-nanoclay reaction model proposed by Tran *et al.* [12].

The type of dispersion of the PGV and PGN nanoclays within the PAA matrix is dependent upon the polymer-nanoclay interaction. Therefore, on the basis of the results obtained from the XRD, it may be suggested that in the solid products recovered from the PAA-PGN reaction, one or more polymer chains might have penetrated in between the silicate plates of PGN and the lamellar structures of nanoclays remain intact resulting in intercalation. On the other hand, the solid residue recovered from PAA-PGV reaction resulted in the separation and random orientation of the silicate plates in nanoclays suggesting full exfoliation of nanoclays in this case [278]. Furthermore, during the interaction of the hydrophilic nanoclay platelet surfaces with PAA, their natural interstitial metal cations (K^+, Na^+, Li^+, Mg^{2+}, Ca^{2+}, etc.) are exchanged with protons and/or released within the organic PAA solution. This cation exchange forms more organophilic galleries within nanoclays enhancing the increase in *d*-spacing and simultaneously reducing the attractive forces between the platelets [12]. PAA can then intercalate more readily and further expand the *d*-spacing in nanoclays, leading to more efficient platelet exfoliation and improved clay dispersion into the polymer solution at the nanometer scale.

4.1.2 XPS analysis

To develop further our understanding about the PAA-PGV and PAA-PGN interactions, element specific X-ray photoemission spectroscopy (XPS) was employed. XPS measurements allowed the determination of elements involved in the PAA-nanoclay reaction, which resulted in an increase of the interlayer space between the silicate plates.

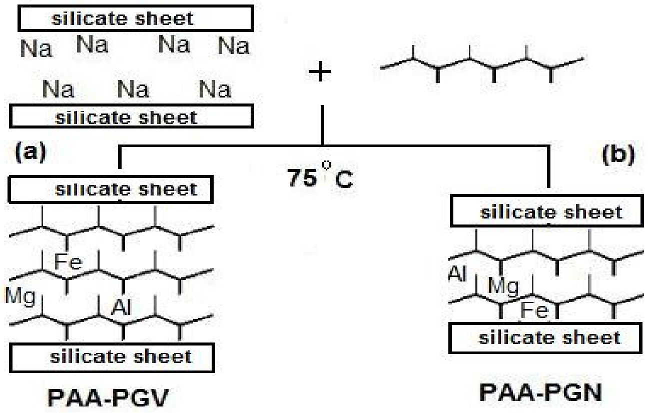

Figure 4. 4: Illustration of the interactions between the polymer-grade nanoclay and the aqueous solution of PAA (model modified based on the model presented in [12]).

Extending the model described above in Figure 4.3 to the XPS results, the expansion (intercalation) of the interlayer space suggested that the interlayer space of the silicate plates may accommodate at least two layers of fully extended PAA chains, which are bounded to the silicate surface via a number of carboxyl groups or to each other via hydrogen bonds. For example, the expansion of clay galleries due to intercalation of nanoclays in the case of PAA-PGN may accommodate a few PAA chains, whereas in the case of PAA-PGV, exfoliation of silicate plates may result in a larger number of PAA chains between the interlayer spaces (Figure 4.4). The results of the XPS study are presented in Figures 3.3, 3.4, 3.5, and 3.6. Si-O-Al linkages can be identified in both PAA-PGV and PAA-PGN treated nanoclays at the lower binding energy of the wide-scan XPS (78-160 eV) which are associated with the Si 2p or Si 2s and Al 2p or Al 2s photoelectrons from the silicate layers. The presence of one additional small peak assigned to Mg KLL at 281 eV in both nanoclays before and after the treatment with PAA, indicates that there is a small amount of Si-O-Mg present in the silicate layers. The intensity of Si 2p, Si 2s, Al 2p, Al 2s and Mg KLL peaks was slightly higher in PAA-PGN and PAA-PGV samples when compared to the respective nanoclays, however it is not clear what is the significance of this observation as all the above peaks present in the treated nanoclays are clearly only associated with the presence of nanoclays (Figures 3.3 and 3.4). On the other hand the presence of O1s peak is clearly associated with both nanoclays and PAA whereas the presence of C1s is obviously associated only with the PAA. The detailed analysis of the peaks at lower binding energy using narrow-angle XPS would be interesting in order to study the influence of cations in the chemisorption of nanoclays and PAA. Unfortunately, these data cannot be presented here as this type of analysis was not conducted. Wide-scan XPS on the other hand, showed that Fe 1p and Fe 2p peaks were also present at 773 eV associated with the presence of Si-O-Fe species in the silicate layers. This is in good agreement with recent studies where X-ray absorption fine structure (NEXAFS) of PAA-MMT was applied and reported by Tran *et al.* [13]. It was shown, that PAA caused oxidation of Fe^{2+} ions resulting in enhanced dispersion of MMT. In this study, the binding energy at 1077 eV was attributed to Na 1s or Na KLL peaks in PGV and PGN nanoclays (Figure 3.3 and 3.4, respectively). However, Na ions were not detected in the wide-scan of both PAA-PGV and PAA-PGN suspensions indicating that they have been removed from the surface of silicate plates during the interaction of PAA with nanoclays at 75°C and are probably replaced by protons from the PAA solution. This finding actually justifies the model described in Figure 4.3.

The narrow-angle scans of C 1s and O 1s are shown in Figures 3.5 and 3.6. The C 1s scan of PAA shows the characteristic peaks of C-C at 287 eV and C-COOH at 293 eV. Leadly and Watts [279] studied the interaction of the X-ray source with PAA thin layers on metallic substrates and reported that changes in the C 1s high resolution spectra of PAA layers in the energy range of 286-287 eV (especially the appearance of a weak shoulder next to the main peak) were due to C-O-C and C-OH rearrangements in PAA chains due to the monochromatic X-ray source. In our case, we did not observe a similar pattern and therefore we are not able to comment on polymer rearrangements due to degradation resulting from the exposition to the monochromatic X-ray source. In PAA-PGV samples there is a broadening and slight shifting of the C-C peaks, however the peak associated with C-COOH at 292 eV became very weak after the treatment of PGV with PAA. The C 1s narrow-scan of PAA-PGN shows clearly that the peaks associated with both C-C and C-COOH moved to higher binding energies when compared to the narrow-scan of PAA indicating interaction with the nanoclays. A small C 1s peak at 536 eV present in both PGV and PGN narrow-scans can only be present due to adventitious carbon as reported elsewhere by Miller and Linton [233]. Both PGV and PGN were supplied by Nanocor Inc. that certified that both types of nanoclays were not treated before by any organic agent [265].

The narrow-scans of PAA-PGV and PAA-PGN for the main peak from O 1s photoelectrons are presented in Figure 3.6. The main peak associated with C=O in PAA-PGV nanoclays appeared broader with higher intensity and shifted towards lower binding energies at 536.65 eV compared to the narrow-scans of PGV and PAA indicating changes in the environment around the chemical species containing oxygen and consequently some interactions with PAA. The main peak from O 1s photoelectrons in the case of PAA-PGN samples on the other hand, is present at 537.84 eV close to the reference peak of PAA. Comparing the changes observed in the above scans for PAA-PGV and PAA-PGN, it is clear that stronger interactions were observed in the first case. This is in good agreement with the XRD analysis that showed that PGV nanoclays were fully exfoliated in PAA, whereas PGV nanoclays were only intercalated in the PAA aqueous suspension.

XPS can be interpreted in terms of both physisorption and chemisorption of PAA molecules on the silicate surface of nanoclays. In terms of physisorption, the increase in the interlayer distance in nanoclays may easily accommodate the PAA molecules which form linear extended chains rather than random coils while interacting with nanoclays [12]. Taylor and Stivala [129] measured the radius of gyration, cross-sectional radius of gyration and persistence length of PAA in water by small angle X-ray scattering while Tran *et al.* [12] investigated PAA-nanoclays interactions and found that the interlayer spacing in intercalated nanoclays was not above 16 Å and considerably smaller than the radius of gyration (597 Å) and persistence length (58.8 Å) of PAA random coils in water. However, the distance was similar to the cross sectional radius of gyration for fully extended PAA chains measured by Taylor and Stivala [129]. Tran *et al.* [12] therefore concluded that extensive reorganisation of PAA at the surface of nanoclays resulted in the formation of linear PAA chains rather than random coils. Extending all the above to their model, Trans *et al.* suggested that since the interlayer distance was measured to be about 16 Å, the interlayer space can only accommodate a maximum of two layers of fully extended PAA chains that are bound to the silicate surface by a number of carboxylic groups or hydrogen bonds. Considering, that the interlayer space of the intercalated nanoclays in the present study was also measured about 16 Å, it was possible to extend the model in our case as it was presented in the XRD section above. In terms of chemisorption, Choi *et al.* [280] reported that the organic molecules can penetrate the interlayer spaces by interacting with nanoclays surface in one of the following ways; (a) cationic bonding, in which protonated molecules can replace the sodium ions in the interlayer spaces of nanoclays, (b) ion-dipole interaction, in which polar organic molecules are related to the sodium ions in the nanoclay plates, (c) dipole-dipole interactions, which include the hydrogen bonding that associate the polar organic molecules with the hydroxyl groups or oxygen in the layers of nanoclays. Moreover, Tran *et al.* [12] studied the formation of siloxanes (C-O-Si) at the surface of the clay plates and the re-arrangement of coordination complexes between the metal ions within the silicate plates and suggested that this may be one of the possible chemisorption mechanisms that could describe the PAA-nanoclay interactions. The same group also performed ^{29}Si NMR studies in the case of leucentite nanoclays which showed that the PAA chains may also react with the octahedral Mg (or Li) present in the silicate plate of leucentite resulting in the formation of –COOMg complexes [267]. In the light of the above explanation, it can be stated that the removal of the cations from the nanoclays interlayer galleries by the PAA chains can significantly reduce the electrostatic Van-der-Waals forces between the silicate plates. Additionally, the steric effect created by the PAA chains on the silicon plates may also prevent the face-to-face interaction of nanoclay plates, which eventually results in intercalation or exfoliation.

4.1.3 FTIR

Fourier Transform Infrared Spectroscopy (FTIR) has widely been used to study the chemical structure of PAA [81, 237, 278, 281-283] , nanoclays [284-288] and their nanocomposites [183, 190, 234, 280, 289, 290]. The understanding of PAA-nanoclay interactions at the molecular level is an important aspect toward the development of the glass-ionomer based clay nanocomposites. In this study, Attenuated Total Reflectance Fourier Transform Infrared (ATR-FTIR) spectroscopy using a mid-infrared source was employed to investigate the adsorption of water soluble polymers (PAA) onto the surface of nanoclays. The ATR technique is very useful to obtain quantitative data on organic-inorganic materials. FTIR has been previously used to monitor the setting reaction in hybrid materials (organic-inorganic composites) but only in a semi-quantitative manner. Young however reported a method using ATR-FTIR that gave high quality quantitative data [81]. Another reason of using the ATR-FTIR setup is that a very good contact of the sample with the diamond cell in the ATR attachment can be established, leading to high quality spectra.

In the FTIR studies of nanoclays, –OH and Si-O groups play an important role in the differentiation of the nanoclays from each other and from the host polymer. In a review paper of FTIR techniques in clay-mineral studies, Madejova [291] suggested that it is useful to measure nanoclays samples in a KBr disk by mixing two to three milligrams of a clay sample dispersed in 200 mg of KBr. This permits detailed examination of -OH stretching vibrations in the nanoclays spectrum at higher wavenumbers and Si-O absorption and -OH bending vibrations in a region bellow 1200 cm $^{-1}$, where intense peaks are present. However, in the present study, the spectra of nanoclays were taken by using powder samples of nanoclays and the ATR-

FTIR method. The liquid samples, for example, PAA-nanoclay suspensions, a drop of PAA suspension after the dispersion of nanoclays was directly in contact with the Golden Gate Single Reflection Diamond ATR attachment and it was expected that some spectral changes may indicate adsorption of PAA onto nanoclays.

Figure 3.7 (a) shows the FTIR spectra of PAA, PAA-PGV after the dispersion in aqueous PAA solutions of different PGV content (D0.5VP to D8.0NP). Figure 3.7 (b) helps to distinguish certain types of groups present in PGV and PGN nanoclays. Both PGV and PGN nanoclays show characteristic bands at 3620 cm^{-1} due to O–H stretching vibrations, at 3370 cm^{-1} due to inter- and intra-layer H-bonded O–H stretching vibrations, at 1654cm^{-1} due to H–O–H bending vibrations, at 973cm^{-1} due to Si–O stretching vibrations, at 913cm^{-1} due to the presence of Al–OH and at 833 and 792cm^{-1} due to (Al, Mg)–OH vibration modes. The sharp peak centred at 973 cm^{-1} in both PGV and PGN nanoclays is attributed to the distinctive nanoplates of the tetra-hydrate layers of silicon. The absorbance at 3620 cm^{-1} in the spectrum of PGV and PGN is typical for montmorillonites with high Al content in the octahedral layer of nanoclay. Madejova studied different types of mineral clays including the 1:1 family of dioctahedral and trioctahedral clays and the 2:1 family of smectites [291]. In the case of smectite montmorillonites, the main peak at 3620 cm^{-1} is associated with the high Al content in the octahedral layer, whereas any peak at around 3567 cm^{-1} is associated with the Fe_2OH groups in the octahedral sheets in Fe rich nontronites [284]. In our case, this peak is not present in any of the nanoclays spectra and therefore, it is well confirmed that the clays belong to a typical high aluminium content type of montmorillonites. Despite the fact that PGN contains a higher amount of Fe than PGV, the peak that corresponds to the Fe_2OH group was missing from both nanoclays spectra. A broad band near 3430 cm^{-1} observed in both nanoclays is due to the H-O-H vibration of adsorbed water but this band was less prominent in PGN (Figure 3.7 (b)). The spectra of nanoclays exhibit peaks associated with Si-O stretching and bending vibrations as well as -OH bending vibrations in the 1300-400 cm^{-1} range [236]. Unfortunately, it was not possible to observe any other peak under 700 cm^{-1} due to equipment limitations and therefore, we cannot comment on the presence of Fe-O out-of-plane vibrations (676 cm^{-1}), Al(Mg)-O-Si vibrations (527 cm^{-1}) and Si-O vibrations (480 cm^{-1}) in nanoclays reported by other researchers [284]. The FTIR spectra of PAA-nanoclay and nanoclays samples support the observations mentioned above on the interactions observed between the nanoclays and PAA. Figure 3.7 (a) shows that the absorbance intensity of the peak observed at 1019 cm^{-1} associated with Si-O-stretching vibrations increased with increasing the clay loading, irrespective of the type of the clay used. In Figure 3.7 (a), it is noticeable that the Si-O vibrations band present in PGV nanoclays at 973 cm^{-1} moved to higher wavenumbers at 1019 cm^{-1} when the nanoclays were dispersed in the aqueous PAA solution. The shift of the peak at 973 cm^{-1} associated with Si-O- stretching vibrations can be due to the change of the chemical environment in the nanoclay-PAA suspensions indicating a strong interaction between the silicate plates of nanoclays with the polymer solution.

Madejova *et al.* reported an FTIR study on the effects of acid treatment on the structural modification of nanoclays and they reported that the acid attack (HCl) lead to the successive release of the central atoms from the octahedral layer and the release of Al from the Si tetrahedral sheets [292]. In the case of PAA which is considered to be a weak acid compared to HCl, it can be suggested that the protons from the –COOH groups may enter the nanoclay layers and attack the structural –OH groups resulting in dehydroxylation of nanoplates connected with the successive release of the central atoms. This can be readily followed by observing the changes in the characteristic absorption bands attributed to the vibration of -OH groups and octahedral cations (3626 and 1642 cm^{-1} as well as 904 and 814 cm^{-1}, respectively). In addition, a gradual transformation of the tetrahedral sheets to protonated amorphous silica can also be observed in the region of the stretching vibrations of the Si-O groups at 973 cm^{-1} which shifted to 1030 cm^{-1} with a simultaneous increase in absorbance indicating interaction of silicate nanoplates in nanoclays with PAA.

ATR-FTIR in previous studies could differentiate between dry polymer films loaded with nanoclays and solvated films. For instance, Hitzky *et al.* [293] claimed that the adsorption of polyethylene oxide (PEO) onto clays led to a splitting of a band at 1350 $cm^{−1}$ to 1360 $cm^{−1}$ and 1345 $cm^{−1}$ in dry samples. A similar peak splitting pattern was observed by Billingham *et al.* [237] in the spectra of poly-ethylene-glycol (PEG) films. In the case of dry PEG films loaded with nanoclays due to the adsorption of PEG onto nanoclay surface peak splitting was observed however, upon addition of water to the dry films, this splitting disappeared leaving only one band at 1350 cm^{-1} associated with a PEG diagnostic band [237]. ATR-FTIR spectra obtained by Billingham *et al.* for PEG-nanoclay films with increased loadings of different molecular weight of PEG showed that the ATR-FTIR method can also differentiate between the different loadings of the polymer used for the treatment of nanoclays [237]. Specifically, the intensity of the PEG diagnostic peaks increased with increasing PEG loading. A similar observation was also made in the present work where the nanoclays diagnostic peaks increased in intensity with increasing the nanoclays content in the aqueous polymer-nanoclay suspensions. For example, in Figure 3.7 (a), it is clear that increasing the content of nanoclays from 0.5 to 8.0 wt % resulted in an increase in the absorbance intensity of Si-O group at 1019 cm^{-1}. Madejova *et al.* [294] also claimed that treatment with HCl resulted in the formation of amorphous silica gel on the surface of treated nanoclays strongly dependent on the temperature and the acid concentration. According to this, the shift of the Si-O stretching vibrations from 973 cm^{-1} in nanoclays to 1019 cm^{-1} in nanoclay-PAA suspensions could be an indication of the result of the PAA interaction with the silicate nanoplates and specifically the formation of an amorphous silica gel layer on the surface of nanoclays after the polyacid (PAA) attack. Another smaller shoulder at 1086 cm^{-1} appeared in the spectra of PAA-PGV suspensions and especially at contents higher than 2 wt % in PGV that unfortunately could not be assigned but it could be connected also with Si-O stretching vibrations. The peaks associated with the carboxylic group are present at 1706 cm^{-1} and at 1629 cm^{-1} and are attributed to the C=O stretching vibrations and –OH bending vibrations in the carboxylic group, respectively.

It is worth noting, that the peak intensity associated with C=O stretching vibrations at 1706 cm^{-1} in the carboxylic group decreased slightly in addition to a minor increase in the intensity of the peak associated with bending vibrations of the –OH groups at 1629 cm^{-1}, when the nanoclays content increased from 1 to 8 wt % (from D1.0VP to D8.0VP) in the PAA-nanoclay suspensions (Figure 3.7 a). The changes in the intensity of the peaks associated with the carboxylic groups in PAA-PGV may suggest the interaction of protons from PAA with the nanoclays [294]. Furthermore, a significant broadening and decrease in intensity of the peak associated with C-O stretching vibrations in PAA at 1266 cm^{-1} was observed in the spectra of D4.0VP, D6.0VP and D8.0VP with the increase in the nanoclays content. It is not clear, however why an increase in nanoclays content would have an effect on C-O stretching vibrations. The presence of a small and sharp peak at 3626 cm^{-1} in PAA-PGV suspension was also observed. It increased in intensity with the increase in the nanoclays content from 1 to 8 wt % in PAA suspension. Madejova reported [291] that a peak at 3620 cm^{-1} is a typical peak present in the spectra of smectites (such as montmorillonites as in the present case) and is associated with H-O-H stretching vibrations of water molecules weakly hydrogen bonded to Si-O groups on the surface, whereas a broad band at 3430 cm^{-1} is due to H-O-H vibrations of adsorbed water. The FTIR results of the PAA-PGV suspension are in good agreement with the results from the XPS and XRD analysis suggesting that the chemisorption and physisorption of PAA on the silicate nanoplates resulted in increasing the interlayer space due to the segregation and adsorption of PAA molecules into the interlayer space.

In order to study the effects of nanoclays dispersion on GICs, nanoclays were mixed in the liquid portion of the two commercial dental restorative cements, Fuji-IX and HiFi according to the protocol mentioned in 2.1.2. Figure 3.8 shows the FTIR spectra of the liquid portion of Fuji-IX (FL) and the FTIR spectra of Fuji IX-nanoclay suspensions after the dispersion of 2 wt % PGV (D2.0VRT, D2.0V75) and 2 wt % PGN (D2.0VRT, D2.0V75). The peak at 1706 cm^{-1} is attributed to the C=O stretching vibrations in the carboxylic group, whereas the peak at 1630 cm^{-1} is associated with –OH bending vibrations in the carboxylic group. In comparison to the FTIR spectra of the PAA-PGV suspensions, the intensity of the peak associated with C=O at 1706 cm^{-1} of the carboxylic group present in the spectrum of FL is slightly higher than the intensity of the peak at 1630 cm^{-1} associated with –OH stretching vibrations.

In contrast to PAA-PGV suspension, the intensity of the peak at 1706 cm^{-1} present in the spectrum of FL was not decreased after the addition of nanoclay both at room temperature and at 75°C. Generally, the FTIR spectra of the Fuji-IX-nanoclay suspensions were not very much dissimilar from the spectrum of FL. Only small differences in the peak intensity of C=O at 1706 cm^{-1} were observed when nanoclays were dispersed at 75°C (D2.0NF75 and D2.0VF75) in FL (Figure 3.9). It is not easy to commend on the effect of temperature on the dispersion and exfoliation of nanoclays in the Fuji IX liquid based on the above observation. Previous studies however [267, 276, 295] suggested that temperature has an effect on both dispersion and exfoliation of nanoclays and it seems that the interlayer spacing in nanoclays increased with increasing the temperature during the heat treatment of nanoclays in aqueous PAA as it was discussed earlier (see paragraph 4.1).

The effect of PAA molecular weight on the dispersion of nanoclays has not been investigated and there is not enough available information in the current literature. Kirwan *et al.* [296] reported that at low pH the attachment of poly-carboxylate molecules on hematite surface was not dependent on the chain length. It is expected however, that the molecular weight of PAA would have an effect on the nanoclays exfoliation and specifically on the interlayer spacing as the number of polymer entanglements would have had an effect on the mobility of the chains within the interlayer spacing. This however cannot be confirmed by the current study or by the available literature. It is therefore important to mention here, that the M_w of PAA employed in PAA-PGV suspension was 110,000 (as reported by the manufacturer) whereas the M_w of FL was measured by GPC at RAPRA and was found to be in the range of 15.000 (see section 3.2).

Comparing the spectra of PAA and Fuji IX liquid (FL) (Figures 3.7 and 3.8, respectively), one can say that the main differences are:

1. The shifting of all characteristic peaks towards lower wavenumbers and
2. The differences in the intensity of both peaks assigned to C=O and –OH stretching vibrations.

One of the reasons for this could be the difference in the molecular weight as well as the concentration of the polymer in the solution. Specifically, in Fuji IX liquid the concentration of PAA in water was measured to be 33 wt %, whereas the PAA solution was measured to be 39 wt % (see paragraph 3.2, Table 3.3). In order to elucidate the effect of the molecular weight and polymer concentration on the dispersion and exfoliation of nanoclays, a more systematic study should be carried out. However, in the present study this was outside the scope of the thesis.

Figure 3.9 shows the FTIR spectra of HiFi liquid (PA) and its solutions prepared after the dispersion of 1 wt % (D1.0NHPAH), 2 wt % (D2.0NHPAH) and 4 wt % (D4.0NHPAH) of PGN nanoclays. The presence of a new peak at 1041 cm^{-1} after the addition of nanoclays is attributed to the Si-O stretching mode in PGN nanoclays. Apparently, the Si-O stretching peak which was present at 973 cm^{-1} in PGN nanoclays moved towards higher intensity at 1041 cm^{-1} and resulted in a stronger peak with increasing the content of PGN in the PA suspension indicating the strong interaction of nanoclays with the PA polymer chains. The absorbance intensity of this peak also increased with increasing the nanoclay content from 1 to 4 wt %. In comparison to the PAA-PGV suspension, a similar trend in the peak height at 1041 cm^{-1} associated with Si-O stretching vibrations was observed, however the peak at 1710 cm^{-1} associated with C=O also depicted the same trend. The M_w analysis of the HiFi polymer powder and solution was determined (measured by RAPRA) in the range of 52,000-56,000 which is higher than the M_w determined for FL but lower than the M_w of PAA used to prepare the PAA-PGV suspensions (section 3.2). Besides, it is worth mentioning that as the content of the nanoclay was raised from 1 to 4 wt % in HiFi suspensions, the viscosity of the resulting PAA solutions also increased due to the adsorption of more random binding of the carboxyl groups to the surface of the clays. This increase in viscosity, especially with the dispersion of 4 wt % of PGN nanoclays, resulted in an increase in the flow resistance behaviour of the PAA solution. The peak at 1358 cm^{-1} associated with Si-OH became also prominent in HiFi-nanoclay suspensions with an increase in nanoclay content in particular more than 2 wt %.

The setting reaction of the GICs prepared in this study was followed by FTIR spectroscopy, which is a very effective method to monitor the setting reaction of GICs as reported previously in the literature [297]. In the FTIR studies of GICs, the adsorption of the carboxylic acid on the glass surface via an acid-base neutralization reaction has been widely explored in the literature [6, 81, 87, 298]. A conventional GIC sets by means of an acid-base reaction between an aqueous PAA solution and a fluoro-alumino silicate glass [242]. It is therefore, important to study the setting reaction of GICs in order to understand what exactly controls the properties of GICs at the molecular level. However, FTIR spectroscopy is only suitable for semi-quantitative analysis, since the loss of the carbonyl group absorption band during the neutralization overlaps with the formation of the asymmetric COO^- salt band [241, 242]. Another problem with the FTIR is that the absorption bands of the poly-carboxylic acid overlap with the strong absorption bands of water at 1642 and 1705 cm^{-1} [299].

The real-time study of the setting reaction of GICs over a period of one hour before and after nanoclay dispersion in Fuji-IX system (Figure 3.11 and 3.12) and in HiFi system (Figure 3.13 and 3.14) was performed during the present research work. It is well established, that the PAA liquid used for the GIC preparation exhibits characteristic absorption bands in the region between 1000 and 2000 cm^{-1} which could be used to assess the degree of neutralisation during the setting reaction. The acid-base neutralization reaction in glass ionomer cements can be presented by the following general chemical reaction:

$$n_a \text{ acid} + n_g \text{ glass} + n_w \text{ water} \longrightarrow n_{s,1} \text{ salt}_1 + n_{s,2} \text{ salt}_2 + \ldots, \text{ [81]}$$

where, n is the number of moles of each component required or formed during the reaction between n_a moles of acid and n_g moles of glass in the presence of a required amount of water to achieve poly-acid neutralisation. Commercially available glass ionomer cement formulations contain both PAA and tartaric acid. Crisp and Wilson, and Nicholson *et al.* studied the effect of tartaric acid on the setting reaction of GICs and they reported, that the main role of tartaric acid is to control the setting reaction by chelating with Ca, delaying initially the setting and enhancing the formation of aluminium poly-acrylates sharpening the final stage of the setting reaction [100, 106]. In the present study, the HiFi cements were produced by using the glass powder provided by the suppliers (Advanced Healthcare Ltd) and 40 wt% aqueous solution of PAA (PPA powder and water). Tartaric acid was not used in the present study because it was important to keep the system simple so that we could investigate any effect the introduction of nanoclays would have on the setting reaction of cements.

In addition from Figure 3.10, it is clear that the HiFi glass powder did not contain tartaric acid as the characteristic peaks at 1088 and 1134 cm^{-1} were not present. On the other hand, Fuji IX liquid contains tartaric acid evidenced by the FTIR spectrum in Figure 3.8. During the setting reaction of GICs, poly-acrylate-salt units and tartrate-salt units appear at different wavenumbers making possible to monitor the activity of various metal cations. The vibration bands from calcium acrylate and aluminium acrylate appear due to the carboxylate stretching vibration [242]. Figure 3.11 and 3.12 shows the bending vibrations at 1594 and 1644 cm^{-1} was attributed to the formation of calcium and aluminium poly-acrylate salts. Symmetric and asymmetric stretching vibrations of COO^- can also be identified at approximately 1420 and 1540 cm^{-1} in C2.0VF75F as well as in Fuji-IX cement. However, in comparison to Fuji-IX cement, the real time spectra of C2.0VF75F shows that the peak at 1625 cm^{-1} moved to higher wavenumber and there was also absence of peak at 1594 cm^{-1} unlike CF-IX spectra after one hour from the start of cement mixing. Additionally, the presence of the strong absorbance band at 948 cm^{-1} in both C2.0VF75F and Fuji-IX cements was due to the stretching vibrations of Si-OH of the glass powder and no significant changes were found in this band over the duration of one hour. The asymmetric stretching vibrations in Si-O of the nanoclays, which are usually present between 940 and 1000 cm^{-1} are very difficult to distinguish during the setting reaction due to the Si-OH vibration of the glass powder element. Figure 3.13 and 3.14 show the real-time setting reaction for one hour of two HiFi cements, CPA-PA and C2.0NPAH. The setting reaction of both cements follows generally the same path. A peak at 1594 cm^{-1} is attributed to the C-O asymmetric stretching vibration in Al-PAA poly-salts. A new peak at 1522 cm^{-1} is most likely associated with –(C=O)O- asymmetric stretching vibrations of Ca-PAA poly-salts. The strong peak at 1451 cm^{-1} is assigned to C-O symmetric stretching vibrations of Ca-PAA in C2.0NPAH. However, the spectra of C2.0NPAH depicted the emergence of two new peaks at 2358 and 2448 cm^{-1}, which increase in intensity and become prominent after one hour of the start of mixing. The exact nature of the presence of the peaks in this band is not clear but it seems that they are connected with the presence of nanoclays in the cement system. The influence of the addition of MMT nanoclays to the chemical reaction and the setting of GICs is not yet fully understood. Although, the rheological characterisation showed, that the addition of nanoclays had a small effect on the working and setting time in both Fuji IX and HiFi systems, it is not well understood what exactly the effect is. It was expected, that the FTIR analysis would give more information on the role of nanoclays in the setting reaction, however the spectra of cements that contained nanoclays did not give a better insight. Three relatively weak peaks in the range of 2325 and 2363 cm^{-1} that seem to be more intense in the case of the nanoclay containing cements for both Fuji IX and HiFi systems, are most likely due to the atmospheric CO_2. It is not known why these peaks are more pronounced in Figures 3.12 and 3.14 but the intensity of the peaks assigned to the presence of CO_2 depends on the existing conditions at the time of the FTIR measurements.

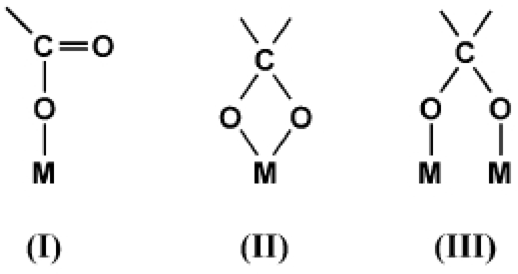

Figure 4. 5: Three types of carboxylate-metal interactions (I) mono-dentate, (II) bidentate chelating, (III) bidentate bridging [296].

Nicholson [300] reported the effect of trivalent nitrates on the setting reaction of GICs and he argued that the precise position of the asymmetric carboxyl band varies according to the structure of the polysalts. He further described that in polyacrylate salts, the bands associated with –COOH appeared due to purely ionic or partially covalent interactions. Furthermore, Deacon and Phillips [301], reported that a carboxylate ion of PAA can coordinate to metal ions in a number of ways by comparing the symmetric and asymmetric frequencies of the carboxylic acid group. Figure 4.5 describes three proposed possibilities by Deacon and Phillips, which can exist in this bonding mechanism, which are; monodentate, chelating bidentate and bridging bidentate structures. It is well documented, that the setting reaction of GICs involves the neutralisation of PAA by the glass powder, which is associated with the formation of calcium and aluminium salt complexes. However, the neutralisation is never complete and there are always un-reacted carboxylic acid groups present within the set cement [95]. Although the setting reaction of GICs has been studied extensively, there is considerable debate and controversy over various aspects of the setting chemistry including, the effect and sequence of metal ions release, whether the setting reaction continues with time and how both the silica gel phase and poly-salt phase influence the long-term mechanical properties of the cements. Young *et al.* [297] suggested, that the main changes in real time FTIR spectra arise from the irreversible formation of poly-acrylate salts, which may be complexed with various metal cations from the dissolution of the glass. Wasson and Nicholson [302] demonstrated, that the initial product of the setting reaction is predominantly calcium salts resulted from the acid attack of the calcium-rich sites in the glass, whereas aluminium salts form later because although aluminium is released at the very early stages of the setting reaction, it is most likely released as a part of more condensed species and it is not readily available for reaction with the carboxylate moieties. However, the FTIR spectra reported in this thesis do not support the same idea. In general, it is difficult to differentiate between Ca-PAA and Al-PAA in the FTIR spectra. Specifically, in the Fuji IX real time FTIR spectrum it is clear, that Al- and Ca-tartrates form almost at the same time. Similarly Al- and Ca-polyacrylates seem to form both at the same time with no evidence that Al-polyacrylates form later. In order to understand the mechanism of the ionic crosslinking of polyacrylic acid by Ca and Al ions, it is important to consider the structure of the ionomer glass used. It is likely, that the ionomer glasses used for the production of the early cements (70's and 80's) were phase separated into one reactive Ca- and F-rich phase and one less reactive Al- and Si-rich phase. Therefore and most likely, the release of Ca ions from the Ca-rich phase occurred prior to the release of Al ions from the Al-rich phase. The idea that Ca-poly-acrylates form earlier than Al-poly-acrylates has been supported by several authors [31, 49, 130, 241, 303-306] but, the main evidence was taken from ion release data. If the ionomer glass used was phase separated as mentioned above, the more reactive phase (in this case the Ca-rich phase) would release ions faster than the less reactive phase. On the other hand, evidence of early release of Ca cations has been also provided by FTIR studies and has been reported in the literature [297, 300, 307-310]. However, often it is difficult to differentiate between Ca-poly-acrylates and Al-poly-acrylates resulting in lack of strong evidence that Ca-poly-acrylates form first. In addition, MAS-NMR spectroscopy studies [83, 311] have shown that octahedral hydrated Al^{3+} (six-fold coordinated aluminium Al(VI)) –the type of Al^{3+} that forms Al-poly-acrylates- forms already at very early stages during the setting reaction. The setting reaction of GICs based on three different fluoro-alumino-silicate glass compositions (LG125, ART10, and LG26Sr) using ^{27}Al MAS-NMR spectroscopy was recently studied by Norhazlin *et al.* [299] and it was reported, that the setting reaction depended strongly on the glass composition used to form the cement. Specifically, when the glass was rich in phosphorus, the presence of Al-O-P species had an influence on the dissolution of the glass during the acid attack and consequently an effect on the ion release. In the case of the Sr substituted glass, the setting reaction was completed already after one day, whereas the setting reaction continued up to 1 year in the case of the low phosphorus containing glass. Furthermore, the presence of Al(VI) was reported as early as 2 minutes after the start of the setting reaction with obvious conversion of Al(IV) to Al(VI) with time irrespective of what was the glass composition used to form the cement. Considering, all the above, it is clear that there is not strong evidence to support the idea that Ca-poly-acrylates form earlier than Al-poly-acrylates and we will accept that Ca and Al compete equally for ionically crosslink the poly-acrylic acid chains during the cement formation. The release of cations such as sodium and silicon during the acid attack was also reported by Wasson and Nicholson [312], who suggested that these elements were involved in forming an inorganic network that can contribute to the increase of compressive strength with the time. Similar observations were reported by Matsuya *et al.* who used combined FTIR and MAS-NMR studies to conclude that re-polymerisation of the silicate network occurred during the setting reaction [313]. This approach although was initially accepted, it is the source of a debate within the glass ionomer cement research community as another approach suggests that it is not the silicate network that contributes to the increase in compressive strength with time but it is the molecular weight and the degree of cross-linking of the polymer chains that control the increase of compressive strength during the setting reaction [96, 98].

4.2 Rheological studies

The dispersion of different amount of nanoclays in PAA at different temperatures may lead to strong variations of the flow properties. For example, when the weight percentage of PGV and PGN nanoclays was increased over 2 wt %, it resulted in an increase in viscosity of both Fuji-IX (FL) and HiFi liquids. At 4 wt % of nanoclays content, the powder did not hand-mix easily with the liquid resulting in an effect of the properties of both cement systems. Therefore, the potential reinforcement of conventional GIC systems with nanoclays at contents more than 2 wt % should be carefully designed. It may become necessary to add certain additives such as surfactants to stabilise the nanoclay particles in the PAA solution or using more dilute PAA solutions. In the present work a ratio of 65 : 35 was employed for water : nanoclays content. When a PAA solution is formed with the plate-like nanoclays particles, three different modes of particle association may occur during the process of dispersion: face-to-face (FF), edge-to-face (EF) and edge-to-edge (EE) as shown in Figure 4.6.

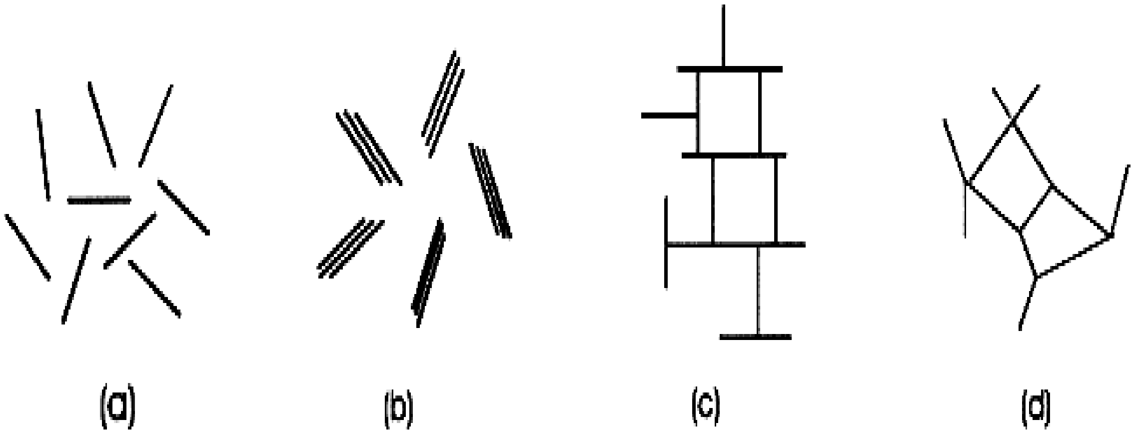

Figure 4. 6: Different mode of nanoclay particle in an aqueous solution of PAA: (a) dispersed; (b) face-to-face (FF); (c) edge-to-face (EF); and (d) edge-to-edge (EE) [314].

In the aqueous solution of PAA, the negative charge of the face/solution interface is due to the isomorphous substitutions of Si and Al atoms in the tetrahedral and octahedral nanoclay sheets, while the charge of the edge/solution interface is determined by the pH of the solution (H^+ is a crucial ion) and can be positive or negative [314]. The rheological properties of the Na montmorillonite suspension in an aqueous solution of polyelectrolytes (PAA) were reported by Tejada *et al.* [315] in order to analyse the changes in the interfacial electric potential of the surface after the dispersion in PAA. Tejada *et al* concluded that the addition of nanoclay can provoke the dramatic changes in the viscoelastic properties of PAA-nanoclay suspensions depending on the pH, polymer charge and concentration.

Ideally, a dental cement should have a long working time after which it should set rapidly (a snap set) [316] to meet the clinical requirement in oral cavity without disturbing the inherited properties of the materials. However, the chemical reactions in dental materials, particularly in dental cements are affected by the change in temperature. An accelerated setting time may adversely affect the properties of the cement due to the manipulation during the hardening phase. Therefore, the appropriate rheological characteristics are one of the prerequisites of dental restorative materials such as GICs. The working and setting times of GICs determined by the Wilson's rheometer are presented in Figure 3.16 and Table 3.4 (section 3.1.5). In order to determine the rheological characteristics of cements, immediately after the start of mixing the powder and liquid constituents, both working and setting times were recorded using a modified Wilson's rheometer (section 2.2.5). The use of the oscillating rheometer provides the means to monitor the setting reaction of GICs while varying the temperature. In the present study, the measurements were conducted at room-temperature. The rheological studies showed that there was a small decrease in both the working and setting times of glass ionomer cements prepared with the polymer liquids formed after the nanoclays dispersion, as compared to control groups (CPA-HP and CF-IX). The slight deflection in the results to the higher values of working and setting time may be due to the room-temperature used during the experiments instead of 37 °C. Furthermore, Pearson and Atkinson [316] studied the effect of temperature on the working and setting characteristics of cements and they observed that the cements (phosphate, poly-carboxylate and glass ionomer cements) exhibited an increase in working and setting time at lower temperatures (e.g., 8 °C). The cements (C1.0NPAH, C2.0NPAH and C4.0NPAH) formed with the HiFi glass powder and the polymer liquids formed after the dispersion of PGN nanoclays (D1.0NPA, D2.0NPA and D4.0 NPA) exhibited a rheological behaviour not very much different from the control cements group of HiFi cement (CPA-HP). However, a decrease of 20-30 seconds was observed in the working and setting time of cements, formed with the Fuji-IX powder (FP) and D2.0VF75, D2.0VFRT, D2.0NF75 and D2.0NFRT when compared to the control group (CF-IC). Generally, HiFi cements exhibits lower working and setting times as compared to Fuji-IX which may be associated with the dispersion of nanoclays with a different processing method. The values of the setting and working times of the control groups determined in the present study are slightly higher than the values reported in the literature [317-320]. However, such variations in the results may be accepted due to the nature of Wilson’s rheometers which is largely dependent upon the elastic tension and the physical properties of the spring coils used in different oscillating rheometer. A stiffer spring would produce lower values of the setting and working times of a material and vice versa. The sensitivity of the oscillating rheometer is usually determined by the spring tension that reduces the motion of the lower platen so that if the chosen springs were weak, the initial changes during the setting reaction would be prominent and if the chosen springs were too strong the final stages of the setting reaction would be more noticeable [316, 321].

The working characteristics of a conventional P/L GIC system (ChemFil) after the addition of two different types of nanoclays i.e., calcium MMT (Ca-MMT) and an organically modified 12-amino-dodecanoic acid treated MMT (ADA-MMT) were determined by Dowling *et al.* [14]. They reported that the working times recorded for the GICs after the addition of nanoclays (Ca-MMT) were not significantly different from the control group when the nanoclays were added to the glass powders. A decrease in the working times was observed on the other hand, when nanoclays were added to the GIC's liquid, prior to mixing. However, a significant increase in the setting time of GICs was observed when nanoclays were added to the liquid portion of the GIC system instead of the glass powder. Dowling *et al.* assumed, that Ca-MMT clays in the glass powder would compete for the available liquid causing a reduction (although not significant) in the associated working time, whereas a slow release of the bounded water during the setting reaction was responsible for extending the setting times. Dowling *et al.* also claimed that by adding the nanoclays in the liquid part of the GICs, the setting times was decreased as the weight percentage of the nanoclays increased (the longest setting times recorded at 0.5 wt.% and the shortest at 2.5 wt %) [14]. The above explanations, related to the tendency of nanoclays to "absorb and release" the water, during the initial and final stages of setting may require some more consideration. The dispersion of nanoclays is a key element to achieve better properties in GIC systems.

The work presented in this thesis aimed to the development of a process strategy based on the dispersion of nanoclays in PAA aqueous suspensions. The success of the processing strategy, however, relies on the actual dispersion of nanoclays, which was described in the section 1.12 and shown in Figure 1.6. Thus, if nanoclays were not penetrated by PAA chains and dispersion was not successful, then agglomeration of nanoclays would have been observed and a micro-composite would have been formed instead of a nanocomposite in the case of a successful dispersion (exfoliation and intercalation) of nanoclays. The rationale adapted by Dowling *et al.* [14] is likely to result in the formation of micro-composites. On the other hand, exfoliation or intercalation of nanoclays in PAA has been achieved in the present study. Therefore, the size of nanoclays, the nanoclay surface modification method and the processing technique used are important factors for the stability of the PAA-nanoclay suspensions formed.

4.3 Mechanical properties

In Chapter 1, the applications of GIC's as luting cements, lining materials, temporary filling materials in the anterior region and as core build-up, orthodontic band cementations and permanent filling materials in the primary dentition were mentioned. It has been shown, that low strength and high abrasiveness of GICs limit the clinical use as permanent filling materials in the posterior region which is subjected to high masticatory loads [158, 322]. Generally, the mechanical performance of a novel system is evaluated by a series of laboratory tests. However, the selection of these tests varies widely in the literature (see section 1.10) and it is entirely upon the discretion of dental materials researchers and manufacturers how to determine the mechanical behaviour of a new material. The most common mechanical properties used for the characterisation of the dental restorative materials are, compressive strength (CS), diametral tensile strength (DTS), bi-axial flexural strength (BSF), flexural strength (FS), micro-hardness (Vickers (HV) or Knoop), fracture toughness (FT), dynamic mechanical properties, impact strength, tear strength and tear energy, bond strength, viscoelastic properties (creep and stress relaxation), fatigue, elastic modulus (E_f) and wear rate [3, 33, 36].

In the present work CS, DTS, FS, E_f, VH and wear resistance of the two GIC systems (Fuji-IX and HiFi) before and after the reinforcement with nanoclays were investigated and the results are described in sections 3.4 and 3.5. The mechanical testing showed that all the glass-ionomer cements became stronger as they matured after 24 hour, 1 week and 1 month of storage in distilled water. Moreover, most glass-ionomer cements formed with modified PAA liquid that contained less than 2 wt % nanoclays, exhibited generally slightly higher CS (range 124–142 MPa), similar DTS (range 12–

20 MPa) and higher flexural strength (range 37–42 MPa) compared to the control cement groups (Fuji-IX and HiFi). However, no significant differences ($P > 0.05$) were observed when the mechanical testing data were statistically analysed with GLM and ANOVA. By changing the processing temperatures during the dispersion of nanoclays in the liquid portion of the Fuji-IX system, no significant difference ($P > 0.05$) was observed in the mechanical testing data. On the other hand, the HiFi system, where a different processing route of nanoclays dispersion was followed compared to Fuji IX system resulted in mechanically superior cements. According to the manufacturer of the HiFi system (AHC Ltd, UK), HiFi generally has an inferior mechanical behaviour compared to Fuji-IX but in the present study, the dispersion of nanoclays in the liquid portion of HiFi system resulted in better mechanical properties than the Fuji-IX system with and without nanoclays. Therefore, it is thought that the processing conditions of nanoclays dispersion in the polymer liquid have an effect on the mechanical properties of the glass ionomer system. Furthermore, the increase in the viscosity of the PAA liquid after the dispersion of nanoclays was not desirable for the successful preparation of cements. The higher nanoclay content in the polymer liquid (4 wt % or more) influenced the manipulation and mixing of cements resulting in difficulties in specimen preparation and therefore inferior mechanical properties.

The mechanical behaviour of materials is described by their deformation and fracture characteristics under applied tensile, compressive or multi-axial stresses [323]. However, the determination of mechanical properties may be influenced by several factors for example, materials variability, nature of applied forces and choice of the test methods. The determination of dental restoratives CS is an essential parameter in order to evaluate the response of restorative materials because most of mastication forces are compressive. Generally, CS is a useful test method for comparing materials having brittle nature and having a weaker performance in tension. During the laboratory testing, when GICs are subjected to compression test, the failure of the test specimens occurs as a result of complex stresses formation in the CS test specimen which are illustrated in Figure 4.7 (A). From the diagram is obvious, that the compression forces applied on the cylindrical specimen (4×6 mm) are resolved into shear forces along a cone-shaped area at both edges and tensile forces subjected in the central portion of the GIC specimen.

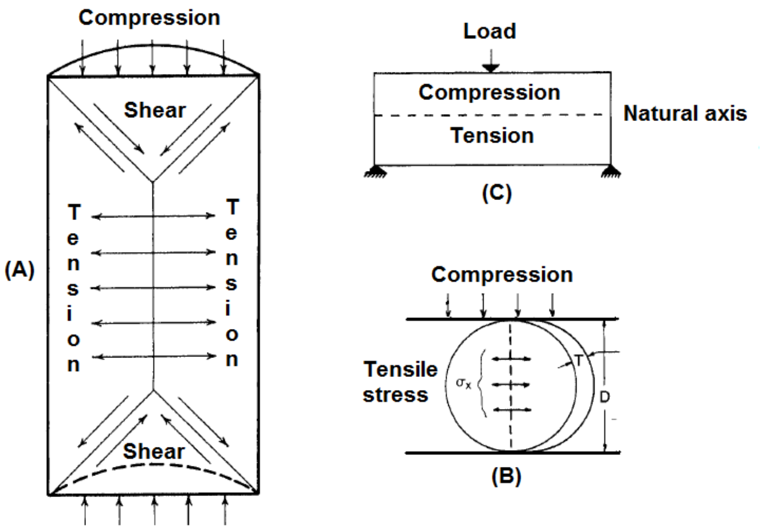

Figure 4. 7: A drawing of the complex stress pattern developed during the testing of GICs (A) CS test, (B) DTS test and (C) three-point bend FS test [3].

Due to the resolution of forces in the body of the specimen, it is necessary to adopt standard dimensions of GICs specimens in order to obtain reproducible results. Craig and Powers in their textbook suggested, that the distribution of forces in the compression testing become more complicated if the CS test specimens are too short or too long [3]. Therefore, Craig and Powers recommended that the cylinder specimens of the CS test should have a length twice that of the diameter in order to obtain most satisfactory results. However, the CS tests in the present study were conducted according to the ISO standard 9917-1 that recommends 4×6 mm^2 cylindrical test specimens [220]. Fracture is one of the major causes for the clinical failure of dental restoratives. The fracture of brittle materials such as GICs, occurs through the propagation of pre-existing cracks under tensile stresses due to micro-structural imperfections or presence of bubbles [324]. Moreover, the crack initiation is strongly affected by the micro-structural characteristics of the materials which may cause stress concentration, surface scratches and micro-cracks [325, 326]. Due to the complexity associated with the tensile strength measurement methods for brittle materials, such as GICs, an alternative method (DTS) to calculate ultimate tensile strength has become popular because of its simplicity and reproducibility of data [3, 327-331]. In the DTS test (Figure 4.7 B), the compressive stresses are applied diametrically to the specimen introducing tensile stresses in the plane of the force application in the disk specimen. The flexural strength of GICs is determined by employing a three point bending test on rectangular bar-shaped specimens ($25\times2\times2$ mm^3) in accordance with the ISO standards 9917-2 and 4049. The distribution of stress forces during the FS test is shown in Figure 4.7 (C).

As discussed above, measuring the FS is a meaningful mechanical property for brittle materials despite the fact that the results from the test cannot be extrapolated to the clinical behaviour without considering the structural reliability of the materials and the flaw distribution. Nonetheless, the *in-vitro* three-point bending test is recommended by the ISO 4049:2000 [221] specification for polymer-based materials and is widely used for comparative purpose. Another important mechanical property derived from the three-point bending test is the flexural modulus (E_f). The E_f was determined in accordance with the ASTM standard D 790-07 [222] and was calculated from the initial straight part of the stress-strain curve obtained from the three-point bending test as described in section 2.2.6.4 and the results are presented in section 3.4.4. One-way ANOVA and Tukey's test comparison of E_f results showed that the modulus of C1.0N PAH (14.8 G Pa) was significantly higher ($P < 0.001$) at a confidence interval of 95%. However, generally no significant difference ($P > 0.05$) between the both cement systems (HiFi and Fuji-IX) was found after the 2 wt % nanoclays dispersion in the liquid portion. Rodrigues *et al.* suggested [332], that different clinical situations demand restorative materials with different moduli of elasticity. For example, Class V cavities require a low modulus restorative material to flex with the teeth while, Class I and II cavities require a restorative material with relatively higher modulus to withstand the occlusal forces on posterior teeth during mastication. Xie *et al.* [158, 333] studied the mechanical behaviour of GICs and reported that conventional GICs had higher values of modulus than RMGICs due to the more flexible polymer matrix. In the present work, it is suggested that the modulus of GICs after the dispersion of 1 wt % of nanoclays may be appropriate for using these materials in load bearing applications as well as for Class V cavities.

Apart from the bulk mechanical properties of cements, the surface properties of dental cements especially when considering that these materials function in the oral environment are as important. The surface hardness of dental cements is frequently used to evaluate the surface resistance to the plastic deformation by indentation [330, 334-338]. The results obtained from the Vickers Hardness (HV) test are summarised in Table 3.6. One-way ANOVA and Tukey's test with 95% confidence interval showed no significant differences ($P > 0.01$) in the HV values of all cements. The average values of hardness were obtained between 68 and 85 HV. The results of hardness presented in Table 3.6, however, showed that there are no statistically significant differences ($P > 0.01$) in the hardness values of GICs and the presence of nanoclays did not influence the hardness of glass ionomer cements.

Generally, the mechanical properties (FS, DTS and CS) of GICs at different setting times (storage time) showed an increase in strength with increasing the storage time. Univariate GLM and two-way ANOVA showed that the ageing time of cements has a significant influence ($P < 0.05$) on the strength after 1 day and 1 month. This is in good agreement with the literature [249, 339-342]. Cattani-Lorente *et al.* [343-345] investigated the mechanical properties (FS, DTS and CS) of twelve commercial GICs at different ageing periods (1 day, 2 months, 6 months and 1 year) and found four different change patterns with time in the mechanical properties when GICs were stored in water. In some cases they observed:

(1) an increase in strength to an upper limit value,
(2) a gain in strength over a period of two to six months, followed by a decrease in strength,
(3) a continuous decrease in strength with time, and
(4) an invariable strength with ageing time.

The authors of the above study concluded, that the strengthening of GICs resulted from addition cross-linking and building-up of a silica phase, while the weakening of cements was the result of erosion and the plasticizing effect of water [344]. While it is reasonable to accept, that storage of GICs in water would have an effect on the mechanical properties and specifically erosion would decrease the strength in these materials, we should be very sceptical regarding the change in strength with time. As it was mentioned above, we now know that the setting reaction of GICs depends strongly on the composition of the ionomer glass used [83, 84, 92, 99, 124]. In some cases the setting reaction seems to complete in 1 day and in some other cases the setting reaction seems to continue a year after the mixing of the powder and the liquid components. Unfortunately, in most commercial cements, the glass compositions are not known and therefore it is difficult to comment on the setting duration. However, it seems that this information results into a better understanding of how the strength of cements changes with time. It is possible, that when Catani-Lorente *et al.* noticed the four different strength changing patterns in the commercial GICs they studied, the glass compositions would have an effect on the setting reaction leading to all these four different behaviours. Here, in the case of Fuji IX cements, it is expected that the setting reaction will continue with time and that the mechanical properties should increase with time, whereas in the case of HiFi it is possible, that the ionomer glass used is a high phosphorus containing glass, that would lead in the early completion of the setting reaction and not significant changes in the strength should be expected with ageing time. According to the mechanical properties results described in section 3.4 this seems to be the case for the HiFi system.

The data measured from the *in-vitro* tests discussed above can give an indication about the clinical performance of dental restorative materials but unfortunately they cannot predict the clinical performance [346]. The evaluation of the strength of GIC systems, e.g., CS, DTS and FS has an important role in the acceptance of novel formulations. In the oral cavity, however under different clinical situations these restorative materials will respond in a different way. The forces acting on teeth and the restorative materials, lead to deformation that ultimately compromises the durability of materials over time. Many brittle materials such as glass ionomer dental cements have a tensile strength markedly lower than the compressive strength. Xie and co-workers [158, 347] reported that GICs fail by crack-propagation which is favoured by tensile rather than compressive loading. Prosser *et al.* [348] on the other hand, reported that the most appropriate measurement of the strength of GICs is probably the FS test. Considering the nature of compressive fracture, Prosser *et al.* claimed that the CS measurement has no fundamental meaning because GICs only fracture at the atomic level by tensile or shear failure. On the other hand, the tensile strength measurement by DTS is only acceptable if there is no significant plastic flow. Prosser *et al.* further suggested, that the FS measurement offers the best practical and reliable estimate of tensile strength, whereas CS is only indirectly related to tensile and/or shear failure in a complex manner. Direct tensile measurements of brittle materials (such as GICs) on the other hand, are inherently invalid due to the technical problems of the test methodology [348].

Dental cements are a versatile class of materials which are utilised clinically in several applications. For each application a specific cement must be selected and developed since one type of cement is unlikely to perform under all conditions [47]. Dental cements and restoratives are commonly supplied as separate powder and liquid constituents which are hand-mixed to a paste consistency and set to form a hard brittle mass within six to eight minutes of mixing. The relative proportions of the powder and liquid constituents are usually dispensed using the manufacturer’s recommended scoop and dropper bottle system prior to hand-mixing. However, the use of scoop and dropper bottle systems can result in powder to liquid mixing ratios that vary considerably from that recommended by the manufacturer [31, 318, 349, 350]. The volume of powder dispensed by the operator depends on the powder packing density achieved on filling the scoop with powder variations of ±10.0 % from that recommended by the manufacturers reported in a laboratory investigation. The dropper bottles can also not be relied upon to dispense calibrated volumes of liquid because of the angle at which the bottle is held and the pressure applied to squeeze a drop will influence the volume of the liquid dispensed [58, 351]. If the dropper bottle is held on its side rather than being inverted, the volume of the drop of liquid dispensed can vary by including an air bubble within the drop. Alternatively, if the bottle is squeezed too much when dispensing the liquid a squirt rather than a drop may be obtained. Considerable variations in test results for dental cements and restoratives are achieved when the manufacturer's recommended powder to liquid mixing ratios are not utilised and emphasis should be placed on the proportioning, manipulation and properties of the cement or restorative produced as a basis for a practical interpretation of its fundamental physical, chemical, biological and mechanical characteristics [2, 318, 352-355].

The reinforcement of GICs in order to improve the mechanical properties of conventional cement systems has been widely studied. The use of glass fibres [356-359], fillers such as hydroxyapatite [136, 157, 360, 361], strontium oxide [362], bioactive glass particles [148, 363, 364], metallic powders [365-370] and montmorillonites [14, 15] has been reported in the literature. Kobayashi [359] *et al.* suggested, that the brittle nature of glass-ionomer cements can be changed to a more ductile or predicable one by fibre incorporation which may prevent the catastrophic fracture caused by the surface and initial flaws that are common to brittle materials. As mentioned previously, Dowling *et al.* [14] reported the addition of nanoclays (Ca-MMT and ADA-MMT) to conventional GIC restoratives and found no significant reinforcement effect or increased performance in the case of Ca-MMT whereas, the addition of organoclays (ADA-MMT) to the powder and liquid elements of the GICs up to 1.0 wt.% had a positive reinforcing effect on the GIC system. The authors attributed the effect of the untreated nanoclays addition on the CS of GICs, at higher clay concentrations (increased MMT additions in excess of 1.5 wt.%), to the nanoclays agglomeration and disorganised structures of stacked clay platelets, which decreased the overall surface area available for reaction thereby minimising any potential reinforcing effect. However, the possibility to achieve optimum nanoclay dispersion in the polymer liquid component of the cement was not explored in the above mentioned study by Dowling *et al.* In the current work, on the other hand, we initially established the dispersion of nanoclays in PAA by selecting the most appropriate commercially available clays (Nanocor Inc. purified nanoclays i.e., PGV and PGN) which did not require any additional pre-treatment to increase the interlayer gallery [265] before the mixing with the aqueous PAA solutions. Although, the dispersion of nanoclays was successfully achieved as shown by the data presented earlier, only a small improvement in the mechanical properties of the GIC systems was observed. There are several factors which can affect the improvement of the mechanical properties in cements, for example the adjustment in the P/L ratio of the GIC systems, the processing technique of nanoclays dispersion in PAA suspensions, the molecular weight of PAA, the polymer concentration of the aqueous PAA solutions and the acquisition of the precise dexterity methodology to prepare the GIC specimens for mechanical testing. In addition, the details on the testing methodology in terms of specimen size, rate of loading (cross-head speed), specimen preparation, storage conditions and time of testing make it very challenging to adequately assess the literature in a scientific manner.

Unfortunately, the manipulation techniques for dental cements, GICs in particular, vary greatly such that this group of restorative dental materials is probably the most abused with respect to the manipulation techniques employed and powder to liquid mixing ratios utilised in clinical practice [36, 371, 372]. Therefore, one cause for failure in restorations is the manipulation of dental materials. The techniques employed in manipulating the GICs in clinical practice frequently involve the mixing of two components, powder and liquid or paste and paste, with the relative proportions being assessed by ‘eye’ or with the aid of a crude operator dependent measuring system and under mixing conditions (time and manipulation technique) which might differ from those employed by the manufacturer to assess the standard material properties [47, 318, 373-377]. As a result, the final materials produced in clinical practice are subject to considerable variations and therefore the physical, chemical, biological and mechanical properties of these materials cannot be consistent [3, 31, 318, 378-381]. Interestingly, dental restoratives are often placed under stressful clinical situations which invariably influence the clinically induced variability and result in poor clinical performance [1, 382]. It is often unknown how the clinical variability impacts on the performance of dental cements. Therefore, the familiarity with the factors affecting the performance of the materials properties can minimise the problem of failure and increase the scope of application.

The addition of nanoclays at low loadings i.e. 5 wt.% was reported that resulted in reinforcing a variety of polymer systems, including, nylon [262, 268, 383], poly-methyl-methacrylate (PMMA) [384, 385], epoxy [184], polyacrylamide [386, 387] and more recently PMMA bone cements [388]. The mechanical properties of nanocomposites determined via a stress–strain testing showed a substantial increase of the elastic modulus of the composite materials compared to the values reported for the pristine matrix materials in several polymer systems. In a review of nanocomposites, Fischers [252] reported, that the elastic modulus of the composites increased by about 60%, while values for the strain at break and the yield stress remained nearly at the same level.

Earlier researchers of Toyota [255] had developed a technique for the incorporation of nanoclays into polypropylene to enhance the mechanical performance of the system. In this procedure, a first ion-exchange step with ammonium cations was followed by the incorporation of oligomeric polypropylene between the organically modified nanoclay sheets and a subsequent mixing with the polymer matrix. In a recent review paper, Okada and Usuki [253], the pioneers of polymer nanocomposites, stated that the difficulties in obtaining molecular level dispersion of hydrophilic nanoclays in polymer systems is a challenging task to develop their novel industrial applications. Nevertheless, nylon-clay nanocomposites, manufactured previously, have been used in automotive parts, food packaging and electrical products with improved mechanical properties [253, 262, 268, 383, 389]. Yoshitsugu *et al.* studied the polymerisation of ε-caprolactam into the interlayer spacing of nanoclays to produce a nylon 6-clay hybrid which had significantly increased tensile strength (107MPa) and tensile modulus (2.1GPa) compared to the pure nylon-6 (69 MPa and 1.1 GPa, respectively) [263].

They attributed the significant increase in mechanical properties to the increased interlayer spacing of the MMT nanoclays which resulted in “an enormous surface area and ionic bonds between the organic polymer and the inorganic silicate sheets”. Similarly, Park and Jana [385] studied the reinforcing ability of organically-modified nanoclays (Cloisites) in PMMA-epoxy blends and reported the significant increase in the tensile strength (69 MPa) and the tensile modulus (0.8 GPa) compared to the non-reinforced control group (27MPa and 0.5GPa, respectively). Park and Jana recognized, that the improvement in the mechanical properties was due to the homogeneous dispersion of MMT clays within the polymer matrix [385]. Thus, it is suggested that the dispersion of nanoclays in lower wt % (1-2 wt %) in GICs may potentially produce cements with better physical properties however, an understanding of the fundamental aspects of nanoclay dispersion and interactions with the polymer, the choice of suitable handling parameters and the employment of appropriate polymers and glass components is mandatory.

4.4 Wear

Wear is a tribological process which results in the loss of a material due to the interfacial contact of the two opposing surfaces. As previously mentioned in Chapter 1, the human oral environment is complex and the wear of tooth surfaces and dental restorative materials may result from a variety of mechanical interactions including, abrasion, attrition, adhesion, fatigue and erosion or any combination of these interactions. The final test of any new dental material is a carefully controlled clinical trial before their application in the oral environment. Therefore a considerable interest has developed in laboratory simulating the clinical environment in order to reduce the number of patients for clinical testing. Thus, it is important to understand the mechanisms of wear operating in the mouth. In the present work, the wear behaviour of GICs was evaluated by employing two wear test machines (section 2.2.7) to develop an understanding of the potential effects of nanoclays on the wear behaviour of the GIC systems. Although, the more reliable way to validate the wear behaviour of the dental restorative materials is to perform *in-vivo* studies. However, these studies are time consuming because of the patient variables (age, chewing habits, diet, biting forces etc.) that can significantly influence the data-collection. It is therefore very difficult to extract precise results and such findings are least likely to apply in the general population [390]. Due to the above difficulties, *in-vitro* studies are a good alternative. Although it is desirable for a restorative material to have a wear resistant behaviour similar to the natural tooth structure but, little is known about the systemic effects that the worn materials may have. For example, the fate of the debris from worn materials, the adverse effect of the debris on the tissues or its incorporation into the body cells and tissues [391].

Unfortunately, the validation and correlation of the *in-vitro* results with the *in-vivo* are very complicated because there are no standards for wear characterisation and there are also a large number of variables involved in *in-vitro* vs *in-vivo* comparison. ISO has published a technical specification ISO 14569-1:1999 (new version: 14569-1:2007) on "Wear by tooth brushing" in 1999 [392] followed by another technical specification, ISO 14569-2:2001 "Wear by two- and/or three-body contact" in 2001 [393]. In the later standard, eight different wear test methods were described but according to Heintze [391], none of them is able to reflect the clinical performance. Therefore, significant variations can be observed in recent studies on the methodology of the wear-test parameters such as the type of the wear machine, the antagonist materials, the contact conditions, the applied load, the contact area load and the presence or absence of the slurry. Most of the studies on the wear behaviour of materials in the metallurgical science are based on experiments using simple, unidirectional or reciprocating movements [224, 248]. However, different types of chewing simulation methods (*in-vitro* wear simulators) like the IVOCLAR [174], the Zurich [175], the MTS [176], the ACTA [177], teh OH&SU [178], the Dento-Munch-Robo-simulator [179] and the University of Alabama [180] wear simulators have been reported in the literature. In a recent critical review of dental wear simulation devices and methods, Heintze [391] indicated that the MTS hydraulic simulator, which was designed by DeLong and Douglas [176], had the best motion control. Furthermore, several antagonist materials such as steel [394, 395], enamel [178, 396, 397], polymers (mainly silicon rubber) [398], ceramics (alumina, carbide steel etc.) [399], steatite [175, 400] and titanium [401] have been reported in the literature. It is therefore nearly impossible to correlate the results of the wear behaviour of GICs considering the variation in methodology reported in the literature.

Despite the number of advantages of GICs such as fluoride release, physicochemical bonding to enamel and dentine and similar coefficient of thermal expansion as of the natural tooth, their main disadvantage is their low wear resistance [402]. In the present study, we proposed the dispersion of nanoclays in the liquid portion of GIC as on way to improve the mechanical properties and the wear behaviour of the resulting GICs. The reciprocating wear test (ball-on-flat) and the OH&SU wear simulation studies were performed in order to investigate the effectiveness of Fuji-IX and HiFi reinforcement with nanoclays. The results of reciprocating wear test of the GICs, both in terms of wear volume and wear depth, are described in section 3.5.1. The results of the reciprocating wear resistance are shown in Table 3.7. In the reciprocating wear test, the cements did not generate wear marks on the alumina antagonist due to the higher values of hardness of alumina. This suggested that the wear scar created during the ball-on-flat abrasion resulted entirely from the wear of the GICs. Although the reciprocating wear test results of the HiFi cements showed that C1.0NHPAH (1 wt % nanoclays) had a better wear resistance (lower values of wear volume) however, no significant difference ($P > 0.05$) in the wear volume was observed in the HiFi-nanoclay system when the data were analysed with ANOVA. Similarly, the Fuji-IX cements showed no significant difference in the statistical analysis however, the highest wear volume was obtained for C2.0NF75F. A comparison between the Fuji-IX and HiFi cements formed after the dispersion of nanoclays, reflects that the HiFi cements always showed better wear resistance than the Fuji-IX. It is proposed, that the improved wear resistance of the HiFi system after the dispersion of nanoclays may be due to a better dispersion of nanoclays. In a study by Ramalho and Antunes [403] on resin-based dental composites it was reported, that there is a linear relationship between the wear resistance and the hardness and therefore higher values of hardness may lead to higher values of wear resistance. The reciprocation wear test results presented in Figure 3.36 shows a linear relationship between the wear volume and hardness values of the HiFi system at different nanoclay content which support the findings of Ramalho and Antunes and are in good agreement with their studies. Ramalho and Antunes [171] also reported that RBCs consisted of 40 μm filler particles sometimes do not follow the above trend of wear-hardness relationship. It was suggested, that this behaviour may be related to the microstructure of composites and was due to the abrasive nature of the tested materials. In the case of GICs, the glass particles that remain as fillers after the setting reaction are not expected to be as large as 40 μm. In most commercial products, the size of the glass particles is ≤ 45 μm. Furthermore, during the setting reaction, the size of the glass particles is expected to decrease significantly. Consequently, the wear resistance now should not be dependent on the size of the glass particles as in the case of the RBCs. It is therefore logical to conclude, that in GICs the main factor remains the wear resistance of the polymer matrix. [404].

The results from OH&SU wear simulations, both in terms of wear volume and wear depth, are described in section 3.5.2 and Table 3.7. The OH&SU oral wear simulator subjected the cement specimens to three wear mechanisms, namely abrasion, three-body abrasion and attrition using a steatite antagonist. The abrasion wear, resulted in material loss from the GIC specimen as the steatite antagonist forced through the exposed glass particles when it travelled along the sliding path [168]. In the three-body abrasion wear, the presence of the food like slurry and the wear debris between the two opposing surfaces (cement and steatite antagonist) abraded further the GIC specimens. This behaviour resembles the mastication process [405]. Finally, in attrition wear, a force was applied upon the specimens which induced the micro-cracks that propagated under the cyclic loading resulting in the removal of material from the GIC surfaces [406]. Table 3.7 depict that of HiFi cement formed after the dispersion of nanoclay generally resulted in an increase in total wear volume of cements however, no significant difference ($P > 0.05$) was found was data was analysed with ANOVA. The reinforcement of 4 wt % nanoclay (C4.0NHPAH) showed highest total wear volume 1.49 (0.24) mm^3 in comparison to 1 wt % 0.97 (0.28) mm^3 (C1.0NHPAH) and 2 wt % 0.94 (0.21) mm^3 (C2.0NHPAH). A schematic evaluation of the values obtained from OH&SU wear simulation of cement groups is presented in Figures 3.31 and 3.32. The total wear volumes and total wear depths were analysed in terms of their relationship to the mean abrasion and the mean attrition. It is obvious from Figures 3.31 that the calculation of total wear volumes was less dependent upon abrasion volume and attrition volume. Conversely, total wear depths were strongly influenced by attrition depth and to some extant by abrasion depth. It is therefore suggested that the determination of the total wear volume is more reliable than the total wear depth. Therefore, the wear regime, from which some of the reinforcing glass particles from the GIC surface were removed continuously exposing the underlying cement matrix, can be studied in a much better way by using wear volume values. Moreover, the wear volume determined by the OH&SU simulator showed a similar trend as the wear volume determined by the ball-on-flat method and the results from both testing methods confirmed that the HiFi cements were more wear resistant than the Fuji-IX cements. The wear of the steatite antagonist in the OH&SU simulation test method may also need to be considered while analysing the wear resistance of GICs. Unfortunately, the wear of steatite antagonist was not determined in the present study. However, it would be interesting to monitor the effects of the wear of antagonist on the wear resistance of GICs. Furthermore, the effect of the nanoclays dispersion on the wear resistance of GICs was not obvious and there was no significant difference when the wear volume data were analysed using ANOVA and Tukey's test. It was also noted that the OH&SU wear simulation produced significantly lower wear values than the ball-on-flat test due to fundamental differences between these two wear testing methods which were described in Table 3.8. Nevertheless, a comparison of the various parameters used in two wear test methods shown in Table 3.8 demands that the wear resistance of GICs obtained from two different machines can not be correlated and it must be analysed independently.

Considering the factors which may affect the wear of material, the applied load or pressure, which is defined as the force applied per unit area, may be a one of the dominating factors in addition to type of antagonist in the determination of wear. One of the factors of fundamental importance, which determines the validation of the *in-vitro* wear determination and, is the size of the contact area. Contact area between the material and the antagonist is inversely proportional to the pressure and consequently can affect the extent and the mechanism of wear in all type of wear studies [166]. In the present work, the ball-on-flat wear test was conducted using alumina ball antagonists whereas, in OH&SU wear simulations steatite antagonists were employed. The relationship between the applied force and the contact are of an antagonist is presented in Figure 4.9. In both test methods, contact area was different which have resulted in different contact forces. For example, when alumina ball antagonist was employed in reciprocating test method (ball-on-flat), it did not show any apparent wear scar. Therefore, the lower contact area due to no wear in alumina antagonist resulted in higher contact forces and more wear of GIC material. Whereas, higher contact area, in case of OH&SU simulation may have resulted due to the simultaneous wear of steatite antagonist and GICs specimens, produced lower contact stresses. Krejci *et al.* [407] evaluated the influence of the size and shape of the contact areas on the wear results and found that the wear of posterior restorative materials was inversely related to the contact area size of the antagonistic cusps. Krejci *et al.* noted a significant decrease of wear when the contact area increased from 0.26 to 1.18 mm^2 but surprisingly found no significant difference in the extent of the wear contact areas increased from 1.18 to 4.10 mm^2. Krejci *et al.* proposed that a standardized enamel antagonist must not have a flat uniform surface but should have a "cupola-like" shape but the radius or potential materials to be used for this purpose were not suggested [407].

Furthermore, several associations of the wear of a material and mechanical properties have been suggested. Wilson *et al.* demonstrated a correlation between the fracture toughness and the wear resistance of glass ionomer cements and reported that wear rate decreased with increasing fracture toughness [408, 409]. Rabinowich, on the other hand, suggested that the wear resistance of materials is often related to their fracture toughness and hardness and proposed the following equation [410]:

$$V = CF/K_{\mathrm{IC}}^{0.75} H^{0.5}$$

Where C is a constant, V is the loss of material's volume, F is the applied load, H is the hardness and K_{IC} is the fracture toughness.

Wilson *et al.* [408, 409] related the Reptation model that was applied by Prentice [404, 411] on the fracture toughness of materials, with the effect of molecular weight of

PAA on the fracture toughness in glass ionomer cements and suggested that the number of entanglements are closely related to the molecular weight. Prentice studied the fracture behaviour of PMMA following the Reptation model (shown in Figure 4.8) and reported that the crack open displacement of PMMA increased linearly with increasing the molecular weight up to a maximum value of molecular weight, above which it is constant. Similarly, Fennel and Hill [412] investigated the influence of PAA molar mass and PAA concentration on the fracture toughness and toughness of cements. Fennel and Hill reported that there was a larger dependence of the cement toughness on the PAA concentration for high molar mass PAA. However, the fracture toughness of cements increased with the molecular weight up to a point where the molecular weight of PAA reached a critical entanglement value.

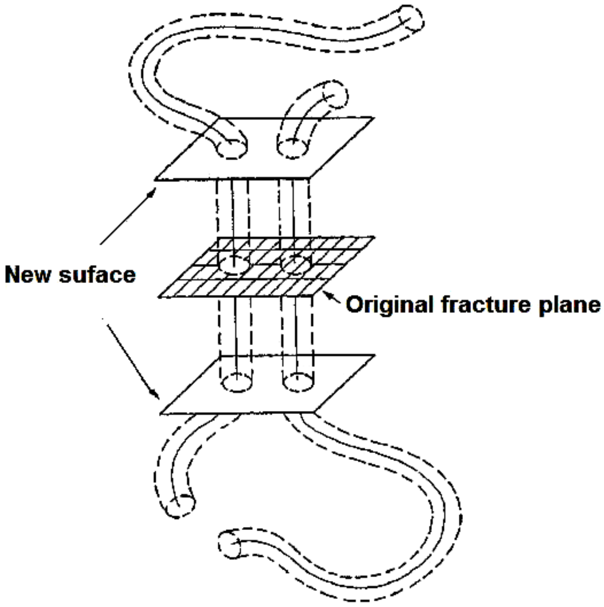

Figure 4. 8: Reptation chain pull-out model for fracture [404].

This is very useful in order to understand better the mechanical behaviour in glass ionomer cements. In practice, there is a molecular weight value of PAA above which the fracture toughness deviates from the Reptation model and the fracture toughness does not increase with increasing the molecular weight further. This value has not been reported in the literature. Another factor that would restrict the use of high molecular weight PAA in glass ionomer cements is viscosity. Consequently, the fracture toughness of glass ionomer cements could theoretically be higher if the molecular weight of the PAA used was higher. Considering all the above and knowing from previous work published by Hill *et al.* that the fracture toughness of GICs depends on the molecular weight and the concentration of the aqueous polymer solutions used in GICs, it is logical to consider that other than the polymer component could play an important role in the reinforcement of the polysalt matrix, e.g. nanoparticles, nanoclays.

In a clinical study by O'Brein and Yee [413], five possible wear mechanisms of composite resins was proposed: (1) wear of the resin matrix, (2) loss of fillers by failure of bonding to the matrix, (3) loss of filler through shearing of exposed particles, (4) loss of filler through cracking and failure of matrix, (5) exposure of entrapped air bubbles. On the other hand Xie *et al.* [158] reported that the wear resistance of GICs may be influenced by several factors such as, the inherent wear resistance of the polymer matrix and the glass particles, the size and quantity of pores, the size and shape of the glass powder and the integrity at the interface between the glass particles and the polymer matrix. Xie *et al.* proposed that the unreacted glass filler particles and the unreacted polymer matrix may constitute the area of the lowest wear resistance for GICs. Dowling and Fleming recently studied the *in-vitro* wear resistance of the Chemfil Superior (GIC) prepared with nanoclays additions to the powder constituent [15]. The addition of ADA-MMT nanoclays to GICs did resulted in significant difference in total wear volume and total wear depth. On the other hand, Ca-MMT nanoclays resulted in significant increase in total wear volume as the concentration of nanoclay was increased. Dowling and Fleming attributed the poor wear resistance of Ca-MMT reinforced cements to agglomeration and the larger particle size of Ca-MMT however, the possibility of such agglomeration in the GICs reinforced with ADA-MMT clay was not discuss in detail. In the present study, it is suggested that due to the interaction between nanoclays and PAA, there might be a fewer amount of unreacted PAA left which may result in less abrasion of the GIC system and improving the wear resistance after the dispersion of nanoclay. However, the quantification of the unreacted PAA may be very difficult and we do not know in what extent this may potentially affect the properties of GICs system.

To date the assessment of the *in-vivo* or *in-vitro* wear resistance of dental restoratives has been evaluated both in terms of the wear depth and the wear area. In a recent review questioning the “need for *in-vitro* wear simulating devices” Ferracane [414], concluded that in order to standardise the wear testing methodologies and data reporting, an appropriate wear quantity namely, area, depth or volume is critical. However, DeLong [415] suggested that the ideal wear quantity for data reporting should be relevant to the clinical practice and measured easily both *in-vivo* and *in-vitro* using similar or comparable methods. In the same paper, DeLong also described the assessment of the *in-vivo* wear of tooth structures and dental restorative materials in terms of area and depth as being “indirect wear measures” since both the wear area and wear depth are dependent upon occlusal factors and vary with time. Finally, DeLong suggested that the assessment of area and depth as appropriate wear quantities are “difficult, if not impossible” to combine. Heintze [416, 417], analysed the reproducibility of the mean wear depth results from different test centres when the

OH&SU was employed to test three conventional resin-based composite materials (Heliomolar, Herculite and Z100) using a 20 N abrasion force (in the presence of a food-like slurry) and differences of 33–56 % were reported. Interestingly, the mean wear depth measurements observed for the attrition regime when the OH&SU was employed using the same methodology varied from 31–78% when attrition loads used varied from 70–90 N. Heintze, therefore, suggested that there are indeed difficulties with using the mean wear depth measurements to report the *in-vitro* wear resistance of dental restorative materials. In the clinical studies however, the influence of the restorative materials, different batches, measuring methods, finishing techniques, and variables such as chewing, age, dietary habits will produce different results between clinical studies with the same materials. Therefore, the wide variations in clinical results make it difficult for significant differences to be found among materials [418]. Enamel-like wear behaviour is one of the major requirements for dental restorations and for the antagonist materials used in the in-vitro studies [405].

4.5 Microscopy

The microscopic observation of GICs revealed that the fractured surface of cement specimens consists of both large and small glass particles which can readily be distinguished from the polymer matrix. It is widely accepted that conventional SEM is not ideal to study the microstructure of glass ionomer cements because of the cracks formations due to the evaporation of water in the SEM vacuum. The resultant SEM micrographs sometimes prevented the interpretation of micro-analytical information of the structure of cements. Such limitation may be avoided by the use of ESEM, cryo-SEM or TEM. Cryo-SEM micrographs presented in section 3.6 did not show the same cracks over the surface of GICs samples if compared to conventional SEM. Such crack formations during SEM observations were due to the dehydration of cements under high vacuum conditions. Figure 3.41 shows that glass particles are embedded in the cement matrix and some of the glass particles are also observed on the surface of cements being dislodged during the three-point test. Although the average size of glass particles was measured under 5 µm in the micro-graph of the Fuji-IX cement, there is a possibility that much smaller glass particles may also be present. However, due to the small wt % of nanoclay used, it was difficult to study the dispersion of nanoclays in GICs by scanning electron microscopy. Therefore, transmission electron microscopy (TEM) was employed to study the structure and interaction of nanoclays and GICs. The TEM study showed that the cement-forming reaction resulted in the dissolution of the glass to form an amorphous gel around the glass particle. Figure 3.42 shows the TEM micrograph of C2.0NF75. TEM micrographs indicated the microstructure of the PAA matrix, glass and the interactions of dispersed nanoclays with PAA and glass particles. The mesoporous appearance of glass particle etched with PAA and its association with the nanoclay can be observed in Figure 3.42. Tay *et al.* [249] described the porous structure of glass filler particles in ChemFlex (GIC) as "seed-like" inclusions. Tay *et al.* [249] reported that "seed-like" inclusions were retained within the silica gel layer after the depletion of ions from the surfaces of glass particles in conventional glass ionomer cements. On the other hand, Barry *et al.* [419] suggested that the porous glass filler or "seed-like" inclusions present in conventional GIC formulations represent segregated regions of a fluoride-rich phase in certain reactive glass compositions. Tay *et al.* [249] observed a 150-300 nm thick siliceous hydrogel phase around the glass core and suggested that smaller glass particles reacted completely with PAA forming siliceous-hydrogel rich phases within the cement matrix. Extending the explanations of Tay *et al.* to the present work, the presence of siliceous hydrogel phases surrounding the remnant glass core was observed in the TEM micrographs of CF-IX. The thickness of this phase seems to be only a few hundred nanometers. The smaller particles forming "fully reacted" hydrogel phases (core glass has fully reacted) are also shown in Figure 3.42 (white bold arrow). Barry *et al.* [419] studied the microstructure of GICs and concluded that the action of PAA is to leach aluminium ions from the alumina-silicate matrix, leaving a silica gel containing particles of fluorite. However, this is the case if the ionomer glass composition is phosphorus free. As mentioned before, if the glass composition contains phosphorus then Al-O-P species are present and the hydrolysis mechanism during the PAA attack on the glass surface is not the same and depleted phosphorus is observed on the glass surface instead. The TEM of GICs reported in the present study, confirmed the presence of porous glass filler particles and our findings are in good agreement with the above mentioned study by Tay *et al.* Moreover, the presence of electron-dense (dark gray) zones in the majority of the polymer matrix (M) shown in

Figure 3.36 was probably due to the formation of a poly-salt matrix when metallic ions reacted with PAA [249]. On the other hand, the bright areas in the cement matrix were most likely non cross-linked PAA. Wilson *et al.* reported the presence of calcium rich droplets in the glass particles shown as bright spots on the glass surface under the SEM. These droplets, however, were not observed in the present work [419]. As discussed above, during the setting of GICs, bonds are formed between the poly-carboxylic from the PAA matrix and aluminium and/or calcium ions from the glass particles resulting in salt bridges. The un-reacted glass filler particles and/or un-reacted PAA matrix may constitute a microstructure with inferior mechanical properties and poor wear resistance. It is therefore, assumed that nanoclay reinforcement may reduce the amount of un-reacted PAA matrix resulting in superior GIC system but it is difficult to comment of such an interaction. Moreover, Dowling *et al.* studied the microstructure of GICs (Chemfil) after the addition of nanoclays (Ca-MMT and ADA-MMT) and proposed that the dehydration cracks travel more easily through the matrix of the Ca-MMT reinforced cements than the ADA-MMT reinforced cements [14].

In relation to the microstructure, the determination of the bond strength between the tooth and GIC is one of the important properties of GICs. The bond strength of GICs is greater to enamel than to dentine due to the chelation of the calcium in the mineral phase of tooth [66]. In ordered to understand the microstructure of glass ionomer cements, Yiu *et al.* [420] studied the GIC-dentin interface of six commercial auto-cure GICs. Yiu *et al.* revealed the presence of “spherical bodies” along the GIC-dentin interface that resembled with hollow eggshells consisted of a silicon-rich GIC phase (Figure 4.9). They suggested that the presence of such inclusions of distinct Si-rich phase within an air-void of GIC-bonded dentin resulted from a continuation of the glass ionomer reaction upon water diffusion from the moist dentine [420].

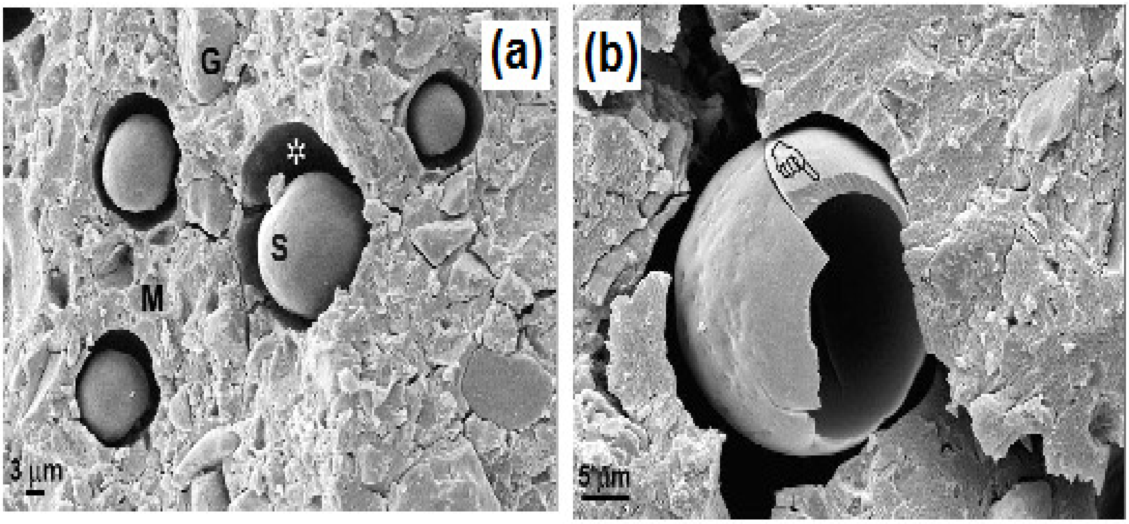

Figure 4. 9: ESEM micrograph showing the presence of spherical bodies (S), glass filler particles (G) and polymer matrix (M) at the GIC-dentin interface [420].

The presence of these spherical bodies in the matrix of GICs was only limited to the GIC-dentin interface and there was no evidence of such structures at 0.5 mm away from dentin. Yiu *et al.* attributed the formation of such structures to the slow permeation of water from dentin into the GIC matrix resulting in Si-rich phase which played an important role in achieving the strength along GIC-dentin bonded interface. One would expect, however to observe similar spherical bodies within the cement matrix if considering that water could be also absorbed from the oral cavity and generally the oral environment. However, such an observation has not been observed in the present work or reported in the available literature.

Generally, the structure of nanocomposites can be studied using XRD and TEM analyses. Due to its easiness and availability, XRD is the most common technique used to probe the nanocomposite structure which was discussed in section 4.1.1. Although XRD offers a convenient and simple method to determine the average interlayer spacing of the nanoclays, it cannot determine the spatial distribution and the microstructure of nanocomposites. Thus, nanocomposite structures cannot be studied solely by XRD patterns. On the other hand, TEM allows a qualitative evaluation of the internal structure and spatial distribution of the various phases through direct visualization and can also prove the occurrence of intercalated and exfoliated nanocomposites. Although TEM represents a powerful tool for the characterization of nanocomposites, problems concerning the tedious sample preparation and may be the modifications of specimens during the sample preparation process have to be considered. Indeed, TEM analysis of PAA-nanoclay dispersion can only be achieved with proper experimental conditions and correct information about the methodology. In the present study, due to certain problems associated with TEM specimens, it was very challenging to obtain thin sections of PAA-nanoclay specimens using an ultra microtome. Unfortunately, we are unable to provide the morphological evidence showing a homogeneous dispersion of nanoclays in aqueous PAA suspensions due to difficulties associated with the TEM specimen preparation and technical limitations of the ultra microtome. However, during this study and for training purposes, the TEM analysis of some polymer-nanoclay systems (poly-propylene and poly-butylene) was successfully conducted. Figure 4.10 showed evidence of exfoliation of nanoclays in poly-propylene and poly-butylene. We expected to obtain similar results for dispersed nanoclays in PAA-nanoclay suspensions as well as nanoclay reinforced GICs. This however, was a difficult task due to unresolved problems in sample preparation.

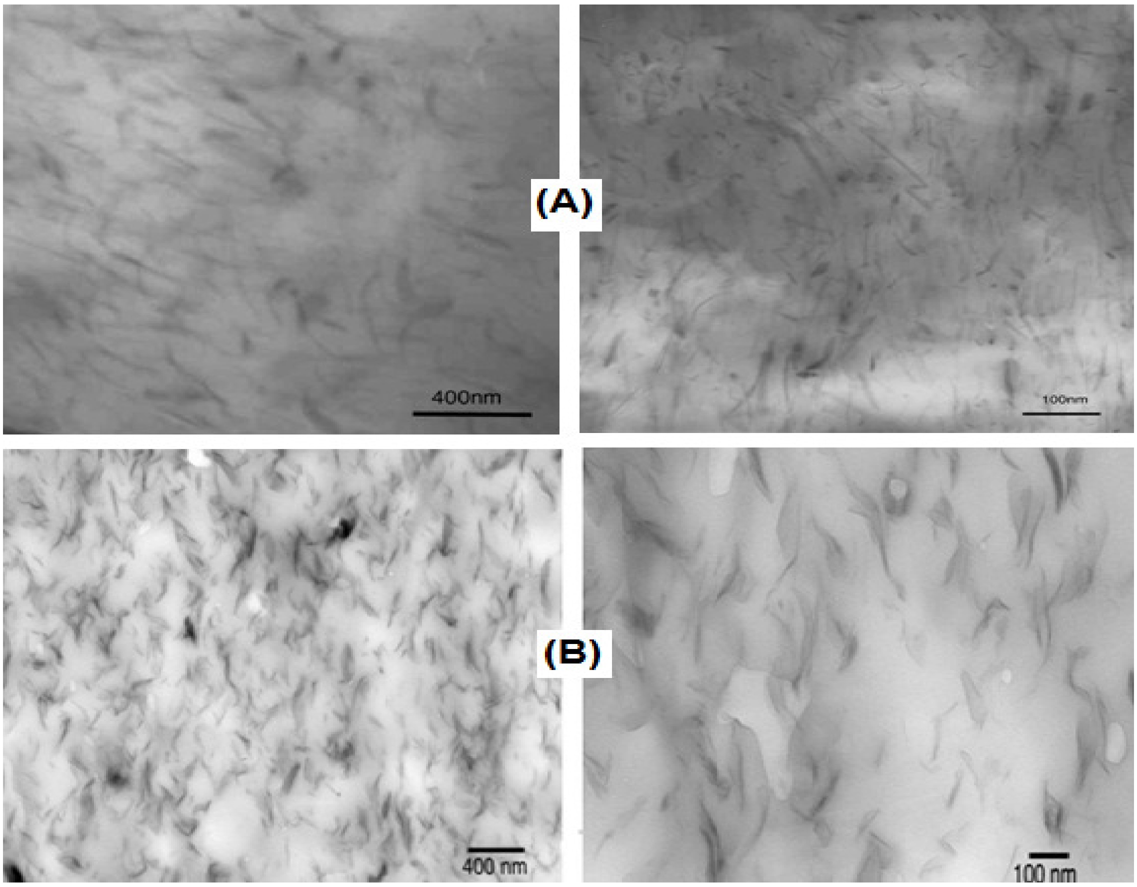

Figure 4. 10: TEM micrographs of two polymer-clay systems, (A) 32% polypropylene and nanoclay and, (B) polybutylene terephthalat and Celosite.

CHAPTER 5

5 CONCLUSIONS

The reinforcing capability of nanoclays is due to their high modulus, high strength and high aspect ratio. PAA-nanoclay interactions were observed when PGV and PGN nanoclays were dispersed in the polymer matrix following a suitable processing method. The dispersion of nanoclays in aqueous PAA suspensions and the reinforcement effect of the dispersed nanoclays on GICs were studied using a combination of analytical tools such as, XRD, XPS, FTIR, GPC, TEM, ESEM and cryo-SEM analyses. Furthermore, the mechanical properties (CS, DTS, FS, E_f and VH) as well as the working and setting times of the GIC systems after the reinforcement with nanoclays were measured. Finally, the wear resistance of cements was evaluated by two wear test methodologies namely, reciprocating wear test and OHSU wear-simulator.

The XRD pattern of nanoclays showed that the main diffraction peak of PGV was present at 2θ ~ 6.95° and the interlayer space was 12.39 Å whereas in PGN the main diffraction peak appeared at 2θ ~ 7.13° and the interlayer space was 12.71 Å. The XRD pattern (no [001] peak at low angle) of PAA-PGV indicated that full exfoliation of the nanoclays in PAA took place. In the case of PAA-PGN, the shifting of 2θ values to a lower angle indicated intercalation due to the small increase (16.03 Å) in the nanoclays interlayer gallery spacing. The interaction of the hydrophilic nanoclay platelets with PAA resulted in the exchange of their interstitial metal cations (K^+, Na^+, Li^+, Mg^{2+}, Ca^{2+}, etc.) with protons and/or released within the organic PAA solution resulting in enhancing the *d*-spacing and simultaneously reducing the attractive forces between the platelets of nanoclays. It was suggested, that during the PAA-PGN interactions, one or more polymer chains penetrated in between the silicate plates of PGN whereas the lamellar structures of nanoclays remained intact resulting in intercalation. On the other hand, the PAA-PGV interaction resulted in the separation and random orientation of the silicate plates in nanoclays indicating exfoliation of nanoclays.

XPS studies resulted in information concerning the adsorption of PAA and the depletion of Na ions at the surface of nanoclays. The presence of O1s peak was associated with both nanoclays (PGV and PGN) and PAA whereas the presence of C1s was associated only with the PAA. The presence of one additional small peak in the wide XPS scan assigned to Mg KLL at 281 eV in both nanoclays before and after the treatment with PAA, indicated that there was a small amount of Si-O-Mg present in the silicate layers. The intensity of Si 2p, Si 2s, Al 2p, Al 2s and Mg KLL peaks was slightly higher in PAA-PGN and PAA-PGV. The presence of a small C 1s peak at 536 eV in both PGV and PGN nanoclays was attributed to adventitious carbon. Comparing the changes observed from O 1s photoelectrons in the narrow angle XPS scans of PAA-PGV and PAA-PGN, it was clear that stronger interactions were observed in the PAA-PGV. The physisorption and chemisorption of PAA molecules on the silicate surface of nanoclays resulted in the release of cations from the interlayer galleries of nanoclays reducing consequently the electrostatic Van-der-Waals forces between the silicate plates. The steric effect created by the PAA prevented the face-to-face interaction of nanoclay plates, which eventually resulted in intercalation or exfoliation.

The FTIR analysis showed that the absorbance intensity of the peak observed at 1019 cm^{-1} associated with Si-O- stretching vibrations increased with increasing the content of nanoclays from 0.5 to 8.0 wt %. The shift of the peak at 973 cm^{-1} associated with Si-O- stretching vibrations in nanoclays to 1019 cm^{-1} in PAA-nanoclay and to 1041 cm^{-1} in HiFi-nanoclay suspensions was linked to the change of the chemical environment in the nanoclay-PAA suspensions. When the nanoclays content increased from 1 to 8 wt % , the peak intensity associated with C=O stretching vibrations at 1706 cm^{-1} in the carboxylic group decreased slightly whereas a minor increase in the bending vibrations at 1629 cm^{-1} of the –OH groups was observed. The FTIR spectra of the Fuji-IX-nanoclay suspensions were not very much different from the spectrum of FL. The real-time study of the setting reaction of GICs over a period of one hour before and after nanoclays dispersion in Fuji-IX system and in HiFi system showed slight differences in the FTIR spectra. During the setting reaction of GICs, relatively weak peaks in the range of 2325 and 2363 cm^{-1} were observed that seem to become more intense in cements containing nanoclays (C2.0VF75F and C2.0NPAH).

GPC analysis showed that the PAA content in the aqueous polymer solution of Fuji IX liquid was 33 wt %, whereas the PAA content for the polymer solution in HiFi was 39 wt%. The M_w of PAA used in the HiFi system was in the range of 52,000-56,000 g/mol, whereas the M_w of FL was found to be very low in the range of 15.000 g/mol. The average M_w of FL was much lower than the expected range for a glass ionomer cement liquid required for posterior restoration cements. It is suggested that the molecular weight of PAA may have an effect on the nanoclays exfoliation and specifically on the interlayer spacing as the number of polymer entanglements would have had an effect on the mobility of the PAA chains within the interlayer space.

The working and setting times of GICs determined by the Wilson's rheometer exhibited a small decrease in both the working and setting times of glass ionomer cements prepared with the polymer liquids formed after the nanoclays dispersion when compared to control groups (CPA-HP and CF-IX). Generally, HiFi cements exhibited lower working and setting times compared to Fuji-IX. The addition of nanoclays of more than 1 % caused changes in the viscosity of PAA-nanoclay suspensions and the polymer suspension containing more than 4 % nanoclays was difficult to mix with the glass powder.

The mechanical properties (CS, DTS, FS, E_f and VH) of GICs were measured after storage in distilled water at various aging times such as, after 1 hour, 1 day, 1 week and 1 month. Generally, the cements containing 2 wt % nanoclays exhibited slightly higher CS (range 124–142 MPa), similar DTS (range 12–20 MPa) and higher biaxial flexural strength (range 37–42 MPa) compared to the control cement groups (Fuji-IX and HiFi). The reinforcement of nanoclays had no significant effect ($P > 0.05$) on the strength of cements however, an increase in strength was observed with increasing the storage time when mechanical testing data were statistically analysed with GLM and ANOVA. Similarly, in Fuji-IX system, no significant difference ($P > 0.05$) was observed in the mechanical testing data when two different processing temperatures (room temperature and 75 ^{o}C) were employed. Moreover, in Fuji IX cements, it was assumed that the setting reaction continued with time and that the mechanical properties increased with time, whereas in the HiFi cements no significant changes in the strength were observed with ageing time indicating that the cements had undergone possibly an early completion of the setting reaction. The flexural modulus E_f that was calculated from the initial straight part of the stress-strain curve obtained from the three-point bending test was significantly higher ($P < 0.001$) in the case of C1.0N PAH (14.8 G Pa). The HV of cements was calculated between 62-89 HV and no significant difference was observed between the GICs when the data were statistically analysed.

Wear tests conducted by the ball-on-flat wear test method and the OH&SU wear simulation method suggested, that the measurement of the wear volume is a more reliable value than the measurement of the wear depth. The total wear volume of the HiFi cements formed after the dispersion of nanoclays generally increased when compared to the control HiFi cements however, no significant statistical differences were observed. A comparison between the Fuji-IX system and the HiFi system reflected that the HiFi cements showed always better wear resistance than the Fuji-IX cements. It was proposed, that the improved wear resistance of the HiFi system after the dispersion of nanoclays may be due to a better methodology of the nanoclay dispersion. It is therefore suggested, that in the HiFi system there might be a fewer amount of unreacted PAA left which may result in less abrasion and improvement of the wear resistance.

The electron microscopy studies revealed the microstructure of the PAA matrix, glass as well as the degree of interaction of nanoclays with PAA. The cryo-SEM was proved to be a good tool for the micro-structural observation of GICs. The micro-structure of porous glass particles and the presence of siliceous hydrogel phases surrounding the unreacted glass core were identified by TEM. In the PAA matrix, the association of porous glass particles with the nanoclays was also observed.

CHAPTER 6

6 FUTURE WORK

In future, more work should be carried out in order to develop a complete understanding of nanoclays dispersion on PAA and the potential reinforcement mechanism of nanoclays in GIC systems. Also, the possibility to develop a commercial novel GIC system with nanoclays reinforcement should be explored on the basis of our current understanding of the PAA-nanoclay interactions. The following points for future work can be suggested:

1. The selection of suitable nanoclays, appropriate processing methodologies, uniform distribution of the nanoclays and interaction of nanoclays with PAA are key elements. Up-to-date knowledge of the literature and the logical design of experimental procedure are very important and should be addressed accordingly.
2. To achieve the maximum reinforcement effects of nanoclays, direct intercalation may be employed. Direct intercalation involves the mixing of the host nanoclay with PAA powder and then pressing the mixture into a pellet and heating at an appropriate temperature. However, the heating temperature will need to be optimised and it should be above the bulk glass transition temperature of PAA to ensure the presence of polymer melt [421]. The resulting product could be used to prepare a PAA solution (35-40 % PAA) to make the GICs restoration. Moreover, a comparative study of PAA-nanoclay prepared by solution-blending and melt-intercalation would be very interesting to optimise the most appropriate model for the exfoliation of nanoclays in PAA [422].

3. One of the possible ways to study the effect of nanoclays in glass ionomer cements is to treat the nanoclays with the PAA solution. After the initial treatment with PAA solution, nanoclays could be extracted by centrifuging and directly be added to the glass powder.
4. After the preparation of PAA-nanoclay suspension, GICs can be studied by modifying and finally optimising the powder : liquid ratios of the existing system.
5. It would be interesting to study the effect of PAA molecular weight and PAA contents in the aqueous suspension on the dispersion of nanoclays. In order to elucidate the effect of the molecular weight and polymer concentration on the dispersion and exfoliation of nanoclays, a more systematic study should be carried out.
6. Low-angle XRD should be employed to study the interlayer spacing along d_{001} direction to optimise the dispersion of nanoclays. Moreover, the presences of certain XRD peaks at higher 2θ values also require further explanation.
7. Narrow-scan XPS at binding energy 78-160 eV which is associated with the Si 2p or Si 2s and Al 2p or Al 2s photoelectrons from the silicate layers would provide a more detailed information of the elements involved in the PAA-nanoclay interaction. Mg KLL peaks observed at 281 eV was slightly higher in PAA-PGN and PAA-PGV when compared to the respective nanoclays and a narrow-scan XPS at 281 eV however, might be helpful to determine the significance of this observation and further understanding the chemisorption of nanoclays and PAA.
8. Although, the exfoliation/intercalation of nanoclays in aqueous PAA suspension was confirmed by XRD and the interaction between the nanoclays and PAA molecules was confirmed by XPS analysis, further details related to chemisorption and physiosorption mechanisms of PAA-nanoclay interaction would still require

attention. A more detailed justification of such interaction in the resultant GICs may also need to be explored.

9. More information is expected to be received from powder FTIR studies of nanoclays and PAA treated nanoclays following the KBr method (2 mg of sample well blended with 200 mg of KBr to form a disk for further FTIR analysis). . This would permit the detailed examination of -OH stretching vibrations in the nanoclays spectrum and Si-O absorption and -OH bending vibrations in a region bellow 1200 cm $^{-1}$, where intense peaks are present [291].
10. The addition of nanoclays can cause dramatic changes in the viscoelastic properties of PAA-nanoclay suspensions. Such changes are related to the pH, polymer charge and concentration of nanoclay and polymer. The determination of the viscoelastic properties of the PAA-nanoclay suspensions would be valuable to achieve the desirable effects of nanoclays reinforcement in GICs.
11. The possibilities to distinguish between the reacted and un-reacted segments of the adsorbed polymer molecules on the surface of nanoclays may be one area of interest. One way of conducting such quantitative analysis is by using NMR spectroscopy. ^{13} C NMR spectra could be used to quantify the number of free –COOH groups or interacted –COO$^-$ groups. Extending this to the setting reaction of the new cements, it would be possible to measure the degree of cross-linking as well as the free –COOH groups in the cement matrix using ^{13}C MAS-NMR spectra.
12. The mechanical properties must be evaluated according to the available test standards such as ISO or ASTM standards. A special care must be observed in the process of mould making. It is preferable to design such a mould which may house maximum 2-3 specimens. Considering the preparation of a larger number of GIC

specimens for determination of several useful properties such as, CS, DTS, FS, HV, BFS and fracture toughness, there should not be any compromise on the quality and quantity of moulds required for specimen preparation.

13. The fracture toughness is an important property of brittle materials such as, GICs. In the present work, however, fracture toughness could not be included due to the challenging nature of mould design and the difficulties involved in specimens preparation. The specifications according to ASTM Standard E399 – 06 [423] were employed to prepare disk shaped GICs specimens. However, disk shaped GICs specimen with a preformed crack was difficult to produce due to technical problems associated with the mould design. It is therefore, suggested that fracture toughness of GICs may be calculated according to the above mentioned ASTM protocol choosing a bar-shaped specimen design instead of a disk shaped design.
14. The validation and correlation of the *in-vitro* wear results obtained from two different test methods is very complicated because there are no standards for wear characterisation. There are also a large number of variables involved in different tests used in the *in-vitro* comparison. Ball-on-flat test may offer useful information about the wear behaviour of GICs, however the test parameter should be optimised very carefully because a slight change in any of the parameters may invalidate the results.
15. Although TEM provides very useful information about the dispersion and structure of nanocomposites, the sample preparation for the TEM study of PAA-nanoclays is a challenging area which should be carefully considered. It is suggested that a different sample preparation technique should be employed. TEM specimens may be prepared by mixing the PAA solution with the nanoclays, forming a thin film of the nanocomposite which will then be directly embedded to epoxy resin from

which a thin section (80-100 nm) will be removed using an ultra-microtome and the sample will be mounted onto a TEM copper grid.

7 REFERENCES

[1] McCabe JF, Walls A. Applied dental materials 9th Edition. Oxford : Blackwell, 2008.

[2] Mount GJ. Glass ionomers: a review of their current status. Operative dentistry 1999;24:115-24.

[3] Craig RG, Powers JM, Wataha JC. Dental Restorative Materials. St. Louis, MO. : Mosby, 2004.

[4] Mount GJ. Glass ionomer cements and future research. American Journal of Dentistry 1994;7:286-92.

[5] Wilson AD, Kent BE. The glass-ionomer cement: A new translucent dental filling material. Journal of Applied Chemistry & Biotechnology 1971;21:313-8.

[6] Wilson AD, Kent BE, Clinton D, Miller RP. The formation and microstructure of dental silicate cements. Journal of Materials Science 1972;7:220-38.

[7] Wilson AD, McLean JW. Glass-ionomer Cement 1st Edition. Chicago: Quintessence. 1988.

[8] Nicholson JW, Royal Society of Chemistry (Great Britain). The chemistry of medical and dental materials 1st Edition [Electronic book]. Cambridge, UK : Royal Society of Chemistry, 2002.

[9] Alexandre M, Dubois P. Polymer-layered silicate nanocomposites: Preparation, properties and uses of a new class of materials. Materials Science and Engineering R: Reports 2000;28:1-63.

[10] Giannelis EP. Polymer layered silicate nanocomposites. Advanced Materials 1996;8:29-35.

[11] LeBaron PC, Wang Z, Pinnavaia TJ. Polymer-layered silicate nanocomposites: An overview. Applied Clay Science 1999;15:11-29.

[12] Tran NH, Dennis GR, Milev AS, Kannangara GSK, Wilson MA, Lamb RN. Interactions of sodium montmorillonite with poly(acrylic acid). Journal of Colloid and Interface Science 2005;290:392-6.

[13] Tran NH, Wilson MA, Milev AS, Dennis GR, Kannangara GSK, Lamb RN. Dispersion of silicate nano-plates within poly(acrylic acid) and their interfacial interactions. Science and Technology of Advanced Materials 2006;7:786-91.

[14] Dowling AH, Stamboulis A, Fleming GJP. The influence of montmorillonite clay reinforcement on the performance of a glass ionomer restorative. Journal of Dentistry 2006;34:802-10.

[15] Dowling AH, Fleming GJP. The impact of montmorillonite clay addition on the in vitro wear resistance of a glass-ionomer restorative. Journal of Dentistry 2007;35:309-17.

[16] Skinner EW, Phillips RW. Skinner's Science of dental materials 8th Edition. Philadelphia ; London : W.B. Saunders, 1982.

[17] Smith DC. Development of glass-ionomer cement systems. Biomaterials 1998;19:467-78.

[18] Craig RG, Powers JM, Wataha JC. Dental materials : properties and manipulation 1st Edition. St. Louis, Mo. : Mosby, 2004.

[19] Kramer IRH, McLean JW. Alterations in the staining reaction of dentine resulting from a constituent of a new self-polymerising resin. British Dental Journal 1952;93:150-3.

[20] Buonocore M, Wileman W, Brudevold F. A report on a dentin composition capable of bonding to human dentin surfaces. Journal of Dental Research 1956;35:846-51.

[21] Bowen RL. Crystalline dimethacrylate monomers. Journal of Dental Research 1970;49:810-5.

[22] Bowen RL, Chandler HH. Experimental metal filled resin composites. Journal of Dental Research 1973;52:32.

[23] Ikemura K, Tay FR, Endo T, Pashley DH. A review of chemical-approach and ultramorphological studies on the development of fluoride-releasing dental adhesives comprising new pre-reacted glass ionomer (PRG) fillers. Dental Materials Journal 2008;27:315-39.

[24] Van Landuyt KL, Snauwaert J, De Munck J, Peumans M, Yoshida Y, Poitevin A et al. Systematic review of the chemical composition of contemporary dental adhesives. Biomaterials 2007;28:3757-85.

[25] Tay FR, Pashley DH. Resin bonding to cervical sclerotic dentin: A review. Journal of Dentistry 2004;32:173-96.

[26] Santini A, Miletic V. Comparison of the hybrid layer formed by Silorane adhesive, one-step self-etch and etch and rinse systems using confocal micro-Raman spectroscopy and SEM. Journal of Dentistry 2008;36:683-91.

[27] Ilie N, Hickel R. Macro-, micro- and nano-mechanical investigations on silorane and methacrylate-based composites. Dental Materials 2009;25:810-9.

[28] Smith DC. A new dental cement. British Dental Journal 1968;124:381-4.

[29] Mizrahi E, Smith DC. The bond strength of a zinc polycarboxylate cement. Investigations into the behaviour under varying conditions. British Dental Journal 1969;127:371-5.

[30] Wilson AD, Kent BE. The glass-ionomer cement: A new translucent dental filling material. J Applied Chemisty & Biotechnology 1971;21:313-8.

[31] Wilson AD, McLean JW. Glass-ionomer Cement 1st Edition. Chicago: Quintessence. 1988.

[32] Whitters CJ, Strang R, Brown D, Clarke RL, Curtis RV, Hatton PV et al. Dental materials: 1997 literature review. Journal of Dentistry 1999;27:401-35.

[33] Anusavice KJ, Phillips RW. Phillips' science of dental materials 11th Edition. St. Louis, Mo. : Saunders, 2003.

[34] Mitra SB. Adhesion to dentin and physical properties of a light-cured glass-ionomer liner/base. Journal of Dental Research 1991;70:72-4.

[35] Nicholson JW. Compomers: Ask the experts. Journal of Esthetic and Restorative Dentistry 2008;20:3-4.

[36] Van Noort R. An introduction to dental materials 3rd Edition. Edinburgh : Mosby, 2007.

[37] Nicholson JW, Royal Society of Chemistry (Great Britain). The chemistry of medical and dental materials 1st Edition [Electronic book]. Cambridge, UK : Royal Society of Chemistry, 2002.

[38] Ngo HC, Mount G, Mc Intyre J, Tuisuva J, Von Doussa RJ. Chemical exchange between glass-ionomer restorations and residual carious dentine in permanent molars: An in vivo study. Journal of Dentistry 2006;34:608-13.

[39] Wilson AD, Batchelor RF. Dental Silicate Cements. I. The Chemistry of Erosion. Journal of Dental Research 1967;46:1075-85.

[40] Kent BE, Wilson AD. Dental Silicate Cements: VIII. Acid-Base Aspect. Journal of Dental Research 1969;48:412-8.

[41] Wilson AD, Batchelor RF. Dental Silicate Cements. II. Preparation and Durability. Journal of Dental Research 1967;46:1425-32.

[42] Wilson AD. A Hard Decade's Work: Steps in the Invention of the Glass-ionomer Cement. Journal of Dental Research 1996;75:1723-7.

[43] Wilson AD. Dental Silicate Cements: VII. Alternative Liquid Cement Formers. Journal of Dental Research 1968;47:1133-6.

[44] Wilson AD, Nicholson J.W. Polyalkenoate Cements. In Acid-base Cements: Their Biomedical and Industrial Applications, Chap. 5, University Press: Cambridge 2003. In: 2003.

[45] Wilson AD, Kent BE. A new translucent cement for dentistry. The glass ionomer cement. British Dental Journal 1972;132:133-5.

[46] Crisp S, Wilson AD. Reactions in Glass Ionomer Cements: I. Decomposition of the Powder. Journal of Dental Research 1974;53:1408-13.

[47] Crisp S, Lewis BG, Wilson AD. Characterization of glass-ionomer cements. 2. Effect of the powder: liquid ratio on the physical properties. Journal of Dentistry 1976;4:287-90.

[48] Crisp S, Ferner AJ, Lewis BG, Wilson AD. Properties of improved glass-ionomer cement formulations. Journal of Dentistry 1975;3:125-30.

[49] Wilson AD, Crisp S, Ferner AJ. Reactions in glass ionomer cements: IV. Effect of chelating comonomers on setting behavior. Journal of Dental Research 1976;55:489-95.

[50] Crisp S, Wilson AD. Reactions in glass ionomer cements: V. Effect of incorporating tartaric acid in the cement liquid. Journal of Dental Research 1976;55:1023-31.

[51] Wilson AD, Crisp S, Ferner AJ. Reactions in Glass-Ionomer Cements: IV. Effect of Chelating Comonomers on Setting Behavior. Journal of Dental Research 1976;55:489-95.

[52] Crisp S, Lewis BG, Wilson AD. Characterization of glass-ionomer cements 1. Long term hardness and compressive strength. Journal of Dentistry 1976;4:162-6.

[53] Barry TI, Clinton DJ, Wilson AD. The structure of a glass-ionomer cement and its relationship to the setting process. Journal of Dental Research 1979;58:1072-9.

[54] Wilson AD, Paddon JM, Crisp S. The hydration of dental cements. Journal of Dental Research 1979;58:1065-71.

[55] Crisp S, Kent BE, Lewis BG, Ferner AJ, Wilson AD. Glass-ionomer Cement Formulations. II. The Synthesis of Novel Polycarboxylic Acids. Journal of Dental Research 1980;59:1055-63.

[56] Garcia-Godoy F, Malone WF. Effect of various etching times on two glass ionomer lining cements. Texas Dental Journal 1987;104:12-5.

[57] Guggenberger R, May R, Stefan KP. New trends in glass-ionomer chemistry. Biomaterials 1998;19:479-83.

[58] Mount GJ. An atlas of glass-ionomer cements 3rd Edition: a clinician's guide. London : Dunitz , 2002.

[59] Nicholson JW, Croll TP. Glass-ionomer cements in restorative dentistry. Quintessence international 1997;28:705-14.

[60] Peutzfeldt A, Garca-Godoy F, Asmussen E. Surface hardness and wear of glass ionomers and compomers. American Journal of Dentistry 1997;10:15-7.

[61] Smith DC. The current status of glass ionomer cements. Ontario Dentist 1985;62:26-9, 31, 34.

[62] Wasson EA, Nicholson JW. Change in pH during setting of polyelectrolyte dental cements. Journal of Dentistry 1993;21:122-6.

[63] Brook IM, Hatton PV. Glass-ionomers: Bioactive implant materials. Biomaterials 1998;19:565-71.

[64] Nicholson JW, Braybrook JH, Wasson EA. The biocompatibility of glass-poly(alkenoate) (Glass-Ionomer) cements: a review. Journal of Biomaterials Science Polymer edition 1991;2:277-85.

[65] Sullivan A, Hill R. Influence of poly(acrylic acid) molar mass on the fracture properties of glass polyalkenoate cements based on waste gasifier slags. Journal of Materials Science 2000;35:1125-34.

[66] Nicholson JW. Adhesive dental materials - A review. International Journal of Adhesion and Adhesives 1998;18:229-36.

[67] Bertolini MJ, Zaghete MA, Gimenes R, Freitas de Souza R, Vaz LG. Preparation of new glass systems by the polymeric precursor method for dental applications. Journal of Non-Crystalline Solids 2004;344:170-5.

[68] Culbertson BM. New polymeric materials for use in glass-ionomer cements. Journal of Dentistry 2006;34:556-65.

[69] Culbertson BM, Thakur A, Xie D, Kao EC. Amino acid modified polyelectrolytes for formulation of improved glass-ionomer (GI) dental restoratives. American Chemical Society, Polymer Preprints, Division of Polymer Chemistry 1997;38:127-8.

[70] Kao EC, Culbertson BM, Xie D. Preparation of glass ionomer cement using N-acryloyl-substituted amino acid monomers--evaluation of physical properties. Dental materials 1996;12:44-51.

[71] Algera TJ, Kleverlaan CJ, De Gee AJ, Prahl-Andersen B, Feilzer AJ. The influence of accelerating the setting rate by ultrasound or heat on the bond strength of glass ionomers used as orthodontic bracket cements. European Journal of Orthodontics 2005;27:472-6.

[72] Alemzadeh K, Raabe D. Prototyping artificial jaws for the Bristol Dento-Munch Robo-Simulator. 'A parallel robot to test dental components and materials'. Conference proceedings : Annual International Conference of the IEEE Engineering in Medicine and Biology Society IEEE Engineering in Medicine and Biology Society Conference 2007;2007:1453-6.

[73] Greenhalgh T. Papers that summarise other papers (systematic reviews and meta-analyses). British Medical Journal 1997;315:672-5.

[74] Lucarotti PSK, Holder RL, Burke FJT. Outcome of direct restorations placed within the general dental services in England and Wales (Part 1): Variation by type of restoration and re-intervention. Journal of Dentistry 2005;33:805-15.

[75] Burke FJT, Lucarotti PSK, Holder RL. Outcome of direct restorations placed within the general dental services in England and Wales (Part 2): Variation by patients' characteristics. Journal of Dentistry 2005;33:817-26.

[76] Lucarotti PSK, Holder RL, Burke FJT. Outcome of direct restorations placed within the general dental services in England and Wales (Part 3): Variation by dentist factors. Journal of Dentistry 2005;33:827-35.

[77] Lutz F. The postamalgam age. Operative dentistry 1995;20:218-22.

[78] Randall RC, Wilson NHF. Glass-ionomer Restoratives: A Systematic Review of a Secondary Caries Treatment Effect. Journal of Dental Research 1999;78:628-37.

[79] Burke FJT, Lucarotti PSK. Re-intervention in glass ionomer restorations: What comes next? Journal of Dentistry 2009;37:39-43.

[80] Yip HK, To WM. An FTIR study of the effects of artificial saliva on the physical characteristics of the glass ionomer cements used for art. Dental Materials 2005;21:695-703.

[81] Young AM. FTIR investigation of polymerisation and polyacid neutralisation kinetics in resin-modified glass-ionomer dental cements. Biomaterials 2002;23:3289-95.

[82] Young AM, Sherpa A, Pearson G, Schottlander B, Waters DN. Use of Raman spectroscopy in the characterisation of the acid-base reaction in glass-ionomer cements. Biomaterials 2000;21:1971-9.

[83] Stamboulis A, Law RV, Hill RG. Characterisation of commercial ionomer glasses using magic angle nuclear magnetic resonance (MAS-NMR). Biomaterials 2004;25:3907-13.

[84] Hill RG, Stamboulis A, Law RV. Characterisation of fluorine containing glasses by 19F, 27Al, 29Si and 31P MAS-NMR spectroscopy. Journal of Dentistry 2006;34:525-32.

[85] Zainuddin N, Karpukhina N, Hill RG, Law RV. A long-term study on the setting reaction of glass ionomer cements by 27Al MAS-NMR spectroscopy. Dental Materials 2009;25:290-5.

[86] Wasson EA, Nicholson JW. Change in pH during setting of polyelectrolyte dental cements. Journal of Dentistry 1993;21:122-6.

[87] Wasson EA, Nicholson JW. Studies on the setting chemistry of glass-ionomer cements. Clinical Materials 1991;7:289-93.

[88] Griffin SG, Hill RG. Influence of glass composition on the properties of glass polyalkenoate cements. Part I: Influence of aluminium to silicon ratio. Biomaterials 1999;20:1579-86.

[89] Crisp S, Lewis BG, Wilson AD. Glass Ionomer Cements: Chemistry of Erosion. Journal of Dental Research 1976;55:1032-41.

[90] Pires RA, Nunes TG, Abrahams I, Hawkes GE. The role of aluminium and silicon in the setting chemistry of glass ionomer cements. Journal of Materials Science: Materials in Medicine 2008;19:1687-92.

[91] Griffin S, Hill RG. Glass composition influence on glass polyalkenoate cement mechanical properties. Journal of Non-Crystalline Solids 1996;196:255-9.

[92] Griffin SG, Hill RG. Influence of glass composition on the properties of glass polyalkenoate cements. Part I: Influence of aluminium to silicon ratio. Biomaterials 1999;20:1579-86.

[93] Crisp S, Wilson AD. Reactions in Glass Ionomer Cements: V. Effect of Incorporating Tartaric Acid in the Cement Liquid. Journal of Dental Research 1976;55:1023-31.

[94] Hatton PV, Brook IM. Characterisation of the ultrastructure of glass-ionomer (poly-alkenoate) cement. British Dental Journal 1992;173:275-7.

[95] Wasson EA, Nicholson JW. New aspects of the setting of glass-ionomer cements. Journal of Dental Research 1993;72:481-3.

[96] Sullivan A, Hill R. Influence of poly(acrylic acid) molar mass on the fracture properties of glass polyalkenoate cements based on waste gasifier slags. Journal of Materials Science 2000;35:1125-34.

[97] Stamboulis A, Matsuya S, Hill RG, Law RV, Udoh K, Nakagawa M et al. MAS-NMR spectroscopy studies in the setting reaction of glass ionomer cements. Journal of Dentistry 2006;34:574-81.

[98] Griffin S, Hill R. Influence of poly(acrylic acid) molar mass on the fracture properties of glass polyalkenoate cements. Journal of Materials Science 1998;33:5383-96.

[99] Griffin SG, Hill RG. Influence of glass composition on the properties of glass polyalkenoate cements. Part IV: Influence of fluorine content. Biomaterials 2000;21:693-8.

[100] Nicholson JW, Brookman PJ, Lacy OM, Wilson AD. Fourier Transform Infrared Spectroscopic Study of the Role of Tartaric Acid in Glass-ionomer Dental Cements. Journal of Dental Research 1988;67:1451-4.

[101] Wilson AD. Developments in glass-ionomer cements. The International journal of prosthodontics 1989;2:438-46.

[102] Walls AWG. Glass polyalkenoate (glass-ionomer) cements: a review. Journal of Dentistry 1986;14:231-46.

[103] Fleming GJP, Kenny SM, Barralet JE. The optimisation of the initial viscosity of an encapsulated glass-ionomer restorative following different mechanical mixing regimes. Journal of Dentistry 2006;34:155-63.

[104] Dowling AH, Fleming GJP. Is encapsulation of posterior glass-ionomer restoratives the solution to clinically induced variability introduced on mixing? Dental Materials 2008;24:957-66.

[105] Nicholson JW, Brookman PJ, Lacy OM, Wilson AD. Fourier transform infrared spectroscopic study of the role of tartaric acid in glass-ionomer dental cements. Journal of Dental Research 1988;67:1451-4.

[106] Crisp S, Wilson AD. Reactions in glass ionomer cements: V. Effect of incorporating tartaric acid in the cement liquid. Journal of Dental Research 1976;55:1023-31.

[107] Nicholson JW. Chemistry of glass-ionomer cements: A review. Biomaterials 1998;19:485-94.

[108] Griffin SG, Hill RG. Influence of glass composition on the properties of glass polyalkenoate cements. Part IV: Influence of fluorine content. Biomaterials 2000;21:693-8.

[109] Hill RG, Wilson AD. Some strtuctural aspects of glass used n ionomer cements. Glass Technology 1988;29:150-9.

[110] Kent BE, Lewis BG, Wilson AD. Glass Ionomer Cement Formulations: I. The Preparation of Novel Fluoroaluminosilicate Glasses High in Fluorine. Journal of Dental Research 1979;58:1607-19.

[111] Crisp S, Wilson AD. Reactions in glass ionomer cements: I. Decomposition of the powder. Journal of Dental Research 1974;53:1408-13.

[112] Clifford A, Hill R. Apatite-mullite glass-ceramics. Journal of Non-Crystalline Solids 1996;196:346-51.

[113] Wood D, Hill R. Glass ceramic approach to controlling the properties of a glass-ionomer bone cement. Biomaterials 1991;12:164-70.

[114] Bengisu M, Brow RK, Yilmaz E, Mogus-Milankovic A, Reis ST. Aluminoborate and aluminoborosilicate glasses with high chemical durability and the effect of P2O5 additions on the properties. Journal of Non-Crystalline Solids 2006;352:3668-76.

[115] Neve AD, Piddock V, Combe EC. Development of novel dental cements. II. Cement properties. Clinical Materials 1992;9:13-20.

[116] Boyd D, Towler MR, Law RV, Hill RG. An investigation into the structure and reactivity of calcium-zinc-silicate ionomer glasses using MAS-NMR spectroscopy. Journal of Materials Science: Materials in Medicine 2006;17:397-402.

[117] Gorman CM, Hill RG. Heat-pressed ionomer glass-ceramics. Part II. Mechanical property evaluation. Dental Materials 2004;20:252-61.

[118] Wilson AD, Crisp S, Prosser HJ, Lewis BG, Merson SA. Aluminosilicate glasses for polyelectrolyte cements. Industrial & Engineering Chemistry Product Research and Development 1980;19:263-70.

[119] Stebbins JF, Xu Z. NMR evidence for excess non-bridging oxygen in an aluminosilicate glass. Nature 1997;390:60-2.

[120] Griffin SG, Hill RG. Influence of glass composition on the properties of glass polyalkenoate cements. Part II: Influence of phosphate content. Biomaterials 2000;21:399-403.

[121] Burke FM, Lynch E. Glass polyalkenoate bond strength to dentine after chemomechanical caries removal. Journal of Dentistry 1994;22:283-91.

[122] Wilson AD, Prosser HJ, Powis DM. Mechanism of Adhesion of Polyelectrolyte Cements to Hydroxyapatite. Journal of Dental Research 1983;62:590-2.

[123] Smith DC, Simonsky R, Lux J. Enamel fluoride uptake from glass-ionomer cement. Journal of Dental Research 1982;61.

[124] Griffin SG, Hill RG. Influence of glass composition on the properties of glass polyalkenoate cements. Part II: Influence of phosphate content. Biomaterials 2000;21:399-403.

[125] Adamczyk Z, Bratek A, Jachimska B, Jasinski T, Warszynski P. Structure of Poly(acrylic acid) in Electrolyte Solutions Determined from Simulations and Viscosity Measurements. The Journal of Physical Chemistry B 2006;110:22426-35.

[126] Finar IL. Organic Chemistry volume 1 The Fundamental Principle. [S.l.] : The English Language Book Society, 1973.

[127] Mandel M. In: Hara M. editor. Polyelectrolytes - Science and technology Chapter 1. 1st Edition. New York: Marcel Dekker: 1992.

[128] Gowarikar VR, Vishwanathan NV, Jayadev S. Polymer Science, Individual polymer Chaper 9. In. Polymer Science: New Age Publications (Academic) India 2006.

[129] Taylor TJ, Stivala SS. Small-angle X-ray scattering study of a weak polyelectrolyte in water. Journal of Polymer Science, Part B: Polymer Physics 41:1263-72. 2003.

[130] Prosser HJ, Richards CP, Wilson AD. NMR spectroscopy of dental materials. II. The role of tartaric acid in glass-ionomer cements. Journal of Biomedical Materials Research 16:431-45, 1982.

[131] Culbertson BM, Xie D, Thakur A. New matrix resins for glass polyalkenoates or glass-ionomers with pendant amino acid residues. Journal of Macromolecular Science - Pure and Applied Chemistry;36 A: 681-96, 1999

[132] Wilson AD, Nicholson JW. Acid-base cements : biomedical and industrial applications 1st Edition. Cambridge : Cambridge University Press, 1993.

[133] Schricker SR, Culbertson BM, Tong Y. Functionalization of poly(acrylic acid) with cyclic imino ethers for biomaterials and coatings applications. American Chemical Society, Polymer Preprints, Division of Polymer Chemistry ;40:181-2, 1999.

[134] Huang Y, Schricker SR, Culbertson BM, Olesik SV. Synthesis of poly(acrylic acid-co-itaconic acid) in carbon dioxide-methanol mixtures. Journal of Macromolecular Science - Pure and Applied Chemistry 39 A:27-38, 2002.

[135] Wilson AD, McLean JW. Glass-ionomer Cement 1st Edition. Chicago: Quintessence. 1988.

[136] Nicholson JW, Hawkins SJ, Smith JE. The incorporation of hydroxyapatite into glass-polyalkenoate ('glass-ionomer') cements: A preliminary study. Journal of Materials Science: Materials in Medicine 4:418-21, 1993

[137] Moshaverinia A, Roohpour N, Ansari S, Moshaverinia M, Schricker S, Darr JA et al. Effects of N-vinylpyrrolidone (NVP) containing polyelectrolytes on surface properties of conventional glass-ionomer cements (GIC). Dental Materials;.25:10 1240-47, 2009.

[138] Yamazaki T, Brantley W, Culbertson B, Seghi R, Schricker S. The measure of wear in N-vinyl pyrrolidinone (NVP) modifed glass-ionomer cements. Polymers for Advanced Technologies 2005;16:113-6.

[139] Xie D, Brantley WA, Culbertson BM, Wang G. Mechanical properties and microstructures of glass-ionomer cements. Dental Materials 2000;16:129-38.

[140] Rojo L, Vazquez B, Roman JS, Deb S. Eugenol functionalized poly(acrylic acid) derivatives in the formation of glass-ionomer cements. Dental Materials 2008;24:1709-16.

[141] Mount GJ, Ngo H. Minimal intervention: A new concept for operative dentistry. Quintessence International 2000;31:527-33.

[142] Williams DF, Smith DC. Biocompatibility of dental restorative materials 1st Edition. Boca Raton, Fla. : CRC Press , 1982.

[143] O'Brien WJ. Dental materials and their selection 3rd Edition. Jackson, Wyo., 2008.

[144] Kawahara H, Imanishi Y, Oshima H. Biological Evaluation on Glass Ionomer Cement. Journal of Dental Research 1979;58:1080-6.

[145] Heys RJ, Fitzgerald M. Microleakage of Three Cement Bases. Journal of Dental Research 1991;70:55-8.

[146] Mount GJ. Minimal intervention dentistry: Rationale of cavity design. Operative Dentistry 2003;28:92-9.

[147] Yesilyurt C, Er K, Tasdemir T, Buruk K, Celik D. Antibacterial activity and physical properties of glass-ionomer cements containing antibiotics. Operative Dentistry 2009;34:18-23.

[148] Xie D, Zhao J, Weng Y, Park JG, Jiang H, Platt JA. Bioactive glass-ionomer cement with potential therapeutic function to dentin capping mineralization. European Journal of Oral Sciences 2008;116:479-87.

[149] Czarnecka B, Nicholson JW. A preliminary study of the interaction of glass-ionomer dental cements with amino acids. Dental Materials 2006;22:133-7.

[150] DeSchepper EJ, Thrasher MR, Thurmond BA. Antibacterial effects of light-cured liners. American Journal of Dentistry 1989;2:74-6.

[151] DeSchepper EJ, Berr 3rd. EA, Cailleteau JG, Tate WH. A comparative study of fluoride release from glass-ionomer cements. Quintessence International 1991;22:215-9.

[152] Scherer W, Lippman N, Kaim J. Antimicrobial properties of glass-ionomer cements and other restorative materials. Operative Dentistry 1989;14:77-81.

[153] Svanberg M, Mjor IA, Orstavik D. Mutans Streptococci in Plaque from Margins of Amalgam, Composite, and Glass-ionomer Restorations. Journal of Dental Research 1990;69:861-4.

[154] Knight GM, McIntyre JM, Craig GG, Mulyani, Zilm PS, Gully NJ. An in vitro investigation of marginal dentine caries abutting composite resin and glass ionomer cement restorations. Australian Dental Journal 2007;52:187-92.

[155] Gilmour ASM, Edmunds DH, Newcombe RG. Prevalence and Depth of Artificial Caries-like Lesions Adjacent to Cavities Prepared in Roots and Restored with a Glass Ionomer or a Dentin-bonded Composite Material. Journal of Dental Research 1997;76:1854-61.

[156] Nicholson JW, Hawkins SJ, Smith JE. The incorporation of hydroxyapatite into glass-polyalkenoate ('glass-ionomer') cements: A preliminary study. Journal of Materials Science: Materials in Medicine 1993;4:418-21.

[157] Moshaverinia A, Ansari S, Movasaghi Z, Billington RW, Darr JA, Rehman IU. Modification of conventional glass-ionomer cements with N-vinylpyrrolidone containing polyacids, nano-hydroxy and fluoroapatite to improve mechanical properties. Dental Materials 2008;24:1381-90.

[158] Xie D, Brantley WA, Culbertson BM, Wang G. Mechanical properties and microstructures of glass-ionomer cements. Dental Materials 2000;16:129-38.

[159] Brook IM, Hatton PV. Glass-ionomers: Bioactive implant materials. Biomaterials 1998;19:565-71.

[160] Joseph H.Koo. Polymer nanocomposites Processing, Characterization and Application 1st Edition. McGraw-Hill Companies Inc, USA. 2006.

[161] Ke YE, Strove P. Polymer-Layered Silicate and Silica Nanocomposites 1st Edition. The Netherland: Elsevier Science; 2005.

[162] Ashcroft Niel W., Mermin DN. Solid State Physics. Published by Holt, Rinehart and Winston, 1976: New York. 1976.

[163] Kaufmann EN. Characterization of materials 1st Edition, Published by Wiley-Interscience. 2003.

[164] Kakaboura A, Eliades G, Palaghias G. An FTIR study on the setting mechanism of resin-modified glass ionomer restoratives. Dental Materials 1996;12:173-8.

[165] OMNIC software help Perkin-Elmer FTIR spectrometer (Spectrum2000), Perkin Elmer, USA. 2009.

[166] ASM Handbook, Mechanical Testing and Evaluation, Chapter: Fraction, wear and surface testing Volume: 8 1st Edition. ASM International 2000.

[167] Ramalho A, Miranda JC. The relationship between wear and dissipated energy in sliding systems. Wear 2006;260:361-7.

[168] Mair LH, Stolarski TA, Vowles RW, Lloyd CH. Wear: Mechanisms, manifestations and measurement. Report of a workshop. Journal of Dentistry 1996;24:141-8.

[169] Mair L, Joiner A. The measurement of degradation and wear of three glass ionomers following peroxide bleaching. Journal of Dentistry 2004;32:41-5.

[170] Leinfelder KF, Taylor DF, Barkmeier WW, Goldberg AJ. Quantitative wear measurement of posterior composite resins. Dental Materials 1986;2:198-201.

[171] Ramalho A, Antunes PV. Reciprocating wear test of dental composites: Effect on the antagonist. Wear 2005;259:1005-11.

[172] Heintze SD. How to qualify and validate wear simulation devices and methods. Dental Materials 2006;22:712-34.

[173] Cvar JF, Ryge G. Reprint of Criteria for the Clinical Evaluation of Dental Restorative Materials. Clinical Oral Investigations 9,215-232: 2005.

[174] Kramer N, Kunzelmann KH, Taschner M, Mehl A, Garcia-Godoy F, Frankenberger R. Antagonist Enamel Wears More Than Ceramic Inlays. Journal of Dental Research 2006;85:1097-100.

[175] Krejci I, Albert P, Lutz F. The Influence of Antagonist Standardization on Wear. Journal of Dental Research 1999;78:713-9.

[176] DeLong R, Douglas WH. An artificial oral environment for testing dental materials. IEEE Transactions on Biomedical Engineering 1991;38:339-45.

[177] De Gee AJ, Pallav P. Occlusal wear simulation with the ACTA wear machine. Journal of Dentistry 1994; 22:1, 21-27.

[178] Condon JR, Ferracane JL. Evaluation of composite wear with a new multi-mode oral wear simulator. Dental Materials 1996;12:218-26.

[179] Alemzadeh K, Hyde RA, Gao J. Prototyping a robotic dental testing simulator. Proceedings of the Institution of Mechanical Engineers, Part H: Journal of Engineering in Medicine 2007;221:385-96.

[180] Suzuki S, Nagai E, Taira Y, Minesaki Y. In vitro wear of indirect composite restoratives. Journal of Prosthetic Dentistry 2002;88:431-6.

[181] Ilie N, Hickel R. Macro-, micro- and nano-mechanical investigations on silorane and methacrylate-based composites. Dental Materials 2009, 25:6, 810-819. .

[182] Ho MW, Lam CK, Lau K, Ng DHL, Hui D. Mechanical properties of epoxy-based composites using nanoclays. Composite Structures 2006;75:415-21.

[183] Pinnavaia TJ, Beall GW. Polymer-clay nanocomposites 1st Edition. Chichester : John Wiley, 2000.

[184] Becker O, Simon GP. Epoxy layered-silicate nanocomposites silicateInorganic polymeric nanocomposites; In. Advences in polymer science (2005) 179: Springer series. 2009.

[185] Pinnavaia TJ, Tzou MS, Landau SD, Raythatha RH. On the pillaring and delamination of smectite clay catalysts by polyoxo cations of aluminum. Journal of Molecular Catalysis 1984;27:195-212.

[186] Utracki LA. Basic elements of polymeric nanocomposites technology. Clay-containing polymeric nanocomposites 2004;1:35-256.

[187] Sinha Ray S, Okamoto M. Polymer/layered silicate nanocomposites: A review from preparation to processing. Progress in Polymer Science. 2003;28:1539-641.

[188] Kojima Y, Usuki A, Kawasumi M, Okada A, Kurauchi T, Kamigaito O. Synthesis of nylon 6-clay hybrid by montmorillonite intercalated with +Á-

caprolactam. Journal of Polymer Science, Part A: Polymer Chemistry 1993;31:983-6.

[189] Product Sheet (05-05-06), G-105 Polymer grade montmorillonite, Nanocor, Inc., Arlington Heights, IL 6004 USA. 2009.

[190] Vaia RA, Maguire JF. Polymer nanocomposites with prescribed morphology: Going beyond nanoparticle-filled polymers. Chemistry of Materials 2007;19:2736-51.

[191] Sinha Ray S, Okamoto M. Polymer/layered silicate nanocomposites: A review from preparation to processing. Progress in Polymer Science.2003;28:1539-641.

[192] Carter LW, Hendricks JG, Bolley DS. United States Patent. 2531396[2531396], assigned. 1950.

[193] Okada A, Fukushima Y, Kawasumi M, Inagaki S, Usuki A, Sugiyama S et al. United States Patent (assigned to Toyota Motor Co., Japan). [4739007]. 1988.

[194] Okada A, Usuki A. The chemistry of polymer-clay hybrids. Materials Science and Engineering: C 1995;3:109-15.

[195] Yoonessi M, Toghiani H, Kingery WL, Pittman CU. Preparation, Characterization, and Properties of Exfoliated/Delaminated Organically Modified Clay/Dicyclopentadiene Resin Nanocomposites. Macromolecules 2004;37:2511-8.

[196] Usuki A, Kojima Y, Kawasumi M, Okada A, Fukushima Y, Kurauchi T et al. Synthesis of nylon 6-clay hybrid. Journal of Materials Research 1993;8:1179-84.

[197] Vaia RA, Jandt KD, Kramer EJ, Giannelis EP. Kinetics of polymer melt intercalation. Macromolecules 1995;28:8080-5.

[198] Biasci L, Aglietto M, Ruggeri G, Ciardelli F. Functionalization of montmorillonite by methyl methacrylate polymers containing side-chain ammonium cations. Polymer 1994;35:3296-304.

[199] Jeon HG, Jung H-T, Lee SW, Hudson SD. Morphology of polymer/silicate nanocomposites: High density polyethylene and a nitrile copolymer. Polymer Bulletin 1998;41:107-13.

[200] Wang Z, Pinnavaia TJ. Nanolayer reinforcement of elastomeric polyurethane. Chemistry of Materials 1998;10:3769-71.

[201] McNally T, Raymond Murphy W, Lew CY, Turner RJ, Brennan GP. Polyamide-12 layered silicate nanocomposites by melt blending. Polymer 2003;44:2761-72.

[202] Fedullo N, Sorlier E, Sclavons M, Bailly C, Lefebvre JM, Devaux J. Polymer-based nanocomposites: Overview, applications and perspectives. Progress in Organic Coatings 2007;58:87-95.

[203] Gunister E, Pestreli D, Unlu CH, Atici O, Gungor N. Synthesis and characterization of chitosan-MMT biocomposite systems. Carbohydrate Polymers 2007;67:358-65.

[204] Depan D, Pratheep Kumar A, Singh RP. Preparation and characterization of novel hybrid of chitosan-g-lactic acid and montmorillonite. Journal of Biomedical Materials Research - Part A 2006;78:372-82.

[205] Pinavaia TJ, Beall G. Polymeric Clay Nanocomposites. Polymeric Clay Nanocomposites 2000.

[206] Sinha Ray S, Maiti P, Okamoto M, Yamada K, Ueda K. New polylactide/layered silicate nanocomposites. 1. Preparation, characterization, and properties. Macromolecules 2002;35:3104-10.

[207] Sinha Ray S, Okamoto M. Polymer/layered silicate nanocomposites: a review from preparation to processing. Progress in Polymer Science 2003;28:1539-641.

[208] Usuki A, Hasegawa N, Kato M. Polymer-clay nanocomposites. 179, 135-195. 2005.

[209] McNally T, Raymond Murphy W, Lew CY, Turner RJ, Brennan GP. Polyamide-12 layered silicate nanocomposites by melt blending. Polymer 2003;44:2761-72.

[210] Ploehn HJ, Liu C. Quantitative analysis of montmorillonite platelet size by atomic force microscopy. Industrial and Engineering Chemistry Research 2006;45:7025-34.

[211] Gilman JW, Jackson CL, Morgan AB, Harris J, Manias E, Giannelis EP et al. Flammability properties of polymer - Layered-silicate nanocomposites. Polypropylene and polystyrene nanocomposites. Chemistry of Materials 2000;12:1866-73.

[212] Billingham J, Breen C, Yarwood J. Adsorption of polyamine, polyacrylic acid and polyethylene glycol on montmorillonite: An in situ study using ATR-FTIR. Vibrational Spectroscopy 1997;14:19-34.

[213] Ruiz-Hitzky E, Aranda P. Polymer-salt intercalation complexes in layer silicates. Advanced Materials 2[11], 545-547. 1990.

[214] Zeng C, Lee LJ. Poly(methyl methacrylate) and polystyrene/clay nanocomposites prepared by in-situ polymerization. Macromolecules 34:12, 4098-4103. 2001.

[215] Sinha Ray S, Okamoto K, Okamoto M. Structure-Property Relationship in Biodegradable Poly(butylene succinate)/Layered Silicate Nanocomposites. Macromolecules 2003;36:2355-67.

[216] Pinnavaia TJ, Beall GW. Polymer-clay nanocomposites 1st Edition. Chichester : John Wiley, 2000.

[217] Billmeyer FWJr. Text Book Of Polymer Science 3rd Edition. New York: Wiley Interscience Publication; 1984.

[218] Cowie JMG, Arrighi V. Polymers : chemistry and physics of modern materials 1st Edition. Boca Raton, Fla. : CRC, 2007.

[219] Bovis SC, Harrington E, Wilson HJ. Setting characteristics of composite filling materials. British dental journal 1971;131:352-6.

[220] ISO 9917-1:2007 Dentistry - water-based cements - part 1: powder/liquid acid-base cements. International Organization for Standardisation 2009.

[221] ISO 4049:2000 Dentistry - polymer-based filling, restorative and luting materials. International Organization for Standardisation 2009.

[222] ASTM D790-07 Standard test methods for flexural properties of unreinforced and reinforced plastic and electrical insulating materials. ASTM international 2007.

[223] ASTM C1327-08 Standard test method for Vickers indentation dardness of advanced ceramics. ASTM international 2008.

[224] ASTM G133 Standard test method for linearly reciprocating ball-on-flat sliding wear. ASTM international 2002.

[225] Nagarajan VS, Jahanmir S, Thompson VP. In vitro contact wear of dental composites. Dental Materials 2004;20:63-71.

[226] Wassell RW, McCabe JF, Walls AW. A two-body frictional wear test. Journal of Dental Research 1994;73:1546-53.

[227] Condon JR, Ferracane JL. Factors effecting dental composite wear in vitro. Journal of Biomedical Materials Research 1997;38:303-13.

[228] Mens JWM, de Gee AWJ. Erosion in seawater sand slurries. Tribology International 1986;19:59-64.

[229] Tran N, Wilson M, Milev A, Dennis G, Kannangara GSK, Lamb R. Mechanism of exfoliation of clays. AIP Conference Proceedings 879, 1642-1645. 2007.

[230] Strawhecker KE, Manias E. Structure and properties of poly(vinyl alcohol)/Na+ montmorillonite nanocomposites. Chemistry of Materials 2000;12:2943-9.

[231] Ho MW, Lam CK, Lau Kt, Ng DHL, Hui D. Mechanical properties of epoxy-based composites using nanoclays. Composite Structures 2006;75:415-21.

[232] Ward LJ, Schofield WCE, Badyal JPS, Goodwin AJ, Merlin PJ. Atmospheric pressure plasma deposition of structurally well-defined polyacrylic acid films. Chemistry of Materials 2003;15:1466-9.

[233] Miller ML, Linton RW. X-ray photoelectron spectroscopy of thermally treated SiO2 surfaces. Analytical Chemistry 1985;57:2314-9.

[234] Gao D, Heimann RB. Structure and mechanical properties of superabsorbent poly(acrylamide)-montmorillonite composite hydrogels. Polymer Gels and Networks 1993;1:225-46.

[235] Shen Z, Simon GP, Cheng YB. Comparison of solution intercalation and melt intercalation of polymer-clay nanocomposites. Polymer 2002;43:4251-60.

[236] Madejova J, Komadel P, Cicel B. Infrared study of octahedral site populations in smectites. Clay Minerals 1993;29:319-26.

[237] Billingham J, Breen C, Yarwood J. Adsorption of polyamine, polyacrylic acid and polyethylene glycol on montmorillonite: An in situ study using ATR-FTIR. Vibrational Spectroscopy 1997;14:19-34.

[238] Crisp S, Pringuer MA, Wardleworth D, Wilson AD. Journal of Dental Research 1974;53:1414-9.

[239] MacDonald SA, Schardt CR, Masiello DJ, Simmons JH. Dispersion analysis of FTIR reflection measurements in silicate glasses. Journal of Non-Crystalline Solids 2000;275:72-82.

[240] Hwa LG, Hwang SL, Liu LC. Infrared and Raman spectra of calcium alumino-silicate glasses. Journal of Non-Crystalline Solids 1998;238:193-7.

[241] Nicholson JW, Brookman PJ, Lacy OM, Wilson AD. Fourier transform infrared spectroscopic study of the role of tartaric acid in glass-ionomer dental cements. Journal of Dental Research 1988;67:1451-4.

[242] Nicholson JW. Chemistry of glass-ionomer cements: A review. Biomaterials 1998;19:485-94.

[243] Young AM, Rafeeka SA, Howlett JA. FTIR investigation of monomer polymerisation and polyacid neutralisation kinetics and mechanisms in various aesthetic dental restorative materials. Biomaterials 2004;25:823-33.

[244] De Maeyer EAP, Verbeeck RMH, Vercruysse CWJ. Infrared spectrometric study of acid-degradable glasses. Journal of Dental Research 2002;81:552-5.

[245] Nicholson JW, Brookman PJ, Lacy OM, Wilson AD. Fourier transform infrared spectroscopic study of the role of tartaric acid in glass-ionomer dental cements. Journal of Dental Research 1988;67:1451-4.

[246] ASM handbook 1st Edition . ASM International.Handbook Committee. Metals Park, Ohio : American Society for Metals International, 2000.

[247] DeLong R. Intra-oral restorative materials wear: Rethinking the current approaches: How to measure wear. Dental Materials 2006;22:702-11.

[248] ASM handbook 1st Edition. Volume:18 Friction, Lubrication and wear technology. Metals Park, Ohio : American Society for Metals International, 2000.

[249] Tay FR, Pashley EL, Huang C, Hashimoto M, Sano H, Smales RJ et al. The Glass-ionomer Phase in Resin-based Restorative Materials. Journal of Dental Research 2001;80:1808-12.

[250] Vaia RA, Jandt KD, Kramer EJ, Giannelis EP. Kinetics of polymer melt intercalation. Macromolecules 1995;28:8080-5.

[251] Ray SS, Bousmina M. Biodegradable polymers and their layered silicate nanocomposites: In greening the 21st century materials world. Progress in Materials Science 2005;50:962-1079.

[252] Fischer H. Polymer nanocomposites: From fundamental research to specific applications. Materials Science and Engineering C 2003;23:763-72.

[253] Okada A, Usuki A. Twenty years of polymer-clay nanocomposites. Macromolecular Materials and Engineering 2006;291:1449-76.

[254] Okada A, Usuki A. The chemistry of polymer-clay hybrids. Materials Science and Engineering: C 1995;3:109-15.

[255] Okada A, Fukushima Y, Kawasumi M, Inagaki S, Usuki A, Sugiyama S et al. United States Patent (assigned to Toyota Motor Co., Japan). [4739007]. 1988.
Ref Type: Patent

[256] Lan T, Pinnavaia TJ. Clay-reinforced epoxy nanocomposites. Chemistry of Materials 1994;6:2216-9.

[257] Lan T, Kaviratna PD, Pinnavaia TJ. Mechanism of clay tactoid exfoliation in epoxy-clay nanocomposites. Chemistry of Materials 1995;7:2144-50.

[258] Kaviratna H, Pinnavaia TJ. Acid hydrolysis of octahedral Mg2+ sites in 2:1 layered silicates: an assessment of edge attack and gallery access mechanisms. Clays & Clay Minerals 1994;42:717-23.

[259] Kojima Y, Usuki A, Kawasumi M, Okada A, Fukushima Y, Kurauchi T et al. Mechanical properties of nylon 6-clay hybrid. Journal of Materials Research 1993;8:1185-9.

[260] Triantafillidis CS, LeBaron PC, Pinnavaia TJ. Thermoset epoxy-clay nanocomposites: The dual role of diamines as clay surface modifiers and polymer curing agents. Journal of Solid State Chemistry 2002;167:354-62.

[261] Koerner H, Misra D, Tan A, Drummy L, Mirau P, Vaia R. Montmorillonite-thermoset nanocomposites via cryo-compounding. Polymer 2006;47:3426-35.

[262] Usuki A, Kojima Y, Kawasumi M, Okada A, Kurauchi T, Kamigaito O. Characterization and properties of nylon 6. Clay hybrid. American Chemical Society, Polymer Preprints, Division of Polymer Chemistry 31[2], 651-652. 1990.

[263] Kojima Y, Usuki A, Kawasumi M, Okada A, Kurauchi T, Kamigaito O. Synthesis of nylon 6-clay hybrid by montmorillonite intercalated with ε-caprolactam. Journal of Polymer Science, Part A: Polymer Chemistry 1993;31:983-6.

[264] Zheng Y, Wang A. Preparation, characterization and swelling behaviours of a novel multifunctional superabsorbent composite based on Ca-Montmorillonite and Sodium Humate. E-Polymers 2007, 127:1-8.

[265] Ying Liang. Technical Sales Manager-Polyamides Nanocor,Inc Chicago IL USA; www.nanocor.com (Personal Communication). 27-9-2006.

[266] Shi H, Lan T, Pinnavaia TJ. Interfacial effects on the reinforcement properties of polymer-organoclay nanocomposites. Chemistry of Materials 1996;8:1584-7.

[267] Tran NH, Wilson MA, Milev AS, Dennis GR, McCutcheon AL, Kannangara GSK et al. Structural-chemical evolution within exfoliated clays. Langmuir 2006;22:6696-700.

[268] Dasari A, Yu ZZ, Mai YW, Hu GH, Varlet J. Clay exfoliation and organic modification on wear of nylon 6 nanocomposites processed by different routes. Composites Science and Technology 2005;65:2314-28.

[269] Baek SH, Kim BS, Kim BK. Hydrogels based on polyurethane-polyacrylic acid multiblock copolymers via macroiniferter technique. Progress in Organic Coatings 2004;49:353-7.

[270] Kooli F, Khimyak YZ, Alshahateet SF, Chen F. Effect of the Acid Activation Levels of Montmorillonite Clay on the Cetyltrimethylammonium Cations Adsorption. Langmuir 2005;21:8717-23.

[271] Modesti M, Lorenzetti A, Bon D, Besco S. Effect of processing conditions on morphology and mechanical properties of compatibilized polypropylene nanocomposites. Polymer 2005;46:10237-45.

[272] Gelfer MY, Burger C, Chu B, Hsiao BS, Drozdov AD, Si M et al. Relationships between Structure and Rheology in Model Nanocomposites of Ethylene and Vinyl-Based Copolymers and Organoclays. Macromolecules 2005;38:3765-75.

[273] Park CI, Kim MH, Park OO. Effect of heat treatment on the microstructural change of syndiotactic polystyrene/poly(styrene-co-vinyloxazolin)/clay nanocomposite. Polymer 2004;45:1267-73.

[274] Becker O, Cheng YB, Varley RJ, Simon GP. Layered Silicate Nanocomposites Based on Various High-Functionality Epoxy Resins: The Influence of Cure Temperature on Morphology, Mechanical Properties, and Free Volume. Macromolecules 2003;36:1616-25.

[275] Kornmann X, Lindberg H, Berglund LA. Synthesis of epoxy-clay nanocomposites. Influence of the nature of the curing agent on structure. Polymer 2001;42:4493-9.

[276] Ngo TD, Ton-That MT, Hoa SV, Cole KC. Effect of temperature, duration and speed of pre-mixing on the dispersion of clay/epoxy nanocomposites. Composites Science and Technology 2009;69:1831-40.

[277] Tekin N, Dinter A, Demirbas I, Alkan M. Adsorption of cationic polyacrylamide onto sepiolite. Journal of Hazardous Materials 2006;134:211-9.

[278] Lin J, Wu J, Yang Z, Pu M. Synthesis and properties of poly(acrylic acid)/mica superabsorbent nanocomposite. Macromolecular Rapid Communications 2001;22:422-4.

[279] Leadley SR, Watts JF. The use of XPS to examine the interaction of poly(acrylic acid) with oxidised metal substrates. Journal of Electron Spectroscopy and Related Phenomena 1997;85:107-21.

[280] Choi YS, Ham HT, Chung IJ. Effect of monomers on the basal spacing of sodium montmorillonite and the structures of polymer-clay nanocomposites. Chemistry of Materials 2004;16:2522-9.

[281] Xie W, Gao Z, Pan WP, Hunter D, Singh A, Vaia R. Thermal degradation chemistry of alkyl quaternary ammonium Montmorillonite. Chemistry of Materials 2001;13:2979-90.

[282] Feng B, Hong RY, Wu YJ, Liu GH, Zhong LH, Zheng Y et al. Synthesis of monodisperse magnetite nanoparticles via chitosan-poly(acrylic acid) template and their application in MRI. Journal of Alloys and Compounds 2009;473:356-62.

[283] Nicholson JW. Metal salts interaction with acrylic acid-maleic acid copolymer: an infrared spectroscopic study. Journal of Applied Polymer Science 2000;78:1680-4.

[284] Farmer VC, Russell JD. The infra-red spectra of layer silicates. Spectrochimica Acta 1964;20:1149-73.

[285] Xie W, Gao Z, Liu K, Pan WP, Vaia R, Hunter D et al. Thermal characterization of organically modified montmorillonite. Thermochimica Acta 2001;367-368:339-50.

[286] Komadel P, Madejova J, Bujduk J. Preparation and properties of reduced-charge smectites - A review. Clays and Clay Minerals 2005;53:313-34.

[287] Shen Z, Simon GP, Cheng YB. Comparison of solution intercalation and melt intercalation of polymer-clay nanocomposites. Polymer 2002;43:4251-60.

[288] Madejova J, Komadel P. Baseline studies of the clay minerals society source clays: Infrared methods. Clays and Clay Minerals 2001;49:410-32.

[289] Yoonessi M, Toghiani H, Kingery WL, Pittman CU. Preparation, Characterization, and Properties of Exfoliated/Delaminated Organically Modified Clay/Dicyclopentadiene Resin Nanocomposites. Macromolecules 2004;37:2511-8.

[290] Xie W, Xie R, Pan WP, Hunter D, Koene B, Tan LS et al. Thermal stability of quaternary phosphonium modified montmorillonites. Chemistry of Materials 2002;14:4837-45.

[291] Madejova J. FTIR techniques in clay mineral studies. Vibrational Spectroscopy 2003;31:1-10.

[292] Madejova J, Bujdak J, Janek M, Komadel P. Comparative FT-IR study of structural modifications during acid treatment of dioctahedral smectites and hectorite. Spectrochimica Acta - Part A: Molecular and Biomolecular Spectroscopy 1998;54:1397-406.

[293] Ruiz-Hitzky E, Aranda P. Polymer-salt intercalation complexes in layer silicates. Advanced Materials 1990;2:545-7.

[294] Madejova J, Bujdak J, Janek M, Komadel P. Comparative FT-IR study of structural modifications during acid treatment of dioctahedral smectites and hectorite. Spectrochimica Acta Part A: Molecular and Biomolecular Spectroscopy 1998;54:1397-406.

[295] Sun L, Gibson RF, Gordaninejad F, Suhr J. Energy absorption capability of nanocomposites: A review. Composites Science and Technology;In Press, Corrected Proof.

[296] Kirwan LJ, Fawell PD, van Bronswijk W. In Situ FTIR-ATR Examination of Poly(acrylic acid) Adsorbed onto Hematite at Low pH. Langmuir 2003;19:5802-7.

[297] Young AM, Rafeeka SA, Howlett JA. FTIR investigation of monomer polymerisation and polyacid neutralisation kinetics and mechanisms in various aesthetic dental restorative materials. Biomaterials 2004;25:823-33.

[298] Nicholson JW, Hawkins SJ, Wasson EA. A study of the structure of zinc polycarboxylate dental cements. Journal of Materials Science: Materials in Medicine 1993;4:32-5.

[299] Zainuddin N, Karpukhina N, Hill RG, Law RV. A long-term study on the setting reaction of glass ionomer cements by 27Al MAS-NMR spectroscopy. Dental Materials 2009;25:290-5.

[300] Nicholson JW. The effect of trivalent metal nitrates on the properties of dental cements made from poly(acrylic acid). Journal of Applied Polymer Science 1998;70:2353-9.

[301] Deacon GB, Phillips RJ. Relationships between the carbon-oxygen stretching frequencies of carboxylato complexes and the type of carboxylate coordination. Coordination Chemistry Reviews 1980;33:227-50.

[302] Wasson EA, Nicholson JW. Study of the relationship between setting chemistry and properties of modified glass-poly(alkenoate) cements. British Polymer Journal 1990;23:179-83.

[303] Crisp S, Pringuer MA, Wardleworth D, Wilson AD. Reactions in Glass Ionomer Cements: II. An Infrared Spectroscopic Study. Journal of Dental Research 1974;53:1414-9.

[304] Barry TI, Clinton DJ, Wilson AD. The structure of a glass-ionomer cement and its relationship to the setting process. Journal of Dental Research 1979;58:1072-9.

[305] Williams JA, Billington RW. Changes in compressive strength of glass ionomer restorative materials with respect to time periods of 24 h to 4 months. Journal of Oral Rehabilitation 1991;18:163-8.

[306] Billington RW, Williams JA, Pearson GJ. Ion processes in glass ionomer cements. Journal of Dentistry 2006;34:544-55.

[307] Kakaboura A, Eliades G, Palaghias G. An FTIR study on the setting mechanism of resin-modified glass ionomer restoratives. Dental Materials 1996;12:173-8.

[308] Nicholson JW, Gjorgievska E, Bajraktarova B, Mckenzie MA. Changes in properties of polyacid-modified composite resins (compomers) following storage in acidic solutions. Journal of Oral Rehabilitation 2003;30:601-7.

[309] Xie D, Chung ID, Wu W, Mays J. Synthesis and evaluation of HEMA-free glass-ionomer cements for dental applications. Dental Materials 2004;20:470-8.

[310] Nicholson JW. Glass-ionomers in medicine and dentistry. Proceedings of the Institution of Mechanical Engineers, Part H: Journal of Engineering in Medicine 1998;212:121-6.

[311] Stamboulis A, Matsuya S, Hill RG, Law RV, Udoh K, Nakagawa M et al. MAS-NMR spectroscopy studies in the setting reaction of glass ionomer cements. Journal of Dentistry 2006;34:574-81.

[312] Wasson EA, Nicholson JW. Studies on the setting chemistry of glass-ionomer cements. Clinical Materials 1991;7:289-93.

[313] Matsuya S, Maeda T, Ohta M. IR and NMR Analyses of Hardening and Maturation of Glass-ionomer Cement. Journal of Dental Research 1996;75:1920-7.

[314] Luckham PF, Rossi S. Colloidal and rheological properties of bentonite suspensions. Advances in Colloid and Interface Science 1999;82:43-92.

[315] Ramos-Tejada MM, Galindo-Gonzalez C, Perea R, Durain JDG. Effect of charged polyelectrolytes on the electrophoretic behavior, stability, and viscoelastic properties of montmorillonite suspensions. Journal of Rheology 2006;50:995-1007.

[316] Pearson GJ, Atkinson AS. Effects of temperature change on the working and setting characteristics of water-based dental cements. Dental Materials 1987;3:275-9.

[317] Dowling AH, Stamboulis A, Fleming GJP. The influence of montmorillonite clay reinforcement on the performance of a glass ionomer restorative. Journal of Dentistry 2006;34:802-10.

[318] Fleming GJP, Zala DM. An assessment of encapsulated versus hand-mixed glass ionomer restoratives. Operative Dentistry 2003;28:168-77.

[319] Crisp S, Lewis BG, Wilson AD. Characterization of glass-ionomer cements. 3. Effect of polyacid concentration on the physical properties. Journal of Dentistry 1977;5:51-6.

[320] Moshaverinia A, Ansari S, Movasaghi Z, Billington RW, Darr JA, Rehman IU. Modification of conventional glass-ionomer cements with N-vinylpyrrolidone containing polyacids, nano-hydroxy and fluoroapatite to improve mechanical properties. Dental Materials 2008;24:1381-90.

[321] Cook WD, Brockhurst P. Materials Science: The Oscillating Rheometer-What Does It Measure? Journal of Dental Research 1980;59:795-9.

[322] Mount GJ. Glass ionomers: a review of their current status. Operative Dentistry 1999;24:115-24.

[323] ASM Handbook. Volume 8: Mechanical testing and Evalution. ASM International.Handbook Committee. 2000.

[324] Manhart J, Chen HY, Hamm G, Hickel R. Review of the clinical survival of direct and indirect restorations in posterior teeth of the permanent dentition. Operative dentistry 2004;29:481-508.

[325] Ichim I, Li Q, Loughran J, Swain MV, Kieser J. Restoration of non-carious cervical lesions. Part I. Modelling of restorative fracture. Dental Materials 2007;23:1553-61.

[326] Loughran GM, Versluis A, Douglas WH. Evaluation of sub-critical fatigue crack propagation in a restorative composite. Dental Materials 2005;21:252-61.

[327] Kerby RE, Bleiholder RF. Physical properties of stainless-steel and silver-reinforced glass-ionomer cements. Journal of Dental Research 1991;70:1358-61.

[328] Mitra SB, Kedrowski BL. Long-term mechanical properties of glass ionomers. Dental Materials 1994;10:78-82.

[329] Xie D, Zhao J, Park JG. A novel light-cured glass-ionomer system for improved dental restoratives. Journal of Materials Science: Materials in Medicine 2007;18:1907-16.

[330] Bertolini MJ, Zaghete MA, Gimenes R, Padovani GC, Cruz CAS. Preparation and evaluation of an experimental luting glass ionomer cement to be used in dentistry. Journal of Materials Science: Materials in Medicine . 2009.

[331] Azillah MA, Anstice HM, Pearson GJ. Long-term flexural strength of three direct aesthetic restorative materials. Journal of Dentistry 1998;26:177-82.

[332] Rodrigues J, Zanchi CH, de Carvalho RV, Demarco FF. Flexural strength and modulus of elasticity of different types of resin-based composites. Brazilian Oral Research 2007;21:16-21.

[333] Xie D, Wu W, Puckett A, Farmer B, Mays JW. Novel resin modified glass-ionomer cements with improved flexural strength and ease of handling. European Polymer Journal 2004;40:343-51.

[334] McKinney JE, Antonucci JM, Rupp NW. Wear and Microhardness of Glass-Ionomer Cements. Journal of Dental Research 1987;66:1134-9.

[335] Forss H, Sepphen L, Lappalaimen R. In vitro abrasion resistance and hardness of glass-ionomer cements. Dental Materials 1991;7:36-9.

[336] Eliades G, Palaghias G. In vitro characterization of visible light-cured glass ionomer liners. Dental Materials 1993;9:198-203.

[337] Yap AUJ, Lye KW, Sau CW. Surface characteristics of tooth-colored restoratives polished utilizing different polishing systems. Operative Dentistry 1997;22:260-5.

[338] Hammouda IM. Reinforcement of conventional glass-ionomer restorative material with short glass fibers. Journal of the Mechanical Behavior of Biomedical Materials 2009;2:73-81.

[339] Watts DC, Kisumbi BK, Toworfe GK. Dimensional changes of resin/ionomer restoratives in aqueous and neutral media. Dental Materials 2000;16:89-96.

[340] Lucksanasombool P, Higgs WAJ, Higgs RJED, Swain MV. Time dependence of the mechanical properties of GICs in simulated physiological conditions. Journal of Materials Science: Materials in Medicine 2002;13:745-50.

[341] Ellakuria J, Triana R, Meinguez N, Soler I, Ibaseta G, Maza J et al. Effect of one-year water storage on the surface microhardness of resin-modified versus conventional glass-ionomer cements. Dental Materials 2003;19:286-90.

[342] Yap AUJ, Yeo EJC, Yap WY, Ong DSB, Tan JWS. Effects of instrumentation time on microleakage of resin-modified glass ionomer cements. Operative Dentistry 2003;28:47-52.

[343] Cattani-Lorente MA, Godin C, Meyer JM. Early strength of glass ionomer cements. Dental Materials 1993;9:57-62.

[344] Cattani-Lorente MA, Godin C, Meyer JM. Mechanical behavior of glass ionomer cements affected by long-term storage in water. Dental Materials 1994;10:37-44.

[345] Cattani-Lorente MA, Dupuis V, Moya F, Payan J, Meyer JM. Comparative study of the physical properties of a polyacid-modified composite resin and a resin-modified glass ionomer cement. Dental Materials 1999;15:21-32.

[346] Huysmans MC, van der Varst PGT, Lautenschalger EP, Monaghan P. The influence of simulated clinical handling on the flexural and compressive strength of posterior composite restorative materials. Dental Materials 1996;12:116-20.

[347] Xie D, Zhao J, Weng Y. Synthesis and Application of Novel Multi-arm Poly(carboxylic acid)s for Glass-ionomer Restoratives. Journal of Biomaterials Application 2008:Vol 00 March.

[348] Prosser HJ, Powis DR, Wilson AD. Glass-ionomer cements of improved flexural strength. Journal of Dental Research 1986;65:146-8.

[349] Billington RW. Relative shear bond strengths of luting media with various core materials. The Journal of prosthetic dentistry 1986;55:284.

[350] Williams JA, Billington RW. Changes in compressive strength of glass ionomer restorative materials with respect to time periods of 24 h to 4 months. Journal of Oral Rehabilitation 1991;18:163-8.

[351] Mount GJ. Clinical placement of modern glass-ionomer cements. Quintessence International 1993;24:99-107.

[352] Iizuka H, Brauer GM, Rupp N, Ohashi M, Paffenbarger G. Forces fracturing cements at die interfaces and their dependence on film thickness. Dental Materials 1987;3:187-93.

[353] Garcia-Godoy F. The preventive glass ionomer restoration. Quintessence International 1986;17:617-9.

[354] Rodrigues Garcia RC, De Gees MF, Del Bel Cury AA. Influence of protecting agents on the solubility of glass ionomers. American Journal of Dentistry 1995;8:294-6.

[355] Tyas MJ, Burrow MF. Clinical evaluation of a resin-modified glass ionomer adhesive system--results at three years. Operative Dentistry 2001;26:17-20.

[356] Kawano F, Kon M, Kobayashi M, Miyai K. Reinforcement effect of short glass fibers with CaO-P2O5-SiO2-Al2O3 glass on strength of glass-ionomer cement. Journal of Dentistry 2001;29:377-80.

[357] Lohbauer U, Frankenberger R, Clare A, Petschelt A, Greil P. Toughening of dental glass ionomer cements with reactive glass fibres. Biomaterials 2004;25:5217-25.

[358] Oldfield CWB, Ellis B. Fibrous reinforcement of glass-ionomer cements. Clinical Materials 1991;7:313-23.

[359] Kobayashi M, Kon M, Miyai K, Asaoka K. Strengthening of glass-ionomer cement by compounding short fibres with CaO-P2O5-SiO2-Al2O3 glass. Biomaterials 2000;21:2051-8.

[360] Yap AUJ, Cheang PHN, Chay PL. Mechanical properties of two restorative reinforced glass-ionomer cements. Journal of Oral Rehabilitation 2002;29:682-8.

[361] Lucas ME, Arita K, Nishino M. Toughness, bonding and fluoride-release properties of hydroxyapatite-added glass ionomer cement. Biomaterials 2003;24:3787-94.

[362] Deb S, Nicholson JW. The effect of strontium oxide in glass-ionomer cements. Journal of Materials Science: Materials in Medicine 1999;10:471-4.

[363] Yli-Urpo H, Vallittu PK, Narhi TO, Forsback AP, Vakiparta M. Release of Silica, Calcium, Phosphorus, and Fluoride from Glass Ionomer Cement Containing Bioactive Glass. Journal of Biomaterials Application 2004;19:5-20.

[364] Yli-Urpo H, Lassila LVJ, Ninrhi T, Vallittu PK. Compressive strength and surface characterization of glass ionomer cements modified by particles of bioactive glass. Dental Materials 2005;21:201-9.

[365] Croll TP. Alternatives to silver amalgam and resin composite in pediatric dentistry. Quintessence International 1998;29:697-703.

[366] Kerby RE, Bleiholder RF. Physical Properties of Stainless-steel and Silver-reinforced Glass-ionomer Cements. Journal of Dental Research 1991;70:1358-61.

[367] Croll TP. Alternatives to silver amalgam and resin composite in pediatric dentistry. Quintessence International 1998;29:697-703.

[368] Dewald JP, Arcoria CJ, Ferracane JL. Evaluation of glass-cermet cores under cast crowns. Dental Materials 1990;6:129-32.

[369] McLean JW, Gasser O. Glass-cermet cements. Quintessence International 1985;16:333-43.

[370] Williams JA, Billington RW, Pearson G. Silver and fluoride ion release from metal-reinforced glass-ionomer filling materials. Journal of Oral Rehabilitation 1997;24:369-75.

[371] Mitchem JC, Gronas DG. Continued evaluation of the clinical solubility of luting cements. The Journal of Prosthetic Dentistry 1981;45:289-91.

[372] Rosenstiel SF, Land MF, Crispin BJ. Dental luting agents: A review of the current literature. The Journal of Prosthetic Dentistry 1998;80:280-301.

[373] Fleming GJP, Narayan O. The effect of cement type and mixing on the bi-axial fracture strength of cemented aluminous core porcelain discs. Dental Materials 2003;19:69-76.

[374] Dowling AH, Fleming GJP. Are encapsulated anterior glass-ionomer restoratives better than their hand-mixed equivalents? Journal of Dentistry 2009;37:133-40.

[375] Mount GJ. Polyacrylic cements in dentistry. American Journal of Dentistry 1990;3:79-84.

[376] Rupp DC, Hermesch CB, Charlton DG. Effect of triturator speed variation on physical properties of encapsulated glass-ionomer luting cements. Operative Dentistry 1996;21:96-102.

[377] Mahmood S, Palin WM, Gbureck U, Addison O, Hofmann MP. Effect of mechanical mixing and powder to liquid ratio on the strength and reliability of a brushite bone cement. Key Engineering Materials 2008;361-363 I:307-10.

[378] Wilder J, Boghosian AA, Bayne SC, Heymann HO, Sturdevant JR, Roberson TM. Effect of powder/liquid ratio on the clinical and laboratory performance of resin-modified glass-ionomers. Journal of Dentistry 1998;26:369-77.

[379] Mitsuhashi A, Hanaoka K, Teranaka T. Fracture toughness of resin-modified glass ionomer restorative materials: Effect of powder/liquid ratio and powder particle size reduction on fracture toughness. Dental Materials 2003;19:747-57.

[380] Knibbs PJ. Glass ionomer cement: 10 years of clinical use. Journal of Oral Rehabilitation 1988;15:103-15.

[381] Knibbs PJ, Walls AW. A laboratory and clinical evaluation of three dental luting cements. Journal of Oral Rehabilitation 1989;16:467-73.

[382] Whitters CJ, Strang R, Brown D, Clarke RL, Curtis RV, Hatton PV et al. Dental materials: 1997 literature review. Journal of Dentistry 1999;27:401-35.

[383] Cho JW, Paul DR. Nylon 6 nanocomposites by melt compounding. Polymer 2001;42:1083-94.

[384] Seakin T, Eunal Y, Aksoy I, Yakinci ME. Synthesis and characterization of novel polyacrylate-clay sol-gel materials. Journal of Materials Science 1996;31:3123-7.

[385] Park JH, Jana SC. The relationship between nano- and micro-structures and mechanical properties in PMMA-epoxy-nanoclay composites. Polymer 2003;44:2091-100.

[386] Wu J, Lin J, Zhou M, Wei C. Synthesis and properties of starch-graft-polyacrylamide/clay superabsorbent composite. Macromolecular Rapid Communications 2000;21:1032-4.

[387] Zhang J, Wang A. Study on superabsorbent composites. IX: Synthesis, characterization and swelling behaviors of polyacrylamide/clay composites based on various clays. Reactive and Functional Polymers 2007;67:737-45.

[388] Soon Yong Kwon, Sung Soo Kim. Preparation and characterization of bone cements incorporated with montmorillonite. Macromolecular Symposia 2007;249:86-95.

[389] Usuki A, Kojima Y, Kawasumi M, Okada A, Fukushima Y, Kurauchi T et al. Synthesis of nylon 6-clay hybrid. Journal of Materials Research 1993;8:1179-84.

[390] DeLong R, Douglas WH. Development of an artificial oral environment for the testing of dental restoratives: bi-axial force and movement control. Journal of Dental Research 1983;62:32-6.

[391] Heintze SD. How to qualify and validate wear simulation devices and methods. Dental Materials 2006;22:712-34.

[392] ISO 14569-1-1999 Dental materials-guidance on testing of wear. Part 1. Wear by tooth brushing. Technical Specification 1999. International Organization for Standardisation 2007.

[393] ISO 14569-2 Dental materials-guidance on testing of wear. Part 2. Wear by two-and/or three body contact. International Organization for Standardisation 2001.

[394] Shortall AC, Hu XQ, Marquis PM. Potential countersample materials for in vitro simulation wear testing. Dental Materials 2002;18:246-54.

[395] De Gee AJ, Van Duinen RNB, Werner A, Davidson CL. Early and long-term wear of conventional and resin-modified glass ionomers. Journal of Dental Research 1996;75:1613-9.

[396] Suzuki S, Leinfelder KF, Shinkai K. Wear resistance of resin cements. American Journal of Dentistry 1995;8:83-7.

[397] De Gee AJ, Van Duinen RNB, Werner A, Davidson CL. Early and long-term wear of conventional and resin-modified glass ionomers. Journal of Dental Research 1996;75:1613-9.

[398] Leinfelder KF, Suzuki S. In vitro wear device for determining posterior composite wear. Journal of the American Dental Association 1999;130:1347-53.

[399] Xu HHK, Quinn JB, Giuseppetti AA. Wear and mechanical properties of nano-silica-fused whisker composites. Journal of Dental Research 2004;83:930-5.

[400] Condon JR, Ferracane JL. Factors effecting dental composite wear in vitro. Journal of Biomedical Materials Research 1997;38:303-13.

[401] Zheng J, Yu HY, Zhou ZR. Comparative study of the three-body abrasive wear behavior of natural human teeth and plastic teeth. Mocaxue Xuebao/Tribology 2004;24:568-71.

[402] Hickel R, Manhart J, Garcia-Godoy F. Clinical results and new developments of direct posterior restorations. American Journal of Dentistry 2000;13.

[403] Antunes PV, Ramalho A. Mechanical characterization of dental restorative composite materials. Materials Science Forum 455-456, 393-397. 2004.

[404] Prentice P. Influence of molecular weight on the fracture of poly(methyl methacrylate) (PMMA). Polymer 1983;24:344-50.

[405] Sulong M, Aziz RA. Wear of materials used in dentistry: A review of the literature. The Journal of Prosthetic Dentistry 1990;63:342-9.

[406] Kunzelmann KH, Brkle V, Bauer C. Two-body and three-body wear of glass ionomer cements. International Journal of Paediatric Dentistry 2003;13:434-40.

[407] Krejci I, Lutz F, Zedler C. Effect of contact area size on enamel and composite wear. Journal of Dental Research 1992;71:1413-6.

[408] Wilson AD, Hill RG, Warrens CP, Lewis BG. The influence of polyacid molecular weight on some properties of glass-ionomer cements. Journal of Dental Research 1989;68:89-94.

[409] Hill RG, Wilson AD, Warrens CP. The influence of poly(acrylic acid) molecular weight on the fracture toughness of glass-ionomer cements. Journal of Materials Science 1989;24:363-71.

[410] Rabinowicz E. Friction and Wear of Materials 1st Edition. Wiley, New York. 1965.

[411] Prentice P. The influence of molecular weight on the fracture of thermoplastic glassy polymers. Journal of Materials Science 1985;20:1445-54.

[412] Fennell B, Hill RG. The influence of poly(acrylic acid) molar mass and concentration on the properties of polyalkenoate cements. Part III: Fracture toughness and toughness. Journal of Materials Science 2001;36:5185-92.

[413] O'Brien WJ, Yee J. Microstructure of posterior restorations of composite resin after clinical wear. Operative Dentistry 1980;5:90-4.

[414] Ferracane JL. Is the wear of dental composites still a clinical concern?. Is there still a need for in vitro wear simulating devices? Dental Materials 2006;22:689-92.

[415] DeLong R. Intra-oral restorative materials wear: Rethinking the current approaches: How to measure wear. Dental Materials 2006;22:702-11.

[416] Heintze SD, Cavalleri A, Forjanic M, Zellweger G, Rousson V. A comparison of three different methods for the quantification of the in vitro wear of dental materials. Dental Materials 2006;22:1051-62.

[417] Heintze SD, Forjanic M, Rousson V. Surface roughness and gloss of dental materials as a function of force and polishing time in vitro. Dental Materials 2006;22:146-65.

[418] Leinfelder KF, Beaudreau RW, Mazer RB. An in vitro device for predicting clinical wear. Quintessence international 1989;20:755-61.

[419] Barry TI, Clinton DJ, Wilson AD. The Structure of a Glass-Io nomer Cement and its Relationship to the Setting Process. Journal of Dental Research 1979;58:1072-9.

[420] Yiu CKY, Tay FR, King NM, Pashley DH, Sidhu SK, Neo JCL et al. Interaction of Glass-ionomer Cements with Moist Dentin. Journal of Dental Research 2004;83:283-9.

[421] Vaia RA, Ishii H, Giannelis EP. Synthesis and properties of two-dimensional nanostructures by direct intercalation of polymer melts in layered silicates. Chemistry of Materials 1993;5:1694-6.

[422] Filippi S, Mameli E, Marazzato C, Magagnini P. Comparison of solution-blending and melt-intercalation for the preparation of poly(ethylene-co-acrylic acid)/organoclay nanocomposites. European Polymer Journal 2007;43:1645-59.

[423] ASTM E399-08 Standard Test Method for Linear-Elastic Plane-Strain Fracture Toughness K Ic of Metallic Materials. ASTM International 2006.

8. CONFERENCES CONTRIBUTIONS

2009	Wear behaviour of novel glass ionomer dental nanocomposites. BSDR Annual meeting 1st-4th September, 2009 Glasgow, UK [Oral presentation]
2009	Glass-Ionomer Dental Nanocomposites: A Study From Conventional to Nano! BSDR Annual meeting 1st-4th September, 2009 Glasgow, UK [Poster presentation]
2009	In-Vitro Wear Determination & Mechanical Properties of Glass-Ionomer Clay Nanocomposites. IADR 87th General Session, Miami, Florida., USA 1-4 April, 2009. [Poster Presentation]
2008	Mechanical Properties and Wear of Glass-Ionomer Restoration After Clay Dispersion. PEF-IADR Conference London, UK 10-12 September, 2008. [Oral Presentation]
2008	Chemical and Mechanical Evolution of Glass Ionomer Clay Nanocomposites. IADR 86th General Session of, Toronto, ON, Canada 1-5 July, 2008. [Oral presentation]
2007	Influence of the Dispersion of Polymer Grade Montmorillonite On The Mechanical Properties Glass Ionomer Cements. 19th European Dental Materials Conference Leeds, UK 29-31 August, 2007. [Poster Presentation]
2007	Dispersion and Interaction of Polymer Grade (PG) Montmorillonite Within Poly(acrylic acid) In Glass Ionomer Cements. Annual Meeting of UK Society of Biomaterials, King's College London 4-6 July, 2007. [Oral presentation]
2007	Novel Dental Nanocomposite. Graduate school poster conference, University of Birmingham UK 12th June, 2007. [Poster presentation]
2007	Dispersion and Interaction of Polymer Grade (PG) Montmorillonite Within Poly(acrylic acid). BSDR/NOF Annual Meeting 2007, University of Durham, UK 3-5 April, 2007. [Oral presentation]

9 APPENDIX

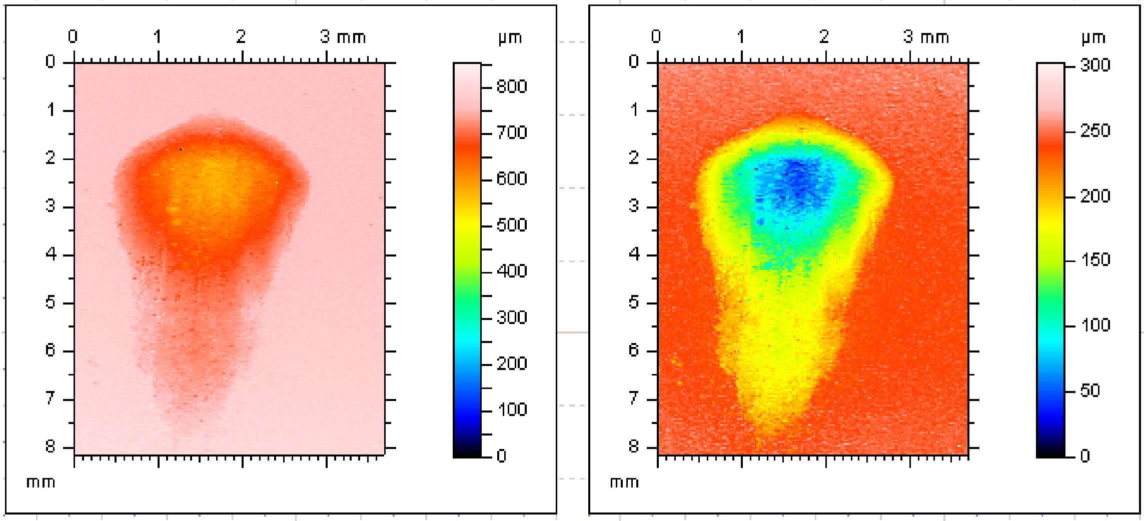

1. Wear scar measurements from HiFi cement with 2 wt % PGN (C2.0NPAH)

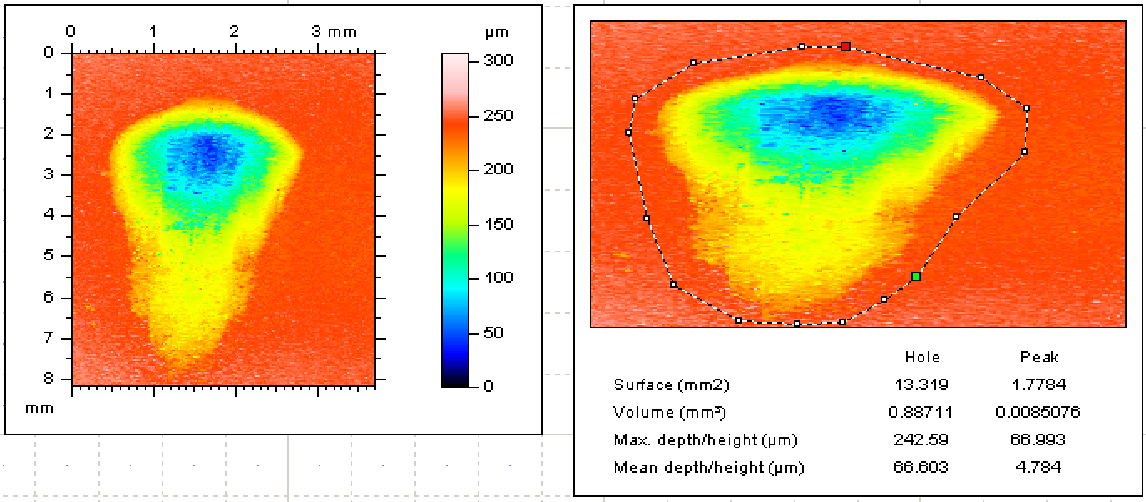

	Hole	Peak
Surface (mm2)	13.319	1.7784
Volume (mm³)	0.88711	0.0085076
Max. depth/height (µm)	242.59	66.993
Mean depth/height (µm)	66.603	4.784

2. Wear volume determination form wear facet of C2.0NPAH.

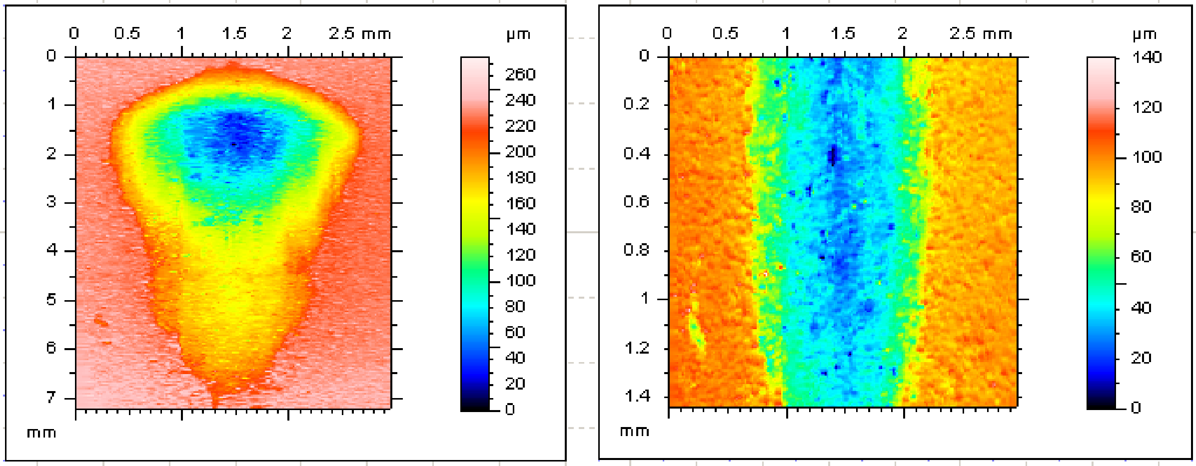

3. Wear volume determination form wear facet of C2.0NPAH.

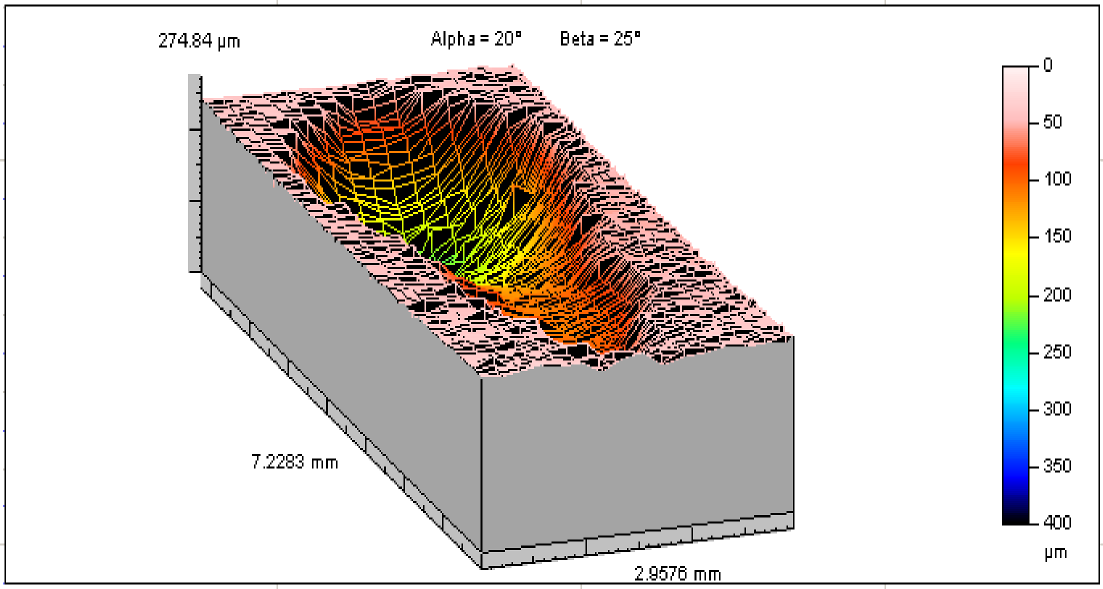

4. Tear-drop shaped wear facet in C2.0NPAH.

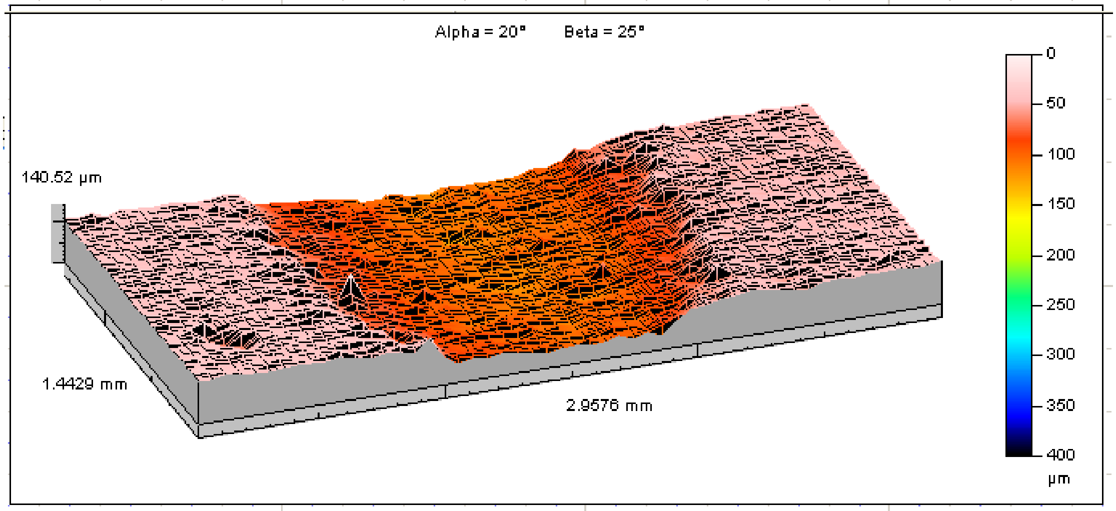

5. Abrasion region in tear-drop shaped wear facet in C2.0NPAH

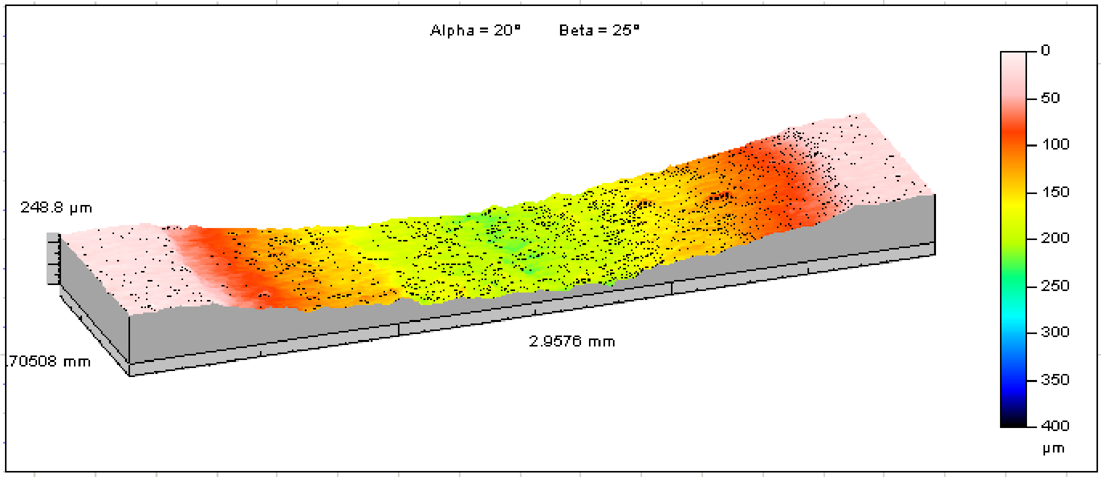

6. Attrition region in tear-drop shaped wear facet in C2.0NPAH

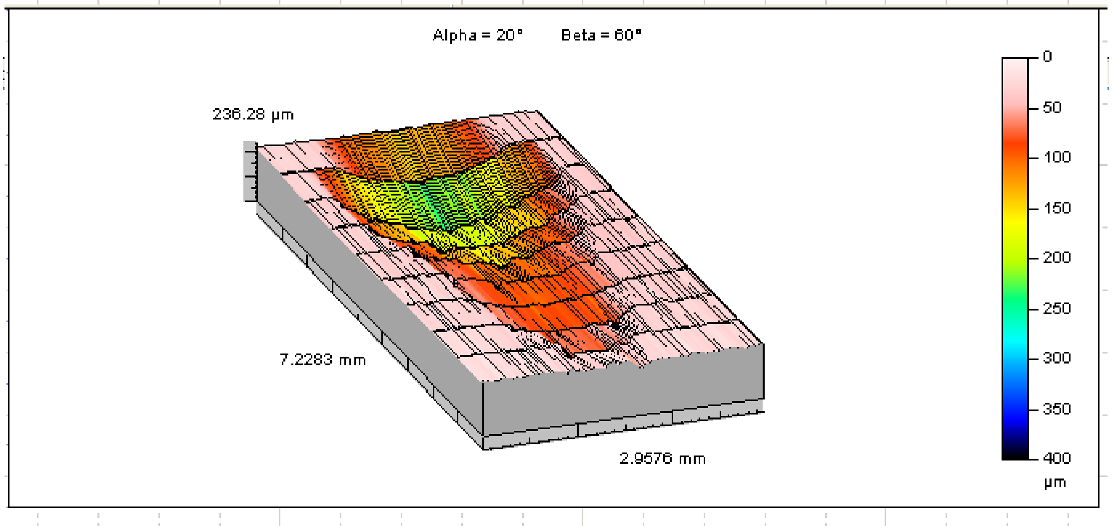

7. Tear-drop shaped wear facet in C2.0NPAH showing 10 scans

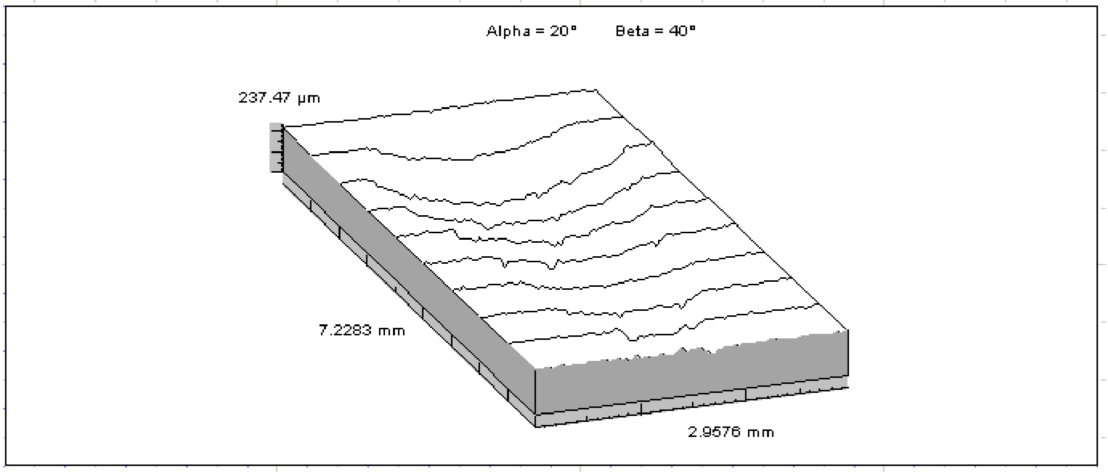

8. Tear-drop shaped wear facet in C2.0NPAH showing 10 scans

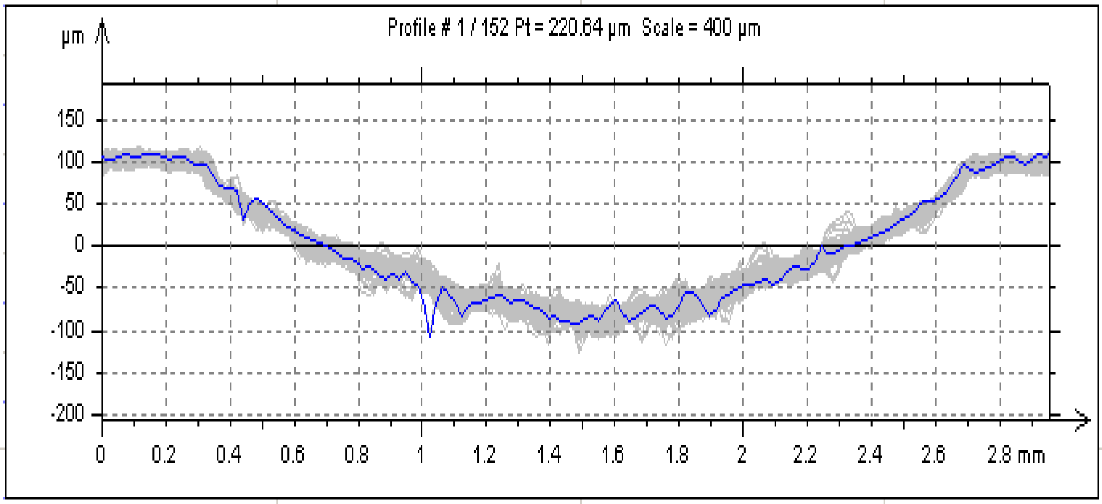

9. Wear facet curve used to calculate wear volume showing the all scans done at 10 micron distance in C2.0NPAH

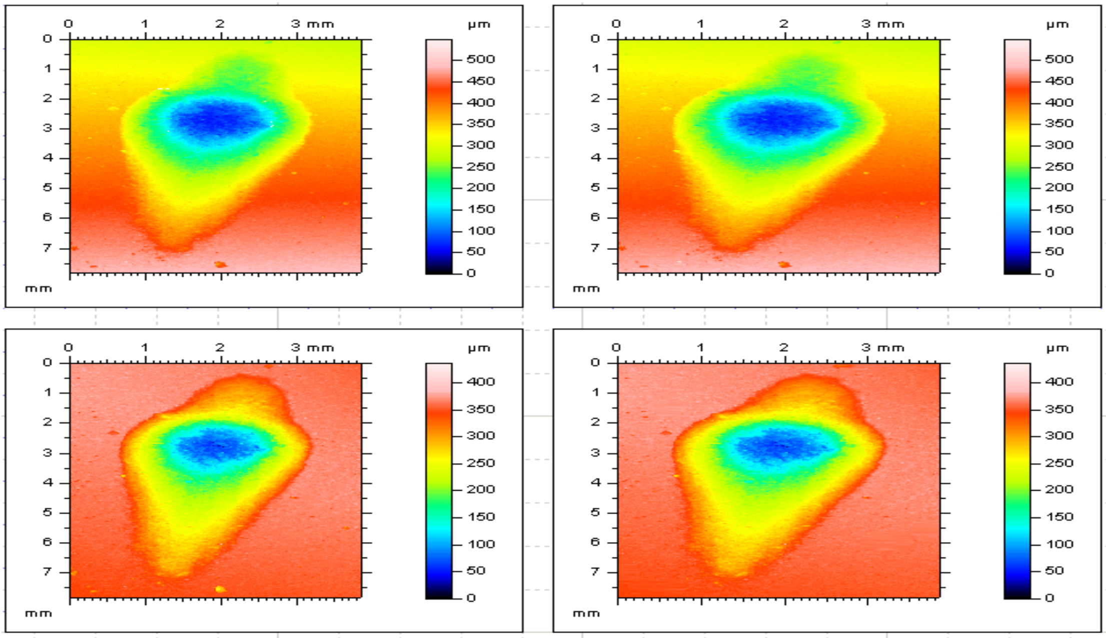

10. Wear scar measurements from Fuji-IX cement with 2 wt % PGN (C2.0NF75F)

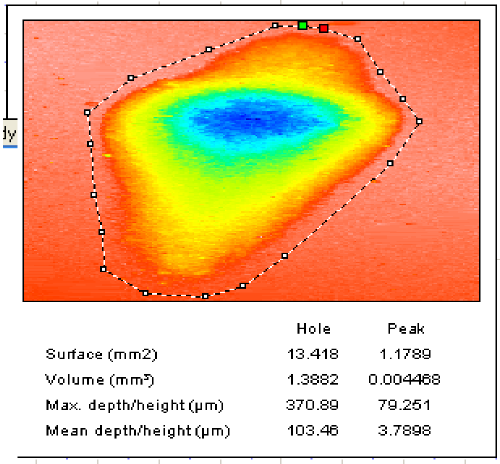

	Hole	Peak
Surface (mm2)	13.418	1.1789
Volume (mm³)	1.3882	0.004468
Max. depth/height (µm)	370.89	79.251
Mean depth/height (µm)	103.46	3.7898

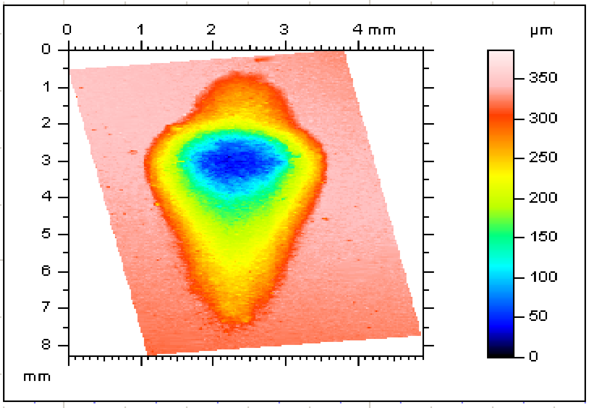

11. Wear scar measurements from Fuji-IX cement with 2 wt % PGN (C2.0NF75F)

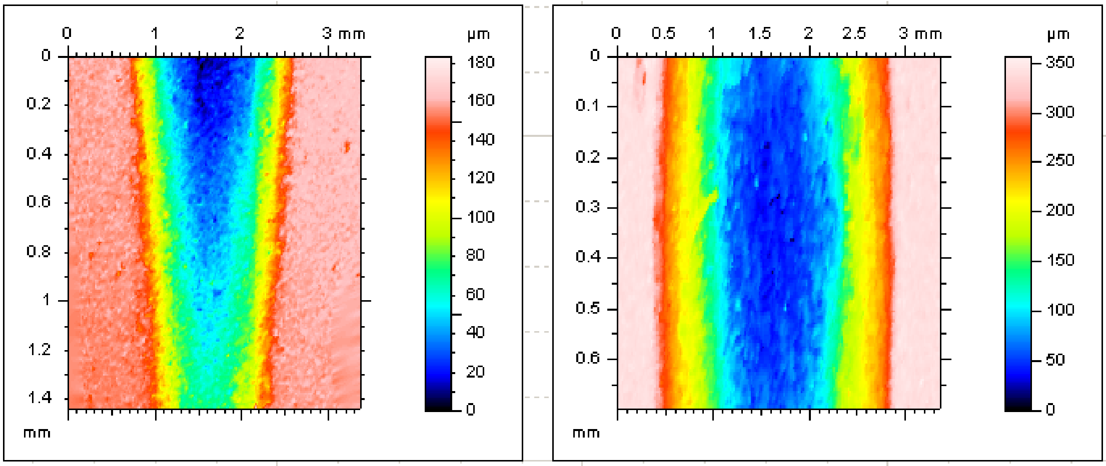

12. Wear scar measurements from Fuji-IX cement with 2 wt % PGN (C2.0NF75F)

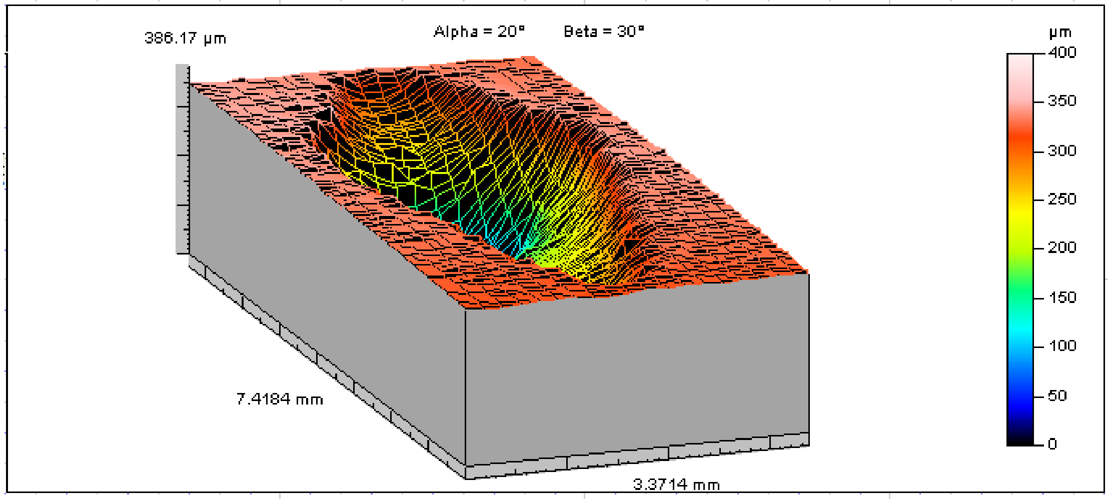

13. A tear-drop shaped in C2.0NF75F

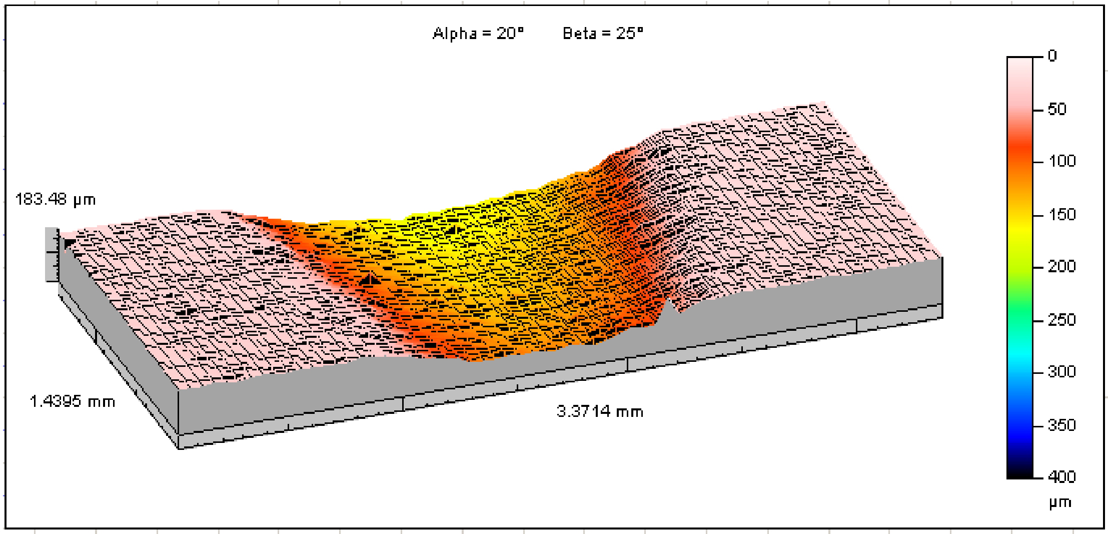

14. Abrasion region in tear-drop shaped in C2.0NF75F

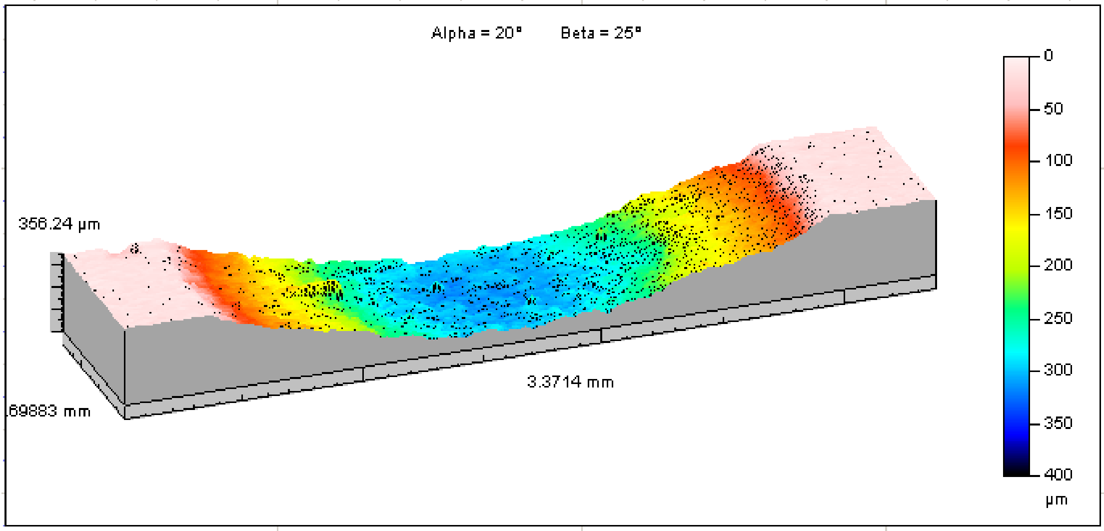

15. Attrition region in tear-drop shaped C2.0NF75F

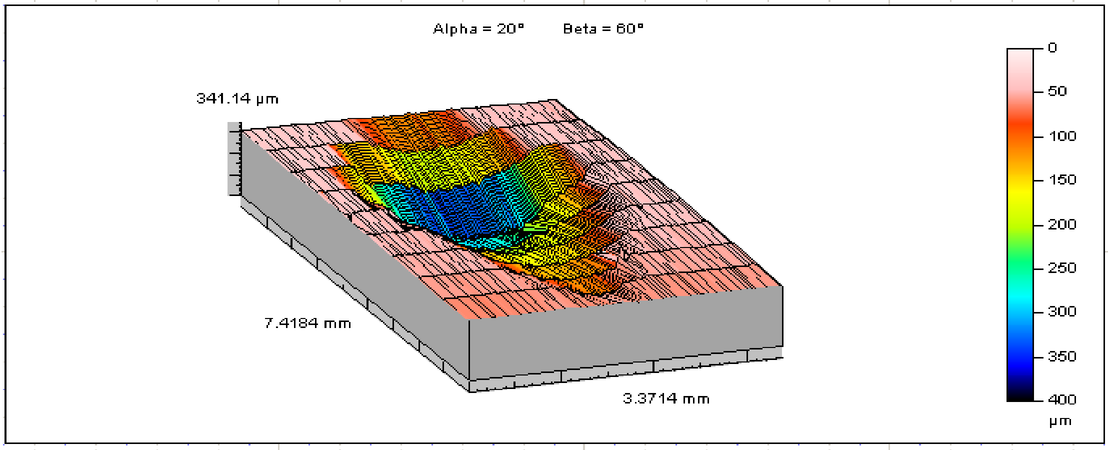

16. Tear-drop shaped wear facet in C2.0NF75F showing 10 scans

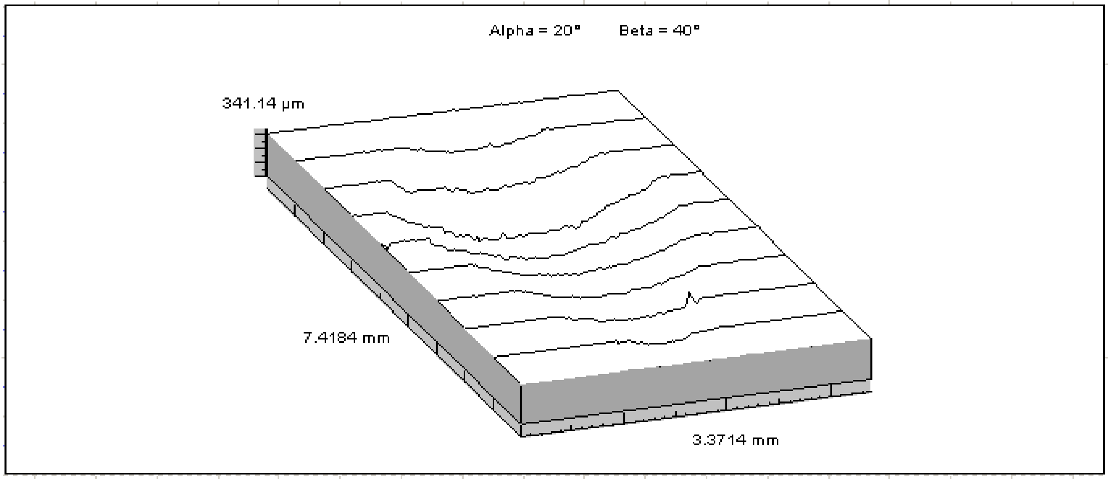

17. Tear-drop shaped wear facet in C2.0NF75F showing 10 scans

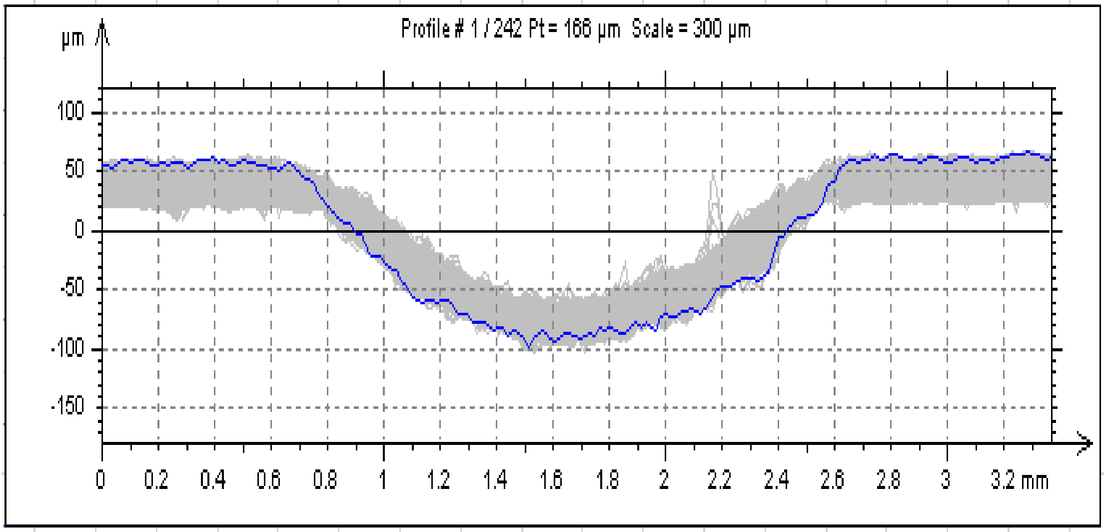

18. Wear facet curve used to calculate wear volume showing the all scans done at 10 micron distance in C2.0NF75F

TEM micrograph of 32% polypropylene + nanoclay (sample-A)

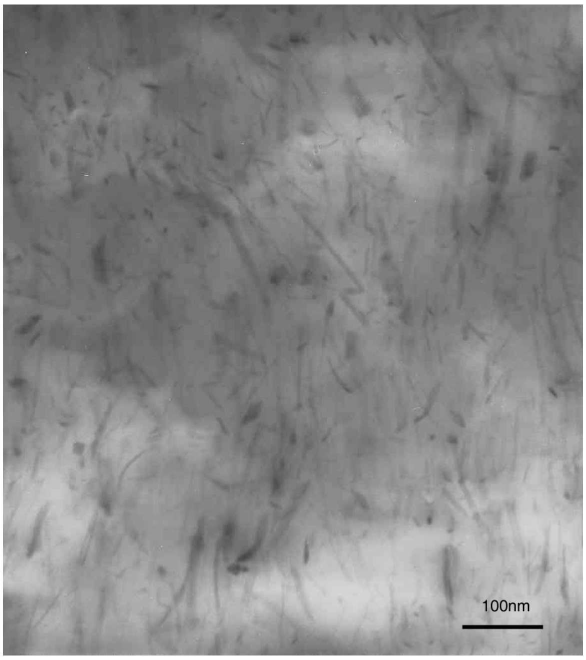

Voltage 100KV , Magnification 27.5K

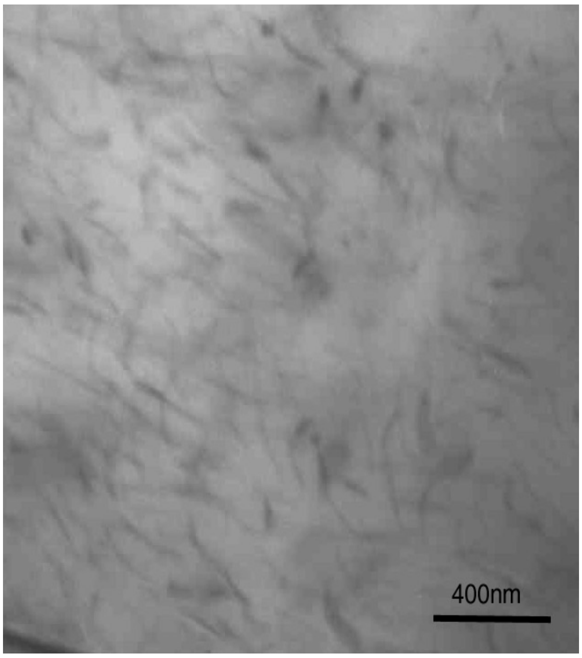

Voltage 100KV , Magnification 38.5K

Sample- B
28% polypropylene + nanoclay

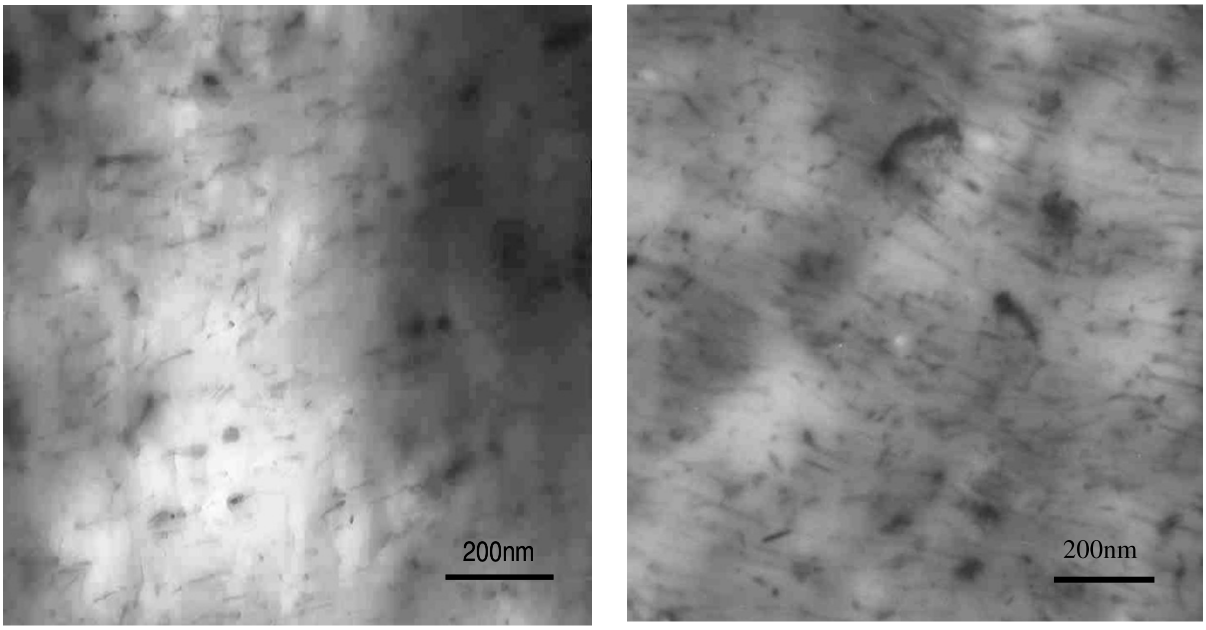

Voltage 200KV , Magnification 20 K